Plasmacytoid Dendritic Cell Activation and Differentiation by the Human Immunodeficiency Virus Type 1 and 2: Implications for HIV Immunopathogenesis

Caroline Margaret Royle

Imperial College London

Department of Medicine

Immunology Section

Chelsea & Westminster Hospital

369 Fulham Road

London, SW10 9NH

A thesis submitted for the degree of Doctor of Philosophy

2014

Declaration of Originality

I, Caroline Royle, declare that the work presented in this thesis is my own and that where appropriate I have acknowledged any outside contribution. Information derived from published work has been clearly indicated in the text and in the list of references.

Copyright Declaration

Abstract

Infection with HIV-1 results in the progressive dysfunction of the immune system eventually leading to AIDS, characterised by low $CD4^+$ T lymphocyte counts and increased susceptibility to opportunistic infections. In contrast to HIV-1, individuals infected with HIV-2 often remain asymptomatic, with lower viral loads and higher $CD4^+$ T cell counts throughout the course of disease. Furthermore, HIV-2^+ individuals display enhanced HIV-specific T cell responses. In addition, HIV-1 disease progression is slower in patients with pre-existing HIV-2 infection. Plasmacytoid dendritic cells (pDCs) are key mediators of the early innate immune response. Upon viral infection, pDCs secrete high levels of type I IFN (IFN-α/β) which limit viral replication and prime the adaptive immune response. Activated pDCs, in particular excessive IFN-α/β, have been implicated in HIV-1 immunopathogenesis. Specifically pDCs may contribute to the recruitment of target cells to the site of HIV-1 infection, increased apoptosis of immune cells and suppression of memory T cell responses.

The aim of this study was to compare the abilities of HIV-1 and HIV-2 to activate pDCs *in vitro*. HIV-1 was a more potent inducer of type I IFN responses in PBMCs compared to HIV-2, measured at both the transcriptional level, and by measuring IFN-α/β secretion into cell culture supernatants. Furthermore, HIV-2, but not HIV-1, inhibited IFN-α production in response to synthetic stimuli. Phenotypic analysis of pDCs by flow cytometry revealed that both HIV-1 and HIV-2 were equally able to induce an up-regulation of co-stimulatory marker expression. Measurement of co-stimulatory molecule expression in conjunction with IFN-α secretion showed that HIV-1 favoured an IFN response, whereas HIV-2 preferentially maturated pDCs towards an antigen-presenting cell (APC) phenotype.

The ability of HIV-2 to mature pDCs into APCs while reducing IFN-α secretion may be an important contributor to more robust T cell responses and therefore slower progressing HIV disease.

Table of Contents

List of Tables

List of Figures

Acknowledgements

First and foremost I would like to thank my supervisor Dr Adriano Boasso for all of your help and support over the last several years. You have always been incredibly understanding and approachable, and for that I am grateful.

I am also indebted to those who took the time to read through my thesis and for their invaluable suggestions and comments: Professor Charles Bangham, Dr Steven Patterson, Dr Nesrina Imami, Dr Shan Herath and Steve Bignell – thank-you.

I cannot forget past and present members of the Immunology Section at the Chelsea & Westminster Hospital. In particular, Anna, Adam, Shan and Marloes: thank-you for your friendship and for preserving my sanity. Louise, Nathali and Charlotte: it's been an absolute pleasure sharing an office with you guys.

My family and friends have also been important in helping me. Mum and John, you have been instrumental in encouraging me to stay in the UK to finish this PhD. Thank-you for believing in me.

And of course, Steve Bignell…… None of this would have been possible without you by my side. I cannot thank you enough for all of the love, support and encouragement you give me.

Abbreviations

1-mT	1-methyl-tryptophan
A T G C	Adenine, Thymine, Guanine and Cytosine
ADAR	Adenosine deaminase acting on RNA
AIDS	Acquired immunodeficiency syndrome
ANOVA	Analysis of variance
APC	Allophycocyanin
APC	Antigen presenting cell
APOBEC	Apolipoprotein B mRNA editing enzyme, catalytic polypeptide-like
ART	Anti-retroviral therapy
At-2	Aldrithiol-2
AZT	Azidothymidine
BD	Becton Dickinson
BDCA	Blood dendritic cell antigen
BST-2	Bone marrow stromal cell antigen-2
BV421	Brilliant Violet 421
CBA	Cytometric bead array
CCL	Chemokine (C-C motif) ligand
CCR	Chemokine (C-C motif) receptor
CD	Cluster of differentiation
cDNA	Copy DNA
CMV	Cytomegalovirus
COA	Certificate of analysis
CpG	Cytosine-phosphate-Guanine
CTL	Cytotoxic T lymphocyte
CTLA-4	Cytotoxic T lymphocyte antigen-4
CV	Coefficient of variation
CXCR	Chemokine (C-X-C motif) receptor
Cy	Cyanine
d4T	2’,3’-didehydro-3’-deoxythymidine
DC	Dendritic cell
DMSO	Dimethyl sulfoxide
DNA	Deoxyribonucleic acid
DR	Death receptor
EDTA	Ethylenediamine tetra-acetic acid
ELISA	Enzyme linked immunosorbent assay
Env	Envelope
FACS	Fluorescence activated cell sorting
FasL	Fas ligand
FBS	Foetal bovine serum
FITC	Fluorescein isothiocyanate
FMO	Fluorescence minus one
Foxp3	Forkhead box P3
FSC-A	Forward scatter-area
FSC-H	Forward scatter-height
FVD	Fixable viability dye
GALT	Gut-associated lymphoid tissue
GCN2	General control non-depressible 2 kinase
GO	Gene ontology
gp	Glycoprotein

HIV	Human immunodeficiency virus
HLA	Human leukocyte antigen
HPLC	High performance liquid chromatography
HRP	Horseradish peroxidase
HSV	Herpes simplex virus
IDO	Indoleamine 2,3-dioxygenase
IFN	Interferon
IFNAR1	Interferon alpha receptor subunit 1
IFNAR2	Interferon alpha receptor subunit 2
IgG	Immunoglobulin G
IL	Interleukin
IQR	Interquartile range
IRF	Interferon regulatory factor
ISG	Interferon stimulated gene
ISRE	IFN-stimulated response element
ITIM	Immunoreceptor tyrosine-based inhibitory motif
Kyn	Kynurenine
LCMV	Lymphocytic choriomeningitis virus
LPS	Lipopolysaccharide
LTNP	Long-term non-progressors
mDC	Myeloid dendritic cell
MFI	Mean fluorescence intensity
MHC	Major histocompatibility complex
MIP	Macrophage inflammatory protein
mRNA	Messenger RNA
Mx	Myxovirus resistance
MyD88	Myeloid differentiation primary response gene 88
NHS	National health service
NK	Natural killer cell
NK-κB	Nuclear factor kappa B
NOD	Nucleotide-binding oligomerisation domain
NRTI	Nucleoside analogue reverse transcriptase inhibitor
OAS	2’,5’-oligoadenylate synthetase
OD	Optical density
ODN	Oligodeoxynucleotides
OPD	o-Phenylenediamine dihydrochloride
PAMP	Pathogen-associated molecular pattern
PBMC	Peripheral blood mononuclear cell
PBS	Phosphate buffered saline
PCA	Principal component analysis
PCR	Polymerase chain reaction
PD-1	Programmed cell death-1
pDC	Plasmacytoid dendritic cell
PD-L1	Programmed cell death ligand-1
PE	Phycoerythrin
PerCP	Peridinin chlorophyll protein complex
PKR	Protein kinase RNA-activated
PMT	Photomultiplier tube
PRR	Pattern recognition receptor
qPCR	Quantitative PCR
RANTES	Regulated on activation, normal T cell expressed and secreted

rcf	Relative centrifugal force
RIG-I	Retinoic acid inducible gene I
RIN	RNA integrity number
RLR	RIG-I like receptor
RMA	Robust multi-array
RNA	Ribonucleic acid
rpm	Rotations per minute
RPMI-1640	Roswell Park Memorial Institute medium-1640
RT	Reverse transcription
RT-qPCR	Reverse transcription-quantitative PCR
SA-HRP	Streptavidin-horseradish peroxidase
SAMHD1	SAM (sterile alpha motif) domain and HD (histidine aspartic) domain-containing protein 1
SIV	Simian immunodeficiency virus
SOCS	Suppressor of cytokine signalling
SPICE	Simplified presentation of incredibly complex evaluations
SSC-A	Side scatter-area
STAT	Signal transducer and activator of transcription
TBK1	TANK-binding kinase-1
TCR	T cell receptor
TGF-β	Transforming growth factor-beta
T_H	T helper cell
TLR	Toll-like receptor
TMB	Tetramethylbenzidine
TNF	Tumour necrosis factor
TRAIL	TNF-related apoptosis inducing ligand
Treg	T regulatory cell
TRIM	Tripartite motif
tRNA	Transfer RNA
Trp	Tryptophan
VSV	Vesicular stomatitis virus
βCD	2-hydroxy-propyl β-cyclodextrin

Publications Arising From This Thesis

Manuscript

Royle CM, Graham DR, Sharma S, Fuchs D, Boasso A. HIV-1 and HIV-2 differentially mature plasmacytoid dendritic cells into interferon-producing or antigen-presenting cells. *Manuscript submitted*.

Oral Presentation

Royle CM, Fuchs D, Graham DR, Boasso A. Comparison of plasmacytoid dendritic cell activation by HIV-1 and HIV-2: implications for HIV immunopathogenesis. Keystone Symposia: Immune Activation in HIV Infection; Basic Mechanisms and Clinical Implications. Colorado, USA. April 2013.

Poster Presentations

Royle CM, Fuchs D, Graham DR, Boasso A. Comparison of plasmacytoid dendritic cell activation by HIV-1 and HIV-2: implications for HIV immunopathogenesis. 5th Blizard Institute HIV Symposium. London, UK. June 2013.

Royle CM, Fuchs D, Graham DR, Boasso A. Comparison of plasmacytoid dendritic cell activation by HIV-1 and HIV-2: implications for HIV immunopathogenesis. Keystone Symposia: Immune Activation in HIV Infection; Basic Mechanisms and Clinical Implications. Colorado, USA. April 2013.

Related Publications Arising During This Thesis

Manuscripts

Royle CM, Tsai MH, Tabarrini O, Massari S, Graham DR, Aquino VN, Boasso A. Modulation of HIV-1-induced activation of plasmacytoid dendritic cells (pDCs) by 6-desfluoroquinolones. AIDS Res Hum Retroviruses 2013; 30(4): 345-354.

Boasso A, Royle CM, Doumazos S, Aquino VN, Biasin M, Piacentini L, Tavano B, Fuchs D, Mazzotta F, Lo Caputo S, Shearer GM, Clerici M, Graham DR. Overactivation of plasmacytoid dendritic cells inhibits antiviral T-cell responses: a model for HIV immunopathogenesis. Blood 2011; 118(19): 5152-5162.

Poster Presentations

Royle CM, Tabarrini O, Graham DR, Boasso A. Unique immunomodulatory properties of the quinolone derivative naphthyridone 3 (HM13N) and its potential for HIV-1 immunotherapy. 19th Conference on Retroviruses and Opportunistic Infections (CROI). Seattle, USA. March 2012.

Royle CM, O. Tabarrini, DR. Graham, A. Boasso. Quinolone derivatives with proven antiretroviral activity dampen HIV-mediated activation of pDC. Keystone Symposia: HIV Evolution, Genomics and Pathogenesis. Whistler, Canada. March 2011.

Royle CM, Tabarrini O, Graham DR, Boasso A. Quinolone derivatives with proven antiretroviral activity dampen HIV-mediated activation of pDC. T lymphocyte dynamics in acute and chronic viral infection. London, UK. January 2011.

Royle CM, Boasso A, Doumazos S, Aquino VN, Biasin M, Piacentini L, Fuchs D, Lo Caputo S, Shearer GM, Clerici M, Graham DR. Permeabilization of HIV via envelope cholesterol depletion enhances HIV recall antigen responses by weakening its immunopathogenic potential. British Society for Immunology (BSI) Congress. Liverpool, UK. December 2010.

Chapter 1 Introduction

1.1 Human Immune Response to Viral Infections

Cells of the innate immune system, which include dendritic cells (DC), natural killer cells (NK), macrophages and neutrophils, are the first to respond to viral infections (Figure 1.1). The innate immune system serves the dual function of limiting the initial replication of a pathogen and favouring the initiation of the adaptive immune response. Innate cells mount a broad response to invading pathogens, releasing inflammatory cytokines and chemokines (Murphy *et al.*, 2008). Dendritic cells and macrophages also act as professional antigen presenting cells (APC), which stimulate cells of the adaptive immune system (Geissmann *et al.*, 2010).

The adaptive immune response, composed of T and B lymphocytes, is able to provide a virus-specific response due to the expression of highly specialised antigen receptors, and is more efficient at clearing infections (Figure 1.1). T lymphocytes, so called because they are derived from immature cells from the thymus, compose the cellular arm of the adaptive immune response. They recognise processed antigens presented to them by APCs (Banchereau and Steinman, 1998, Murphy *et al.*, 2008). B lymphocytes are derived from the bone marrow and form the humoral arm of the adaptive response, secreting antigen specific antibodies. Unlike T cells, B cells recognise native antigens (Banchereau and Steinman, 1998, Murphy *et al.*, 2008). Once the infection is cleared, some activated lymphocytes persist and differentiate into memory cells. Memory lymphocytes are more rapidly activated during subsequent encounters with the same pathogen, and quickly differentiate into effector cells (Murphy *et al.*, 2008).

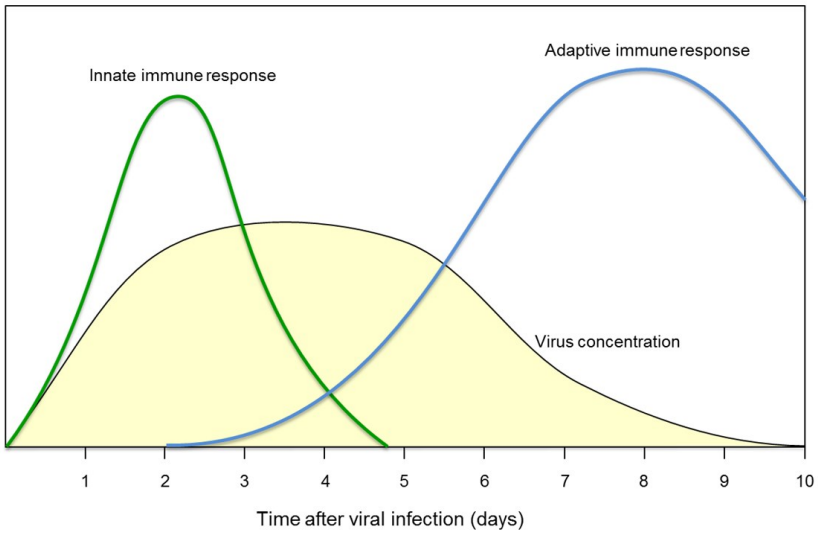

Figure 1.1. Generalised immune response to viral infection. Adapted from (Murphy *et al.*, 2008).

1.1.1 T Lymphocytes

Each T cell expresses a unique T cell receptor (TCR), which is generated by DNA rearrangement during cellular development, and is specific for a certain antigen (Abbey and O'Neill, 2008). T cells which have not yet encountered their antigen, termed naïve, circulate the body until they encounter their specific foreign antigen presented on MHC (major histocompatability complex) molecules. Ligation of the TCR expressed on the surface of T cells, with the MHC molecule presenting peptide, results in T cell activation. In addition to the TCR/MHC interaction, a secondary signal is also required to activate naïve T cells, which is provided by the co-stimulatory molecules expressed on APCs. The most well described co-stimulatory molecules are CD80 and CD86 (also referred to as B7 molecules), which bind to CD28 expressed on T cells and exert a positive signal for T lymphocyte activation (Sharpe and Freeman, 2002). In addition, the activation of T cells is also influenced by secreted cytokines, such as IFN-α and IL-12 (Felix *et al.*, 2010).

There are two main types of T cells, which are divided based on the expression of either CD4 or CD8. $CD4^+$ T cells recognise antigen presented on MHC class II molecules (MHC-II), while $CD8^+$ T cells recognise antigen presented on MHC class I (MHC-I) molecules (Kaye *et al.*, 1989, Teh *et al.*, 1988).

Classically, MHC-I molecules present cytoplasmic derived peptides, while MHC-II molecules present peptides from the extracellular environment (Rammensee *et al.*, 1993).

Upon recognition of antigen, through the TCR/MHC-II interaction, activated $CD4^+$ T cells can differentiate into multiple functional subsets, such as T helper cells type 1 (T_H1), T_H2, T_H17 and T regulatory cells (Treg) (Hirahara *et al.*, 2013). The phenotype of the activated $CD4^+$ T cell is determined by the nature of the pathogenic insult and the resulting inflammatory reaction, which determine the cytokine milieu in which T cell activation occurs. T_H1 cells mainly produce interferon (IFN)-γ and tumour necrosis factor (TNF) and are involved in defence against intracellular pathogens, providing help to $CD8^+$ T cells and macrophages to achieve clearance of infected cells (Abbas *et al.*, 1996, Hirahara *et al.*, 2013). T_H2 cells produce interleukin (IL)-4, IL-5 and IL-13 and are involved in defence against extracellular microbes, promoting and modulating B cell activity (Abbas *et al.*, 1996, Hirahara *et al.*, 2013). T_H17 cells secrete IL-17 and are involved in defence at mucosal surfaces, enhancing the neutrophil response to extracellular pathogens (Khader *et al.*, 2009). T regulatory cells exert suppressive activity on other effector cells of the adaptive immune response, and are important in preventing uncontrolled immune reactions (Hirahara *et al.*, 2013). T regulatory cells can be generated by ligation of the inhibitory molecule cytotoxic T lymphocyte antigen (CTLA)-4, expressed on the surface of T cells, to CD80/86 on APCs (Felix *et al.*, 2010).

Upon activation, $CD8^+$ T cells differentiate into cytotoxic T lymphocytes (CTL) (Zhang *et al.*, 2009). As mentioned, CTLs may also require the help of $CD4^+$ T cells, such as by the secretion of IFN-γ, for effective activation (Janssen *et al.*, 2003, Zhang *et al.*, 2009). CTLs migrate to the site of infection where they release perforin and granzymes, which induce apoptosis of virus-infected cells (Russell and Ley, 2002). In addition to cytotoxic functions, activated $CD8^+$ T cells can also secrete pro-inflammatory cytokines such as IFN-γ, TNF-α, and chemokines such as MIP-1α (CCL3), MIP-1β (CCL4) and RANTES (CCL5), which attract leukocytes to the site of infection (Cocchi *et al.*, 1995, Jassoy *et al.*, 1993).

1.1.2 Dendritic Cells

Dendritic cells, so called based on their classic morphology of cytoplasmic protrusions called dendrites, are a heterogeneous population which play an important role in the innate immune response (Liu, 2001, Merad *et al.*, 2013). They act as sentinels patrolling mucosal sites and the blood for invading pathogens. Upon encountering a pathogen, DCs recognise conserved structures known as PAMPs (pathogen-associated molecular pattern) by use of host expressed PRRs (pattern recognition receptor), which activate DCs and promotes their maturation (Kawai and Akira, 2007). Mature DCs exert anti-viral functions and have the ability to prime T lymphocytes. Activated DCs migrate to the lymph nodes and display captured viral antigens on MHC molecules for recognition by T cells via the TCR. Importantly, activated mature DCs also provide the co-stimulatory signal which is critical for naïve T cell activation (Lanzavecchia and Sallusto, 2001, Liu, 2001, Merad *et al.*, 2013).

Circulating blood DCs consist of myeloid DCs (mDC) and plasmacytoid DCs (pDC), which differ in morphology, phenotype and function (Merad *et al.*, 2013, Ziegler-Heitbrock *et al.*, 2010, Mathan *et al.*, 2013). Myeloid DCs, also known as classical or conventional DCs, are derived from a myeloid progenitor and recognise a broad range of pathogens due to the expression of several PRRs known as toll-like receptors (TLR) (Geissmann *et al.*, 2010, Schreibelt *et al.*, 2010) (Table 1.1). Myeloid DCs are characterised by the expression of CD11c, blood dendritic cell antigen-1 (BDCA1) (also known as CD1c) and the lack of any lineage-specific markers (CD3, CD14, CD19, CD56) (Ziegler-Heitbrock *et al.*, 2010). In addition, a subset of mDCs expressing BDCA3 (CD141), rather than BDCA1, has also been identified (Ziegler-Heitbrock *et al.*, 2010). Upon activation mDCs up-regulate co-stimulatory molecules, such as CD80 and CD86, and migrate to the lymph nodes where they present MHC-associated peptides to T cells (Derby *et al.*, 2011, Schreibelt *et al.*, 2010). In addition to providing the co-stimulatory signal required for naïve T cell activation, mDCs also secrete a wide range of cytokines which modulate the differentiation of $CD4^+$ T lymphocytes into T_H1, T_H2, T_H17 or Treg cells (Banchereau and Steinman, 1998, Merad *et al.*, 2013).

Plasmacytoid DCs can originate from either a myeloid or lymphoid progenitor cell (Reizis, 2010). Immature pDCs have a round morphology and abundant endoplasmic reticulum, and upon activation assume a more classical DC morphology (Asselin-Paturel and Trinchieri, 2005). Human pDCs are CD11c negative and are phenotypically defined based on their unique expression of BDCA2 (also known as CD303), BDCA4 and high levels of the interleukin-3 receptor CD123 (Colonna *et al.*, 2004, Mathan *et al.*, 2013). In comparison to mDCs, pDCs display a far more restricted breadth of TLRs, expressing only TLR-7 and TLR-9 (Schreibelt *et al.*, 2010). Both TLR-7 and TLR-9 are located within endosomal compartments and recognise single-stranded RNA and unmethylated CpG-rich DNA, respectively, which are typically associated with viral nucleic acids. The specificity of TLR-7 and TLR-9 for nucleic acids confers pDCs the ability to recognise and be activated by engulfed viral pathogens (Mathan *et al.*, 2013). Similar to mDCs, activated pDCs migrate to the lymph nodes and up-regulate the expression of co-stimulatory molecules as well as MHC-II following activation, and are capable of activating T cells (Cella *et al.*, 1999, Lore *et al.*, 2003, Mathan *et al.*, 2013).

Table 1.1. TLR Expression on mDCs and pDCs (Schreibelt *et al.*, 2010)

TLR	mDC Expression	pDC Expression
Cell surface		
1	+	-
2	+	-
4	+	-
5	+	-
6	+	-
Intracellular		
3	+	-
7	+	+
8	+	-
9	-	+

The main function of activated pDCs is considered to be the production of high amounts of type I interferon (IFN-α/β) (Mathan *et al.*, 2013). Upon TLR-7/9 engagement pDCs can secrete 1000 fold more IFN-α than any other cell type in response to viral stimuli (Siegal *et al.*, 1999). Indeed, pDCs were originally identified as natural interferon producing cells which were required to activate NK mediated killing of virus infected cells (Asselin-Paturel and Trinchieri, 2005). The ability of pDCs to rapidly

secrete high levels of IFN-α is a result of both the constitutive expression of interferon regulatory factor 7 (IRF-7) (O'Brien *et al.*, 2011) and of a potent positive type I IFN feedback loop which maintains the secretion of this cytokine (Asselin-Paturel and Trinchieri, 2005). Type I IFN induces an anti-viral state by stimulating the transcription of intracellular proteins which are able to inhibit viral replication, as well as inducing apoptosis of infected cells. Type I IFN-induced proteins which exert anti-viral activity include, but are not limited to, RNA-dependent protein kinase (PKR), 2',5'-oligoadenylate synthetase (OAS), RNA-specific adenosine deaminase (ADAR) and Myxovirus Resistance (Mx) GTPases, which are involved in inhibiting viral mRNA translation as well as destabilising viral RNA (Samuel, 2001). The IFN-induced protein Mx2 was recently described as a potent inhibitor of HIV-1 DNA integration (Goujon *et al.*, 2013). In addition, type I IFN also promotes an APC phenotype on DCs and macrophages by increasing the expression of co-stimulatory molecules and MHC class I and II, thus indirectly promoting the activation of virus-specific T cells (Keir *et al.*, 2002, McKenna *et al.*, 2005, Santini *et al.*, 2000).

Many cells of the immune system express the immune suppressive enzyme indoleamine 2,3-dioxygenase (IDO), including DCs and macrophages (Mellor and Munn, 2003). Activated pDCs in particular express high levels of IDO (Munn *et al.*, 2004a). Different from type I IFN, IDO expression in pDCs is primarily induced by TLR-7 mediated activation of the noncanonical NF-κB pathway (Manches *et al.*, 2012). IDO is an intracellular immunoregulatory enzyme that catalyses the degradation of the essential amino acid, tryptophan (Trp), into kynurenine (Kyn), and is encoded by the gene *IDO1*. The imbalance in the Kyn-to-Trp ratio (Kyn/Trp) ultimately results in a reduction in T cell proliferation and activity (Munn *et al.*, 2005). By depriving the surrounding extracellular environment of Trp, uncharged Trp-specific transfer RNA (tRNA) accumulates in the cytoplasm (Munn *et al.*, 2005). Free tRNA binds to and activates GCN2, an important enzyme involved in the cellular stress response mechanism, which subsequently results in a series of events leading to cell cycle arrest (Munn *et al.*, 2005). In addition to its enzymatic function, IDO also acts as an intracellular signalling molecule (Pallotta *et al.*, 2011).

Pallotta *et al* (2011) showed that in response to TGF-β, pDCs phosphorylate immunoreceptor tyrosine-based inhibitory motifs (ITIMs) on IDO. Phosphorylated IDO then initiates a cascade of intracellular signalling events leading to up-regulation in IDO expression, increased type I IFN, and ultimately resulting in a regulatory pDC phenotype. These regulatory pDCs exhibit an increased capacity to induce the differentiation of naïve $CD4^+$ T cells into Tregs, mediated by TGF-β signalling (Pallotta *et al.*, 2011). A tight relationship exists between Tregs and IDO. Previous work has shown that IDO is also capable of inducing a Treg phenotype in naïve $CD4^+$ T cells as a result of GCN2 mediated expression of the transcription factor Foxp3 (Fallarino *et al.*, 2006). In turn, Tregs induce IDO expression in APCs via interaction of the inhibitory molecule CTLA-4 with CD80 or CD86 (Boasso *et al.*, 2005, Grohmann *et al.*, 2002, Munn *et al.*, 2004b). Perturbations in IDO activity have been suggested to play a role in the development of autoimmune conditions such as multiple sclerosis (Sakurai *et al.*, 2002), cancer (Friberg *et al.*, 2002, Munn *et al.*, 2004a), and rejection of semiallogeneic foetuses (Munn *et al.*, 1998).

1.2 Human Immunodeficiency Virus

The human immunodeficiency virus (HIV) was discovered 30 years ago as the causative agent of the acquired immunodeficiency syndrome (AIDS) (Barre-Sinoussi *et al.*, 1983). AIDS is characterized by progressive weakening of the immune system and loss of the ability to fight otherwise innocuous infections and control malignancies. There is currently no cure or vaccine against HIV and it is now estimated that 35.3 million people worldwide are infected with HIV (UNAIDS, 2013). New HIV infections are on the decline, with a 33% reduction since 2001, which is mainly a result of education for safer sexual behaviour as well as increased access to anti-retroviral therapy (ART) (UNAIDS, 2013). However, a greater understanding of the immunopathogenesis of HIV is still needed in order to help direct future vaccine development and to explore other immunotherapeutic options.

1.2.1 Virology

HIV belongs to a group of retroviruses called the lentiviruses of which there are two types known to infect humans: HIV-type 1 (HIV-1) and HIV-type 2 (HIV-2). HIV-1 is derived from zoonotic transfer of SIV_{CPZ} (simian immunodeficiency virus infecting chimpanzees) to humans (Hahn *et al.*, 2000), and is the cause of the global pandemic. HIV-1 viruses are divided into 3 groups; M, N and O, based upon their genetic make-up. Group M, the main cause of the HIV-1 pandemic, has been further classified into 9 sub-types/clades, with sub-type C accounting for over 50% of worldwide infections (Simon *et al.*, 2006). Each HIV-1 virion consists of 2 copies of an RNA genome, which are packaged in the capsid along with the reverse transcriptase enzyme (Figure 1.2). The HIV-1 capsid, of which the main protein is p24, is contained within the viral envelope; a lipid bi-layer of host cell origin (Rubbert *et al.*, 2012). The main viral proteins associated with the envelope are the glycoproteins gp120 and gp41. Trimeric gp120 and gp41 form the outer spikes of the virion (Engelman and Cherepanov, 2012). The viral genome consists of 3 main structural genes; *gag*, *pol* and *env*. *Gag* and *env* encode the nucleocapsid proteins and the envelope glycoproteins respectively, while *pol* encodes the reverse transcriptase, integrase and protease enzymes. In addition, the HIV-1 genome contains the accessory and regulatory genes *vif, vpr, vpu, nef, rev* and *tat*, which encode proteins that are involved in the regulation of transcription and infectivity, among other functions (Rubbert *et al.*, 2012).

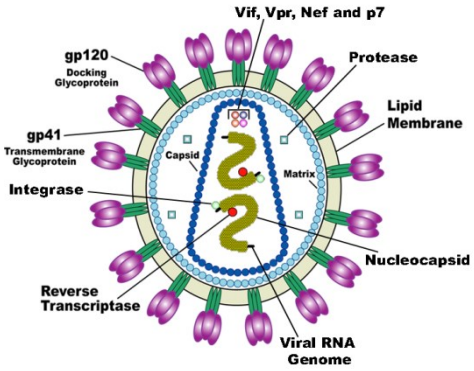

Figure 1.2. HIV-1 Structure (credit NIAID)

1.2.2 HIV Entry & Life Cycle

HIV-1 enters the host cell via binding of the external HIV-1 envelope glycoprotein, gp120, to CD4 receptors on the cell surface (Engelman and Cherepanov, 2012, Simon *et al.*, 2006) (Figure 1.3). $CD4^+$ T lymphocytes, monocytes/macrophages and dendritic cells all express CD4 and have been shown to be susceptible to HIV-1 infection (Dalgleish *et al.*, 1984). Subsequent protein interactions occur between the virus and the chemokine receptors CCR5 or CXCR4, which are therefore referred to as HIV-1 co-receptors (Engelman and Cherepanov, 2012). The co-receptor that HIV-1 uses to enter the host cell determines the cellular tropism of the virus. Most new infections are established by CCR5-tropic founder viruses, which use CCR5 as a co-receptor for cellular entry, whereas CXCR4-tropic viruses generally appear later during infection and have been associated with increased pathogenicity and disease progression (Simon *et al.*, 2006). The interaction between viral gp120 and CD4 expressed on the cell surface causes a conformational change in gp120 that exposes the co-receptor binding site. The binding of gp120 to CCR5 or CXCR4 then activates the viral gp41 (Berger *et al.*, 1999, Simon *et al.*, 2006). HIV-1 gp41 catalyses fusion of the viral envelope with the membrane of the target cell causing the release of the viral capsid into the cytoplasm (Engelman and Cherepanov, 2012, Simon *et al.*, 2006). The viral core disassembles in the cytoplasm, releasing the viral RNA genomes which are reverse transcribed into DNA using the virus's own reverse transcriptase (Simon *et al.*, 2006). The viral reverse transcriptase does not perform 3'-5' exonuclease proof reading activity and the reverse transcription process is therefore error prone, often resulting in viral variants (Simon *et al.*, 2006). Once converted into double-stranded DNA, the viral genome migrates to the nucleus where the viral protein integrase works in conjunction with cellular enzymes to insert it into transcriptionally active regions of the host cell's genome (Simon *et al.*, 2006). Depending on the type of host cell as well as its activation status, the virus can either remain latent or initiate replication. The proviral genome is transcribed into viral messenger RNA (mRNA) and full length RNA viral genomes. Immature viral polyproteins are produced by translation of mRNA by cellular ribosomes. Mature viral proteins are produced after cleavage of the Env and Gag-Pol polyprotein by the viral protease (Simon *et al.*, 2006).

Mature proteins and viral RNA genomes assemble to generate new viral particles (Simon *et al.*, 2006). Viral budding from the host cell takes advantage of vesicular sorting pathways normally involved in endosome egress (Simon *et al.*, 2006). As the viral capsule buds from the host's cell membrane, the newly produced viral particles bear surface proteins of the cells from which they were produced.

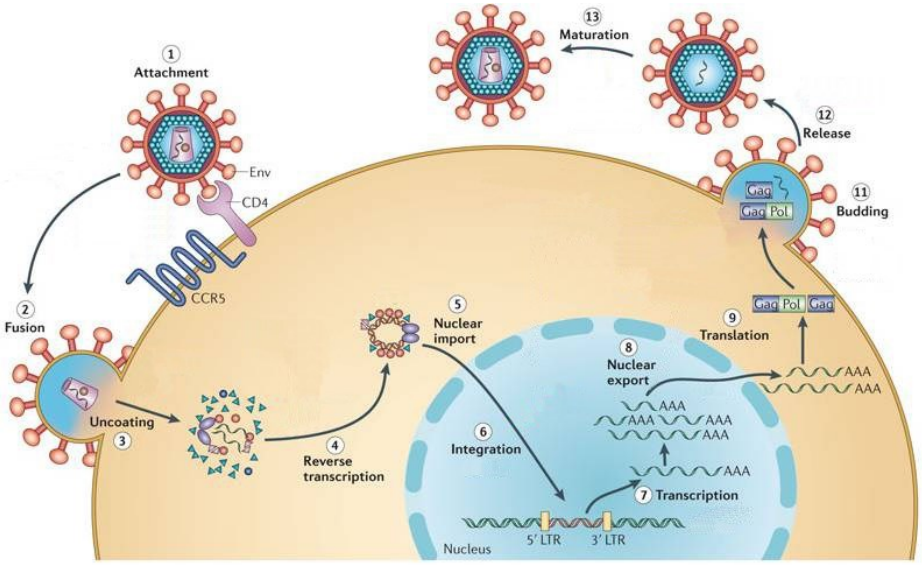

Figure 1.3. HIV-1 life cycle. Adapted from (Engelman and Cherepanov, 2012).

1.2.3 Course of HIV Infection

SIV infection in disease-susceptible non-human primate models, such as rhesus macaques, have afforded a reliable *in vivo* model to closely study the events characteristic of the early stages of HIV-1 infection (Haase, 2010). Within hours of crossing the mucosal barrier, HIV-1/SIV establishes a small founder population of infected cells. Cells of the innate immune system are the first to detect HIV-1 and produce a rapid inflammatory response, including increased secretion of IFN-α, which activates and recruits cells of the adaptive immune system. It is likely that this innate immune response serves to fuel the infection as it recruits further target cells to the site of infection (Li *et al.*, 2009). Recent data has also indicated that HIV-1 founder viruses are resistant to the anti-viral effects of type I IFN, potentially allowing for uncontrolled viral replication during the acute stages of infection (Fenton-May *et al.*, 2013). Within this first week the founder population continues to undergo local expansion

generating sufficient virus and infected cells to disseminate and establish a systemic infection throughout the lymphoid system. Early infection with HIV-1/SIV is characterised by extensive depletion of mucosal $CD4^+$ T cells, which is only partially reflected in the periphery (Veazey *et al.*, 1998). It is of note that the main cell population targeted by HIV-1 is the $CCR5^+$ $CD4^+$ activated T lymphocyte subset (Veazey *et al.*, 2000). The majority of $CD4^+$ T cells reside in lymphoid tissues, in particular within the gastrointestinal tract, and these cells are largely memory $CD4^+$ T cells which co-express CCR5, thus explaining the primary loss of gut $CD4^+$ T cells (Picker and Watkins, 2005, Veazey *et al.*, 2000). By the second week of SIV infection, viraemia levels reach their peak as replication of the virus within the lymphoid tissues is rampant, most likely due to availability of target cells within close proximity (Haase, 2010). In humans however, plasma viral load often peaks after 6 weeks of infection with HIV (Munier and Kelleher, 2007, Pantaleo and Fauci, 1996) (Figure 1.4). The appearance of the adaptive immune response, in particular the virus-specific CTLs, is partially successful in reducing viral replication (Letvin and Walker, 2003). Cells within the infected lymphatic tissues now constitute a reservoir for the virus as the patient enters the chronic phase of infection, which typically lasts for around 10 years if left untreated, during which time a slow decrease in peripheral $CD4^+$ T cell numbers is observed (Levy, 2009). Established HIV-1 infection is initially diagnosed based on the detection of HIV-1-specific antibodies, and the progression of the disease can be monitored by measuring the concentration of $CD4^+$ T cells per µl of blood (CD4 count) and viraemia, measured as viral RNA copies/ml of plasma (Simon *et al.*, 2006). The susceptibility to opportunistic infections increases dramatically when the CD4 count falls below 200 cells/µl of blood, marking the onset of AIDS (Pantaleo and Fauci, 1996).

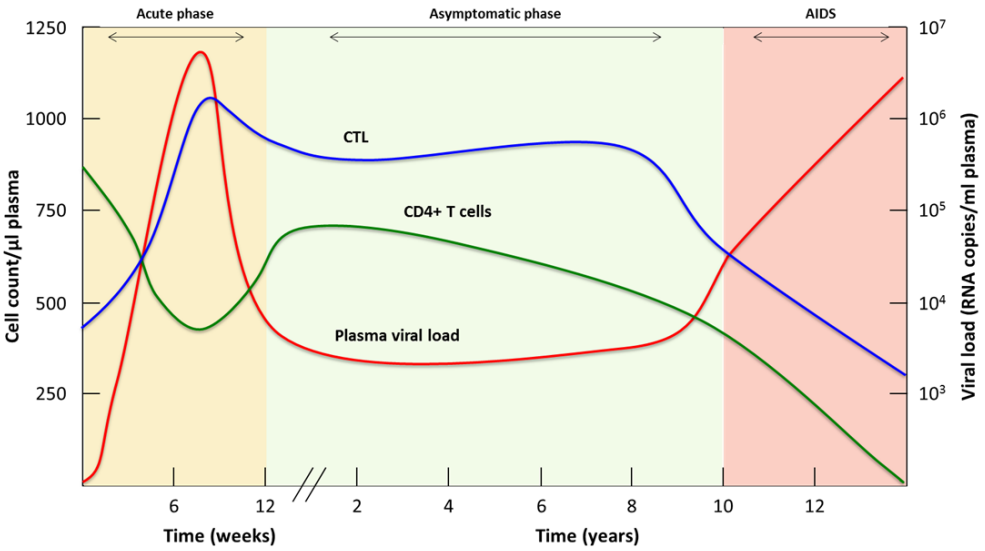

Figure 1.4. Schematic of the course of HIV-1 disease progression. Adapted from (Munier and Kelleher, 2007).

1.3 Immune Dysregulation during Progressive HIV-1 Infection

AIDS was originally identified as a severe weakening of the immune system, exposing the host to a plethora of opportunistic infections. Over the years, and with the better understanding of the immune system itself, several alterations of immune function have been described in HIV-1 infected individuals. A dramatic decline in peripheral $CD4^+$ T helper cells was observed since the first reports of AIDS (Gerstoft *et al.*, 1982, Gottlieb *et al.*, 1981). When HIV was identified as the cause of the disease it was initially thought that this reduction in $CD4^+$ T cells was a result of the direct cytopathic effect of the virus. However, it is now understood that the frequency of infected circulating $CD4^+$ T cells is too low (0.01 – 1%) to completely account for the decline in $CD4^+$ T lymphocytes during chronic infection (Brenchley *et al.*, 2006a). Uninfected T cells from HIV-1^+ patients show an increased rate of apoptosis both *in vivo* in lymph nodes (Finkel *et al.*, 1995) and *in vitro* (Meyaard *et al.*, 1992). It has been proposed that the lower threshold for apoptosis is linked to the cell cycle dysregulation seen in $CD4^+$ and $CD8^+$ T cells from HIV-1 infected patients (Cannavo *et al.*, 2001). T cells from HIV-1^+ patients appear partially activated, but are unable to progress through the cell cycle and this impairment can be corrected by exogenous administration of IL-2 (Paiardini *et al.*, 2001). T cells from HIV-1^+ patients

also display altered production of cytokines in response to activating stimuli. A study by Ullum *et al* (1997) reported increased IFN-γ in HIV-1 infected individuals who have not progressed to AIDS, followed by a decrease in patients who developed AIDS. Furthermore, as a result of HIV-1 infection, IL-2 production and T cell proliferation in response to antigen-specific and mitogen stimulation is progressively impaired (Clerici *et al.*, 1989). T cell responses against HIV-1 antigens are also impaired, likely due to persistent viral replication and chronic stimulation (Appay and Sauce, 2008, Migueles *et al.*, 2009), resulting in increased expression of inhibitory molecules, in particular PD-1, associated with exhaustion of HIV-1-specific $CD8^+$ T cells and disease progression (Day *et al.*, 2006, Trautmann *et al.*, 2006).

Concurrent to the functional impairment of immune responses is a paradoxical state of chronic immune activation, initially described as lymphadenopathy and increased numbers of circulating $CD8^+$ T cells (Gerstoft *et al.*, 1982, Gottlieb *et al.*, 1981). High levels of secreted pro-inflammatory cytokines such as TNF-α, IL-6 and IL-1β are detected in both the serum and from *ex vivo* analysis of monocytes of HIV infected individuals (Weiss *et al.*, 1989, Birx *et al.*, 1990, Kobayashi *et al.*, 1990). Infection with HIV-1 also results in elevated secretion of chemokines such as MIP-1α, MIP-1β and RANTES (Canque *et al.*, 1996, Cotter *et al.*, 2001). Chronic immune activation is also manifested in alterations of the phenotype of immune cells, in particular by increased expression of activation markers, such as CD38 and HLA-DR on T cells of HIV-1 infected patients (Giorgi *et al.*, 1993, Lin *et al.*, 1988). Furthermore CD38 expression on $CD8^+$ T cells represents the best predictor for disease progression, more so than viral load or CD4 count (Giorgi *et al.*, 1999, Liu *et al.*, 1997).

Chronic $CD4^+$ T cell activation may produce a vicious cycle during which HIV-1 replication promotes T cell activation, and immune activation subsequently promotes HIV-1 replication (Appay and Sauce, 2008). Current therapy for HIV-1 infection focuses on inhibiting HIV-1 replication by interfering with different aspects of the viral life cycle, and therefore reducing the viral load of the patient (Engelman

and Cherepanov, 2012). Although this has shown remarkable benefits, abnormalities of the immune function are often still observed despite efficient suppression of viral activity (Cadogan and Dalgleish, 2008).

The mechanisms of HIV-1 induced immunopathogenesis are not fully characterised and they are likely to be multifactorial, however many of the defects observed may be associated with chronic immune activation. The best supporting evidence in favour of the immune activation hypothesis lies perhaps in studies carried out in sooty mangabeys and African green monkeys, the natural hosts for SIV. Sooty mangabeys and African green monkeys do not show signs of pathogenesis nor persistent systemic immune activation despite high levels of viral replication throughout the duration of infection, in contrast to SIV infected disease-susceptible rhesus macaques, in which the infection was introduced experimentally (Hirsch, 2004, Silvestri, 2005). SIV infected sooty mangabeys do not develop AIDS and usually maintain normal CD4 counts. In addition, natural SIV infection is characterized by high viral replication, often with viraemia levels even higher than HIV-1 infected patients (Silvestri *et al.*, 2003). These natural hosts of SIV display low levels of abnormal immune activation, with a lack of lymphadenopathy and minimal levels of activation and proliferation markers on T cells (Hirsch, 2004). Of note, uninfected sooty mangabeys have lower frequencies of $CCR5^+$ $CD4^+$ T cells compared to uninfected rhesus macaques, and after *in vitro* stimulation with mitogens sooty mangabey $CD4^+$ T cells fail to up-regulate CCR5 expression unlike rhesus macaques (Paiardini *et al.*, 2011).

Chronic stimulation of the immune system may lead to its progressive weakening, and thus to the clinical characteristics of immunodeficiency that manifest themselves as disease progresses. In a study by Tesselaar *et al* (2003), persistent activation of the immune system via CD27-CD70 interactions eventually led to immune exhaustion, with loss of the naïve T cell population and vulnerability to opportunistic infections. Persistent activation and subsequent proliferation of cells of the immune

system is known to lead to senescence, apoptosis and overall immune exhaustion (Appay and Sauce, 2008, Effros and Pawelec, 1997).

1.4 Hypotheses for HIV-1 Immunopathogenesis

It is still unclear how HIV-1 infection results in immune dysfunction and chronic immune activation and several non-mutually exclusive mechanisms have been proposed to contribute to HIV-1 pathogenesis.

1.4.1 Preferential Targeting and Loss of $CCR5^+$ $CD4^+$ Mucosal Effector Memory T Cells

Reports of the early depletion of $CCR5^+$ $CD4^+$ mucosal effector memory T cells have led to the hypothesis that the immune system is irreversibly damaged during the early stages of infection, and struggles to recover from the imbalance in T cell populations (Brenchley *et al.*, 2004, Mehandru *et al.*, 2004, Picker and Watkins, 2005). Even when viral replication is suppressed by effective anti-retroviral therapy, the mucosal compartment of $CCR5^+$ $CD4^+$ T lymphocytes is not reconstituted (Mehandru *et al.*, 2004). The loss of a specific T cell sub-population may result in abnormal and accelerated turn-over in the remaining T cell subsets, which eventually provides more target cells for infection. It is thought that this vicious cycle of infection and accelerated T cell turn-over drives chronic immune activation (Cadogan and Dalgleish, 2008).

1.4.2 Gut Microbial Translocation

In physiologic conditions, the physical barrier of the epithelium and the immune components of the intestinal mucosal sites prevent systemic translocation of potentially harmful intestinal flora. Brenchley *et al* (2006a) proposed that the extensive depletion of mucosal $CD4^+$ T cells during the acute phase of infection compromises the integrity of this barrier. They reported that plasma levels of lipopolysaccharide (LPS), a structural component of bacterial walls, and a potent activator of the innate immune system, were increased during HIV-1/SIV infection. Systemic immune activation then

ensues as a result of bacteria and bacterial components infiltrating the blood and activating innate immune cells, resulting in the subsequent activation of both $CD4^+$ and $CD8^+$ T lymphocytes (Brenchley *et al.*, 2006a, Marchetti *et al.*, 2013). Non-pathogenic SIV hosts however show no sign of microbial translocation despite similar levels of mucosal $CD4^+$ T cell depletion during acute infection (Brenchley *et al.*, 2006b). Although, it is noteworthy that the depletion of mucosal $CD4^+$ T cells is transient in African green monkeys, whereas rhesus macaques suffer a permanent loss of mucosal T cells (Pandrea *et al.*, 2007).

1.4.3 Regulatory T Cells and T_H17

Another hypothesis which has been considered to explain the persistent immune activation observed during HIV-1 infection relies on the observed depletion of immunosuppressive Tregs from the blood of HIV-1 infected patients (Eggena *et al.*, 2005, Oswald-Richter *et al.*, 2004). It has been suggested that the loss of immune regulatory cells contributes to uncontrolled immune activation, thus studies have also reported a positive correlation between Treg depletion and the increase in $CD4^+$ T cell activation (Eggena *et al.*, 2005, Oswald-Richter *et al.*, 2004). In addition, long-term non-progressors (LTNP, defined as HIV^+ patients who remain asymptomatic or maintain normal CD4 counts in the absence of treatment) maintain a normal Treg population during chronic infection, which is associated with reduced T cell activation (Chase *et al.*, 2008).

However, a number of studies have reported that the reduction of Treg numbers in the periphery is associated with the accumulation of Tregs in both the gut (Epple *et al.*, 2006) and lymph nodes (Nilsson *et al.*, 2006) of HIV^+ patients. Thus, it is possible that Tregs are not lost during HIV-1 infection, but rather relocate to the lymphoid tissues, where active viral replication and immune activation occur. These findings suggest that an excessive Treg response could lead to an environment in which anti-viral T cell responses are suppressed, therefore allowing HIV to persist, further driving viral replication and immune activation (Cadogan and Dalgleish, 2008).

The loss of T_H17 cells within the gastrointestinal tract of SIV infected rhesus macaques as well as HIV infected patients has been reported (Brenchley *et al.*, 2008, Cecchinato *et al.*, 2008). This reduction in T_H17 cells correlated with viral load in SIV infected macaques (Cecchinato *et al.*, 2008). T_H17 cells are involved in the immune response against commensal bacteria at mucosal surfaces. Thus, the depletion of the T_H17 population of lymphocytes is thought to contribute to microbial translocation. The balance of T_H17 and Treg cells at mucosal surfaces has also been studied. A study conducted by Favre *et al* (2009) found that acute pathogenic SIV infection of macaques resulted in a decline in the T_H17/Treg ratio, due to both the selective depletion of T_H17 cells and an increase in the percentage of Tregs. This was in contrast to the non-pathogenic SIV infection of African green monkeys, in which the T_H17/Treg balance remained stable. Furthermore, the reduction in the T_H17/Treg ratio correlated with systemic immune activation (Favre *et al.*, 2009).

1.4.4 Innate Immune Response

Excessive or chronic stimulation of the innate immune system has been hypothesised to contribute to HIV-1 pathogenesis, in particular the activation of pDCs (Boasso and Shearer, 2008, Miedema *et al.*, 2013). Studies performed in mice have shown that systemic stimulation of pDCs by injection of TLR-7 or TLR-9 agonists induces a phenotype similar to that observed in AIDS patients, with lymphadenopathy and a decrease in circulating T lymphocytes that simultaneously displayed an activated phenotype (Baenziger *et al.*, 2009, Heikenwalder *et al.*, 2004). Administration of CpG-rich oligodeoxynucleotide (ODN) sequences to mice lacking the IFN-α receptor resulted in a significantly milder syndrome, indicating that the immune alterations observed were dependent on type I IFN signalling (Heikenwalder *et al.*, 2004).

The innate immune response is the first line of defence against invading pathogens and is most critical in the first few weeks of infection, before an adaptive response can be established. The loss of $CCR5^+$ T cells, the reduction in T_H17/Treg and the subsequent loss of mucosal integrity leading to microbial translocation, all occur during acute infection. Thus, early events are critical in determining disease

outcome. In support of this, increasing evidence shows that inhibition of viral activity by administration of anti-retroviral treatment during early infection preserves immune function and favours long term disease control (Berrey *et al.*, 2001, Fidler *et al.*, 2013, Hecht *et al.*, 2006, Jain *et al.*, 2013, Le *et al.*, 2013). Moreover, the stabilised plasma viral load reached soon after acute infection, known as the viral set point, has been shown to be predictive of disease outcome (Lyles *et al.*, 2000). This thesis will focus on the hypothesis that pDC activation, one of the earliest events occurring during the innate response against viral pathogens, contributes to immunopathogenesis during HIV-1 infection.

1.5 Dendritic Cells & HIV-1

1.5.1 Viral Entry

Both pDCs and mDCs express the HIV-1 receptor CD4 and the co-receptors CXCR4/CCR5, and are receptive to HIV-1 infection (Donaghy *et al.*, 2003, Patterson *et al.*, 2001). In comparison to T cells, DCs are less susceptible to productive infection, however they can fuel the infection by transferring HIV-1 to T cells, a process known as transinfection (Manches *et al.*, 2013). Activation of human pDCs by HIV-1 requires gp120 ligation to CD4 and subsequent endocytosis of the virion (Beignon *et al.*, 2005), however, productive infection is not required for the activation of DCs (O'Brien *et al.*, 2011). The integrity of the endocytotic pathway, including endosome acidification, is required to expose the viral RNA to TLR-7 (Beignon *et al.*, 2005). Interestingly, while TLR-7 is constitutively expressed by pDCs, it is elevated in HIV-1^+ patients compared with healthy controls, possibly as a consequence of chronic pDC stimulation (Hardy *et al.*, 2007). Conversely, immature mDCs are not directly activated by HIV-1, even though they express TLR-7. Rather, secreted products from HIV-1-activated pDCs, such as type I IFN or TNF-α can induce bystander maturation of mDCs (Fonteneau *et al.*, 2004).

1.5.2 Plasmacytoid DC Activation during HIV-1 Infection

Several studies have reported that the frequencies of both blood DC subsets (mDCs and pDCs) are significantly decreased in the periphery during HIV-1 infection, which often correlates with high plasma viral load, and reduced $CD4^+$ T cell counts (Barron *et al.*, 2003, Donaghy *et al.*, 2003, Sabado *et al.*, 2010). In the specific case of pDCs, the decreased frequencies observed in HIV-1 infected patients are thought to be a result of activation and migration to lymphoid tissues, rather than depletion due to the direct cytopathic effect of HIV-1 or apoptosis. A study conducted by Hardy *et al* (2007) found that exposure to HIV-1 favoured pDC survival *in vitro* rather than contributing to cell death. Following TLR-mediated activation *in vitro*, pDCs have been shown to acquire chemotactic abilities. Thus, CCR7 is up-regulated on pDCs upon exposure to HIV-1, and $CCR7^+$ pDCs are receptive to chemoattraction by CCL19, the ligand for CCR7 which is secreted in lymphoid tissues (Fonteneau *et al.*, 2004). Furthermore, expression of the gut homing integrin α4β7 is up-regulated on pDCs during both SIV and HIV-1 infection, and correlates with pDC migration to the gastrointestinal tract in pathogenic SIV infection of rhesus macaques (Kwa *et al.*, 2011). In chronically HIV infected ART naïve patients, circulating pDCs were found to express high levels of the gut homing integrin CD103 (also known as integrin αE) (Lehmann *et al.*, 2014). In addition, the authors reported an increased frequency of pDCs in the gut-associated lymphoid tissue (GALT), which correlated with high serum concentrations of IFN-α (Lehmann *et al.*, 2014). Increased pDC numbers in the lymph nodes of SIV infected macaques (Malleret *et al.*, 2008), as well as high IFN-α levels in the tonsils of HIV-1 infected patients have also been reported (Herbeuval *et al.*, 2006). However, a study conducted in rhesus macaques infected by intravenous injection of SIV reported that both cell migration to the lymph nodes as well as cell death are likely to contribute to the loss of pDCs (Brown *et al.*, 2009). It is therefore possible that the continual activation of pDCs both recruits them to lymph nodes as well as increases cell turnover.

High plasma concentrations of IFN-α during both acute and chronic infection are associated with disease progression (von Sydow *et al.*, 1991). *Ex vivo* analysis of DCs from chronic $HIV\text{-}1^+$ patients has

shown that both pDCs and mDCs become impaired in their ability to stimulate allogeneic T cell proliferation (Donaghy *et al.*, 2003). However, stimulation of PBMCs from chronic HIV-1^+ patients with TLR-7 agonists induced similar up-regulation of CD86 on pDCs, although expression of CD83 and secretion of IFN-α was significantly reduced compared to healthy controls (Martinson *et al.*, 2007). Sabado *et al* (2010) investigated DC dysregulation during acute HIV-1 infection, and reported that both pDCs and mDCs from HIV-1^+ patients were able to stimulate allogeneic T cell proliferation to a similar degree as observed in uninfected controls. Similar to work by Martinson *et al* (2007), DCs from acute HIV^+ patients preserved the ability to up-regulate co-stimulatory molecules in response to TLR-7/-8 agonists (Sabado *et al.*, 2010). The authors also measured IFN-α secretion from purified pDCs stimulated with either replication deficient HIV-1 or synthetic TLR-7/-8 agonist and found pDCs from acute HIV-1^+ individuals produced significantly higher concentrations of IFN-α compared to controls (Sabado *et al.*, 2010).

In response to activating stimuli, pDCs are reported to become refractory, thus limiting further type I IFN secretion. However, O'Brien *et al* (2011) found that, dissimilar to viruses such as influenza, pDCs do not become refractory after HIV-1 stimulation, which may account for ongoing IFN-α production during HIV-1 infection.

Plasmacytoid DCs have been identified as a major source of IDO following HIV-1 stimulation *in vitro* (Boasso *et al.*, 2007). Increased IDO activity has been reported in HIV-1 infected patients and is also associated with disease progression (Boasso *et al.*, 2007, Fuchs *et al.*, 1991, Huengsberg *et al.*, 1998, Nilsson *et al.*, 2006). Engagement of CTLA-4 is known to activate IDO (Boasso *et al.*, 2005, Grohmann *et al.*, 2002, Munn *et al.*, 2004b) and it is noteworthy that HIV-1 is approximately 10-fold more potent than CTLA-4 in inducing IDO mRNA expression in PBMCs *in vitro* (Boasso *et al.*, 2007). Plasma concentrations of type I IFN have been shown to correlate with IDO activity (Malleret *et al.*, 2008). However, while type I and II IFN are able to induce IDO, these soluble mediators are not strictly

necessary for IDO expression in pDCs in the context of HIV-1 stimulation, which may directly promote IDO expression via TLR-mediated pDC activation (Boasso *et al.*, 2007).

1.6 Plasmacytoid DCs and Immunopathogenesis

By secreting IFN-α as well as expressing IDO, pDCs may contribute to both immune activation and immunosuppression, which characterise HIV-1 immunopathogenesis.

1.6.1 Recruitment of Target Cells

Studies performed in SIV infected rhesus macaques have shown that pDCs are one of the first cell types to be recruited to the site of infection (Li *et al.*, 2009). Accumulation of pDCs beneath the mucosal layer was described at one day post infection. In addition to secreting IFN-α, activated pDCs produce high amounts of the chemokines MIP-1α and MIP-1β which serve to attract $CCR5^+$ $CD4^+$ T cells (Li *et al.*, 2009). Plasmacytoid DCs are therefore involved in the initial recruitment of $CD4^+$ T lymphocytes to the site of infection and are implicated in fuelling the infection by providing further target cells, as well as indirectly contributing to the loss of mucosal $CCR5^+$ T lymphocytes.

1.6.2 Apoptosis & Exhaustion

Type I IFN plays a critical role in dampening viral replication and aiding the priming of adaptive immune responses. However, excessive production of type I IFN can be detrimental, increasing the expression of apoptotic and immunosuppressive ligands, thus resulting in suppression of T cell responses by reducing their survival and proliferative capacity. TNF-related apoptosis-inducing ligand (TRAIL) is a member of the TNF-superfamily, which induces apoptosis of cells expressing either of the functional death receptors, DR4 and DR5 (Herbeuval *et al.*, 2005c). The TRAIL/DR5 pathway contributes to the apoptosis of uninfected $CD4^+$ T cells during HIV-1 infection and elevated levels of $CD4^+$ T cells expressing both TRAIL and DR5 are found in the blood of HIV-1 infected patients (Herbeuval *et al.*, 2005b). Furthermore, plasma levels of the soluble functional form of TRAIL directly

correlate with viral load in HIV-1 infected individuals (Herbeuval *et al.*, 2005a). Expression of TRAIL on monocytes and pDCs is known to be induced by IFN-α (Griffith *et al.*, 1999, Hardy *et al.*, 2007). Moreover, $CD4^+$ T cells undergo apoptosis via a TRAIL-DR5 dependent mechanism upon exposure to HIV-1 *in vitro,* which is inhibited by anti-type I IFN antibodies (Herbeuval *et al.*, 2005b). Other members of the TNF receptor family, Fas and its ligand, FasL, are also involved in apoptosis. The expression of Fas and FasL is increased in the lymph nodes of HIV-1 infected patients (Herbeuval *et al.*, 2006), furthermore, $CD4^+$ and $CD8^+$ T cells from HIV-1^+ patients undergo Fas/FasL induced apoptosis *ex vivo* (Fraietta *et al.*, 2013). Similar to TRAIL, HIV-1-induced apoptosis mediated by Fas/FasL is induced by type I IFN and TLR-7/9 ligation (Fraietta *et al.*, 2013).

The PD-1/PD-L1 pathway is another signalling system that has been proposed to suppress efficient T cell responses against chronic viral infections, including HIV-1 (Boasso *et al.*, 2008b, Maier *et al.*, 2007, Yao and Chen, 2006). The binding of PD-L1 to PD-1 exerts a negative co-stimulatory signal to T cells, thus reducing proliferation, cytokine production and cytolytic activity. HIV-1-specific T cells have been reported to express high levels of PD-1 (Trautmann *et al.*, 2006). Increased expression of PD-L1 on monocytes, B cells and $CCR5^+$ T cells has also been reported in both HIV-1^+ individuals as well as after healthy PBMCs were exposed to HIV-1 *in vitro* (Boasso *et al.*, 2008b, Trabattoni *et al.*, 2003). Furthermore, PBMC stimulation with either IFN-α or TLR-7/9 agonists resulted in similar PD-L1 up-regulation (Boasso *et al.*, 2008b). The selective up-regulation of PD-L1 in the $CCR5^+$ T cell subset was found to be due to the restricted expression of subunit 2 of the IFN-α receptor complex (IFNAR2) to $CCR5^+$ T cells (Boasso *et al.*, 2008b). $CCR5^+$ $CD4^+$ T lymphocytes are rapidly depleted during the early phases of HIV-1 infection, and their responsiveness to type I IFN signalling may account for the enhanced susceptibility to IFN-α-induced apoptosis (Boasso *et al.*, 2008b).

1.6.3 T Cell Activation

In addition to contributing to the immune impairment seen during HIV-1 infection, some studies have also linked pDC activation with chronic T cell activation. Boasso *et al* (2008a) showed that *in vitro*

treatment with IFN-α induces phenotypic activation of T cells, demonstrated by an increase in CD38 and CD69 cell surface expression, and that addition of blocking antibodies against IFNAR2 largely diminished HIV-1-induced CD38 and CD69 expression on $CD4^+$ and $CD8^+$ T cells. Similarly, Rodriguez *et al* (2006) found that IFN-α induced CD38 expression on $CD8^+$ T cells from HIV-1 infected individuals.

A longitudinal study examining pDCs in the blood and gut mucosa of HIV-1 infected individuals found an increased frequency of pDCs in the gut compared to HIV negative controls (Lehmann *et al.*, 2014). The authors reported a positive correlation between the percentage of pDCs in the GALT, IFN-α expression and the frequency of HLA-DR^+ $CD38^+$ $CD8^+$ T lymphocytes (Lehmann *et al.*, 2014). Furthermore, Brenchley *et al* (2006b) observed a positive correlation between plasma IFN-α and LPS concentrations. Together these data suggest that the excessive production of IFN-α from pDCs in the gut may contribute to the loss of integrity of the mucosal barrier and microbial translocation, which subsequently leads to systemic immune activation (Lehmann *et al.*, 2014).

1.6.4 T_H17 & Treg Cells

Although IFN-α may suppress Treg activity by down-regulating the production of the survival cytokine IL-2 (Golding *et al.*, 2010), several studies have documented a role for pDCs in the induction of $CD4^+$ or $CD8^+$ Tregs, both *in vivo* and *in vitro* (Gilliet and Liu, 2002, Moseman *et al.*, 2004, Ochando *et al.*, 2006). HIV-1-activated pDCs can induce the differentiation of Tregs from naïve $CD4^+$ T cells in a TLR-7-, IDO-dependent mechanism (Manches *et al.*, 2008). In addition, several studies have described the accumulation of Tregs in lymphoid tissues where IDO is over expressed during HIV-1 or SIV infection (Andersson *et al.*, 2005, Estes *et al.*, 2006, Nilsson *et al.*, 2006). Similarly, pDC-mediated IDO activity modulates the balance between T_H17 and Treg differentiation. Treatment of PBMCs from healthy donors with tryptophan catabolites resulted in reduced frequencies of IL-17A producing cells (Favre *et al.*, 2010). Furthermore, the expression of IDO1 mRNA in mucosal biopsies from HIV^+ individuals was inversely related to the T_H17/Treg ratio (Favre *et al.*, 2010). The T_H17/Treg balance at mucosal surfaces has also been documented to be critical in maintaining the integrity of the mucosal barrier, and a

decrease in this ratio correlates with microbial translocation and increased immune activation (Favre *et al.*, 2009, Favre *et al.*, 2010, Jenabian *et al.*, 2013). A study conducted in non-human primates found a disturbance in the T_H17/Treg ratio in SIV infected macaques who progress to AIDS, while this balance was maintained in non-pathogenic SIV infection of African green monkeys (Favre *et al.*, 2009). It is therefore conceivable that pDC activation could directly contribute to attenuated mucosal immunity thus leading to microbial translocation.

1.6.5 Non-Human Primate Models: Pathogenic versus Natural Hosts

Studies performed in non-human primate models have also implicated the innate immune response, in particular pDCs, in SIV immunopathogenesis. Comparisons between pathogenic SIV infection of rhesus macaques with non-pathogenic natural hosts of SIV, sooty mangabeys and African green monkeys, have highlighted substantial differences in the innate response. In particular, both sooty mangabeys and African green monkeys mount robust IFN-driven responses, epitomised by elevated expression of IFN-stimulated genes (ISGs), during the acute phase of infection. However, when transition to the chronic phase occurs, both species exhibit a contraction of IFN responses, despite consistently high levels of peripheral viraemia. In contrast, SIV infected rhesus macaques maintain high levels of ISG expression beyond the acute and through to the chronic phase of infection, and eventually progress to symptomatic disease (Bosinger *et al.*, 2009, Harris *et al.*, 2010, Jacquelin *et al.*, 2009).

1.6.6 Modulation of pDC Activation *in Vivo*

Studies on animal models and clinical trials have been undertaken in order to determine if inhibiting pDC activation or type I IFN secretion during SIV/HIV-1 infection would improve disease outcome, however the results are inconsistent. In clinical trials conducted in the late 1990's, HIV-1 infected individuals were vaccinated with recombinant IFN-α2b with the aim of eliciting antibodies against IFN-α2b, and thereby blocking the effects of an over production of IFN-α. These studies found a correlation between AIDS-related clinical manifestations and high titres of circulating IFN-α. The

authors reported low immunogenicity of the vaccine, however, a more favourable disease prognosis was seen in patients who responded compared to patients receiving placebo (Gringeri *et al.*, 1999, Gringeri *et al.*, 1996). Chloroquine and hydroxychloroquine have also been studied as immunotherapeutic approaches for HIV infection. Chloroquine interferes with the process of endosomal acidification, which is necessary for TLR-7/9 activation (Rutz *et al.*, 2004). *In vitro,* the addition of chloroquine to HIV-1-stimulated PBMCs inhibits IFN-α secretion by pDCs (Beignon *et al.*, 2005, Martinson *et al.*, 2009, Royle *et al.*, 2013). HIV-1 infected ART naïve patients treated for 2 months with chloroquine displayed a reduction in T cell activation, measured as the frequency of $CD38^+$ HLA-DR^+ T cells (Murray *et al.*, 2010). Furthermore, the administration of hydroxychloroquine for 6 months to HIV^+ patients receiving ART resulted in increased peripheral $CD4^+$ T lymphocyte numbers, decreased frequencies of activated T cells measured by Ki67 expression, increased Tregs and reduced inflammatory cytokine production (Piconi *et al.*, 2011). However, a more recent study in which HIV^+ ART naïve patients were treated with hydroxychloroquine for 48 weeks, found no reduction in $CD8^+$ T cell activation, an increase in viral replication and a reduction in $CD4^+$ T cell numbers compared to placebo (Paton *et al.*, 2012). A similar outcome was observed in SIV-infected rhesus macaques treated with chloroquine during acute infection, with treated animals displaying higher viral loads and a trend towards increased T cell activation (Vaccari *et al.*, 2013). A study conducted in rhesus macaques infected intravenously with SIV and simultaneously treated with TLR-7/9 blockers found no reduction in the frequencies of activated memory T cell subsets or viral load compared to untreated SIV infected animals (Kader *et al.*, 2013).

Thus, it is still unclear whether inhibiting IFN-α responses during HIV-1 infection is beneficial or not to disease outcome.

1.7 HIV-2

In 1986, HIV-2 was identified as another retrovirus causing AIDS in West Africa (Clavel *et al.*, 1986). Compared to HIV-1, HIV-2 has a limited worldwide distribution, being endemic to West Africa (Campbell-Yesufu and Gandhi, 2011). Different from HIV-1, which originated from the chimpanzee retrovirus SIV_{CPZ}, HIV-2 derived from the sooty mangabey virus SIV_{SM} (Hahn *et al.*, 2000). HIV-2 shares approximately 60% identity with HIV-1 at the amino acid level for Gag and Pol, and only 30-40% homology in the regions coding for Env (Guyader *et al.*, 1987). The main HIV-2 capsid protein is p26 and the main envelope-associated glycoproteins are gp125 and gp36, which exert similar functions as HIV-1 p24, gp120 and gp41, respectively (Cavaleiro *et al.*, 2009a, Reeves and Doms, 2002). The HIV-2 genome also contains accessory and regulatory genes similar to HIV-1, with the exception of the accessory gene *vpx*, in place of *vpu* (Reeves and Doms, 2002). Several distinct HIV-2 groups have been described, of which only A and B have led to continued transmission in humans (de Silva *et al.*, 2008, Nyamweya *et al.*, 2013).

HIV-1 and HIV-2 isolates are reported to have similar levels of replicative efficiency *in vitro* (Schramm *et al.*, 2000), although *in vivo* replication rates for HIV-2 are significantly lower (Popper *et al.*, 2000). Similar to HIV-1, HIV-2 infects $CD4^+$ T cells by binding to the CD4 receptor via the envelope glycoprotein, gp125, although some degree of CD4-independence has been reported for HIV-2 (Reeves and Doms, 2002). While HIV-1 mainly utilises the co-receptors CCR5 and CXCR4 to gain entry to cells, HIV-2 is more promiscuous and can infect target cells using a wider range of co-receptors (McKnight *et al.*, 1998). However, HIV-2 is less pathogenic than HIV-1 and individuals infected with HIV-2 display a slower rate of disease progression compared to those infected with HIV-1 (Marlink *et al.*, 1994). HIV-2 infected patients often remain asymptomatic with mortality rates more common among older age groups (de Silva *et al.*, 2008). The largely geographical confinement of the virus to West Africa is thought to correlate with its low transmission rates (Campbell-Yesufu and Gandhi, 2011, de Silva *et al.*, 2008), and epidemiological data suggests that HIV-2 infection rates are declining (Nyamweya *et al.*,

2013). However, upon progression to AIDS, clinical manifestations in HIV-2^+ patients are indistinguishable from HIV-1 infection (Martinez-Steele *et al.*, 2007).

HIV-2 infection is associated with lower plasma viral RNA levels compared to HIV-1 (Popper *et al.*, 1999), and the majority of asymptomatic HIV-2^+ patients maintain an undetectable viral load (Popper *et al.*, 2000). The lower viraemia alone is unlikely to account for the reduced pathogenicity of HIV-2 as HIV-2 viral loads remain low even during advanced disease stage (Andersson *et al.*, 2000). In a study examining mortality rates, patients with plasma viral loads of less than 10,000 RNA copies/ml infected with HIV-1 had significantly higher rates of mortality compared to HIV-2^+ patients with similar viraemia. Whereas, at higher viral loads, mortality was similar between the two infections (Hansmann *et al.*, 2005). Interestingly, proviral DNA levels are comparable between HIV-1^+ and HIV-2^+ patients, suggesting that the slower progression of HIV-2 disease may not be due to a quantitative difference in the rate of infection (Cavaleiro *et al.*, 2013, Popper *et al.*, 2000). HIV-2 infection has also been associated with greater $CD4^+$ T cell counts throughout infection. Thus, even at the onset of disease, HIV-2^+ patients tend to display higher $CD4^+$ T cell numbers compared to HIV-1 (Martinez-Steele *et al.*, 2007).

1.7.1 Immune Activation during HIV-2 Infection

Reports have shown reduced immune activation after HIV-2 infection when compared to HIV-1. PBMCs from healthy donors show lower rates of apoptosis after *in vitro* infection with HIV-2 than that observed with HIV-1 (Machuca *et al.*, 2004), and HLA-DR expression on T cells is greatly reduced in HIV-2^+ compared to HIV-1^+ patients (Michel *et al.*, 2000). A study by Sousa *et al* (2002) suggested that immune activation, rather than viral load, is linked to $CD4^+$ T cell depletion in both HIV-1 and HIV-2 infection. Thus, when HIV-1^+ and HIV-2^+ patients with similar levels of $CD4^+$ T cell loss were compared, they also showed similar increases in the proportion of activated T cells, despite the lower viral loads in HIV-2^+ patients (Sousa *et al.*, 2002).

The slow rate of $CD4^+$ T cell decline and the low to undetectable viral loads in the majority of HIV-2 infected patients are consistent with the hypothesis that HIV-2 infection is controlled by a more efficient cellular immune response compared to HIV-1. Many studies have focused on the adaptive immune response to HIV-2, however the literature shows conflicting results. When comparing asymptomatic HIV-1 and HIV-2 infected patients, some reports showed no differences in the frequency of HIV-specific T cells or the magnitude of responses against Gag peptides (Foxall *et al.*, 2008, Jaye *et al.*, 2004, Ondondo *et al.*, 2008, Zheng *et al.*, 2004). However, other reports show enhanced HIV-specific memory $CD4^+$ T cell responses in asymptomatic HIV-2^+ compared to HIV-1^+ patients. In particular, $CD4^+$ T cells from HIV-2^+ patients show an earlier differentiated phenotype, as measured by the lack of CD57 expression, and preserve their proliferative capacity (Duvall *et al.*, 2006). In contrast to HIV-1, T cells from HIV-2^+ individuals preserve the ability to secrete IL-2 (Sousa *et al.*, 2001) and display an increased frequency of polyfunctional $CD4^+$ and $CD8^+$ T cells (Duvall *et al.*, 2008). Furthermore, *ex vivo* analysis from HIV-2 infected patients showed that the frequency of $CD4^+$ T cells producing IL-2 and IFN-γ in response to stimulation with HIV-2 Gag peptides is similar to that observed following stimulation with cytomegalovirus (CMV) peptides (Alatrakchi *et al.*, 2006). This is in contrast to HIV-1^+ individuals in whom HIV-specific T cell responses are often diminished in comparison to CMV (Komanduri *et al.*, 2001, Papagno *et al.*, 2002, Pitcher *et al.*, 1999). Other studies have compared HIV-2 progressors, patients with plasma viral loads greater than 100 copies/ml, to HIV-2 controllers, defined as asymptomatic patients with viral loads of less than 100 copies/ml of plasma. In these patients Leligdowicz *et al* (2007) observed an association between the magnitude of HIV-2 Gag-specific T cell responses and undetectable viral loads. This correlation was later found to be largely due to a highly restricted breadth in the $CD8^+$ T cell response directed against Gag (de Silva *et al.*, 2013). In particular the authors reported that the bulk of the $CD8^+$ T cell response was accounted for by cells targeting one immunodominant peptide (de Silva *et al.*, 2013). Furthermore, $CD8^+$ T cell polyfunctionality is associated with viral control, similar to what has been observed in HIV-1

controllers (de Silva *et al.*, 2013). However, it is unclear whether an enhanced cellular immune response is the cause or consequence of low levels of circulating virus.

The study of HIV-2 provides a unique tool to explore which aspects of virus-host interaction may contribute to immunopathogenesis and therefore disease outcome.

1.7.2 HIV-2 & Dendritic Cells

A study by Duvall *et al* (2007) demonstrated that both primary mDCs and pDCs are poorly susceptible to HIV-2 infection *in vitro* and that, in contrast to HIV-1, mDCs exposed to HIV-2 do not transfer virus to autologous $CD4^+$ T cells. Furthermore, while HIV-1 Env proteins are known to promote DC activation (Fonteneau *et al.*, 2004), HIV-2 Env has no effects on DC differentiation or maturation *in vitro*, defined as expression of HLA-DR and co-stimulatory molecules (Cavaleiro *et al.*, 2009a). In a similar manner, exposure to HIV-2 does not cause significant alterations in PD-L1 expression on DCs (Cavaleiro *et al.*, 2009a), whereas HIV-1 induces increased PD-L1 expression in DCs, monocytes and $CCR5^+$ T cells (Boasso *et al.*, 2008b, Meier *et al.*, 2008).

HIV-1 and HIV-2 infected individuals, stratified according to $CD4^+$ T cell frequency, exhibited similar reductions in circulating mDCs and pDCs compared to healthy controls (Cavaleiro *et al.*, 2009b, Cavaleiro *et al.*, 2013). The extent of the reductions in DC numbers directly correlated with the degree of $CD4^+$ T cell depletion and T cell activation in both infections, despite the lower viraemia observed in HIV-2^+ patients (Cavaleiro *et al.*, 2009b, Cavaleiro *et al.*, 2013). In addition, CD86 and PD-L1 expression were similarly up-regulated on pDCs and mDCs in both HIV-1 and HIV-2 cohorts at comparable disease stages (Cavaleiro *et al.*, 2009b, Cavaleiro *et al.*, 2013). In contrast to pDCs from HIV-1^+ patients, pDCs from HIV-2^+ patients preserve the ability to secrete high amounts of IFN-α upon TLR-9 ligation with CpG type-A (CpG-A) ODN, which is inversely correlated with viral load (Cavaleiro *et al.*, 2009b). However, expression of the *MxA* gene, an ISG which is a reliable marker of IFN-α production *in vivo*, is significantly higher in PBMCs from HIV-1 compared to HIV-2 infected patients (Cavaleiro *et al.*, 2009b).

These findings suggest that pDCs are not chronically stimulated *in vivo* during HIV-2 infection, and are therefore not refractory to further *in vitro* stimulation.

Taken together, these *in vitro* and *ex vivo* data support the hypothesis that excessive type I IFN secretion occurs during HIV-1 but not HIV-2 infection.

1.8 Hypothesis & Aims

The overall hypothesis of this thesis is that the activation of pDCs is an important factor in determining the outcome of HIV disease. Plasmacytoid DC activation by HIV-1 has been well studied. However, HIV-2 infection in humans represents a significantly less pathogenic disease compared to HIV-1, and the relative ability of HIV-2 to induce pDC activation has not previously been reported.

Due to the dramatic differences in disease outcome of HIV-1 and HIV-2 infection, I hypothesise that *in vitro* activation of pDCs by HIV-1 will significantly differ from that induced by HIV-2.

Specifically this work aims to investigate:

- The secretion of type I IFN (Chapter 3)
- Inflammatory pathways potentially regulating the type I IFN response (Chapter 4)
- The phenotypic maturation of APCs (Chapter 5)

Chapter 2 Materials and Methods

2.1 Viral Isolates

For the majority of the experiments described in this study I have used two viruses, HIV-1_{MN} and HIV-2_{NIH-Z}. HIV-1_{MN} is a lab-adapted CXCR4 tropic virus, and was grown in an H9 CL.4 T cell line (NIH AIDS Research & Reference Reagent Program, Bethesda, MD, USA). HIV-2_{NIH-Z} is also a lab-adapted virus originally isolated from a symptomatic patient and grown in an HuT 78 T cell line (Advanced Biotechnologies, Columbia, MD, USA). Unless otherwise specified these are referred to as HIV-1 and HIV-2 respectively. In some experiments described in Chapter 3 I have also used other HIV-1 and HIV-2 isolates; a full list of all viral isolates used in this study is shown in Table 2.1. All HIV-1 isolates used are classified as clade B and both HIV-2 isolates are classified as sub-type A.

Table 2.1. List of HIV-1 and HIV-2 isolates

Virus	Strain	Aldrithiol-2 treatment	Cell line used for propagation	Source
HIV-1	MN	No	H9 CL.4	NIH AIDS Research & Reference Reagent Program
HIV-1	MN	Yes	H9 CL.4	NIH AIDS Research & Reference Reagent Program
HIV-1	MN	No	CL.4/CEMx174	NIH AIDS Research & Reference Reagent Program
HIV-1	MN	Yes	CL.4/CEMx174	NIH AIDS Research & Reference Reagent Program
HIV-1	Ada	Yes	SupT1-CCR5 CL.30	NIH AIDS Research & Reference Reagent Program
HIV-1	IIIB	No	H9	Advanced Biotechnologies
HIV-2	NIH-Z	No	HuT 78	Advanced Biotechnologies
HIV-2	ST	No	CEMx174	NIH AIDS Research & Reference Reagent Program

2.2 Viral RNA Quantification

Viral isolates were normalised based on RNA content to ensure that during cell culture experiments DCs were exposed to the same amount of TLR ligand (viral RNA) across all viruses used.

2.2.1 RNA Extraction

RNA from purified viral samples was extracted using the QIAamp UltraSens Virus kit (QIAGEN, Manchester, UK), which utilises spin columns containing a QIAamp membrane that selectively binds nucleic acids. All samples were centrifuged in a Micro Centaur (MSE, London, UK).

Viral samples were prepared by diluting the virus in 600 µl PBS (PAA Laboratories, Pasching, Austria) in a 1.5 ml tube, which was vortexed and briefly centrifuged to ensure there was no residual liquid in the lid. Subsequently, the viral sample was lysed and the nucleic acids precipitated by the addition of 800 µl of AC buffer. Lysed samples were mixed thoroughly by vortexing and incubated at room temperature for 10 minutes. The viral lysates were centrifuged at 10,000 rotations per minute (rpm) for 3 minutes, the supernatants were discarded leaving the pellets containing nucleic acid complexes. In order to digest residual proteins, 300 µl of AR buffer, pre-warmed to 60°C in a water bath, and 20 µl proteinase K solution were added to each tube and mixed thoroughly by vortexing. Samples were incubated at 40°C for 10 minutes in a heated plate and vortexed at 5 minute intervals. Tubes were briefly centrifuged before the addition of 300 µl of AB buffer. This procedure yielded a volume of approximately 600 µl of RNA complexes in suspension, which was transferred to a spin column and centrifuged at 4000 rpm for 1 minute in order to bind the nucleic acids to the membrane. The spin column was transferred to a new collection tube and the old one containing filtrate discarded. The membrane was then washed by adding 500 µl of AW1 buffer to the spin column and centrifuged at 5000 rpm for 1 minute. Again the spin column was transferred to a new collection tube, and the old one discarded. A second wash step was performed, by adding 500 µl of AW2 buffer to the spin column and centrifuged at 13,000 rpm for 3 minutes. The spin column was then transferred to a new 1.5 ml tube and 30 µl of AVE buffer added directly onto the membrane of the column. The sample was centrifuged at 5000 rpm for 1 minute to elute the RNA. In order to maximise RNA recovery, an additional 30 µl of AVE was added to the membrane and again centrifuged at 5000 rpm for 1 minute.

The quantity of RNA extracted was checked by measuring the optical density (OD) of the preparation at 260 nm using the NanoDrop 1000 (Thermo Scientific, Leicester, UK). RNA concentration was calculated using the following equation:

RNA Concentration (µg/ml) = (OD 260 nm) x (40 µg RNA/ml)

In addition, the NanoDrop also measures the OD of the RNA preparation at 280 nm and the ratio between the OD 260 nm and OD 280 nm was used to ascertain the purity of the RNA. The optimal 260 nm/280 nm ratio ranges between 1.7 – 2.0. Values lower than 2 can be indicative of protein contamination, whilst ratios higher than 2 can be a result of ethanol in the preparation.

An optimal volume of virus to use for the RNA extraction was determined. Viral RNA was extracted from a range of volumes of purified virus and the concentration of RNA recovered was measured using the NanoDrop. The resulting concentrations of RNA were plotted against the volume of virus added to the extraction column to determine the correlation between volume of virus suspension and RNA yield. The optimal volume of virus to use for RNA extraction was chosen within the region in which the correlation followed a linear trend (example shown in Figure 2.1).

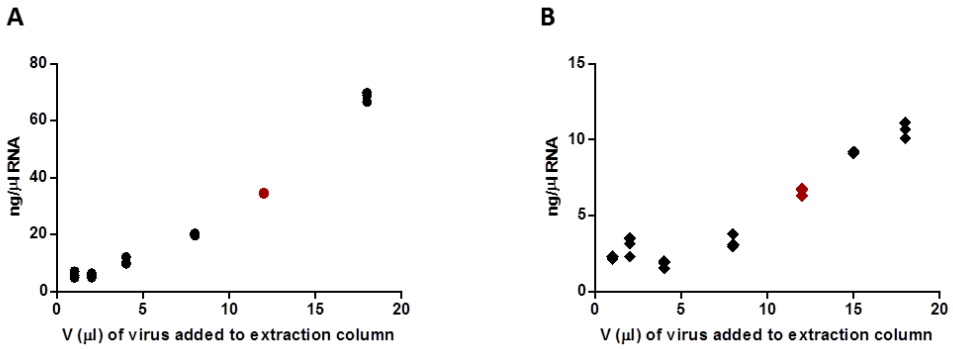

Figure 2.1. Example of RNA extraction optimisation. Dot plots representing the concentration of eluted RNA (y-axes) versus the volume of virus preparation added to the extraction columns (x-axes) for HIV-1_{MN} (A) and HIV-2_{NIH-Z} (B). The volume chosen for subsequent RNA extraction was 12 µl (shown in red).

2.2.2 RT-qPCR

2.2.2.1 Reverse Transcription

Reverse transcription of RNA was carried out using the SuperScript III First-Strand Synthesis SuperMix kit (Invitrogen, Paisley, UK).

To a 0.2 µl thin walled PCR tube, the following reagents were added: 4 µl RNA, 1 µl random hexamers (50 ng/µl), 1 µl annealing buffer and 2 µl water. An RNA negative control was added with water in place of RNA. Tubes were incubated in a pre-heated thermal cycler (PTC-255 thermal cycler, MJ Research, Waltham, MA, USA) at 65°C for 5 minutes and immediately placed on ice for a minimum of 1 minute. The contents of the tube were then collected by brief centrifugation. Keeping the tubes on ice, 10 µl of 2x First-Strand reaction mix and 2 µl of SuperScript III/RNAaseOUT enzyme mix were added to give a final volume of 20 µl. An RT control was added, replacing the enzyme mix with water. Samples were briefly vortexed, centrifuged and incubated using the following protocol: 25°C for 10 minutes, 50°C for 50 minutes and 85°C for 5 minutes. Tubes were placed on ice and cDNA was stored at -20°C. Reactions were performed in triplicate for each virus.

2.2.2.2 Primer Design

Multiple alignment analysis was performed with ClustalW (EMBL-EBI, Cambridge, UK, available online http://www.ebi.ac.uk/Tools/msa/clustalw2/) using the sequences listed below. The area of highest homology was chosen for primer design. Primers were designed using the Primer-BLAST Primer designing tool (NCBI, Bethesda, MD, USA, available online http://www.ncbi.nlm.nih.gov/tools/primer-blast/). Both HIV-1 and HIV-2 primers were manufactured by Invitrogen.

HIV-1: HIV-1_{MN} (GenBank: M17449.1) and HIV-1_{Ada} (GenBank: AF004394.1)

HIV-2: HIV-2_{ST} (GenBank: M31113.1) and *gag* gene sequences from 3 HIV-2 isolates (GenBank: AJ008534.1, AJ008495.1 and AJ008497.1).

Table 2.2. Primer sequences for qPCR

Gene	Forward Primer Sequence (5' – 3')	Reverse Primer Sequence (5' – 3')
HIV-1 *gag*	GGC TTT CAG CCC AGA AGT AAT ACC C	TTG CAT GGC TGC TTG ATG TCC CC
HIV-2 *gag*	TGT GGG CGA CCA TCA AGC AGC	CCG CTG GTA AGG GGC CTG GTA

2.2.2.3 Quantitative Real Time PCR (qPCR)

Quantitative real time PCR was carried out using a Light Cycler 480 (Roche Diagnostics, West Sussex, UK). SYBR Green I was used as a detector which binds all double-stranded DNA molecules and emits a fluorescent signal at 521 nm. Reactions were carried out in 96 well PCR plates with a total volume of 20 µl, all reagents included in each reaction are summarized in Table 2.3 and the amplification protocol is described in Table 2.4. Plates were briefly centrifuged before beginning the incubation. SYBR Green I fluorescence was detected during the elongation step at 72°C. Each reaction was performed in triplicate.

Table 2.3. qPCR reaction mix

Reagent	Final Concentration/Volume
2x QuantiTect SYBR Green RT-PCR Master Mix* (QIAGEN)	1x
Forward primer	0.5 µM
Reverse primer	0.5 µM
Nucleic Acid (vector for standards, cDNA for samples)	2 µl
Water	7 µl

*contains: HotStarTaq DNA polymerase, QuantiTect SYBR Green RT-PCR buffer (Tris-Cl, KCl, $(NH_4)_2SO_4$, 5 mM $MgCl_2$, pH 8.7), dNTP mix (dATP, dCTP, dGTP and dTTP/dUTP), and SYBR Green I and ROX fluorescent dyes.

Table 2.4. Cycling conditions for qPCR

Incubation Step	Temperature	Time	Cycles
Pre-incubation	95°C	15 minutes	1
Denaturation	94°C	15 seconds	30
Annealing	60°C	30 seconds	30
Elongation	72°C	30 seconds	30

2.2.2.4 Standard Curve

In order to create standards for absolute quantification, the amplified product was cloned into a pMA-T vector by GENEART (Regensburg, Germany) (Table 2.5).

Table 2.5. Insert sequences cloned into pMA-T vectors to be used as standards for qPCR

Standard	Insert Sequence	Vector Molecular Weight (Da)
HIV-1	GTA AAA GTA GTA GAA GAG AAG GCT TTC AGC CCA GAA GTA ATA CCC ATG TTT TCA GCA TTA TCA GAA GGA GCC ACC CCA CAA GAT TTA AAC ACC ATG CTA AAC ACA GTG GGG GGA CAT CAA GCA GCC ATG CAA ATG TTA AAA GAG ACC ATC AAT GAG GAA GCT GCA GAA TGG GAT AGA TTG CAT CCA GTG CAT GCA GGG CCT ATT	1600022.4
HIV-2	TGT GGG CGA CCA TCA AGC AGC TAT GCA AAT AAT CAG GGA AAT TAT TAA TGA AGA AGC AGC AGA TTG GGA CGC ACA ACA CCC AAT ACC AGG CCC CTT ACC AGC GG	1535852.56

A standard curve was generated for both HIV-1 and HIV-2 by serial diluting these vectors 1:5 in water to produce a range from 2000 pg – 0.64 pg. Final values were expressed as RNA copy number, calculated using the following equation:

$$\text{RNA copy number} = \text{Moles of vector (g/MW)} \times \text{Avogadro's constant } (6.022 \times 10^{23}/\text{mole})$$

Standards were amplified alongside samples using the Light Cycler 480, as well as a negative control in which the nucleic acid samples were replaced with water.

The amplification of pre-quantified standards was also used to assess the efficiency of the reaction. The efficiency assesses the ability of the reaction to double the amount of DNA after each cycle. An efficiency of 100% is therefore observed when amplification profiles of two standards with a concentration ratio of 2:1 reach the fluorescence signal threshold at one cycle distance from each other. An efficiency of 80% to 100% was considered acceptable, to ensure that the gene expression in the unknown samples would not be over or underestimated. The following equation was used to calculate the efficiency:

$$E = (10^{-1/\text{gradient of standard curve}}) - 1$$

2.2.2.5 Melt Curve

A melt curve was generated after every qPCR run to assess the specificity of the amplified product. The temperature of the PCR product was gradually increased at a rate of 0.11°C/second to a maximum temperature of 95°C and the SYBR Green fluorescence measured 5 times per degree. As the temperature increased the fluorescence decreased as a result of the denaturation of double-stranded DNA. The negative first derivative of the temperature versus fluorescence (-dF/dT) was then plotted against the temperature. The resulting curve has a parabolic profile, in which the peak corresponds to the temperature of maximal –dF/dT, or the temperature at which 50% of the DNA molecules in the reaction are in double-stranded form (melting temperature). Each PCR product has a unique melting temperature, as both the size of the fragment and the base pair composition affect the melting temperature. The presence of a single peak in the melt curve shows that there is only one product being amplified in the PCR reactions, excluding the presence of contaminants, primer-dimer or mis-priming products.

2.3 Cell Culture

All centrifuge speeds are quoted as rpm and were performed in a Mistral 3000E centrifuge (MSE).

2.3.1 PBMC Isolation

Blood from healthy subjects was obtained either from the NHS Blood and Transplant Service in the form of component donation leucocyte cones (also known as leucoreduction system chambers) or volunteers from within the Immunology Section at the Chelsea & Westminster Hospital collected into BD vacutainer lithium heparin tubes (whole blood) (Becton Dickinson, Oxford, UK). The contents of the leucocyte cone was emptied into a 50 ml tube and topped to approximately 50 ml with PBS (PAA Laboratories) + 2% FBS (Sigma-Aldrich, Dorset, UK). One quarter of the volume was transferred to a new 50 ml tube and an equal volume of PBS + 2% FBS was added. Whole blood was simply diluted 1:2 with PBS. Approximately 10 ml of Lymphocyte separation medium 1077 (PAA Laboratories) was

layered underneath the blood and the sample centrifuged at 2000 rpm for 20 minutes with the brake off. The resulting interface of PBMCs was collected into a new 50 ml tube, washed twice with 40 ml of PBS + 2% FBS for leucocyte cones or just PBS for whole blood and centrifuged at 1500 rpm for 10 minutes. Before the second wash, 100 µl of diluted cell suspension was set aside to perform a cell count. Cells were diluted in trypan blue (Sigma-Aldrich) and counted using a haemocytometer. The following equation was then used to determine the cell count:

(Number of cells in 9 squares) x (dilution factor) x (total volume) x (10^4) = total number of cells

Cells were then re-suspended in culture media containing RPMI-1640 + 10% FBS + 2 mM L-Glutamine + 100 U/ml Penicillin and 0.1 mg/ml Streptomycin (all PAA Laboratories unless otherwise stated) at a final concentration of 2 x10^6 cells/ml.

2.3.2 Depletion of pDCs from PBMCs

After PBMCs were isolated, as detailed above, 2 – 3 x10^6 cells were re-suspended in 300 µl of MACS buffer: PBS + 2 mM EDTA (Gibco, Paisley, UK) + 2% FBS, and incubated in the fridge with 100 µl BDCA4 microbeads + 100 µl FcR blocking reagent (Miltenyi Biotec, Surrey, UK). After 15 minutes cells were washed in 10 ml of MACS buffer and centrifuged at 300 rcf (relative centrifugal force) for 10 minutes at 4°C. Cells were then re-suspended in 500 µl of MACS buffer and applied to a pre-rinsed LS column (Miltenyi Biotec) placed onto a magnetic MACS separator. The unlabelled fraction of cells that passed through the column was collected into a 50 ml tube. The column was rinsed three times with 3 ml of MACS buffer, again collecting the cells that passed through the column. The total effluent represented the pDC-depleted PBMC population. Cells were then counted and re-suspended at a final concentration of 2 x10^6 cells/ml in culture media. The efficiency of pDC depletion was tested by flow cytometry: 1 x10^6 cells of both the untouched PBMC fraction and pDC-depleted population were stained with CD123-PE-Cy7 (Biolegend, London, UK), BDCA2-APC (Miltenyi Biotec) and CD14-APC-H7

(Becton Dickinson) conjugated antibodies as detailed in section 2.4.1 and acquired on a BD LSR-II flow cytometer (Becton Dickinson).

2.3.3 Cell Culture

PBMCs were cultured at 37°C with 5% CO_2 for different periods of time ranging from 3 to 48 hours. Cells were cultured in the presence or absence of varying concentrations of HIV-1 or HIV-2 as indicated in the results. In some experiments CpG-A (ODN 2216, InvivoGen, San Diego, CA, USA) or LPS (Sigma-Aldrich) were also used to stimulate PBMCs at a final concentration of 0.5 µM and 1 ng/ml respectively, unless otherwise stated. Mouse anti-human IFN-α receptor chain 2 (MMHAR-2, PBL Interferon Source, Piscataway, NJ, USA) antibody was used in cell cultures at a final concentration of 10 µg/ml. Rabbit anti-human IFN-α and IFN-β were added together at final concentrations of 10 µg/ml (PBL Interferon Source). All antibodies were pre-incubated with PBMCs for 30 minutes before adding any other stimulus. Universal Type I IFN (PBL Interferon Source) was added to pDC-depleted cells at concentrations indicated in results. The nucleoside analogue reverse transcriptase inhibitors (NRTI), azidothymidine (AZT) (Sigma-Aldrich) and 2',3'-didehydro-3'-deoxythymidine (d4T) (Sigma-Aldrich), both of which inhibit HIV-1 and HIV-2 replication *in vitro* (Smith *et al.*, 2008), were solubilised in DMSO (Sigma-Aldrich) and used at concentrations from 50 µM to 0.5 nM with a final maximum DMSO concentration of 0.1% in culture.

Cultures were conducted in 24, 48 or 96 well plates depending on the experimental read-out. Cells were harvested after 9 and 24 hours culture for analysis by flow cytometry (Section 2.4), and after 6 and 12 hours culture for whole genome expression analysis (Section 2.7). Supernatants were collected at up to seven different time points (3, 6, 9, 12, 18, 24 and 48 hours) and immediately frozen at -80°C for future analysis of soluble proteins (Section 2.5) and IDO activity (Section 2.6).

2.4 Flow Cytometry

Flow cytometry was performed on a BD LSR-II using FACSDiva software (Becton Dickinson), and FlowJo software (Treestar, Ashland, OR, USA) was used for data analysis. Compensation was performed using plus size anti-mouse compensation beads (Becton Dickinson) stained with each specific fluorochrome conjugated antibody, unless otherwise specified.

2.4.1 Surface staining

Cells were collected into FACS tubes and centrifuged at 1500 rpm for 10 minutes. Supernatants were set aside and frozen at -80°C for future analysis. Cell pellets were resuspended and incubated with different combinations of fluorescently conjugated monoclonal antibodies (Table 2.6 and Table 2.7) for 20 minutes in the dark, at room temperature. Cells were then washed twice with 1 ml of BD stain buffer (Becton Dickinson) and fixed in 200 µl BD stabilising fixative (Becton Dickinson). Isotype matched controls were used as a control for background fluorescence signal and aspecific staining to determine the threshold of positivity for markers of interest and identify frequencies of CD80, CD83 or CD86 expressing pDCs and monocytes and CD80, CD86 or HLA-ABC expressing mDCs.

Table 2.6. Flow cytometry antibody panel for pDCs and monocytes

Target	Conjugate	Clone	Source
CD80	FITC	2D10.4	eBioscience (Hatfield, UK)
CD83	PE	HB15e	eBioscience
CD86	PerCP-Cy5.5	IT2.2	BioLegend
CD123	PE-Cy7	6H6	BioLegend
BDCA2	APC	AC144	Miltenyi Biotec
CD14	APC-H7	MϕP9	Becton Dickinson
IgG1	FITC	P3.6.2.8.1	eBioscience
IgG1	PE	P3.6.2.8.1	eBioscience
IgG2b	PerCP-Cy5.5	MPC-11	BioLegend

Table 2.7. Flow cytometry panel for mDCs

Target	Conjugate	Clone	Source
Lineage Cocktail 1*	FITC	(multiple antibodies)	Becton Dickinson
HLA-ABC	PE	DX17	Becton Dickinson
CD86	PerCP-Cy5.5	IT2.2	BioLegend
CD11c	PE-Cy7	3.9	BioLegend
CD80	APC	2D10	BioLegend
HLA-DR	APC-Cy7	L243	BioLegend
IgG1	PE	P3.6.2.8.1	eBioscience
IgG2b	PerCP-Cy5.5	MPC-11	BioLegend
IgG1	APC	P3.6.2.8.1	eBioscience

*Consists of anti-human CD3, CD14, CD16, CD19, CD20 and CD56

2.4.1.1 Gating Strategy

Figure 2.2 shows a representation of the gating strategy used to identify monocytes and pDCs. The gating strategy employed to identify mDCs is shown in Figure 2.3. In both cases, matched isotype controls were used to set the thresholds of positivity and determine the frequencies of markers of interest. An alternative gating strategy to confirm the mDC population identified is shown in Appendix 4.

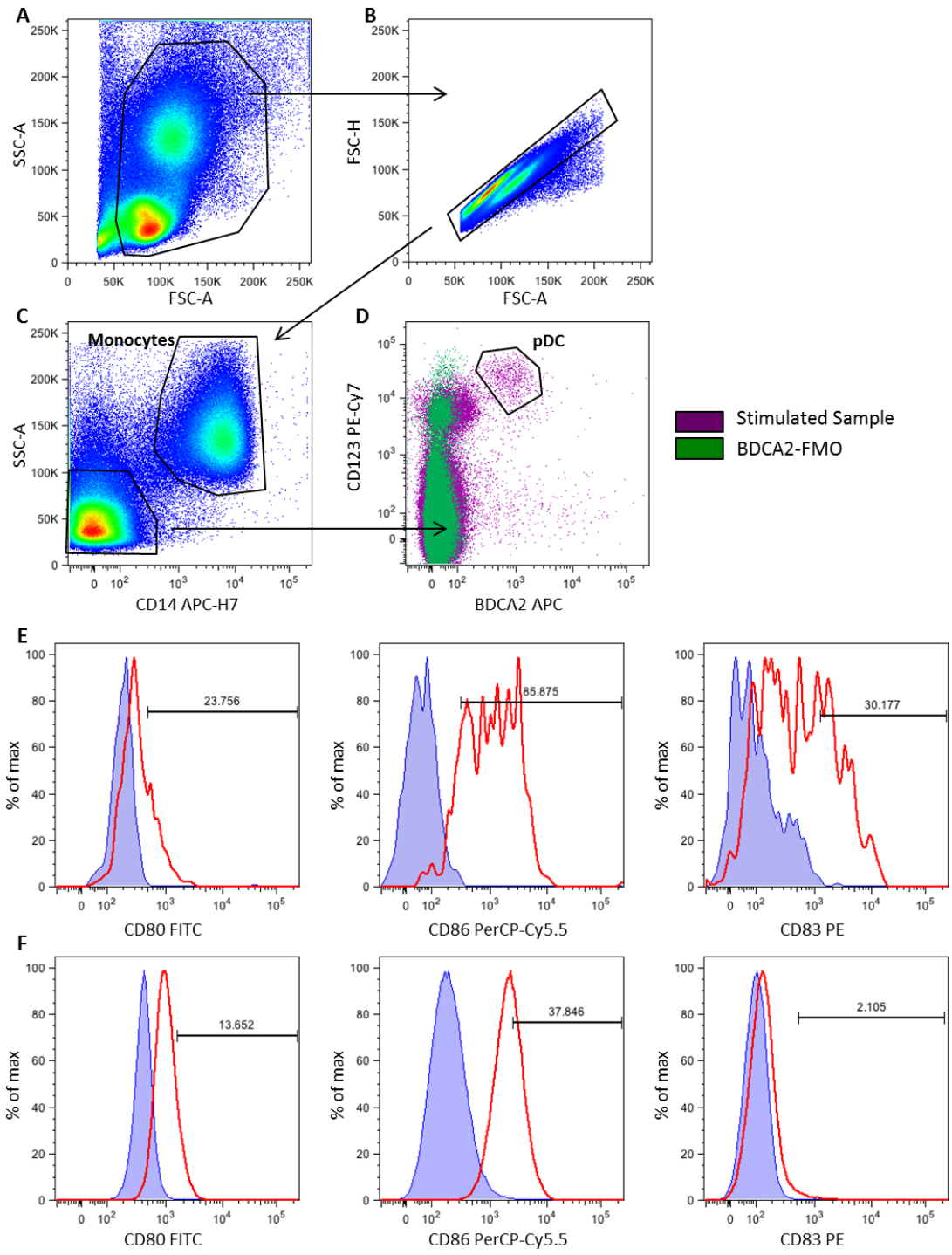

Figure 2.2. Gating strategy for pDCs and monocytes. (A) PBMCs were gated based on side scatter (SSC-A) and forward scatter (FSC-A). (B) Doublets were excluded using FSC height (FSC-H) versus FSC-A. (C) The monocyte population was identified as $CD14^{+}$ SSC-A high. Plasmacytoid DCs were identified as $CD14^{-}$ SSC-A low (C) and $BDCA2^{+}$ $CD123^{+}$ (D). Fluorescence-minus-one (FMO) for BDCA2-APC is shown in green to help identify the pDC population (D). Panels (E) and (F) show the isotype gating (solid blue histograms) used to identify CD80, CD86 and CD83 positive populations for pDCs and monocytes respectively. Open red histograms show a stimulated sample.

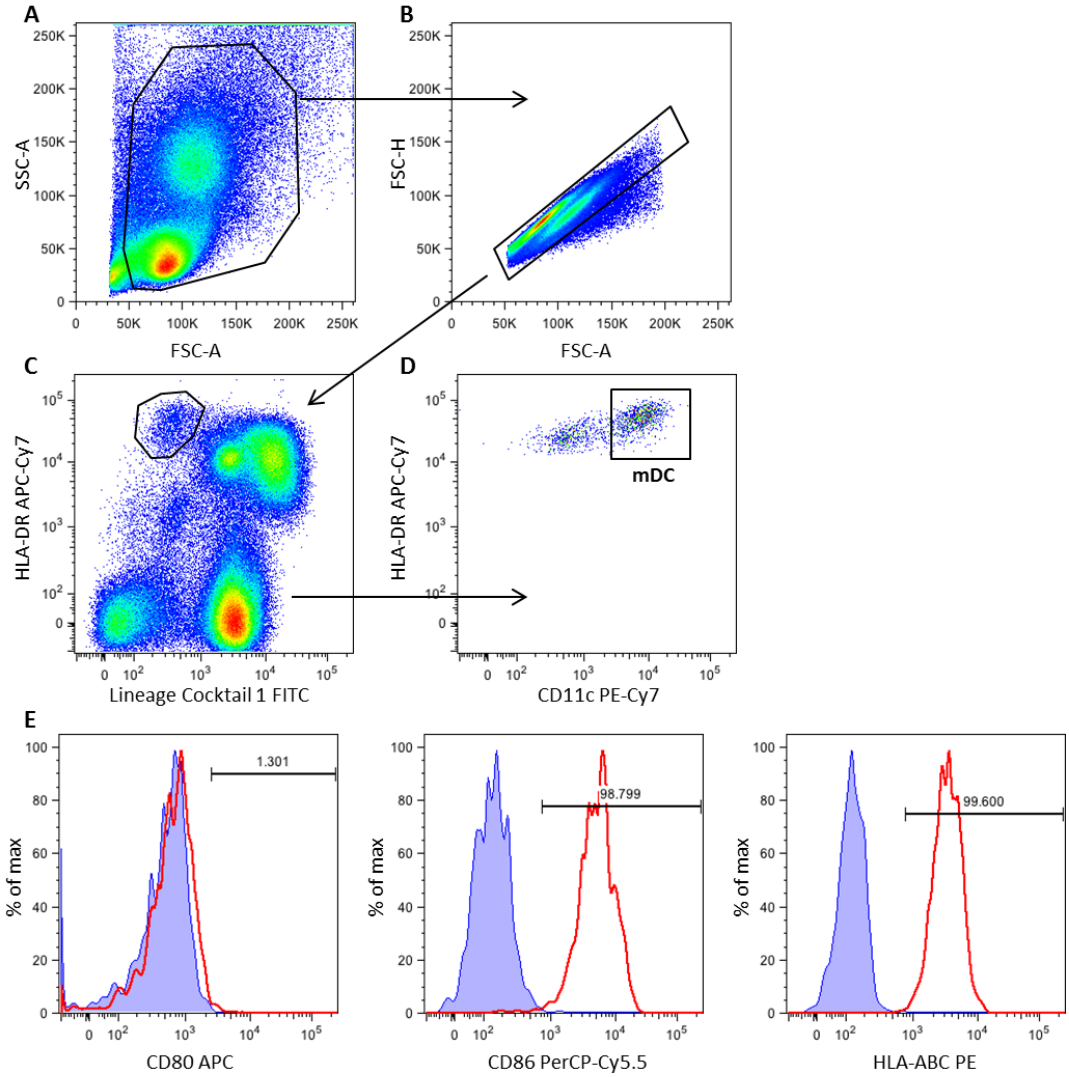

Figure 2.3. Gating strategy for mDCs. (A) PBMCs were gated based on side scatter (SSC-A) and forward scatter (FSC-A). (B) Doublets were excluded using FSC height (FSC-H) versus FSC-A. (C) Myeloid DCs were identified as HLA-DR$^+$ Lineage$^-$ (C) and CD11c$^+$ (D). Panel (E) shows the isotype gating (solid blue histograms) used to identify CD80, CD86 and HLA-ABC positive populations. Open red histograms show a stimulated sample.

2.4.2 Cell Viability

In addition to surface staining for markers of activation, some samples were also tested for cell viability. Cells were incubated with a combination of fluorescently conjugated antibodies listed in Table 2.8 and Table 2.9 for 20 minutes at room temperature, in the dark. The cells were then washed in PBS and incubated with Fixable Viability dye (FVD) eFluor 506 (eBioscience) for 30 minutes at 4°C. FVD reacts with free amines in the cytoplasm of cells, therefore only in dead cells is the dye able to

cross the plasma membrane, whereas in live cells the intact plasma membrane will exclude the dye. Following this, cells were washed in 1 ml of BD stain buffer and fixed in 200 µl of BD stabilising fixative. Plasmacytoid DCs, monocytes and mDCs were identified as in Figure 2.2 (A - D) and Figure 2.3 (A - D) and then the MFI of FVD eFluor 506 was examined (Figure 2.4). Compensation for FVD was performed using 1:1 mixture of live and heat inactivated PBMCs (heat inactivation was performed at 96°C for 10 minutes), all other markers were compensated using beads.

Table 2.8. Cell viability staining for pDCs and monocytes

Target	Conjugate	Clone	Source
CD123	PE-Cy7	6H6	BioLegend
BDCA2	APC	AC144	Miltenyi Biotec
CD14	APC-H7	MϕP9	Becton Dickinson

Table 2.9. Cell viability staining for mDCs

Target	Conjugate	Clone	Source
Lineage Cocktail 1*	FITC	(multiple antibodies)	Becton Dickinson
CD11c	PE-Cy7	3.9	BioLegend
HLA-DR	APC-Cy7	L243	BioLegend

*Consists of anti-human CD3, CD14, CD16, CD19, CD20 and CD56

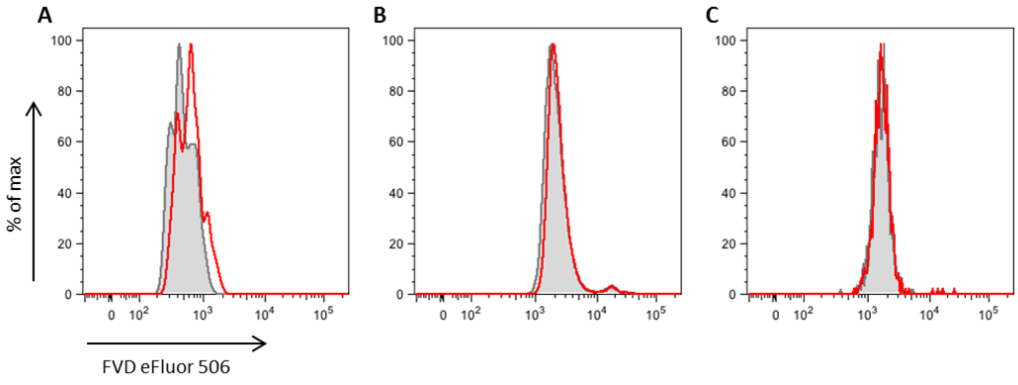

Figure 2.4. Histograms showing FVD eFluor 506 staining for cell viability. Plasmacytoid DCs (A), monocytes (B) and mDCs (C) were examined for dead cells following overnight PBMC stimulation. Solid grey histograms show an unstimulated sample (media alone) and open red histograms represent a stimulated sample.

2.4.3 Cytometric Bead Array (CBA)

Concentrations of cytokines in cell culture supernatants were measured using the BD cytometric bead array (Becton Dickinson), which allows for detection of multiple cytokines in one reaction. The assay utilises capture beads coated with antibodies specific for a soluble protein. Each capture bead has a unique fluorescence which can be detected by flow cytometry. The detection reagent consists of PE-conjugated antibodies specific for each soluble protein, therefore sandwiching the protein of interest. The PE fluorescent signal is thus proportional to the concentration of bound protein.

Defrosted samples were diluted in media and stored at 4°C until required. CBA standards were prepared by pooling all supplied lyophilised standards into one 15 ml tube and reconstituted with 4 ml of supplied assay diluent. The standard was then serially diluted 1:2 to generate a range from 2500 pg/ml to 10 pg/ml. CBA capture beads were prepared by pooling 100 µl of each capture bead (specific for each cytokine) and diluting them according to the manufacturer's instructions. Detection antibody was also prepared by pooling all individual detection antibodies and again diluting them according to the manufacturer's instructions. 50 µl of diluted standards and samples were added to FACS tubes and mixed with 50 µl of prepared CBA capture beads. After one hour incubation at room temperature, 50 µl of prepared detection antibody was added to each tube and then incubated for a further two hours. Samples and standards were then washed once by adding 1 ml of provided wash buffer and centrifuging at 200 rcf for 5 minutes. The supernatant was then discarded and the beads re-suspended in 300 µl of BD stabilising fixative. Samples were subsequently acquired by flow cytometry.

2.4.4 IFN-α Secretion Assay

Plasmacytoid DCs that were actively secreting IFN-α were identified using the IFN-α Secretion Assay from Miltenyi Biotec. After 9 or 24 hours culture in the presence or absence of either HIV-1 or HIV-2, cells were collected into 15 ml tubes and washed in MACS buffer, centrifuged at 1500 rpm for 10 minutes. Cells were then labelled with IFN-α catch antibody (Miltenyi Biotec) for 15 minutes on ice. In

order to allow for the cells to secrete IFN-α, cells were diluted in 1 ml culture media (RPMI-1640 + 10% FBS + 2 mM L-Glutamine + 100 U/ml Penicillin and 0.1 mg/ml Streptomycin) per 1 million cells. Tubes were then placed at 37°C with 5% CO_2 for 20 minutes, and rotated every 5 minutes to resuspend settled cells. Cells were then washed in MACS buffer and incubated with IFN-α detection antibody conjugated to PE (Miltenyi Biotec) plus a combination of fluorescently conjugated monoclonal antibodies (Table 2.10) for 20 minutes in the dark, at room temperature. Following this, cells were washed in PBS and incubated with FVD eFluor 506 for 30 minutes at 4°C. Cells were then washed again in MACS buffer and fixed in BD stabilizing fixative. Isotype controls were used to identify frequencies of CD83 or CD86 expressing pDCs, and unstimulated cells were used to identify frequencies of IFN-α secreting pDCs. In addition to FlowJo, SPICE (NIAID, Bethesda, MD, USA, available online http://exon.niaid.nih.gov/spice/) was also used for data analysis.

Table 2.10. Antibody panel for IFN-α secretion assay

Target	Conjugate	Clone	Source
CD83	Brilliant Violet 421	HB15e	Biolegend
CD86	PerCP-Cy5.5	IT2.2	BioLegend
CD123	PE-Cy7	6H6	BioLegend
BDCA2	APC	AC144	Miltenyi Biotec
CD14	APC-H7	MϕP9	Becton Dickinson
IgG1	Brilliant Violet 421	MOPC-211	BioLegend
IgG2b	PerCP-Cy5.5	MPC-11	BioLegend

2.4.4.1 Gating Strategy

Figure 2.5 shows the gating strategy used for analysis of the IFN-α secretion assay.

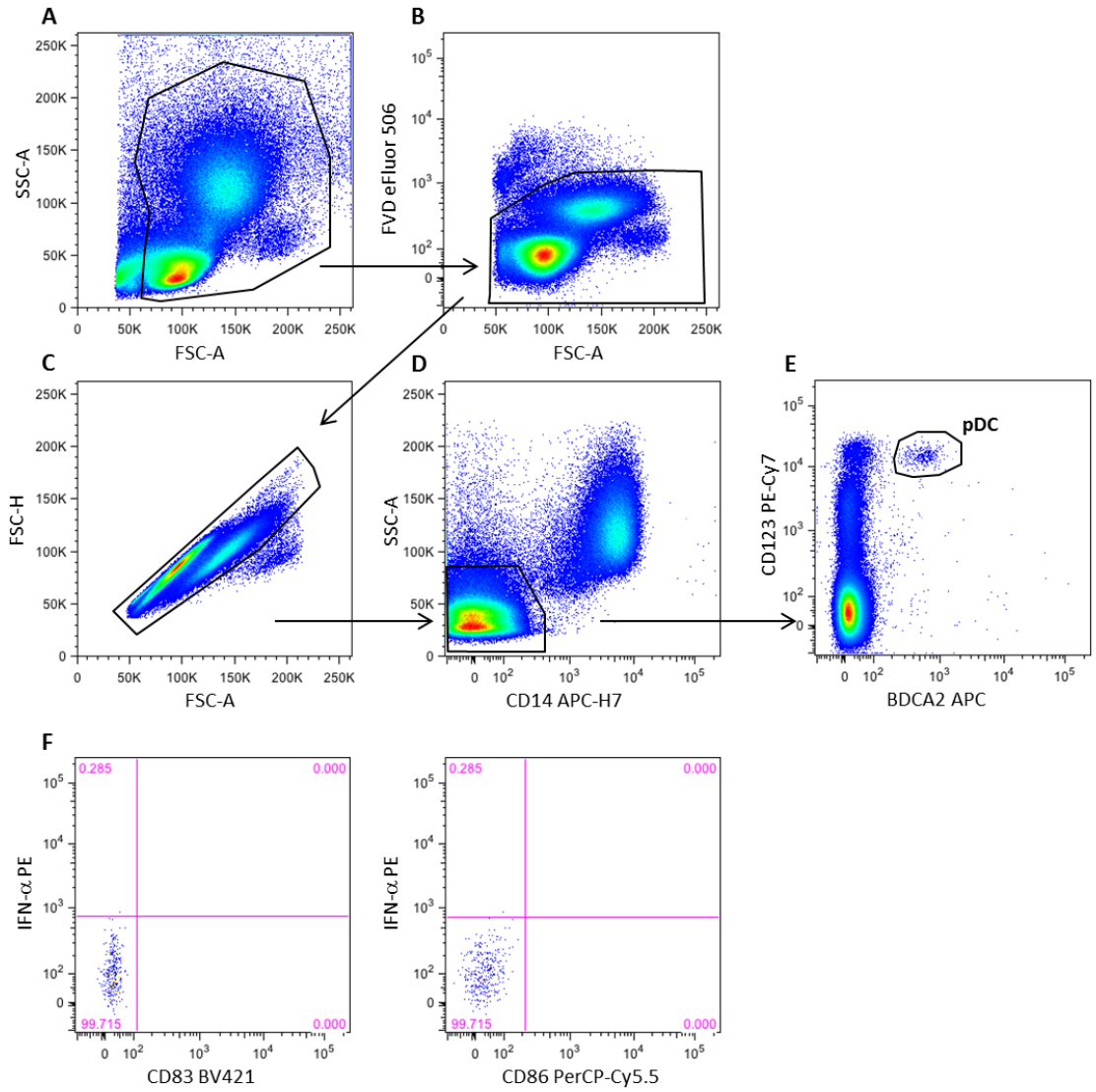

Figure 2.5. IFN-α secretion assay gating strategy. (A) PBMCs were gated based on side scatter (SSC-A) and forward scatter (FSC-A). (B) Dead cells were excluded based on negative staining for FVD. (C) Doublets were excluded using FSC-H versus FSC-A. (C) Plasmacytoid DCs were identified as $CD14^-$ SSC-A low (C) and $BDCA2^+$ $CD123^+$ (D). Panel (F) shows the gating used to identify $CD83^+$ and $CD86^+$ pDCs by isotype staining. The gate for IFN-α-secreting cells was based on these unstimulated cells.

2.5 Enzyme Linked Immunosorbent Assay

Concentrations of different proteins in cell culture supernatants were measured using commercially available enzyme linked immunosorbent assay (ELISA) kits. Analysis was performed using Microsoft Excel (Reading, UK).

2.5.1 IFN-α ELISA

Concentrations of IFN-α were measured using the human IFN-α multi-subtype ELISA kit (PBL Interferon Source). According to the manufacturer's protocol, 100 µl of diluted standards, controls and samples were added in duplicate to a pre-coated microtitre plate. The supplied standard was appropriately diluted in dilution buffer and serially diluted 1:2 to generate a range from 5000 pg/ml to 78.125 pg/ml. A control was also prepared from the standard at a concentration of 625 pg/ml and used six times in each plate to monitor inter- and intra-assay variability, calculated as:

Intra-assay CV = (standard deviation of 3 internal controls/average of 3 internal controls)*100

Inter-assay CV = (standard deviation of intra-assay CVs/average of intra-assay CVs)*100

Sample supernatants were diluted 1:2.5 in dilution buffer and dilution buffer used as a negative control. Diluted standards, controls and samples were added in volumes of 100 µl in duplicate to a pre-coated microtitre plate. The plate was incubated at room temperature for one hour then washed once with diluted wash buffer and the wells aspirated and tapped dry. The supplied antibody concentrate was diluted in dilution buffer according to the lot-specific Certificate of Analysis (COA) and 100 µl of antibody preparation was added to each well. The plate was incubated for one hour at room temperature. After three washes, 100 µl of diluted horseradish peroxidase (HRP) conjugate, prepared in HRP conjugate diluent as per the lot-specific COA, was added to each well and the plate incubated at room temperature for one hour. After four washes, 100 µl of tetramethylbenzidine (TMB) substrate solution, warmed to room temperature, was added to each well and the plate incubated in the dark for approximately 15 minutes. The reaction was then terminated with 100 µl stop solution and the absorbance measured at 450 nm using a plate reader (Anthos 2020, Anthos Labtec Instruments, Salzburg, Austria).

2.5.2 IFN-β ELISA

Concentrations of IFN-β were measured using the human IFN-β ELISA kit (PBL Interferon Source). According to the manufacturer's protocol, the supplied standard was appropriately diluted in cell culture media and serially diluted to generate a range from 4000 pg/ml to 50 pg/ml. A control was prepared from the standard at a concentration of 1000 pg/ml and used six times in each plate to monitor inter- and intra-assay variability. Cell culture media was used as a negative control. Standards, controls and negatives were then diluted 1:2 and supernatant samples diluted either 1:2 or 1:2.5 in sample diluents. Diluted standards, controls and samples were added in volumes of 100 µl in duplicate to a pre-coated microtitre plate. The plate was incubated at room temperature for one hour then washed three times with diluted wash buffer and the wells aspirated and tapped dry. The supplied antibody concentrate was diluted in concentrate diluent according to the lot specific COA and 100 µl of antibody preparation was added to each well. The plate was incubated for one hour at room temperature. The plate was subsequently washed three time and 100 µl of diluted HRP conjugate, prepared in concentrate diluent as per the lot specific COA, was added to each well and the plate incubated at room temperature for one hour. After three washes, 100 µl TMB substrate solution, warmed to room temperature, was added to each well and the plate incubated in the dark for approximately 20 minutes. The reaction was then terminated with 100 µl of stop solution and the absorbance measured at 450 nm using a plate reader (Anthos 2020, Anthos Labtec Instruments).

2.5.3 IL-6, IL-8, IL-1β and TNF-α ELISA

Concentrations of IL-6, IL-8, IL-1β and TNF-α were measured in cell culture supernatants using Quantikine ELISA kits (R&D Systems, Abingdon, UK). Firstly, according to the manufacturer's protocol, assay diluent was added to each well of pre-coated microplates (Table 2.11). Diluted standards, controls and samples were then added in duplicate to the appropriate wells (Table 2.11) and the plates incubated at room temperature for two hours. A control was prepared from the supplied standard (Table 2.11) and used six times in each plate to monitor inter- and intra-assay variability. The

appropriate Calibrator Diluent served as a negative control. Following incubation, plates were washed with 400 µl/well of the supplied diluted wash buffer, using an automated plate washer (Asys Atlantis, Biochrom, Cambridge, UK). Washing was carried out four times for IL-6, IL-8 and TNF-α, and three times for IL-1β. After the last wash plates were tapped dry to remove any remaining wash buffer. The supplied HRP conjugate was then added to all wells, and the plates incubated at room temperature for either one hour (IL-8, IL-1β and TNF-α) or two hours (IL-6). Following incubation, the wash step was repeated and 200 µl of substrate solution (TMB) was added to each well and the plates allowed to develop at room temperature, protected from the light, for between 10 – 20 minutes. The reaction was then terminated with 50 µl of stop solution (2N sulfuric acid) and the absorbance measured at 450 nm with a wavelength correction at 540 nm, using a plate reader (Infinite M200 Pro, Tecan, Reading, UK).

Table 2.11. List of reagents for R&D ELISA kits

	IL-6	**IL-8**	**IL-1β**	**TNF-α**
Assay Diluent (µl/well)	RD1W (100 µl)	RD1-85 (100 µl)	None	RD1F (50 µl)
Dilution buffer for standards, controls and samples	Calibrator Diluent RD5T	Calibrator Diluent RD5P (1x)	Calibrator Diluent RD5-5	Calibrator Diluent RD6-35 (1x)
Standard curve range (pg/ml)	300 – 3.12	2000 – 31.2	250 – 3.9	1000 – 15.6
Control (pg/ml)	25	250	31.2	125
Standards, controls and samples (µl/well)	100 µl	50 µl	200 µl	200 µl
Conjugate (µl/well)	Anti-IL-6 pAb-HRP (200 µl)	Anti-IL-8 pAb-HRP (100 µl)	Anti-IL-1β pAb-HRP (200 µl)	Anti-TNF-α pAb-HRP (200 µl)

2.6 IDO

IDO activity was quantified as the ratio of kynurenine and tryptophan in the culture supernatants. Kynurenine and tryptophan were detected by high performance liquid chromatography (HPLC) (Widner *et al.*, 1997). This analysis was kindly performed by Professor Dietmar Fuchs (Division of Biological Chemistry Biocentre, Innsbruck Medical University, Austria).

2.7 Whole Genome Expression

2.7.1 RNA Extraction from PBMCs

PBMCs were isolated from whole blood (healthy volunteers recruited from the Immunology Section at the Chelsea & Westminster Hospital) and stimulated with 13 x10^9 RNA copies/ml of HIV-1 or HIV-2, or 0.5 µM of CpG-A (ODN 2216, InvivoGen). Cell culture media alone was used as an unstimulated control. Cells were collected after 6 and 12 hours stimulation. Cultures were run in duplicate with 5 x10^6 cells/well. Duplicates were collected separately into 15 ml tubes and centrifuged at 1500 rpm for 5 minutes (Mistral 3000E, MSE). Supernatants were collected and frozen at -80°C. Cell pellets were then resuspended in 1 ml PBS and transferred to a 1.5 ml tube and centrifuged at 2000 rpm for 5 minutes in the microcentrifuge (Micro Centaur, MSE). The PBS was aspirated and the pellets frozen at -80°C in the residual PBS.

Duplicates were pooled for RNA extraction for a total of 10 x10^6 cells. RNA extraction was firstly performed using the RNeasy Mini kit (QIAGEN). Centrifuge speeds are quoted in rpm and were performed in a Micro Centaur (MSE) centrifuge. PBMCs were lysed in 600 µl of RLT buffer and then homogenised by pipetting the lysate into a QIAShredder spin column (QIAGEN) and centrifuged for 2 minutes at 13,000 rpm. 600 µl of 70% ethanol was then added to the filtrate. 600 µl of the ethanol filtrate mix was then added to an RNeasy spin column placed in a 2 ml collection tube and centrifuged at 13,000 for 15 seconds. The filtrate was discarded and the remaining 600 µl of ethanol filtrate mix was added to the spin column and the centrifugation repeated. Again the filtrate was discarded and the spin column was then washed with 350 µl of RW1 buffer and centrifuged at 13,000 rpm for 15 seconds, discarding the filtrate afterwards. DNase digestion was then performed directly on the extraction columns to remove any contaminating genomic DNA. Briefly, 10 µl of DNase I was added to 70 µl of buffer RDD (RNase-Free DNase Set, QIAGEN), the solution mixed and then added directly onto the spin column membrane and incubated at room temperature for 15 minutes. Following this, the

column was washed again in 350 µl of RW1 buffer and centrifuged at 13,000 rpm for 15 seconds. After the filtrate was discarded the spin column was washed twice in 500 µl of RPE buffer by centrifugation at 13,000 rpm for 15 seconds in the first wash and 2 minutes in the second wash in order to completely dry the membrane. The spin column was then transferred to a new 2 ml collection tube, the old one discarded, and centrifuged for 1 minute at 13,000 rpm to remove any residual ethanol. The spin column was transferred to a new 1.5 ml tube, again discarding the old one. The RNA was eluted by adding 50 µl of RNase-free water directly onto the membrane and spun at 13,000 rpm for 1 minute. To maximise the amount of RNA eluted, this step was repeated so that the total elution volume was 100 µl.

In order to concentrate the RNA the RNeasy MinElute Cleanup kit (QIAGEN) was used following the RNeasy Mini Kit. To the 100 µl of RNA, 350 µl of RLT buffer was added. The solution was mixed by pipetting and then 250 µl of 96 – 100% ethanol was added, bringing the total volume to 700 µl, which was then transferred to an RNeasy MinElute spin column placed in a 2 ml collection tube, and centrifuged at 13,000 rpm for 15 seconds. The column was moved to a new collection tube and the old one containing the filtrate discarded. The spin column was then washed in 500 µl of RPE buffer and centrifuged again at 13,000 rpm for 15 seconds. The filtrate was discarded and the column washed twice in 500 µl of 80% ethanol and centrifuged for 2 minutes at 13,000 rpm. Before the second spin, the column was left on the bench top for 3 minutes with the 80% ethanol, to dry and remove as much salt contaminants as possible. The spin column was again transferred to a new collection tube, and the old one discarded. The column was then centrifuged with the lid open at 13,000 rpm for 5 minutes, in order to dry the membrane and remove any residual ethanol. The spin column was transferred to a new 1.5 ml tube, again the old collection tube discarded, and the RNA eluted in 14 µl of RNase-free water by centrifuging at 13,000 rpm for 1 minute.

The quantity of RNA was measured using the NanoDrop 1000 (Thermo Scientific). The optimal conditions to perform a gene array required that all samples contained a minimum of 800 ng of RNA, normalised to a final concentration of 100 ng/µl. All 260/280 ratios were between 1.95 – 2.10 and 260/230 ratios were all above 1.8. The quality of the RNA was checked using the Agilent Bioanalyzer, which allows for detection of RNA degradation, and only samples with an RNA Integrity Number (RIN) of 7.5 were used.

2.7.2 Microarray

Whole genome expression was performed in collaboration with Dr Simone Sharma (Wolfson Institute for Biomedical Research, University College London, UK). Ambion WT Expression kit (Affymetrix, High Wycombe, UK) was used to prepare the cDNA, which was then labelled using the GeneChip WT Terminal Labeling kit (Affymetrix). Samples were run on the Human Gene 1.0ST version 2 array (Affymetrix), which contains probe sets for 40,716 transcripts. Partek Genomics 6.6 software (Partek, Saint Louis, MO, USA) was used for data analysis. Individual CEL files were corrected using RMA (robust multi-array) background correction. Normalisation was performed using quantiles and median polish used for probe set summarisation. Results were expressed as log2. Data sets from different time points were treated separately.

2.8 Statistical Analysis

2.8.1 ELISA, Flow Cytometry & IDO

Statistical analysis was performed using SPSS version 20.0 (IBM, Portsmouth, UK). Different culture conditions were compared using a non-parametric Friedman test. Pair wise comparisons were subjected to Dunn's post test for correction of multiple analyses. Spearman rank tests were performed for correlation analysis using GraphPad Prism version 5.0 (GraphPad Software, La Jolla, CA, USA). In all cases P values of less than 0.05 were considered significant.

2.8.2 Microarray

Statistical analysis for the gene array data was performed with Partek genomics using a 2-way ANOVA, cross-comparing HIV-1, HIV-2 and CpG to media alone, setting the donor variable as a random variable. Only genes which had a two-fold change in expression relative to media and yielded a p-value <0.05 after Benjamini & Hochberg correction were considered statistically significant and selected for further analysis. The Partek Gene Ontology (GO) enrichment function was used to identify groups of genes based on their biological function. Gene enrichment was performed on 3 separate lists of genes; those showing significant changes in expression compared to media in response to: i) both HIV-1 and HIV-2, ii) HIV-1, and not HIV-2, iii) HIV-2, and not HIV-1.

Chapter 3 Type I IFN Secretion

3.1 Introduction

Activation of pDCs is most commonly measured as type I IFN secretion (Asselin-Paturel and Trinchieri, 2005). Most human cells, including leucocytes, are able to secrete type I IFN in response to viral infections (Samuel, 2001). However, pDCs can secrete 1000 fold more IFN-α than any other cell type following viral exposure, earning themselves the title of natural interferon producing cells (Fitzgerald-Bocarsly, 1993, Siegal *et al.*, 1999). In humans there are five subtypes of type I IFN; IFN-α, IFN-β, IFN-ε, IFN-κ and IFN-ω of which, IFN-α is split into 13 further sub species (Borden *et al.*, 2007). All type I IFNs signal through a common receptor, which is composed of two subunits, IFNAR1 and IFNAR2 (Borden *et al.*, 2007). Interferons draw their name from their ability to interfere with the replication of several viruses (Isaacs and Lindenmann, 1957). In fact, type I IFNs are the most potent natural anti-viral soluble factors, and they exert their anti-viral activity by both stimulating intracellular factors which inhibit viral replication and by inducing cell apoptosis. For example, type I IFN induces the transcription of genes coding for enzymes which degrade viral RNA, thus inhibiting its translation into viral proteins (Samuel, 2001). In addition to halting viral replication, type I IFNs are also important in promoting activation of the adaptive immune system. They promote an antigen-presenting phenotype on macrophages and DCs by increasing the expression of co-stimulatory molecules and MHC class I and II, thereby favouring the priming and activation of virus-specific cytotoxic T lymphocytes (CTL) (Keir *et al.*, 2002, McKenna *et al.*, 2005, Santini *et al.*, 2000). Production of type I IFN is therefore important during the early stages of viral infections (Samuel, 2001). However, in certain persisting viral infections type I IFN is produced continuously through to the chronic phase of infection, which may have deleterious effects on disease outcome (Bosinger *et al.*, 2009, Harris *et al.*, 2010, Jacquelin *et al.*, 2009, Teijaro *et al.*, 2013, Wilson *et al.*, 2013).

Recent publications using a mouse model of lymphocytic choriomeningitis virus (LCMV) highlight the importance of tapering IFN-α production during chronic infections (Teijaro *et al.*, 2013, Wilson *et al.*, 2013). The authors used two different strains of LCMV, an acute strain which initiates a robust T cell response able to clear the virus, and a second strain that establishes a chronic infection. During acute LCMV infection, removal of IFN-α/β signalling, using IFNAR1 blocking antibodies, lead to viral persistence, which is not surprising considering the role type I IFN plays in inhibiting viral replication. However, blockade of type I IFN during the chronic form of disease actually improved disease outcome. These mice had heightened virus specific $CD4^+$ T cell responses and reduced expression of immunosuppressive molecules, such as PD-L1, ultimately leading to improved viral control (Teijaro *et al.*, 2013, Wilson *et al.*, 2013).

We have previously demonstrated the ability of IFN-α to dampen HIV-specific T cell responses using a strain of HIV-1 which had been treated with the starch derivative 2-hydroxy-propyl β-cyclodextrin (βCD), rendering it incapable of inducing an IFN-α response in PBMC cultures *in vitro* (Boasso *et al.*, 2011). Treatment with βCD removes cholesterol from the viral envelope, which consequently destabilises the envelope and removes the ability of HIV to infect $CD4^+$ cells *in vitro*. We reported that re-activation of Gag-specific memory $CD8^+$ T cell responses was enhanced in PBMCs from HIV-exposed individuals when cells were stimulated with βCD-HIV-1 compared to wild type HIV-1. The frequency of IFN-γ positive $CD8^+$ T cells was subsequently reduced when cells were stimulated with βCD-HIV-1 in the presence of recombinant IFN-α, indicating the dependence of this effect on IFN-α.

Studies examining SIV in non-human primates have further highlighted the effect of type I IFN on disease outcome. In the natural hosts of SIV, sooty mangabeys and African green monkeys, infection does not result in immunodeficiency in contrast to SIV infection of rhesus macaques in which immune deficiencies occur. Harris *et al* (2010) reported that sooty mangabeys, African green monkeys and rhesus macaques all produce a rapid type I IFN response to SIV infection. However, only in the sooty

mangabeys and African green monkeys, the natural hosts, is the type I IFN response attenuated during the transition to the chronic stage of infection. Conversely, pathogenic SIV infection in rhesus macaques is associated with the protraction of IFN-α responses through to the chronic phase of infection. This is further illustrated in studies measuring the expression of type I IFN-stimulated genes (ISG), which showed a robust innate immune response in both natural hosts and rhesus macaques during acute SIV infection (Bosinger *et al.*, 2009, Jacquelin *et al.*, 2009). The expression of ISGs returns to basal levels only in sooty mangabeys and African green monkeys, whereas rhesus macaques maintain high ISG expression throughout the chronic phase (Bosinger *et al.*, 2009, Jacquelin *et al.*, 2009). Furthermore, a recent study has shown that upon acute activation of PBMCs with SIV *in vitro*, a significantly reduced number of sooty mangabey pDCs stained positive for IFN-α compared to those from the rhesus macaque (Bosinger *et al.*, 2013). This therefore suggests that during controlled infection of sooty mangabeys, pDCs have a reduced capacity to secrete IFN-α during the early stages of infection, potentially contributing to the improved disease outcome observed in these natural hosts.

In the context of HIV, high levels of IFN-α have been reported in the tonsils of HIV-1 infected patients (Herbeuval *et al.*, 2006) suggesting there is chronic production of IFN-α in these patients. Furthermore, expression of the *MxA* gene, an ISG, is significantly higher in PBMCs from HIV-1 compared to HIV-2 infected patients (Cavaleiro *et al.*, 2009b).

It is worth noting that although pDCs are the main producers of type I IFN during the acute innate response, their importance in chronic type I IFN production may be mitigated by the emergence of other populations of type I IFN-producing cells during the course of infection (Kader *et al.*, 2013). Therefore this study aimed to examine the ability of both HIV-1 and HIV-2 to stimulate IFN responses from pDCs during the acute stages of infection.

Another hallmark of pDC activation is the expression of high levels of the immunoregulatory enzyme IDO. Increased levels of IDO are found in lymphoid tissues during HIV-1 and SIV infection (Nilsson *et al.*, 2006), and in PBMCs from HIV-1 infected individuals (Boasso *et al.*, 2007). Furthermore, increased plasma Kyn/Trp ratios, the marker for IDO activity, have been reported in HIV-1 infected patients (Fuchs *et al.*, 1991, Huengsberg *et al.*, 1998). High levels of IDO activity have been implicated with viral persistence. In a mouse model of HIV-1 encephalitis, animals treated with 1-mT, an inhibitor of IDO activity, showed increased numbers of virus-specific CTLs, resulting in a significant reduction in HIV-1 infected macrophages within the brain (Potula *et al.*, 2005).

The concomitant secretion of IFN-α, which possesses both immune stimulating and immune dampening capacities, and the immunosuppressive enzyme IDO by pDCs highlights their important role in helping to shape the adaptive response from the early stages of infection. Thus, the dynamics of pDC activation may be critical in tweaking the balance between a robust anti-viral and an immunosuppressive response. While the ability of HIV-1 to activate pDCs has been well established, the comparative ability of HIV-2 to induce pDC activation and IFN-α secretion is yet to be determined.

3.2 Hypothesis & Aims

In humans, infection with HIV-2 is generally well controlled and progression to disease is significantly less frequent compared to individuals infected with HIV-1. The hypothesis of this chapter is that HIV-1 favours viral persistence by creating an immunosuppressive environment characterized by more potent pDC-induced IFN-α secretion and higher IDO activity compared to HIV-2.

Specifically I aim:

- To test if there is a difference in the kinetic and viral dose-dependency of IFN-α secretion after *in vitro* stimulation of PBMCs with HIV-1 and HIV-2.

- To determine if there is an association between IFN-α production, viral replication and co-receptor usage
- To measure the levels of IDO activity induced by both HIV-1 and HIV-2.

3.3 Results

3.3.1 Virus Titration and Type I IFN Kinetic

PBMCs from three donors were cultured with different concentrations of HIV-1 or HIV-2 ranging from 0.039 $x10^9$ to 13 $x10^9$ RNA copies/ml over a 48 hour time period. Supernatants were collected at 3, 6, 9, 12, 18, 24 and 48 hours. Concentrations of type I IFN were measured in the supernatants by ELISA (Figure 3.1 and Figure 3.2). The intra- and inter-assay variabilities for the IFN-α ELISA were 3.43% and 14.72% respectively. For the IFN-β ELISA the intra- and inter-assay variabilities were 4.39% and 7.96% respectively.

Great variability in IFN-α production was observed among donors in response to both viruses. However, in all cases there was no IFN-α secretion detected at 3 or 6 hours even in response to the highest concentration of virus. Furthermore, there was no measureable IFN-α in the supernatants after culture with the two lowest viral concentrations tested (0.039 $x10^9$ and 0.13 $x10^9$ RNA copies/ml). In all three donors IFN-α production was greater in response to HIV-1 than HIV-2 (Figure 3.1) at the same concentration of viral RNA. IFN-β levels were negligible in the majority of cell culture supernatants tested, even after viral stimulation (Figure 3.2). Only one of the three donors tested showed IFN-β production in response to the two highest concentrations of HIV-1, but not HIV-2. IFN-β secretion was transient, increasing rapidly at 12 hours, and progressively declining at 18 and 24 hours, returning to baseline levels at 48 hours. No detectable levels of IFN-α were found in supernatants from PBMCs cultured in the absence of stimuli. Based on these results, IFN-α analysis was repeated on

another six donors, focussing on the four highest concentrations at time points between 9 and 48 hours (Figure 3.3).

After 9 hours incubation, IFN-α production was significantly higher in response to both 13 $x10^9$ and 3.9 $x10^9$ RNA copies/ml of HIV-1 compared to media alone (Figure 3.3A & B). Secretion of IFN-α was significantly higher compared to unstimulated cells at all time points starting from 12 hours onwards, independent of the concentration of HIV-1. In contrast, HIV-2 stimulation induced statistically significant IFN-α production compared to media alone only after 48 hours incubation, independent of viral concentration.

Based on the results obtained for the IFN-α kinetic in response to both HIV-1 and HIV-2, the time points at 9 and 24 hours after stimulation were chosen to further study IFN-α secretion. These time points were chosen as they represented the earliest time point at which IFN-α secretion could be detected, and the time point at which IFN-α production reached the peak of detection, respectively. Based on the results obtained with different virus concentrations, 13 $x10^9$, 3.9 $x10^9$ and 1.3 $x10^9$ RNA copies/ml were selected as optimal concentrations for PBMC stimulation. IFN-α secretion was measured in the supernatants from PBMCs cultured for 9 and 24 hours in the presence or absence of the three selected viral concentrations (Figure 3.4). HIV-1, but not HIV-2, induced a statistically significant increase in IFN-α production after 9 hours of culture, independent of the virus concentration. After 24 hours, IFN-α secretion was significantly increased by both HIV-1 and HIV-2 at all virus concentrations compared to media alone. However, HIV-1 was significantly more potent than HIV-2 at stimulating IFN-α production after 24 hours of culture, independent of the virus concentration. As shown in Figure 3.5, stimulation with both viruses achieved the maximum response within the range of concentrations used and confirms that the differences in the levels of IFN-α secreted by HIV-1 and HIV-2 cannot be overcome by simply increasing the concentration of HIV-2.

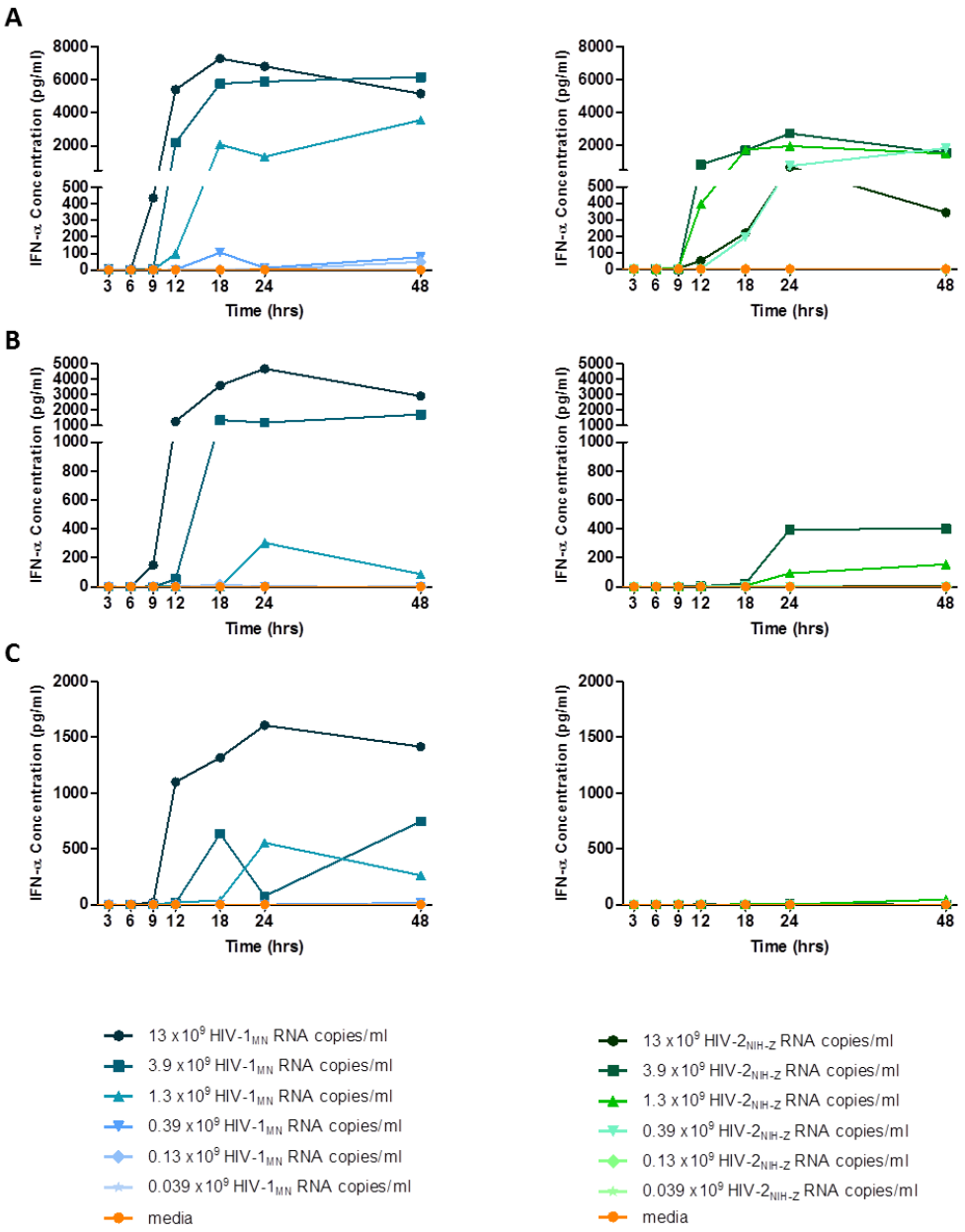

Figure 3.1. Virus titration and IFN-α kinetics from 3 independent donors. Graphs (A), (B) and (C) represent different healthy donors whose PBMCs were stimulated for periods of time ranging from 3 to 48 hours. IFN-α responses to HIV-1 stimulation are indicated in blue (left panels) and responses to HIV-2 are shown in green (right panels). Each symbol is indicative of an IFN-α response to the concentration of HIV-1 or HIV-2 shown in the key. Responses from unstimulated cells (media alone) are shown in orange.

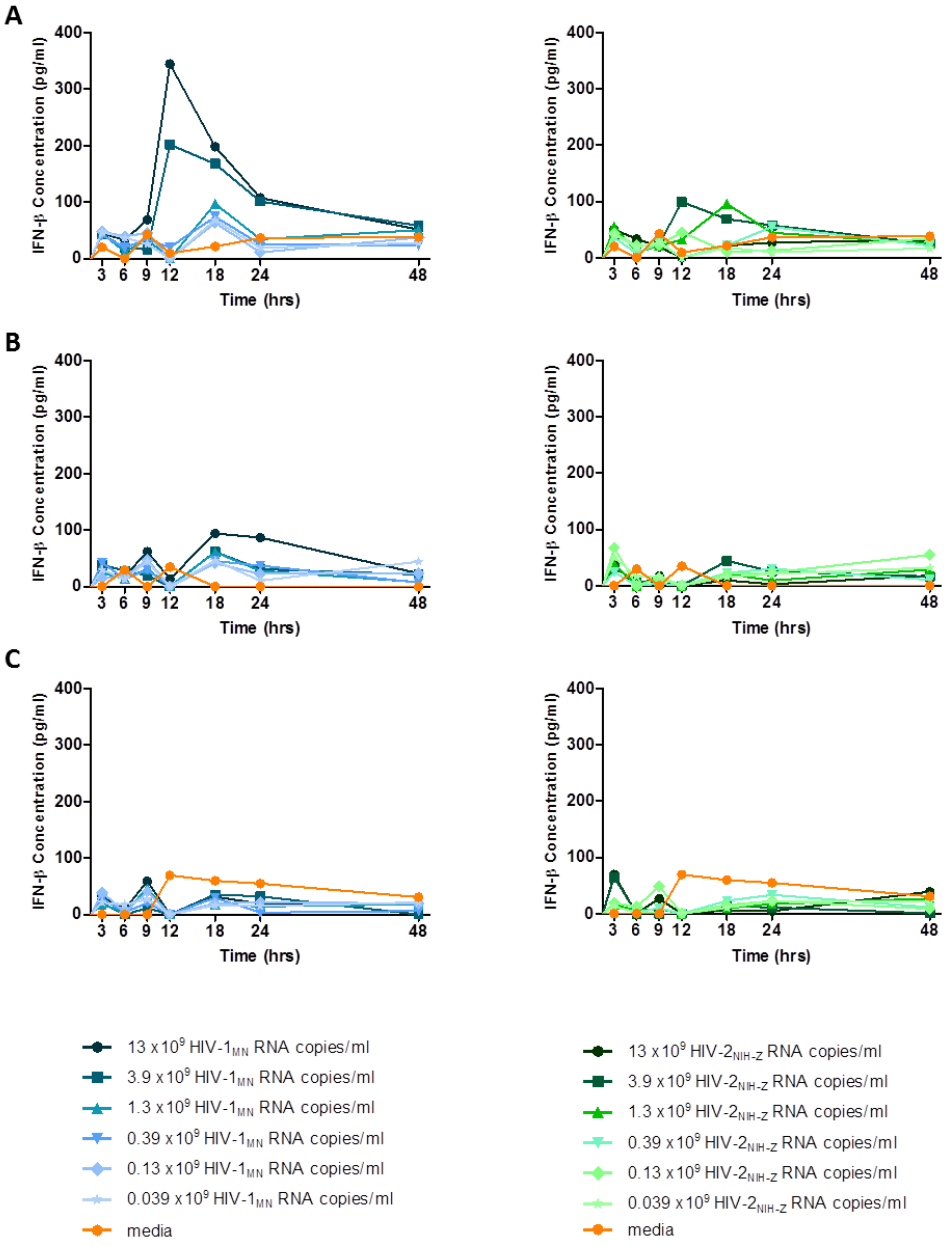

Figure 3.2. Virus titration and IFN-β kinetics from 3 independent donors. Graphs (A), (B) and (C) represent different healthy donors whose PBMCs were stimulated for periods of time ranging from 3 to 48 hours. Responses to HIV-1 stimulation are indicated in blue (left panels) and responses to HIV-2 are shown in green (right panels). Each symbol is indicative of an IFN-β response to the concentration of HIV-1 or HIV-2 shown in the key. Responses from unstimulated cells (media alone) are shown in orange.

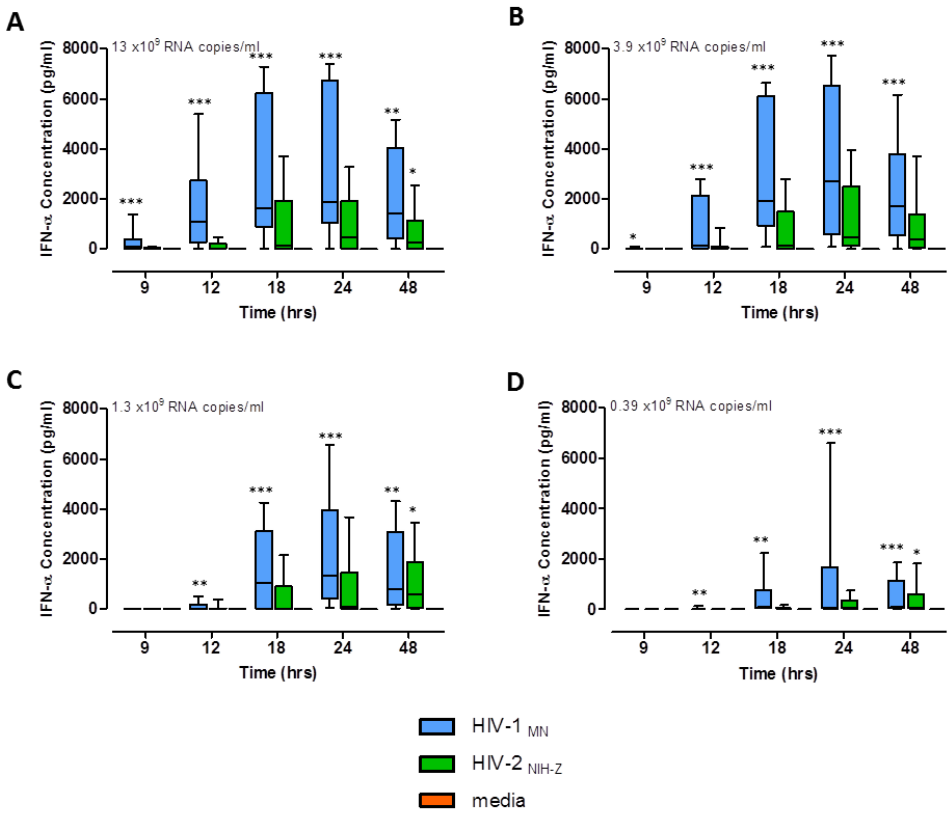

Figure 3.3. Virus titration and IFN-α kinetic. IFN-α responses to HIV-1 stimulation are indicated in blue, responses to HIV-2 are in green and responses to media alone (unstimulated cells) are shown in orange. Horizontal lines within bars represent median values, solid bars represent the interquartile range (IQR) and vertical lines extend to the 5th and 95th percentiles (N = 9). Graphs (A) to (D) represent different virus concentrations used. Responses to HIV-1, HIV-2 and media within individual time points and virus concentrations were compared using a Friedman test with a Dunn's post test for multiple analyses. *HIV vs media p<0.05, **HIV vs media p<0.01, ***HIV vs media p<0.001.

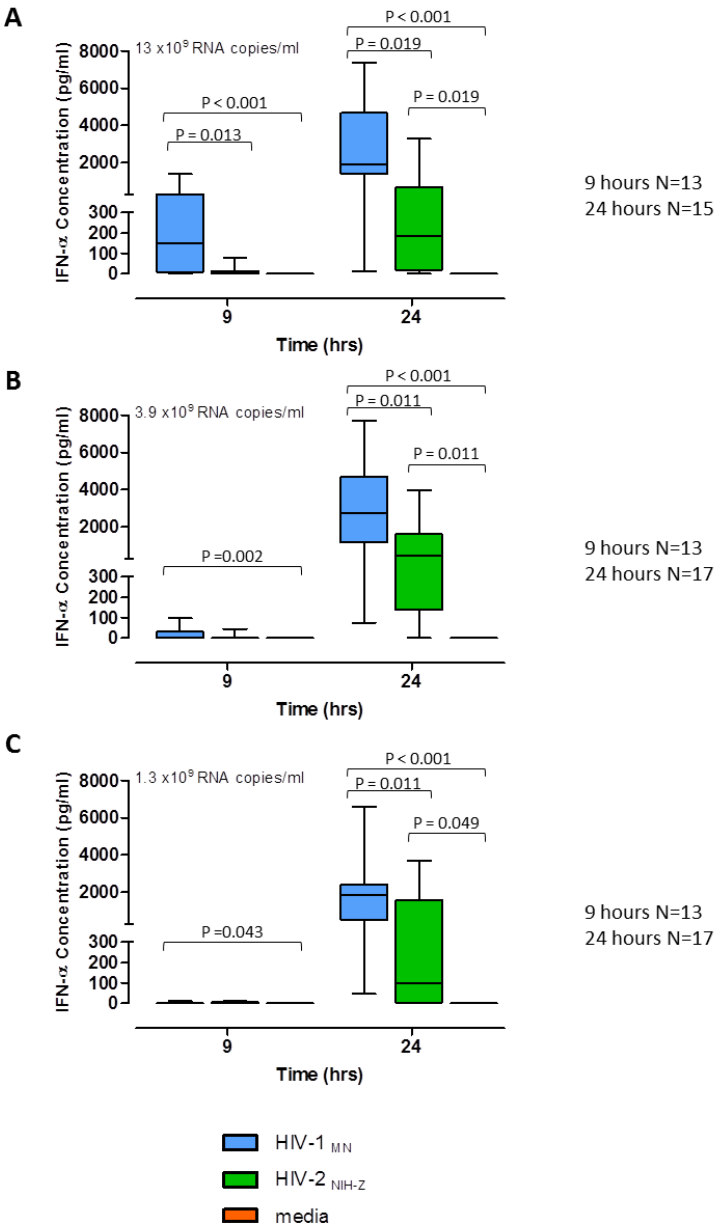

Figure 3.4. IFN-α secretion from PBMCs after incubation with HIV-1 or HIV-2 after 9 and 24 hours. IFN-α responses to HIV-1 stimulation are indicated in blue, responses to HIV-2 are in green and responses to media alone (unstimulated cells) are shown in orange. Horizontal lines within bars represent median values, solid bars represent the IQR and vertical lines extend to the 5th and 95th percentiles. Graphs (A), (B) and (C) represent different virus concentrations used. Responses to HIV-1, HIV-2 and media within individual time points and virus concentrations were compared using a Friedman test with a Dunn's post test for multiple analyses.

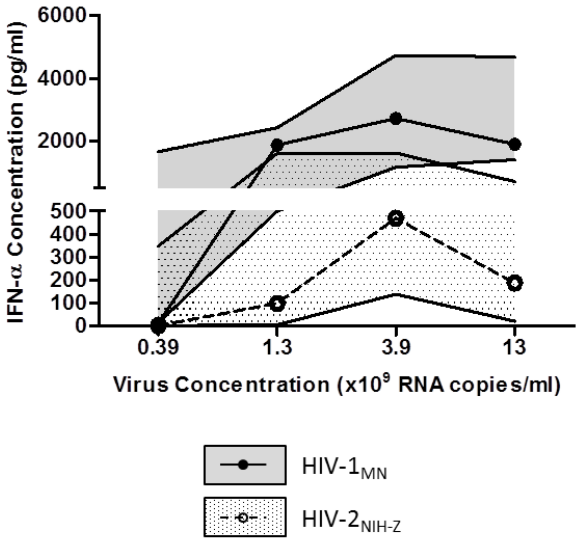

Figure 3.5. IFN-α secretion after 24 hours. Concentrations of secreted IFN-α after 24 hours only across all four concentrations of virus used. Symbols represent the median values, with HIV-1 denoted as solid circles and HIV-2 as open circles. Shaded areas extend to the interquartile range (IQR). The solid grey and patterned areas represent the IQR for HIV-1 and HIV-2 responses respectively.

3.3.2 Identification of pDCs as the main producers of IFN-α

Interferon-α secreting (IFN-α^+) pDCs were identified by flow cytometry after 9 and 24 hours stimulation with high (13 x10^9 RNA copies/ml) and low concentrations (1.3 x10^9 RNA copies/ml) of both HIV-1 and HIV-2. Supernatants from these cultures were also set aside for measurement of secreted IFN-α by ELISA. Figure 3.6 shows the correlation of the frequency of IFN-α^+ pDCs detected by flow cytometry and the concentration of IFN-α measured in cell culture supernatants. A significant correlation was observed at both 9 and 24 hours using all samples.

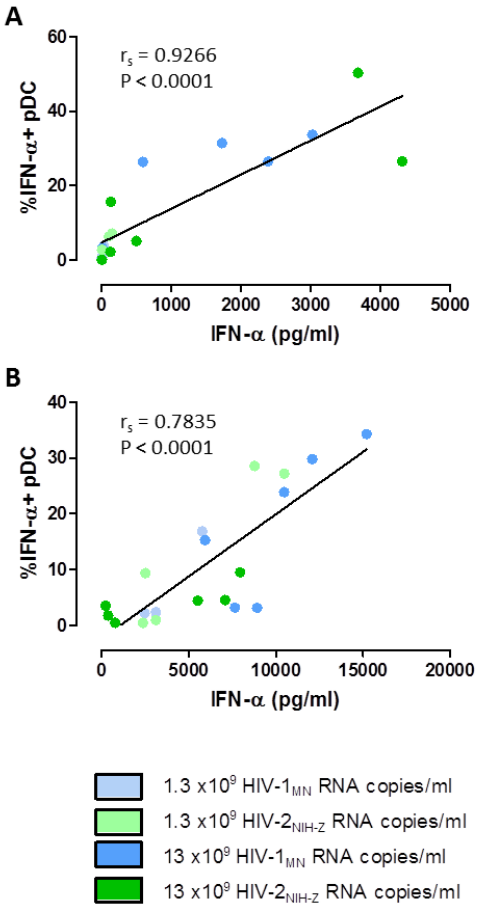

Figure 3.6. Correlation of IFN-α concentrations and IFN-α-producing cells. IFN-α concentrations measured in cell culture supernatants by ELISA, were correlated to the frequency of IFN-α secreting pDCs as detected by flow cytometry, after 9 (A) and 24 hours (B) viral stimulation. Responses to HIV-1 are shown in blue (light blue: low viral concentration, dark blue: high viral concentration) and responses to HIV-2 are represented in green (light green: low viral concentration, dark green: high viral concentration). Correlations were performed using a Spearman rank test.

3.3.3 Effect of Other Viral Isolates on IFN-α Secretion

Other viral isolates were also tested for their ability to induce IFN-α production from healthy PBMCs after overnight culture (Figure 3.7). A total of six different HIV-1 and two different HIV-2 isolates were tested using several different concentrations of virus. Live HIV-1_{MN} grown in either H9 or CEMx174 cells demonstrated similar abilities to induce IFN-α secretion. Live HIV-1_{IIIB} was still able to induce IFN-α secretion, although at levels slightly reduced compared to HIV-1_{MN} when used at 3.9 x10^9 and 1.3 x10^9 RNA copies/ml (Figure 3.7A). HIV-1 isolates which were rendered replication incompetent by treatment with aldrithiol-2 (At-2) were also used to stimulate PBMCs. All three viruses used; At-2 HIV-1_{MN} grown in either H9 or CEMx174 cells, and HIV-1_{Ada}, showed similar abilities to induce IFN-α secretion (Figure 3.7B). However, when used at concentrations of 3.9 x10^9 and 13 x10^9 RNA copies/ml, minimal IFN-α was detected in the cell culture supernatants. When compared to HIV-2_{NIH-Z}, HIV-2_{ST} showed a reduced ability to induce IFN-α production (Figure 3.7C). Measureable levels of IFN-α could only be detected after stimulation with concentrations between 13 and 130 x10^9 RNA copies/ml of HIV-2_{ST}. Whereas, IFN-α responses to HIV-2_{NIH-Z} began to decline when used at concentrations above and including 13 x10^9 RNA copies/ml. When all viral strains were compared at a concentration of 1.3 x10^9 RNA copies/ml it was observed that HIV-1 induced a greater production of IFN-α, independent of viral replication, the cell line used to propagate the virus, and co-receptor usage (Figure 3.8). Thus, all HIV-1 isolates tested were, on average, more potent stimuli for IFN-α secretion compared to HIV-2 when the viruses were used at similar concentrations.

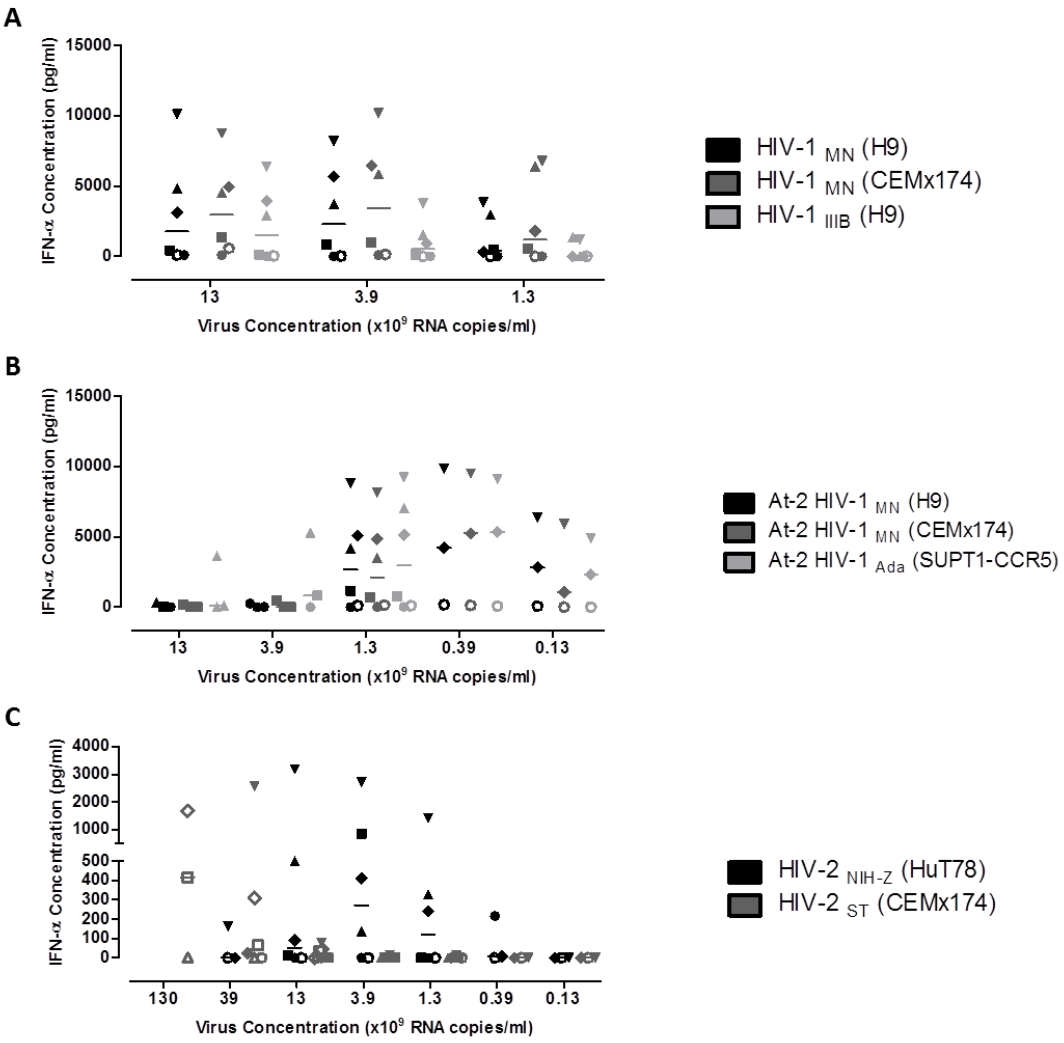

Figure 3.7. IFN-α response from PBMCs stimulated with different HIV-1 and HIV-2 isolates. (A) IFN-α secretion in response to live HIV-1_{MN} grown in H9 cells (black), live HIV-1_{MN} grown in CEMx174 cells (dark grey) and live HIV-1_{IIIB} grown in H9 cells (light grey). (B) IFN-α secretion in response to At-2 inactivated viruses: HIV-1_{MN} grown in H9 cells (black), HIV-1_{MN} grown in CEMx174 cells (dark grey) and HIV-1_{Ada} grown in SUPT1-CCR5 cells (light grey). (C) IFN-α secretion in response to live HIV-2_{NIH-Z} grown in HuT 78 cells (black) and live HIV-2_{ST} grown in CEMx174 cells (dark grey). Individual donors are represented by different symbols. Horizontal bars represent median values. Supernatants were tested after overnight incubation.

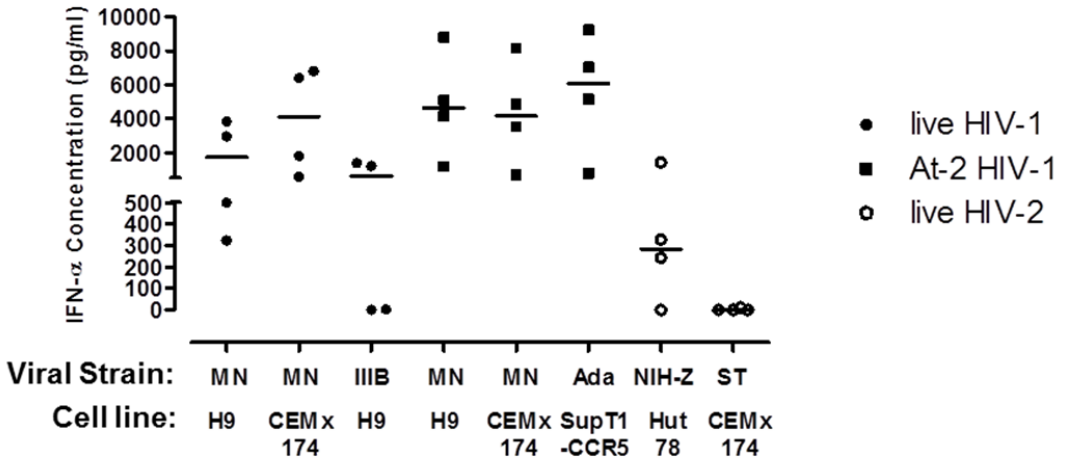

Figure 3.8. Summary of the IFN-α response to different HIV-1 and HIV-2 isolates. Live HIV-1 isolates are represented by filled black circles, At-2 inactivated HIV-1 isolates are denoted by filled black squares, and live HIV-2 isolates are shown as open circles. All viruses were used at a concentration of 1.3 x10^9 RNA copies/ml. Only donors responding to a minimum of one viral isolate are represented. Horizontal bars represent median values. Supernatants were tested after overnight incubation.

3.3.4 Effect of Viral Replication on IFN-α Secretion

The effect of viral replication on the IFN-α response was examined further by the addition of the anti-retrovirals AZT and d4T to PBMCs stimulated overnight with either HIV-1 or HIV-2 (Figure 3.9). In three independent donors, the addition of either AZT or d4T had no effect on the levels of IFN-α produced in response to either HIV-1 or HIV-2.

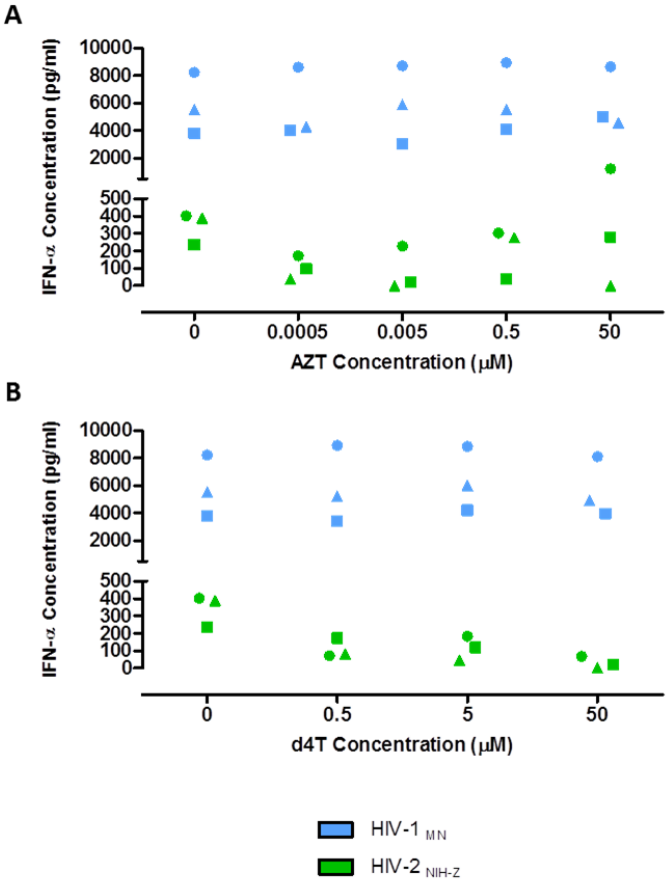

Figure 3.9. IFN-α response from PBMCs stimulated with HIV-1 and HIV-2 in the presence of anti-retrovirals. Graphs show the effect of the reverse transcription inhibitors AZT (A) and d4T (B) on IFN-α secretion following PBMC stimulation with HIV-1 and HIV-2. Responses to HIV-1 are shown in blue and those to HIV-2 are shown in green. A viral concentration of 13 x10^9 RNA copies/ml was used. Graphs show response to 3 individual healthy donors after overnight incubation. Each symbol is indicative of one individual donor.

3.3.5 IDO Activity

IDO activity was quantified by measuring the ratio of Kyn and Trp in the cell culture supernatants; a higher Kyn/Trp ratio indicates higher levels of enzymatic activity. PBMCs were incubated for 9 and 24 hours with three different concentrations of either HIV-1 or HIV-2 (13 $x10^9$, 3.9 $x10^9$ and 1.3 $x10^9$ RNA copies/ml) and IDO activity was subsequently quantified.

At 9 hours post incubation no measurable IDO activity was observed for all three concentrations of both HIV-1 and HIV-2 tested (Figure 3.10). After 24 hours, HIV-1 induced significantly higher levels of IDO activity compared to unstimulated cells, irrespective of the concentration of virus used. In contrast, Kyn/Trp ratios after culture with HIV-2 did not differ significantly from media. Furthermore, at the highest concentration of virus used, the levels of IDO activity induced by HIV-1 were significantly higher than that induced by HIV-2.

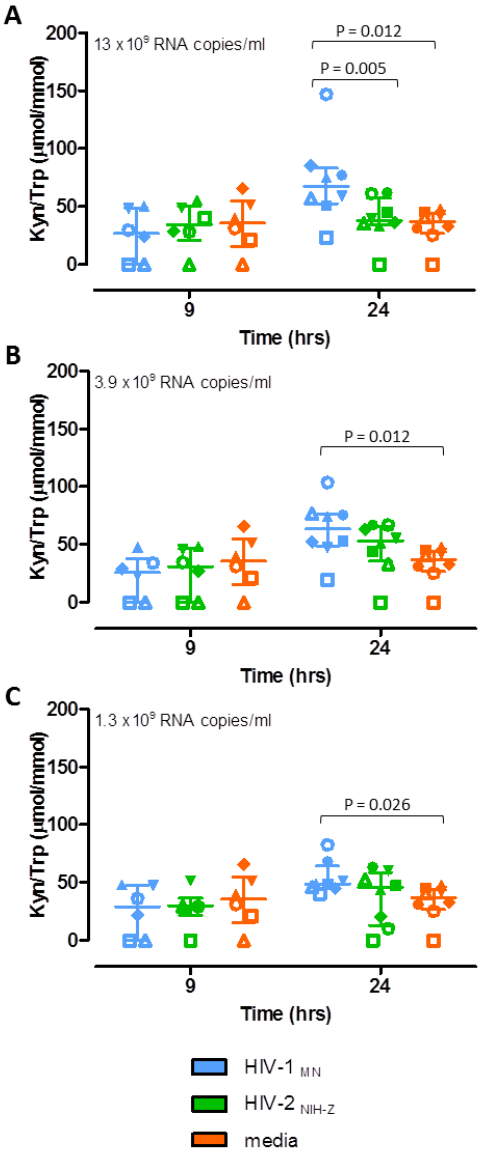

Figure 3.10. HIV-1 induces higher levels of IDO activity compared to PBMCs cultured with HIV-2. Graphs (A), (B) and (C) represent responses to different virus concentrations, as indicated in the top left of each graph, at both 9 and 24 hours. Responses to HIV-1 are shown in blue, HIV-2 in green and responses to media alone, representing unstimulated cells, are shown in orange. Horizontal lines represent median values and vertical lines show the IQR. Each symbol is indicative of one individual donor. Responses to HIV-1, HIV-2 and media within individual time points and virus concentrations were compared using a Friedman test with a Dunn's post test for multiple comparisons.

3.4 Discussion

It has previously been shown that depletion of pDCs from PBMCs and subsequent stimulation with influenza virus resulted in a greater than 90% reduction in IFN-α secretion when compared to whole PBMC populations (Jego *et al.*, 2003). This suggests that within whole PBMC populations pDCs are the main producers of IFN-α. Consistent with this report, pDCs were identified as the main source of IFN-α after HIV-1 and HIV-2 stimulation of PBMCs, illustrated in Figure 3.6. The frequency of IFN-α secreting (IFN-α^+) pDCs detected by flow cytometry correlated directly with the concentration of IFN-α measured in cell culture supernatants by ELISA at both 9 and 24 hours. The high correlation coefficients (r_s = 0.93 and r_s = 0.78 at 9 and 24 hours, respectively) suggest that the amount of IFN-α measured in the cell culture supernatants is determined by the frequency of IFN-α producing pDCs, indicating that pDCs are the main source of IFN-α in these conditions.

Upon exposing PBMCs to HIV-1 or HIV-2, large variations in IFN-α responses were observed from donor to donor. For example, with 13 x10^9 RNA copies/ml of HIV-1, the highest concentration of virus used, IFN-α concentrations ranged from 15 pg/ml to 7000 pg/ml after 24 hours culture (Figure 3.3A). Despite this variability there was consistently more potent IFN-α production in response to HIV-1 than HIV-2. IFN-α was not detectable after 3 and 6 hours of incubation even in response to the highest concentration of HIV-1. The lowest concentrations of HIV-1 tested (0.039 x10^9 and 0.13 x10^9 RNA copies/ml) also failed to induce detectable IFN-α responses (Figure 3.1). I therefore decided to focus on the time points and virus concentrations at which IFN-α secretion could be detected in the supernatants. Results from nine healthy donors showed that HIV-1 induced significantly higher levels of IFN-α secretion compared to media at all concentrations tested and all time points. In contrast, IFN-α responses to HIV-2 were not significantly different from media, except after 48 hours incubation (Figure 3.3). While IFN-α secretion was observed as early as 9 hours after PBMC incubation with HIV-1, measureable IFN-α secretion was only detected after 18 hours stimulation with HIV-2. As the concentration of HIV-1 and HIV-2 was decreased, both a delay and a reduction in the magnitude of

IFN-α production was observed. It is noteworthy that significant differences may be masked by the high variation of IFN-α production between donors. Based on these observations, analysis was focussed on 9 and 24 hours, which represent the earliest time of detectable IFN-α and the peak of production, respectively. Increased study numbers at 24 hours revealed significant differences between the levels of IFN-α produced, with HIV-1-exposed PBMCs secreting significantly higher levels of IFN-α than both HIV-2 and media, independent of the concentration of virus added to culture (Figure 3.4). HIV-2 also induced a significant increase in IFN-α production by PBMCs compared to media, but the levels were consistently below those induced by HIV-1.

Differences in the kinetics of different stimuli to induce IFN-α secretion are not surprising. O'Brien *et al* (2011) reported that pDCs activated using the synthetic TLR-7 ligand, imiquimod, secrete IFN-α within 30 minutes of stimulation, however, HIV-1 did not induce IFN-α production until 6 hours after stimulation. Furthermore, HIV-1 induces a delayed IFN-α response compared to other viruses such as influenza, which has been attributed to ligation of the scavenger receptor, BDCA2, with HIV gp120 (Lo *et al.*, 2012). Based on the data shown here, HIV-2 stimulation of PBMCs resulted in a significantly slower kinetic of IFN-α secretion than HIV-1.

Detectable IFN-β in the supernatants was only observed in a limited number of donors following PBMC exposure to HIV-1 (Figure 3.2). This may be due to the fact that while the IFN-α ELISA detects five different subtypes of IFN-α, there is only one type of IFN-β secreted by human cells, and perhaps the secretion levels are below the limit of assay detection in this experimental setup. Nonetheless, even in samples in which low levels of IFN-β were detected in response to HIV-1, no measurable IFN-β was observed in response to HIV-2, consistent with the results obtained for IFN-α. These results also suggest that IFN-β is secreted at early time points and only transiently. This is supported by reports showing that IFN-β is involved in initiating the type I IFN positive feedback loop and is therefore one of the earlier type I IFN genes to be transcribed (Honda and Taniguchi, 2006, Sato *et al.*, 1998).

To ensure the differences in IFN-α secretion observed in response to HIV-1_{MN} and HIV-2_{NIH-Z} stimulation were not restricted to these two particular strains, other HIV-1 and HIV-2 isolates were also tested for their ability to stimulate IFN-α secretion in PBMCs from healthy donors. HIV-2_{ST} was derived from an asymptomatic patient which may explain the less potent IFN-α response compared to HIV-2_{NIH-Z}. Overall, it appeared that HIV-1 strains were more potent than HIV-2 isolates at inducing IFN-α secretion *in vitro* (Figure 3.8).

In addition to different isolates, viruses grown in different cells lines were also tested. The HIV envelope is derived from the host cell from which the virus buds. Therefore, the cell line from which a virus is propagated can potentially affect its ability to gain entry and thus activate cells, as different cellular proteins will be incorporated into the viral envelope (Stefano *et al.*, 1993). In this experimental set up HIV-1_{MN} grown in the T cell line H9, as well as in the T cell/B cell hybrid CEMx174 were used, allowing a direct comparison of the effect of the cell line on virus induced IFN-α. Similar levels of IFN-α were observed after PBMC stimulation with either of these viruses. Furthermore, whether HIV-1 or HIV-2 were grown in a T cell line (HIV-1_{MN} and HIV-2_{NIH-Z}) or a T cell/B cell hybrid (HIV-1_{MN} and HIV-2_{ST}), HIV-1 was still able to induce a greater level of IFN-α secretion.

The differences in IFN-α production induced by HIV-1 and HIV-2 could reflect CD4 binding efficiencies. However, a previous report found no difference between HIV-1 and HIV-2 Env affinity for CD4. In fact, HIV-2 Env-mediated fusion with CD4 occurred within half the time of that by HIV-1 Env (Gallo *et al.*, 2006), thus suggesting that different mechanisms must be at play which result in the reduced IFN-α secretion observed in response to HIV-2.

While entry into pDCs occurs via CD4-dependent endocytosis, co-receptor binding could affect viral uptake efficiency and therefore pDC activation. In order to determine if the higher levels of IFN-α observed with HIV-1 compared to HIV-2 were not a result of different co-receptor usage, a CCR5-

tropic and a CXCR4-tropic HIV-1 strain were compared. Both At-2 HIV-1_{Ada} (CCR5-tropic) and At-2 HIV-1_{MN} (CXCR4-tropic) induced greater levels of IFN-α than HIV-2, indicating that it is not the co-receptor usage which defines HIV-1 as a stronger stimulus for IFN-α production. Indeed, previous studies have also shown that blocking co-receptor binding with neutralising antibodies (Schmidt *et al.*, 2005) or the CXCR4 and CCR5 antagonists, AMD-3100 and RANTES respectively (Beignon *et al.*, 2005, Herbeuval *et al.*, 2005c), does not affect HIV-1 endocytosis-dependent activation of pDCs. Furthermore, HIV-2 is more promiscuous in its use of co-receptors in order to facilitate cellular entry compared with HIV-1 (McKnight *et al.*, 1998), suggesting that restricted co-receptor binding is unlikely to affect pDC activation and thus IFN-α production.

As both HIV-1_{MN} and HIV-2_{NIH-Z} used in this study are live, replication competent viruses, it is possible that the higher concentrations of IFN-α measured in the supernatants in response to HIV-1 reflect faster or more efficient viral replication, and therefore increased concentrations of HIV-1 than HIV-2 overtime. However, IFN-α is a strong inhibitor of HIV-1 replication (Agy *et al.*, 1995) and the counter argument could be made that in conditions of high IFN-α production, HIV-1 replication may be suppressed. In addition, it is unlikely that significant viral replication occurred in this setting as the T cells were not stimulated: T cell stimulation (e.g. with anti-CD3/CD28 antibodies) is necessary for efficient infection and replication. PBMC stimulation with both live and replication incompetent (At-2 treated) HIV-1 showed no difference in IFN-α production, consistent with previous findings (O'Brien *et al.*, 2011), therefore excluding the possibility that HIV-1 replication contributes to enhanced IFN-α production. Interestingly, concentrations of At-2 HIV-1 higher than 1.3 $x10^9$ RNA copies/ml resulted in an almost complete abrogation of IFN-α secretion, which was observed with all three isolates tested (Figure 3.7B). Treatment of HIV with At-2 covalently alters the nucleocapsid zinc finger motifs required for reverse transcription (Arthur *et al.*, 1998). It is possible that this At-2-induced alteration in the secondary structure of the viral RNA modulates the virus's ability to induce IFN-α secretion at high concentrations. Consistent with this hypothesis, it has previously been demonstrated that while low

concentrations of CpG type-B (CpG-B) ODN sequences are able to induce the secretion of type I IFN, when pDCs are stimulated with high concentrations of CpG-B the type I IFN response is inhibited (Waibler *et al.*, 2008).

For technical reasons I was unable to use At-2 treated HIV-2 in this experimental setting. This was due to poor recovery of re-concentrated HIV-2 following At-2 treatment. Therefore to further exclude the possibility that viral replication may affect IFN-α production, PBMCs were incubated with either HIV-1 or HIV-2 in the presence of the reverse transcription inhibitors, AZT, or d4T. Both AZT and d4T are members of the class of anti-retrovirals known as nucleoside analogue reverse transcription inhibitors (NRTI) which compete with natural deoxynucleotides and upon incorporation into the growing DNA strand halt further transcription (Arts and Wainberg, 1996). *In vitro* both HIV-1 and HIV-2 display similar sensitivities to AZT and d4T (Smith *et al.*, 2008). The IFN-α profile remained unchanged when these anti-retrovirals were added to the culture system (Figure 3.9), indicating that neither HIV-1 nor HIV-2 replication affected pDC activation, as measured by IFN-α secretion.

In response to PBMC exposure to HIV-1 *in vitro*, pDCs have been reported as the main producers of the immunosuppressive enzyme IDO (Boasso *et al.*, 2007). However the effect of HIV-2 on IDO activity is yet to be investigated. These results show that after 24 hours of viral stimulation, HIV-1 induced a significantly greater level of IDO activity, as measured by the Kyn/Trp ratio in PBMC culture supernatants, compared to unstimulated cells (Figure 3.10). This effect was independent of the concentration of stimulus used. Furthermore, using the highest concentration of virus, the level of enzymatic activity induced by HIV-1 was significantly higher than that induced by HIV-2. The low levels of IDO activity observed after HIV-2 stimulation suggest that pDCs may not exert an immunosuppressive function via IDO-mediated Trp catabolism in response to HIV-2 in this acute setting. Perhaps another possibility is that the lower levels of inflammatory IFN-α in the setting of HIV-2 do not require a simultaneous increase in immunosuppressive pathways to potentially protect cells

from the harmful effects of intensified local inflammation. While type I IFN is not essential for IDO expression, it has been shown to increase IDO (Boasso *et al.*, 2007, Manches *et al.*, 2012). In a study examining acute SIV infection *in vivo*, Malleret *et al* (2008) reported a significant increase in the Kyn/Trp ratio, which correlated with both plasma IFN-α/β concentrations and viraemia. In the same study the authors found acute IDO activity correlated with an expansion in $CD8^+$ Tregs as well as a reduction in $CD4^+$ T cell activation (Malleret *et al.*, 2008). In my experimental setting it is possible that the lower concentrations of IFN-α induced by HIV-2 do not further enhance IDO expression, in contrast to HIV-1, where there are heightened levels of IFN-α after stimulation, possibly driving further IDO expression.

A wide range of viral concentrations was tested in this study, with only higher concentrations (greater than or equal to 0.39 $x10^9$ RNA copies/ml) able to induce detectable IFN-α secretion. During the acute phase of infection, after seroconversion, *in vivo* estimates of viral RNA have been reported as high as $10^4 – 10^6$ copies/ml (Berrey *et al.*, 2001, Fidler *et al.*, 2013, Hecht *et al.*, 2006, Jain *et al.*, 2013, Le *et al.*, 2013). Upon activation pDCs migrate to lymph nodes, which represent one of the major sites for viral replication (Hufert *et al.*, 1997). There are few estimates of viral concentrations in lymphoid tissues and how they correlate with plasma viral load, particularly during acute infection. A recent study however found that the infection rate of $CD4^+$ T cells within lymph nodes can be 2 – 17 fold higher than that observed in the periphery (Josefsson *et al.*, 2013), thus, *in vivo* pDCs are likely to encounter high titres of virus during acute infection. The biological relevance of these results would however need to be confirmed *in vivo* using viral loads similar to those seen during HIV transmission. During the clinical course of infection with HIV, high plasma concentrations of IFN-α have been reported (Stacey *et al.*, 2009), therefore suggesting that PBMCs *in vivo* do respond to these lower viral concentrations. Differences are likely to exist between how cells respond *in vivo* and *in vitro*, and it is possible that PBMCs require a more potent stimulus in order to respond in the artificial *in vitro* system. It is worth noting that the range of viral concentrations used in this study is similar to previous publications

(Beignon *et al.*, 2005, Boasso *et al.*, 2008b, Schmidt *et al.*, 2005, Lo *et al.*, 2012). Furthermore, these viral concentrations are similar to those used in sexual transmission studies performed in non-human primate models (Miller *et al.*, 2005).

Overall, these results show that HIV-2 is a weaker stimulus for pDC-mediated IFN-α production, compared to HIV-1. It is possible that the increased levels of type I IFN induced by HIV-1 help to limit early HIV-1 infection, however, this is inconsistent with HIV-2 being better controlled. Thus, similar to results found in the natural host of SIV (Bosinger *et al.*, 2013), lower IFN-α activation during the acute stages of infection, in addition to reduced IDO activity, may help to enhance HIV-specific T cell responses, thereby contributing to the lower pathogenicity of HIV-2. Whether HIV-2 simply represents a less potent stimulus for pDC activation compared to HIV-1 or if other mechanisms are reducing the HIV-2-induced type I IFN response will be further explored in Chapters 4 and 5.

Chapter 4 Mechanisms Influencing Type I IFN Secretion

4.1 Introduction

The production of type I IFN is one of the host's first defence responses against viral pathogens (Samuel, 2001). It plays a crucial step in establishing an anti-viral state as well as priming the adaptive immune system (McKenna *et al.*, 2005, Samuel, 2001). Type I IFN secretion occurs in two phases; initially, the host cell recognises PAMPs from the invading virus, through ligation with PRRs, resulting in the first wave of IFN-α/β secretion (Tailor *et al.*, 2006). Toll-like receptors and retinoic acid inducible gene I (RIG-I)-like receptors (RLRs) are the main PRRs involved in type I IFN signalling (Kawai and Akira, 2007). This initial secretion of type I IFN induces a positive feedback loop, giving rise to the second wave of type I IFN (Honda *et al.*, 2005c, Taylor and Mossman, 2013). The production of IFN-α/β is regulated at a transcriptional level, namely involving IFN regulatory factor (IRF) protein family members. There are nine IRF proteins currently identified, of which it has been shown that IRF-7 is the most critical for IFN signalling (Honda *et al.*, 2005b, Honda *et al.*, 2005c). Secretion of type I IFN by pDCs occurs by TLR-7 and TLR-9 recognition of single-stranded RNA or unmethylated CpG-rich DNA respectively (Lore *et al.*, 2003). Activation of TLR-7 or TLR-9 by their respective ligands induces recruitment of the signalling adaptor protein MyD88 (Kawai *et al.*, 2004). This results in a signalling cascade ultimately leading to phosphorylation and dimerisation of IRF-7, which translocates to the nucleus and initiates type I IFN gene transcription via binding to positive regulatory domains within type I IFN genes (Honda *et al.*, 2004) (Figure 4.1). The importance of IRF-7 in pDC induction of IFN-α/β secretion has been shown using knock-out mouse models. Thus, pDCs derived from Ifr-$7^{-/-}$ mice exhibited significant defects in the ability to secrete IFN-α/β in response to either viral challenge or synthetic CpG-rich ODN type A (CpG-A) (Honda *et al.*, 2005b). The ability of pDCs to rapidly secrete high concentrations of type I IFN is in part attributed to the constitutive expression of IRF-7, most likely supported by low levels of autocrine type I IFN (O'Brien *et al.*, 2011).

Other cell types, which do not express TLR-7 or TLR-9, are able to initiate type I IFN signalling through other PRRs, such as TLR-3 and RIG-I. TLR-3 recognises double-stranded RNA and, similar to TLR-7 and TLR-9, is expressed within endosomes (Kawai and Akira, 2007). Conversely, RIG-I is a cytosolic sensor of viral nucleic acids (Kawai and Akira, 2007). Engagement of these PRRs induces a signalling pathway independent of MyD88, mediated by TANK-binding kinase-1 (TBK1), which phosphorylates IRF-7 and IRF-3, resulting in IFN-α/β production (Honda *et al.*, 2005c, Borden *et al.*, 2007) (Figure 4.1).

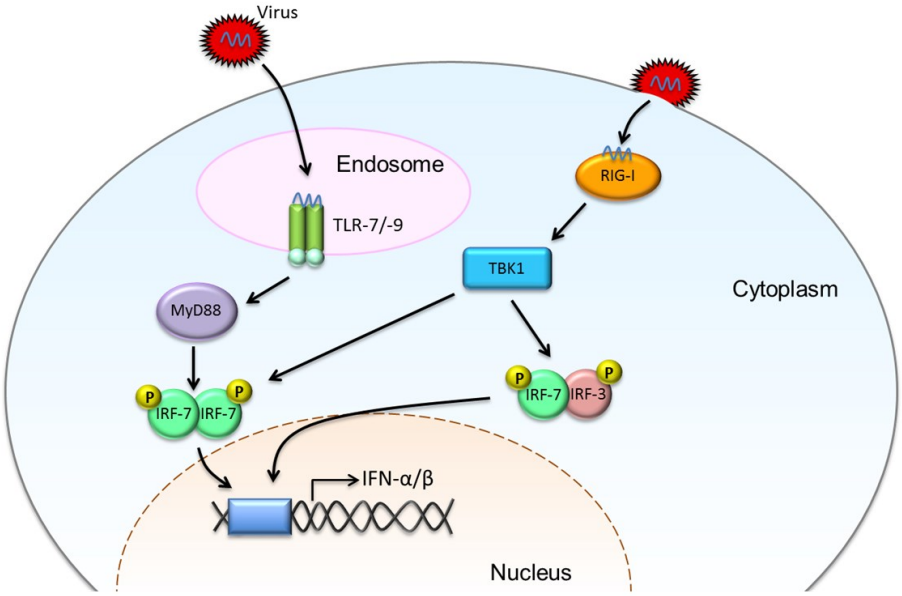

Figure 4.1. Viral induction of type I IFN production. Adapted from (Borden *et al.*, 2007).

This first wave of type I IFN acts in both an autocrine and paracrine fashion to further enhance the IFN response. The type I IFN receptor complex is composed of a dimer of two subunits, IFNAR1 and IFNAR2 (Borden *et al.*, 2007). Ligation of IFN-α/β with the IFN receptor complex activates the Jak kinase proteins, Tyk2 and Jak1, leading to phosphorylation of tyrosine residues on IFNAR1 (Honda *et al.*, 2005c). STAT1 and STAT2 proteins are subsequently recruited to the phosphorylated type I IFN receptor complex, and are also phosphorylated by Tyk2 and Jak1 (Honda *et al.*, 2005c). These activated STAT1 and STAT2 proteins together with IRF-9 form the ISGF3 complex. ISGF3 translocates to the nucleus and induces further expression of IRF-7 as well as expression of other IFN-stimulated

genes (ISG) via binding to an IFN-stimulated response element (ISRE) (Honda *et al.*, 2005c) (Figure 4.2). It is this second induction of type I IFN, via the IFN-receptor, which is thought to contribute to the majority of IFN-α/β secreted. In fact, the use of blocking antibodies against IFNAR2, which inhibit ligation of type I IFN with its receptor, almost completely ablates the IFN response to HIV-1 (O'Brien *et al.*, 2011).

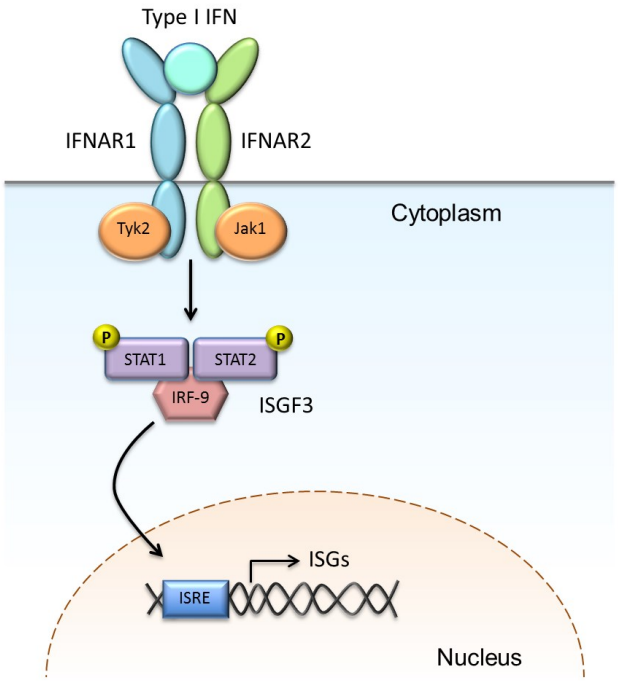

Figure 4.2. Type I IFN receptor signalling. Adapted from (Borden *et al.*, 2007).

In order to circumvent this potent type I IFN response, viruses have developed mechanisms to either evade detection or to reduce IFN-α/β production. As significant differences in the abilities of HIV-1 and HIV-2 to induce IFN-α secretion were observed (described in Chapter 3) the possibility that HIV-2 may attenuate type I IFN production was thus explored. Of particular note, suppressor of cytokine signalling (SOCS) proteins are induced by IFN and negatively regulate Jak kinase activity, therefore limiting the type I IFN feedback loop (Taylor and Mossman, 2013, Vlotides *et al.*, 2004). Increased expression of SOCS proteins has previously been reported in the tonsils of HIV infected individuals (Moutsopoulos *et al.*, 2006). Dengue virus also inhibits type I IFN signalling by down-regulating STAT2

expression, which renders viral replication insensitive to type I IFN once infection has been established (Jones *et al.*, 2005).

Cytokine expression can also influence IFN-signalling. The immunoregulatory cytokine IL-10 has been well studied for its ability to control pro-inflammatory cytokine expression (Sabat *et al.*, 2010). Dendritic cells express the IL-10 receptor and are sensitive to IL-10 (Payvandi *et al.*, 1998). Exogenous IL-10 was found to reduce IFN-α production in response to herpes simplex virus (HSV) stimulation. Likewise, in the same study, use of IL-10 receptor blocking antibodies increased the concentration of IFN-α secreted in response to HSV (Payvandi *et al.*, 1998). In addition, both IL-10 and TNF-α are reported to inhibit IFN-α production from pDCs stimulated with Sendai virus and HSV (Gary-Gouy *et al.*, 2002). The inflammatory cytokine IL-6 can also potentially dampen the IFN-response via up-regulation of SOCS3 (Taylor and Mossman, 2013). Furthermore, the cytokine environment in which pDCs are matured can influence IFN-signalling. Plasmacytoid DCs cultured in IL-4 containing media exhibit a reduced ability to produce IFN-α upon TLR-7 activation with the synthetic ligand imiquimod, compared to cells cultured in the presence of IFN-γ and IL-12 (Bratke *et al.*, 2011).

4.2 Hypothesis & Aims

The aim of this chapter is to test the hypothesis that the reduced potency with which HIV-2 activates IFN-α production may be a secondary result of immune regulatory mechanisms that are selectively activated by HIV-2 and not HIV-1.

Specifically the aim is to:

- Test whether HIV-2 inhibits the secretion of IFN-α. To this end, PBMCs were stimulated with either HIV-1 or HIV-2 in the presence of the synthetic TLR-9 ligand, CpG-A.

- Investigate whether the production of pro-inflammatory or regulatory cytokines are differentially affected by HIV-1 and HIV-2.
- Test the hypothesis that different gene expression profiles and pathways are activated after HIV-1 or HIV-2 stimulation

4.3 Results

4.3.1 HIV-2 Reduces the IFN-α Response to CpG-A

CpG-A was added to PBMC cultures overnight in the presence or absence of HIV-1 or HIV-2 in order to determine if addition of the virus would alter the level of IFN-α production induced by CpG-A alone. Secretion of IFN-α into cell culture supernatants was quantified by ELISA (intra- and inter-assay variabilities were 4.24% and 4.14% respectively). A titration matrix was performed on three individual healthy donors using CpG-A concentrations ranging from 0.018 to 0.5 μM and HIV-1 or HIV-2 ranging from 0.39 $x10^9$ to 13 $x10^9$ RNA copies/ml. No IFN-α was detected in supernatants of cells cultured with the lowest concentrations of CpG-A tested (0.018 and 0.05 μM) (data not shown). When used at 0.5 or 0.167 μM, CpG-A induced IFN-α secretion in all three donors (Figure 4.3). Secreted IFN-α concentrations were reduced by 76%, 73% and 20%, in each donor respectively, when 13 $x10^9$ RNA copies/ml of HIV-2 was added together with 0.5 μM CpG-A, compared to CpG-A alone. In contrast, 10%, 28% and 13% reductions were observed with 13 $x10^9$ RNA copies/ml of HIV-1 (Figure 4.3). Similarly, when 13 $x10^9$ RNA copies/ml of HIV-2 was added together with 0.167 μM CpG-A there was a 39%, 55% and 7% reduction in secreted IFN-α compared to 0.167 μM of CpG-A alone. Whereas a 10%, 12% and 62% increase in secreted IFN-α was observed, in each donor respectively, when 13 $x10^9$ RNA copies/ml of HIV-1 was added to 0.167 μM CpG-A (Figure 4.3). The inhibition of CpG-A-induced IFN-α was not observed when lower concentrations of HIV-2 were used. It is worth noting that the levels of IFN-α detected using HIV-2 + CpG-A were much higher than those induced by HIV-2 alone, suggesting that the majority of IFN-α secreted was most likely a result of CpG-A stimulation.

Based on these results, the assays were repeated using larger study numbers with 13 x 10^9 RNA copies/ml of virus and 0.5 µm CpG-A (Figure 4.4). A non-parametric Friedman test comparing CpG-A alone, HIV-1 + CpG-A and HIV-2 + CpG-A revealed that HIV-2 + CpG-A induced significantly less IFN-α compared to both CpG-A alone and HIV-1 + CpG-A. Similar results were also found when PBMCs were pre-incubated with HIV for three hours prior to the addition of CpG-A (Figure 4.4B).

A

	CpG 0.5 µM	CpG 0.167 µM	CpG 0 µM
13x HIV-1	2827.06	1202.87	2615.10
3.9x HIV-1	4223.52	4449.66	4753.40
1.3x HIV-1	5286.14	5150.32	1389.62
0.39x HIV-1	5063.20	3962.75	646.11
13x HIV-2	765.51	669.51	33.49
3.9x HIV-2	2945.04	2481.95	294.46
1.3x HIV-2	4635.61	3576.22	36.68
0.39x HIV-2	5303.54	4625.59	48.75
CpG alone	3149.23	1096.51	

B

	CpG 0.5 µM	CpG 0.167 µM	CpG 0 µM
13x HIV-1	4230.12	5024.94	6974.95
3.9x HIV-1	6637.47	7749.05	7357.86
1.3x HIV-1	8214.11	8032.78	5085.17
0.39x HIV-1	8259.70	7048.49	1259.57
13x HIV-2	1614.29	1994.02	433.71
3.9x HIV-2	4274.51	5078.15	1997.57
1.3x HIV-2	7973.04	6350.47	1893.34
0.39x HIV-2	6768.75	6106.79	163.88
CpG alone	5903.24	4468.44	

C

	CpG 0.5 µM	CpG 0.167 µM	CpG 0 µM
13x HIV-1	8104.35	11485.96	10812.01
3.9x HIV-1	10598.85	11178.01	10738.75
1.3x HIV-1	10356.95	10482.64	7202.19
0.39x HIV-1	9937.38	10462.14	2904.99
13x HIV-2	7496.84	6551.00	2664.00
3.9x HIV-2	10511.95	8971.34	3038.84
1.3x HIV-2	10006.37	9439.82	2430.90
0.39x HIV-2	10715.05	9680.28	19.40
CpG alone	9333.37	7079.19	

Figure 4.3. Heat map of IFN-α secretion induced by CpG-A in the presence or absence of HIV-1 or HIV-2. (A), (B) and (C) represent results from 3 independent donors. Values represent IFN-α concentration (pg/ml) as measured by ELISA in cell culture supernatants. Low concentrations are shown in yellow and high concentrations are in red. HIV concentrations are quoted as RNA copies/ml ($x10^9$).

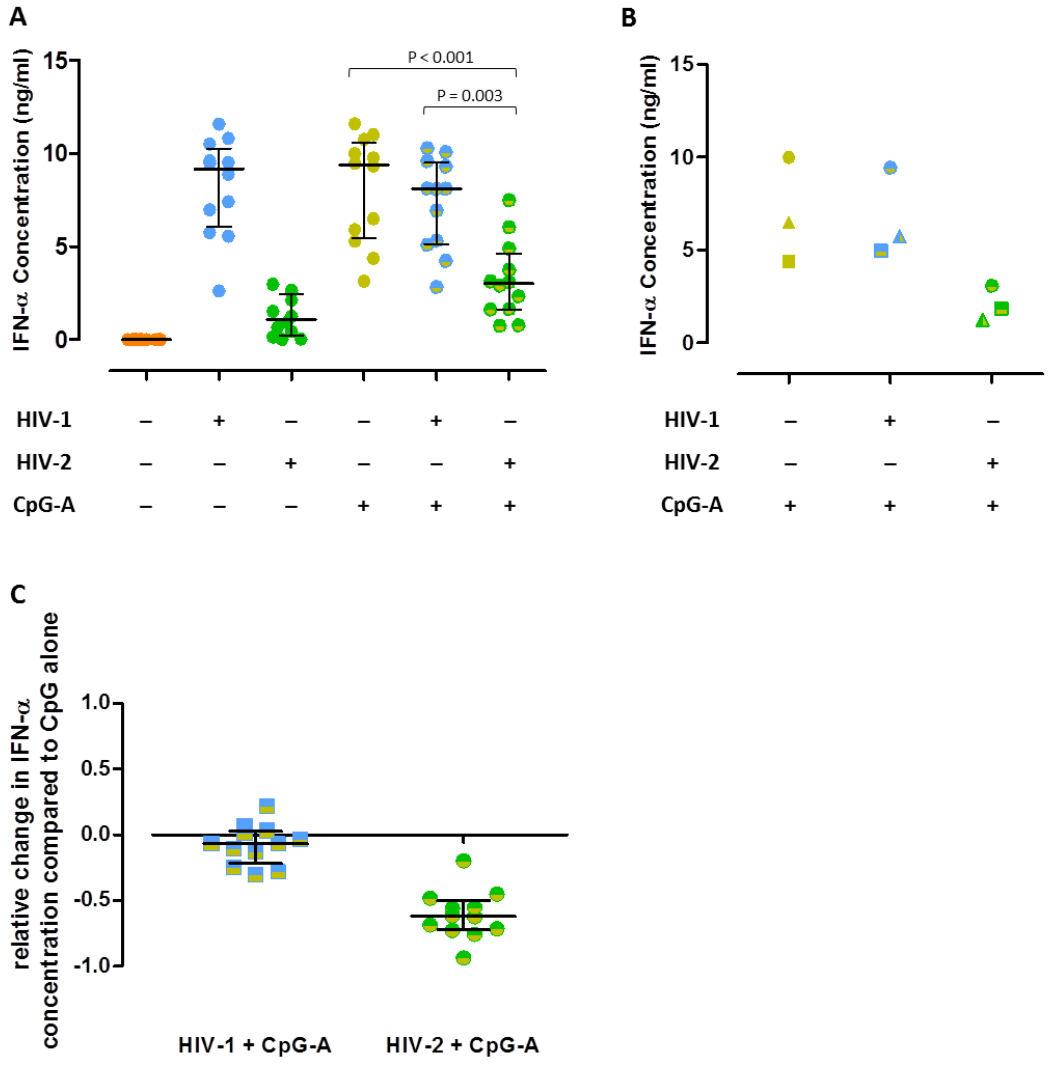

Figure 4.4. IFN-α secretion after PBMC stimulation with CpG-A in the presence or absence of HIV-1 or HIV-2. (A) PBMCs were stimulated for 24 hours with or without CpG-A (0.5 µM), HIV-1 or HIV-2 (13 x10^9 RNA copies/ml). Concentrations of IFN-α in cell culture supernatants were determined by ELISA. Horizontal bars represent median values and vertical lines show the IQR. (B) Three donors were pre-incubated with either HIV-1 or HIV-2 for 30 minutes prior to the addition of CpG-A. Symbols denote individual samples. (C) Graph showing the relative change in IFN-α concentration compared to CpG-A alone. This was calculated as ((HIV+CpG-A)-CpG-A)/CpG-A). Horizontal bars represent median values and vertical lines show the IQR.

4.3.2 Cytokines & Chemokines

The secretion of selected cytokines and chemokines was measured by flow cytometry in cell culture supernatants after PBMC incubation with HIV-1 or HIV-2 after 24 hours using a cytometric bead array (CBA, Becton Dickinson). Concentrations of IL-12p70 were undetectable in all samples (data not shown), while IFN-γ, IL-17A, IL-4 and IL-10 were below the detection level of the assay in more than two thirds (67%) of stimulated samples, reported values therefore had to be extrapolated from the standard curve (Figure 4.5). Measurable concentrations of IL-6 and IL-8 were observed in response to viral stimulation (Figure 4.5). Concentrations of TNF-α and IL-1β were minimal, however, as they have been reported to induce IL-6 secretion (Akira *et al.*, 1990), I decided to further explore their secretion in response to HIV-1 and HIV-2, in addition to IL-6 and IL-8. Thus, the experiment was repeated and the levels of selected cytokines were quantified using ELISA kits.

Concentrations of IL-8, IL-1β, TNF-α and IL-6 were measured by ELISA in cell culture supernatants after 24 hours stimulation of PBMCs with 13 $x10^9$ RNA copies/ml of either HIV-1 or HIV-2 (Figure 4.6). No significant difference in IL-8, IL-1β or TNF-α secretion was observed after viral stimulation compared to media alone. Concentrations of IL-1β and TNF-α remained relatively low, whereas IL-8 secretion was generally above 1423 pg/ml (IQR: 448.9 – 2528 pg/ml) even in the absence of stimulation. Secretion of IL-6 was increased following stimulation with both viruses, and reached statistical significance in response to HIV-2.

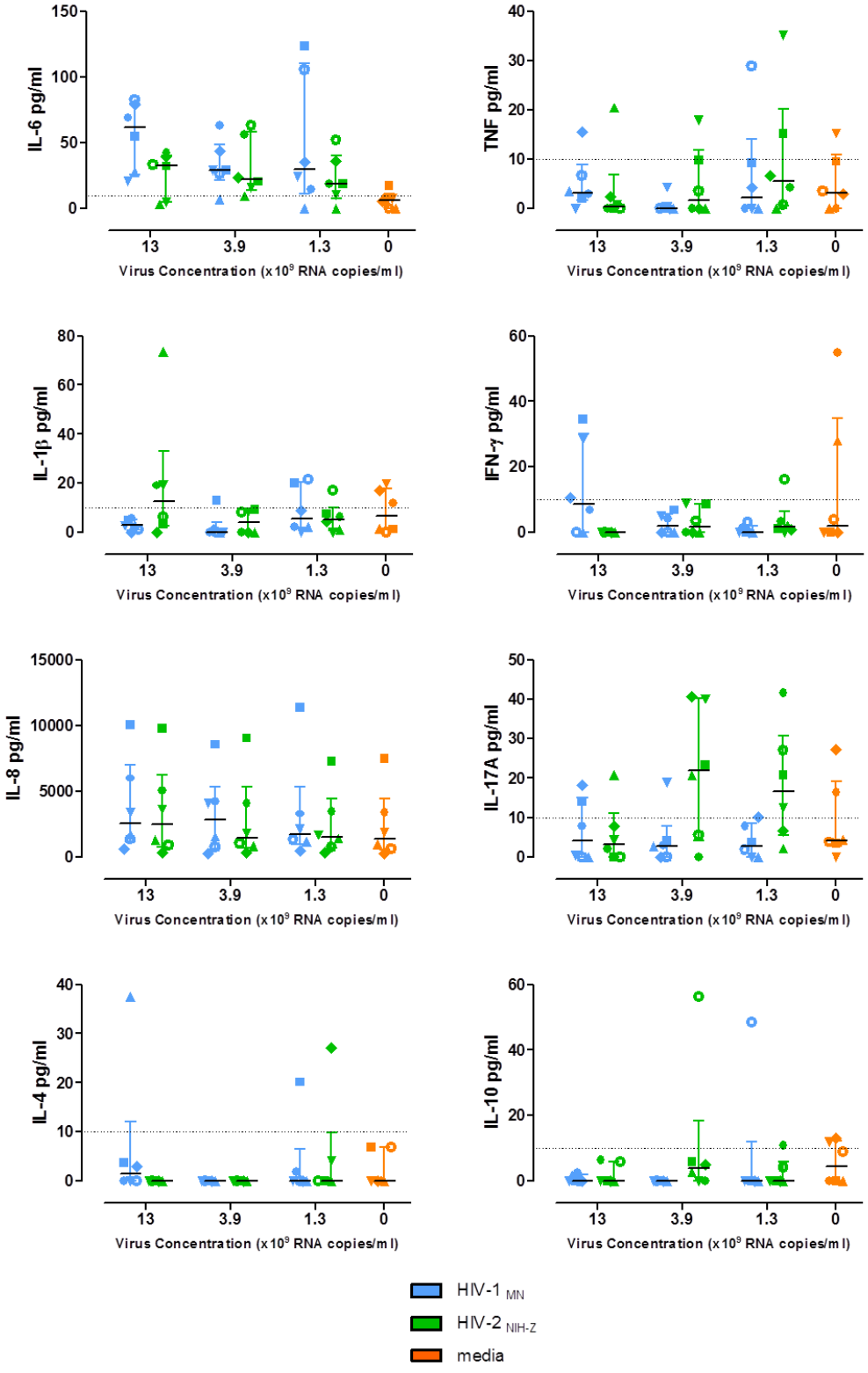

Figure 4.5 Cytokine secretion after PBMC stimulation with HIV-1 or HIV-2 after 24hours as measured by CBA. Multiple cytokines were measured in cell culture supernatants by flow cytometry, using a CBA kit. Responses to HIV-1 are indicated in blue, responses to HIV-2 are shown in green and responses to media alone, representing unstimulated cells are in orange. Horizontal lines represent median values and vertical lines show the IQR. Each symbol is indicative of one individual donor. The limit of assay sensitivity was 10 pg/ml and is shown by a dashed line.

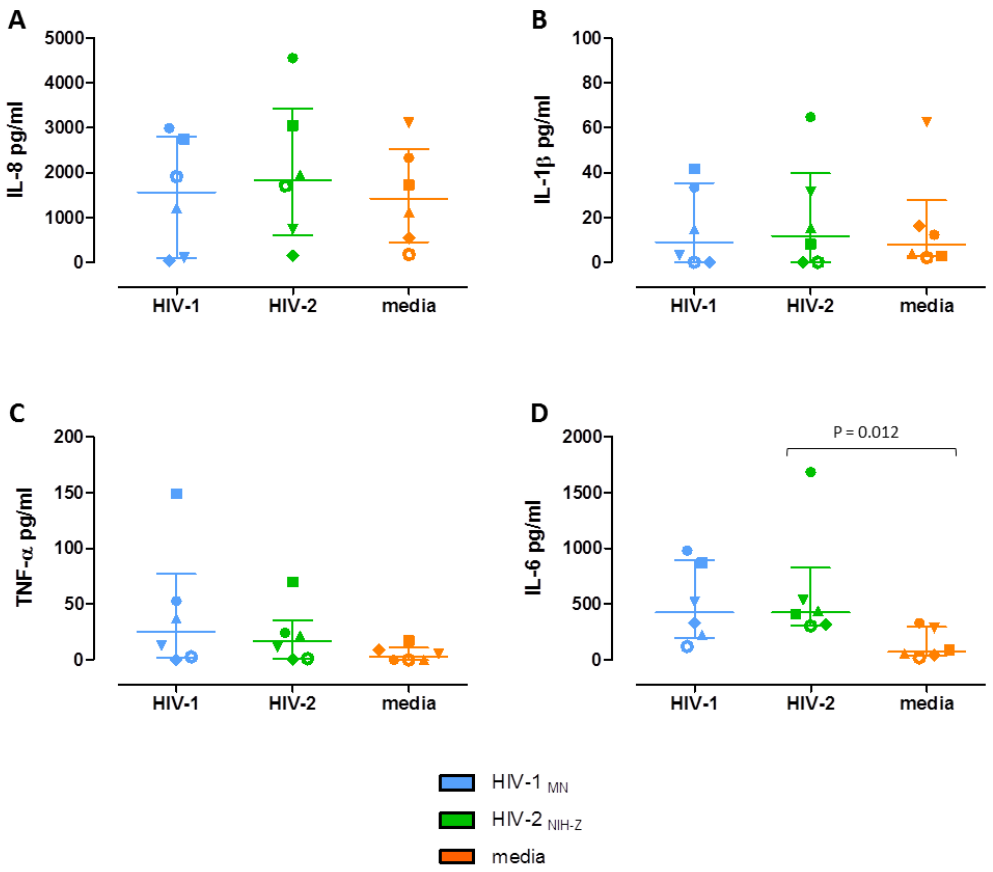

Figure 4.6. Cytokine secretion after PBMC stimulation with HIV-1 or HIV-2 after 24 hours, as measured by ELISA. Concentrations of (A) IL-8, (B) IL-1β (C) TNF-α and (D) IL-6 were measured in PBMC culture supernatants after 24 hours exposure to 13 x10^9 RNA copies/ml of either HIV-1 (shown in blue), or HIV-2 (shown in green), with media alone as a control for unstimulated cells (shown in orange). Horizontal lines represent median values and vertical lines show the IQR. Each symbol is indicative of one individual donor.

4.3.3 Type I IFN and IL-6 Interaction

As IFN-α was the main cytokine produced in response to viral stimulation, the effect of type I IFN signalling on IL-6 secretion was subsequently tested. Figure 4.7A shows the IL-6 response in PBMCs stimulated with HIV-1 or HIV-2 in the presence of antibodies directed against type I IFN or the IFN-α receptor subunit 2 (IFNAR2) (n=3). Both the anti-IFNAR2 neutralising antibody and anti-IFN-α/β antibodies resulted in a dramatic increase in IL-6 secretion, independent of stimulation. A matched isotype control had no effect on IL-6 production (data not shown). The effect of removing type I IFN from the culture system on IL-6 secretion was further explored by depleting pDCs from PBMCs. IL-6 can be produced by many different cell types, monocytes in particular respond to LPS by potent IL-6 secretion (Guha and Mackman, 2001). Thus the TLR-4 ligand, LPS, was used to stimulate IL-6 production in the pDC-depleted population. Figure 4.7B shows the results of one sample after pDCs were depleted from PBMCs (84% pDC depletion by magnetic bead separation, confirmed by flow cytometry). Stimulation of pDC-depleted PBMCs with LPS induced higher levels of IL-6 secretion compared to non-depleted PBMCs (123.8 ng/ml compared to 103.3 ng/ml). Conversely, when pDC-depleted cells were stimulated with LPS in the presence of exogenous type I IFN, the concentration of IL-6 was reduced to levels comparable to those observed using non-depleted PBMCs. Stimulation of pDC-depleted cells with type I IFN alone did not induce any IL-6 (data not shown). The concentrations of exogenous type I IFN used were chosen based on the range of secreted IFN-α measured after HIV stimulation of PBMCs (shown in Chapter 3, Section 3.3.1).

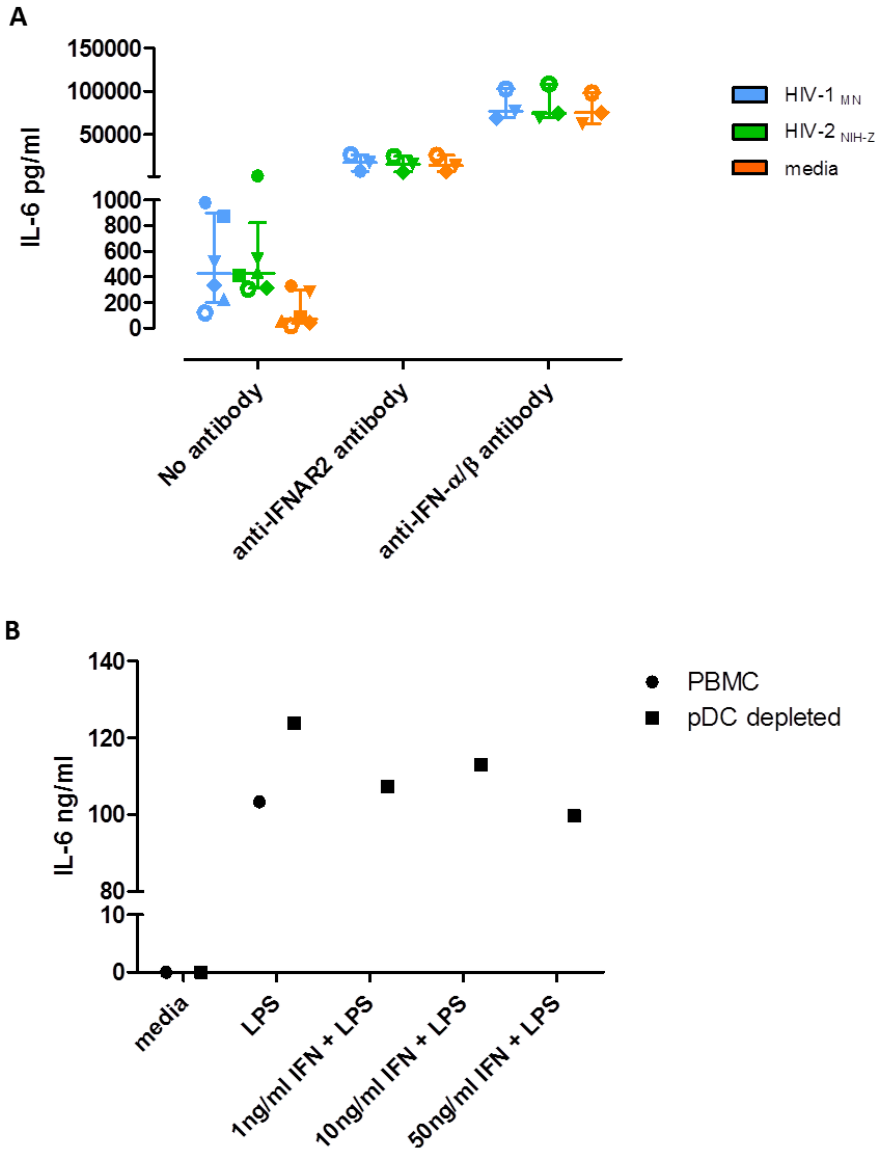

Figure 4.7 Effect of IFN-α on IL-6 secretion. (A) IL-6 secretion in response to PBMC stimulation with either HIV-1 (shown in blue) or HIV-2 (shown in green) at concentrations of 13 x10^9 RNA copies/ml or media alone (shown in orange) in the presence or absence of anti-IFNAR2 or anti-IFN-α/β antibodies. (B) IL-6 concentrations detected in the supernatants of cultured PBMCs from one donor. Responses observed in non-depleted PBMCs (media alone and LPS) are represented by circles, responses observed in PBMCs depleted of pDC (media alone, LPS and LPS + type I IFN) are indicated by squares.

4.3.4 Human Genome Array

A genome wide array was performed on PBMCs from three independent donors cultured with HIV-1, HIV-2, CpG-A or cell culture media alone for 6 and 12 hours. Principal component analysis (PCA) revealed that responses against HIV-1 and CpG-A largely overlapped, whereas responses against HIV-2 after 6 hours clustered separately (Figure 4.8A). This difference was no longer observed after 12 hours (Figure 4.9A). Analysis of gene expression compared to media alone by ANOVA showed that HIV-2 induced the differential expression of fewer genes compared to HIV-1 and CpG-A at both 6 and 12 hours (Figure 4.8B and Figure 4.9B). Furthermore, only 21 genes at 6 hours and 22 genes at 12 hours were differentially regulated by HIV-2 alone (list of genes is shown in Appendix Tables 5.1 and 5.2). Gene enrichment was subsequently performed on genes which showed modified expression in response to both HIV-1 and HIV-2, as well as in response to the two viruses separately (Figure 4.8C and Figure 4.9C), as described in Chapter 2 (Section 2.8.2) (a full list of the enriched genes is shown in Appendix Tables 5.3 – 5.8). The enriched genes were then classified into sub groups using the online database AmiGO (http://amigo1.geneontology.org/cgi-bin/amigo/go.cgi, Version 1.8, GO database release 2013-11-09) and available literature. At both 6 and 12 hours, expression of IFN genes was increased in response to all three stimuli, although expression levels were markedly higher in PBMCs stimulated with HIV-1 or CpG-A compared to HIV-2 (Figure 4.10A and Figure 4.11A). The type I IFN expression profile induced by HIV-2 after 12 hours was more similar to media alone than HIV-1 or CpG-A. Despite the differences in the expression of type I IFN genes, a similar increase in the expression of genes involved in IFN signalling (*IRF* and *STAT*) as well as ISGs was observed among all three stimuli at both time points tested (Figure 4.10 and Figure 4.11). Furthermore, a similar expression pattern was observed with HIV-1, HIV-2 and CpG-A for PRRs and PRR-associated genes, apoptosis-related genes and viral restriction factors (Figure 4.12 and Figure 4.13), with the exception of three PRR genes (*CLEC4A*, *CLEC5A* and *NLRC4*), which after 12 hours showed a more potent down-regulation in response to HIV-1 and CpG-A compared to HIV-2. After 6 hours, a small number of genes associated with the induction and regulation of adaptive immune responses were down-regulated in

response to viral stimulation, but remained higher in cells exposed to HIV-2 compared to HIV-1 or CpG-A (Figure 4.16A). The expression pattern of cytokine and chemokine genes was similar across HIV-1, HIV-2 and CpG-A stimulated samples after 6 hours (Figure 4.16B). Following 12 hours of stimulation, the expression profile of genes associated with the adaptive immune response was similar among the three stimuli (Figure 4.17A). However, expression of *CXCL3*, *CXCL5*, *CXCL6*, *CCL20* and *IL1A* was reduced in response to HIV-1 and CpG compared to media, an effect which was less pronounced in response to HIV-2 (Figure 4.17B).

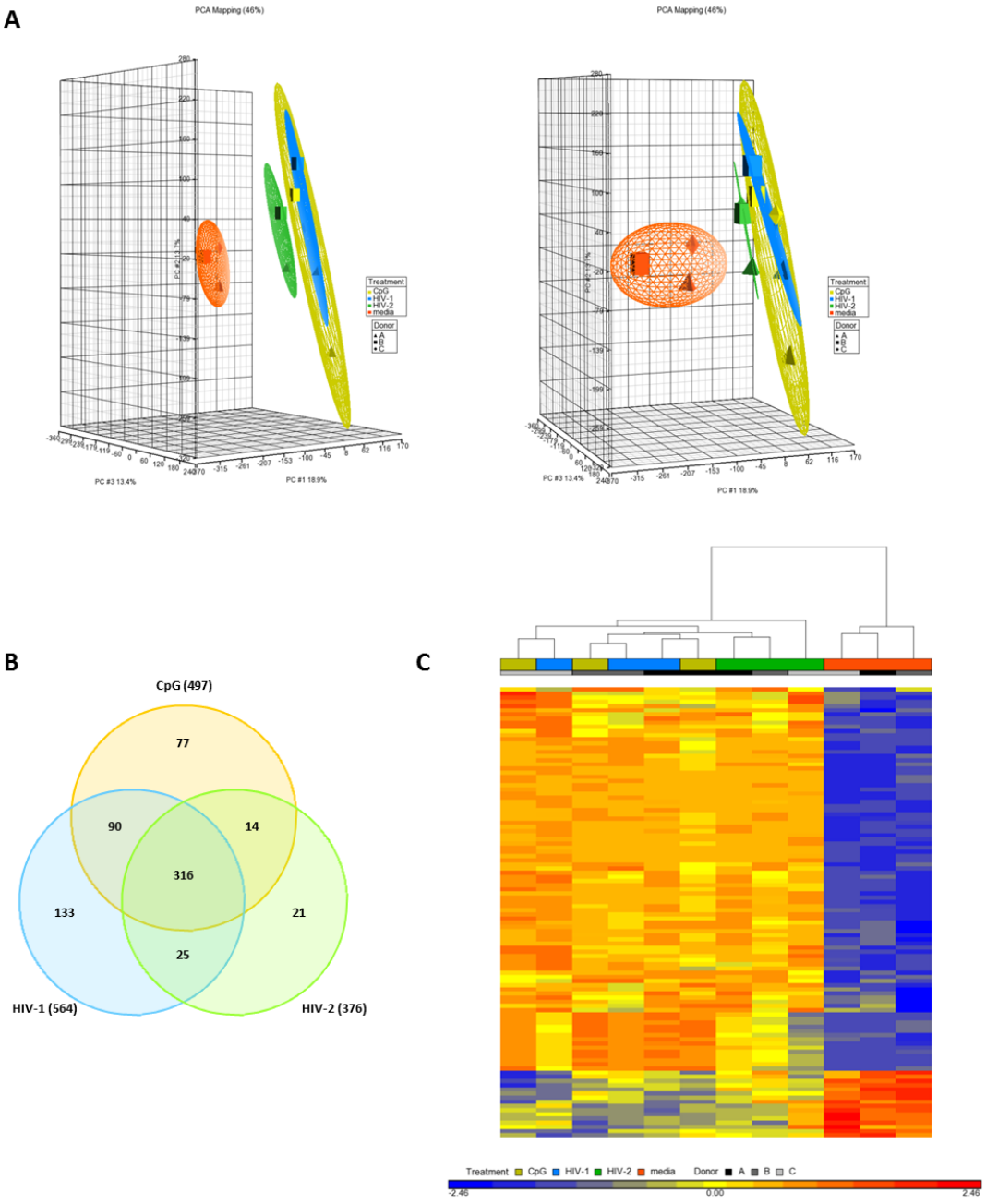

Figure 4.8. Gene expression profile in PBMCs stimulated with HIV-1, HIV-2 or CpG for 6 hours. (A) PCA performed on complete gene expression profiles of PBMCs stimulated for 6 hours with HIV-1 (blue), HIV-2 (green), CpG-A (yellow) and unstimulated cells (orange). The three independent donors are represented by different symbols. The graphs show two different viewpoints of the same 3-dimensional graph. (B) Venn diagram indicating the overlap of genes differentially regulated by HIV-1, HIV-2 and CpG-A compared to media, as determined by ANOVA. (C) Heat map of enriched genes. Each column represents the response from a single donor to HIV-1 (blue), HIV-2 (green), CpG-A (yellow) and media alone (orange). Gene expression levels are indicated by colour transitions from blue (lowest expression) to red (highest expression) according to the legend displayed below the heat map.

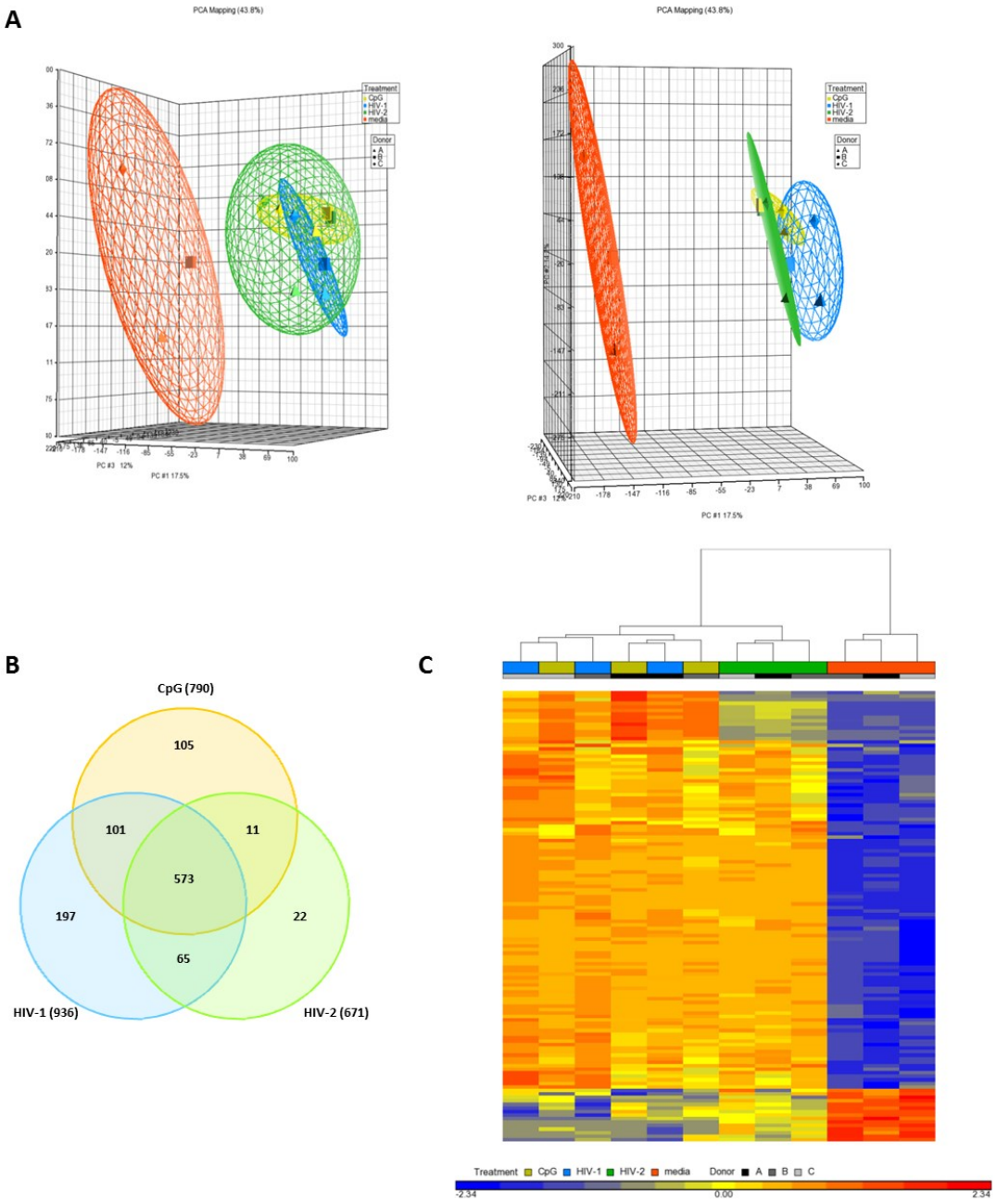

Figure 4.9. **Gene expression profile in PBMCs stimulated with HIV-1, HIV-2 or CpG for 12 hours.** (A) PCA performed on complete gene expression profiles of PBMCs stimulated for 12 hours with HIV-1 (blue), HIV-2 (green), CpG-A (yellow) and unstimulated cells (orange). The three independent donors are represented by different symbols. The graphs show two different viewpoints of the same 3-dimensional graph. (B) Venn diagram indicating the overlap of genes differentially regulated by HIV-1, HIV-2 and CpG-A compared to media, as determined by ANOVA. (C) Heat map of enriched genes. Each column represents the response from a single donor to HIV-1 (blue), HIV-2 (green), CpG-A (yellow) and media alone (orange). Gene expression levels are indicated by colour transitions from blue (lowest expression) to red (highest expression) according to the legend displayed below the heat map.

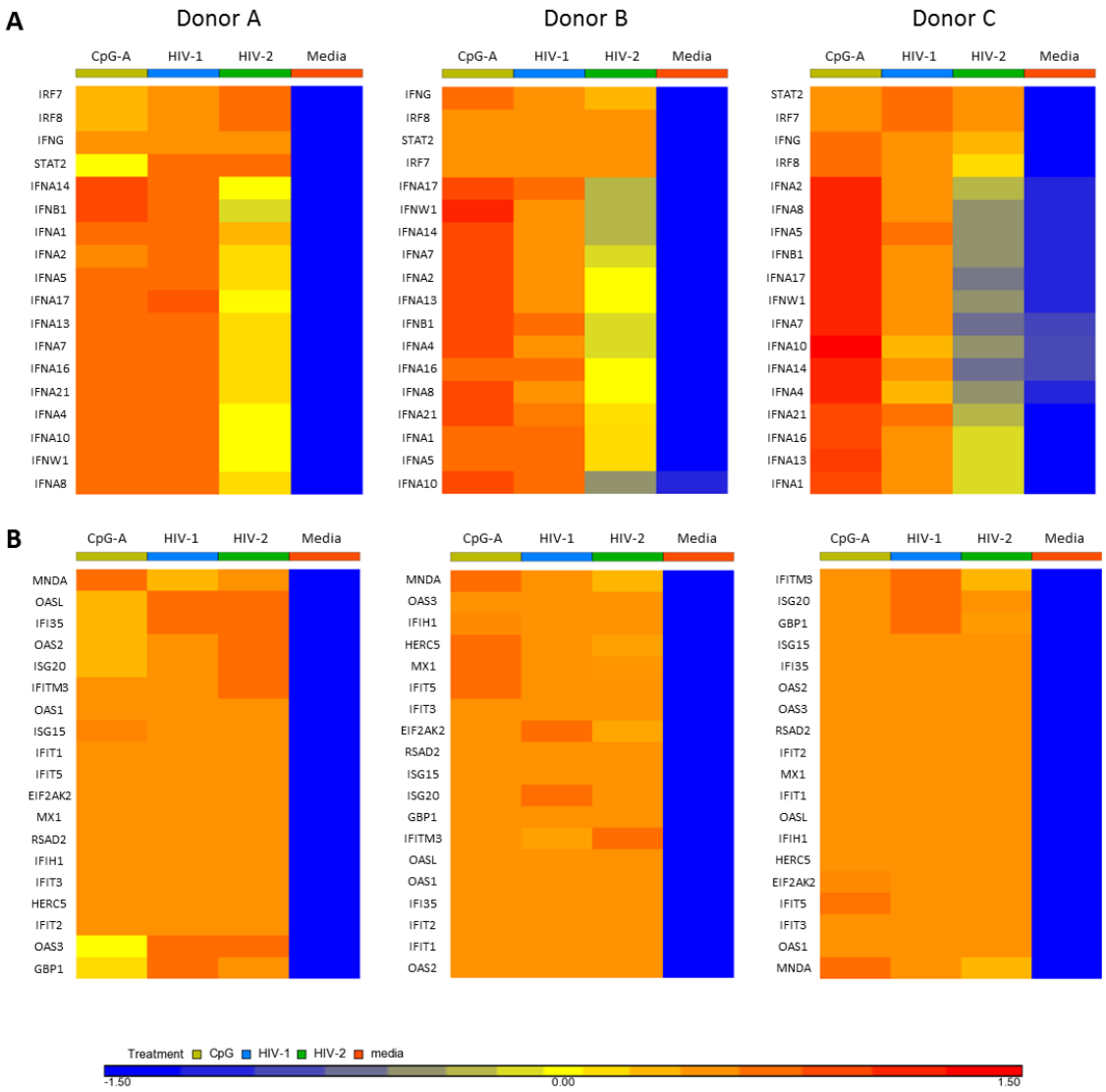

Figure 4.10. Expression of enriched genes associated with the IFN response after 6 hours of stimulation. (A) Heat map of IFN-I and IFN-II genes, as well as genes involved in IFN signalling: *IRF* & *STAT*. (B) Heat map of ISGs. Each heat map represents responses from an individual donor. Each column represents a different treatment: HIV-1 is headed in blue, HIV-2 in green, CpG-A in yellow and PBMCs incubated with cell culture media alone are shown in orange. Gene expression levels are indicated by colour transitions from blue (lowest expression) to red (highest expression) according to the legend displayed below the heat maps.

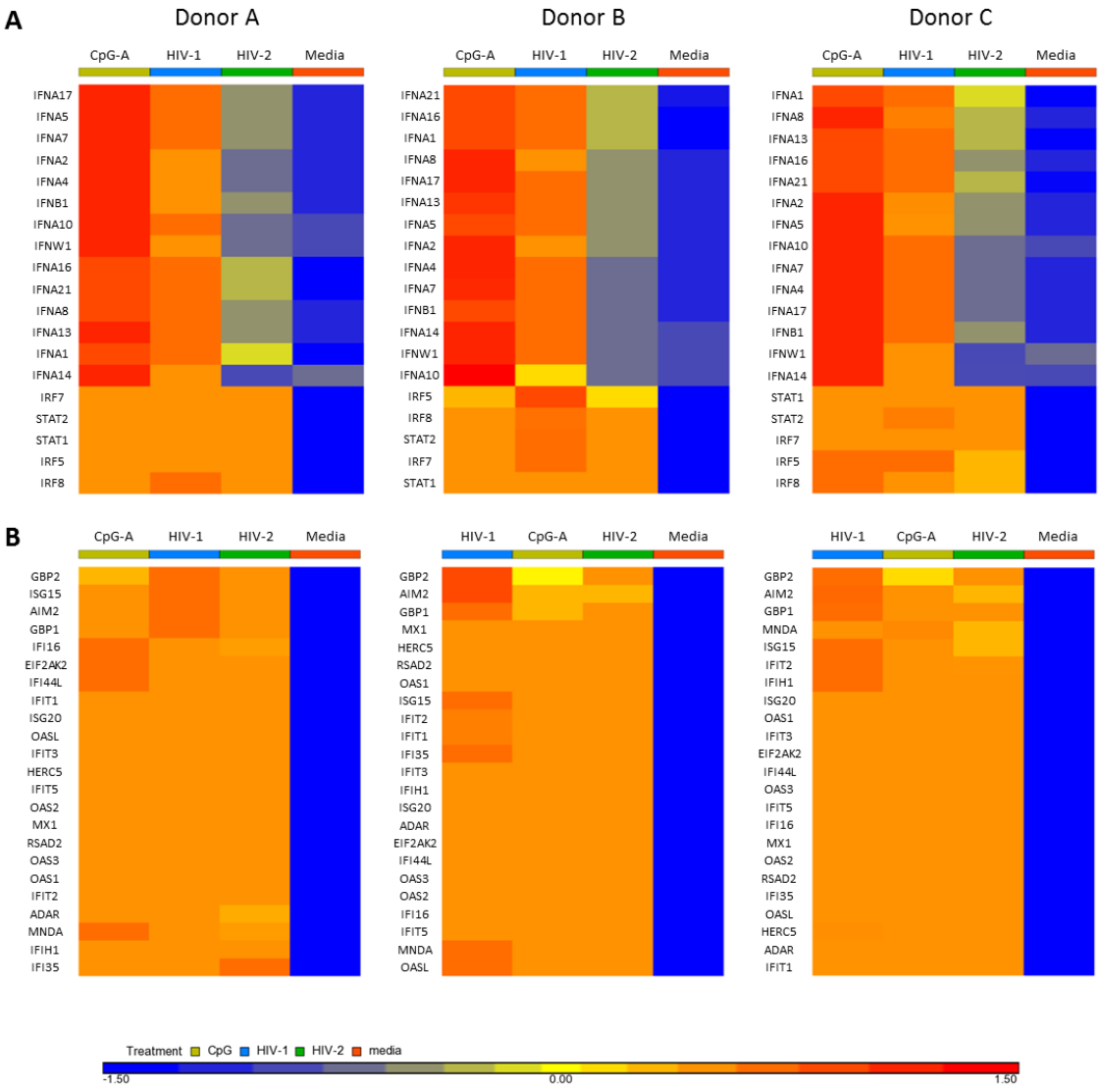

Figure 4.11. Expression of enriched genes associated with the IFN response after 12 hours of stimulation. (A) Heat map of IFN-I and IFN-II genes, as well as genes involved in IFN signalling: *IRF* & *STAT*. (B) Heat map of ISGs. Each heat map represents responses from an individual donor. Each column represents a different treatment: HIV-1 is headed in blue, HIV-2 in green, CpG-A in yellow and PBMCs incubated with cell culture media alone are shown in orange. Gene expression levels are indicated by colour transitions from blue (lowest expression) to red (highest expression) according to the legend displayed below the heat maps.

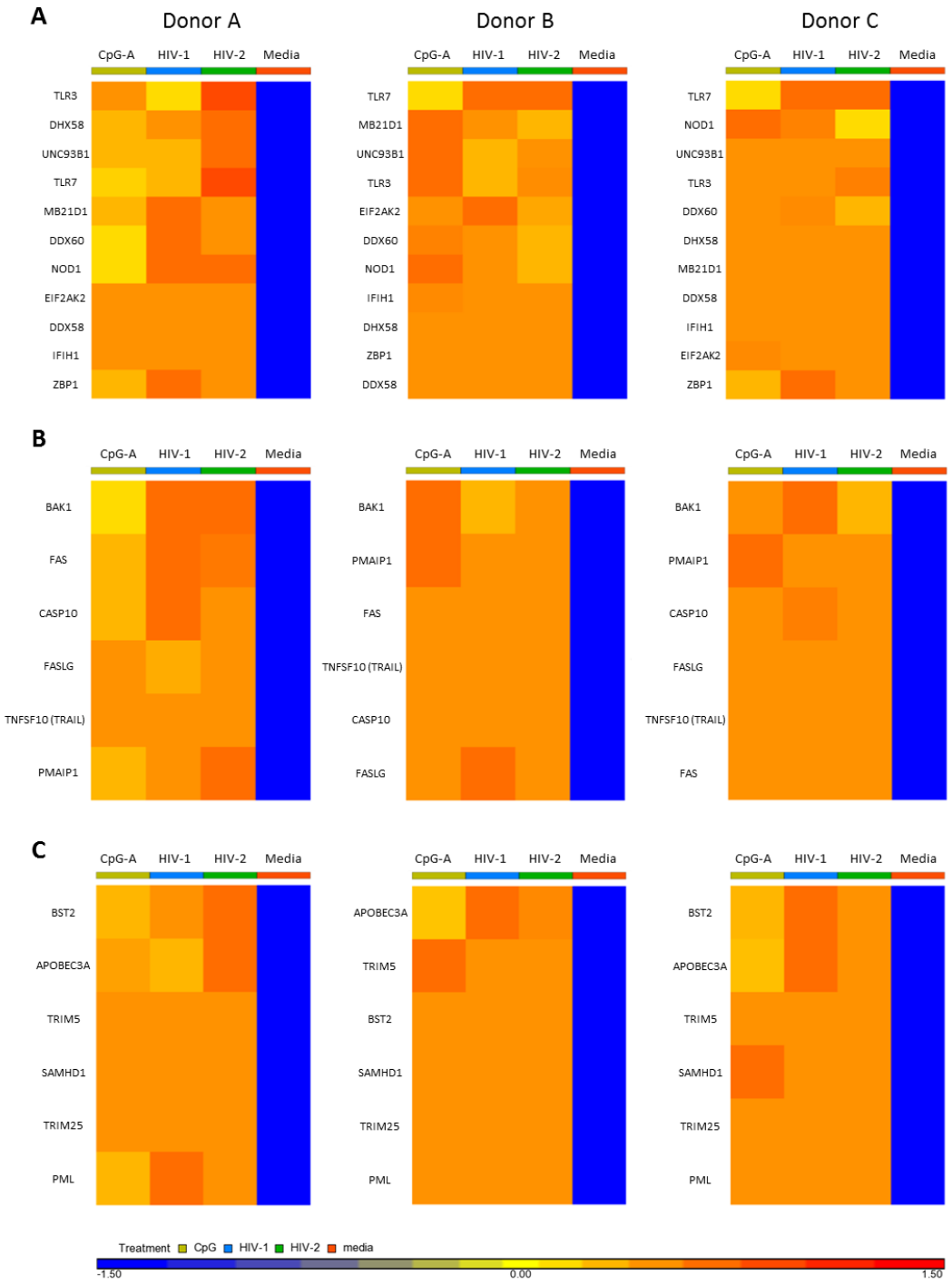

Figure 4.12. Heat map of PRR, apoptosis and viral restriction genes after 6 hours of stimulation. Expression of (A) PRRs and genes associated with PRRs, (B) genes associated with apoptosis and (C) viral restriction factors. Each heat map represents responses from an individual donor. Each column represents a different treatment: HIV-1 is headed in blue, HIV-2 in green, CpG-A in yellow and unstimulated PBMCs (incubated with cell culture media alone) are shown in orange. Gene expression levels are indicated by colour transitions from blue (lowest expression) to red (highest expression) according to the legend displayed below the heat maps.

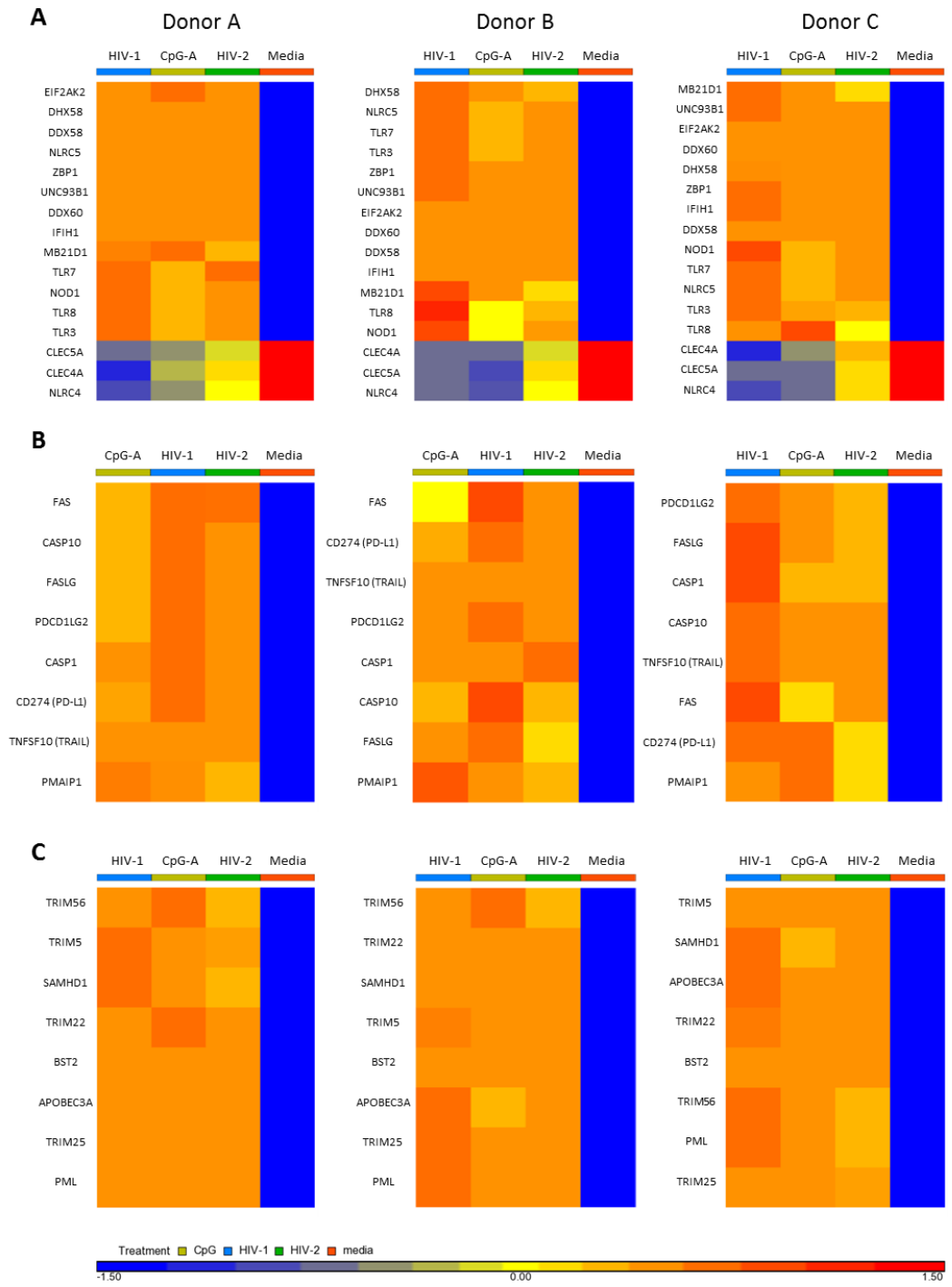

Figure 4.13. Heat map of PRR, apoptosis and viral restriction genes after 12 hours of stimulation. Expression of (A) PRRs and genes associated with PRRs, (B) genes associated with apoptosis and (C) viral restriction factors. Each heat map represents responses from an individual donor. Each column represents a different treatment: HIV-1 is headed in blue, HIV-2 in green, CpG-A in yellow and unstimulated PBMCs (incubated with cell culture media alone) are shown in orange. Gene expression levels are indicated by colour transitions from blue (lowest expression) to red (highest expression) according to the legend displayed below the heat maps.

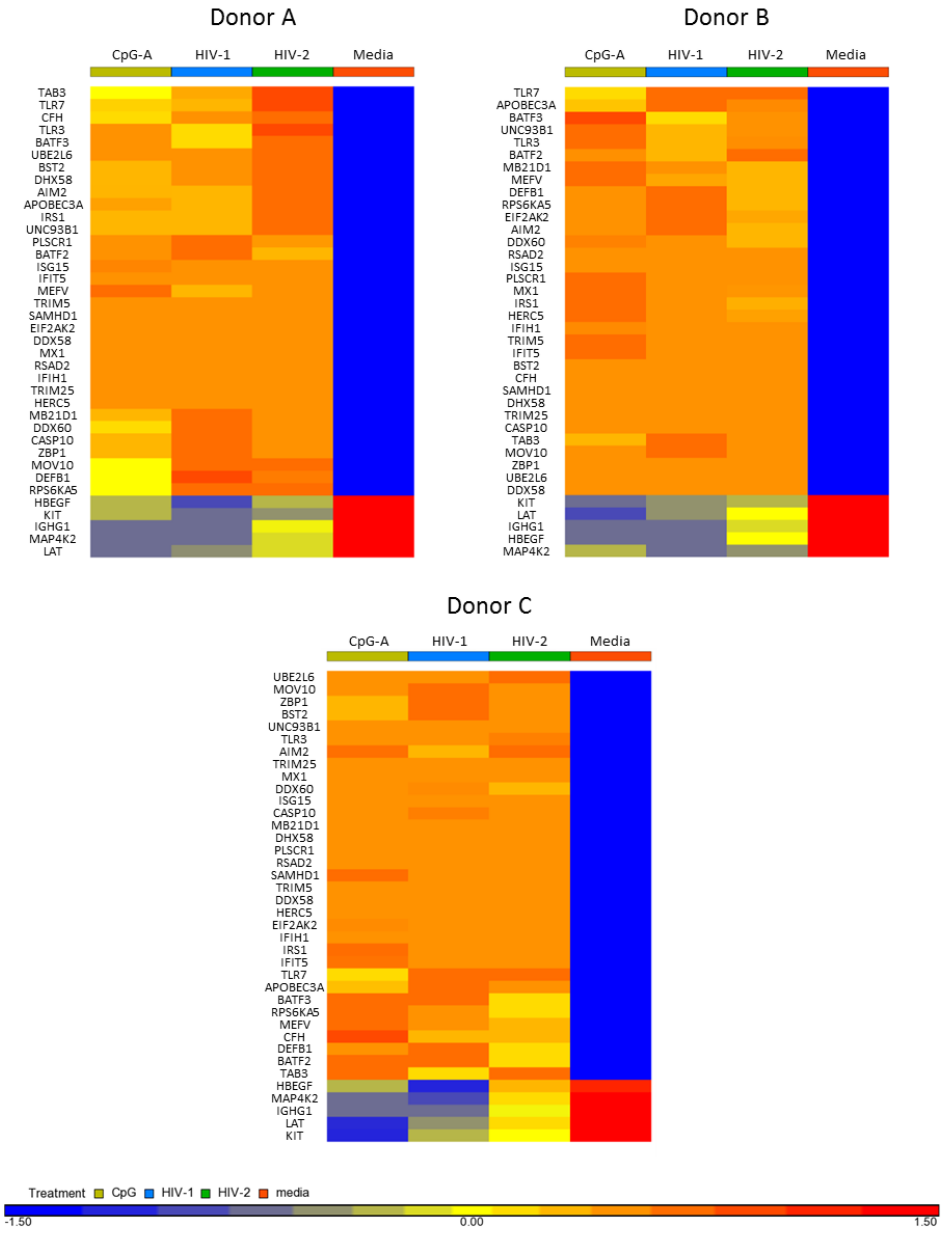

Figure 4.14. Heat map of enriched genes associated with innate immunity after 6 hours of stimulation. Each heat map represents responses from an individual donor. Each column represents a different treatment: HIV-1 is headed in blue, HIV-2 in green, CpG-A in yellow and PBMCs incubated with cell culture media alone are shown in orange Gene expression levels are indicated by colour transitions from blue (lowest expression) to red (highest expression) according to the legend displayed below the heat maps.

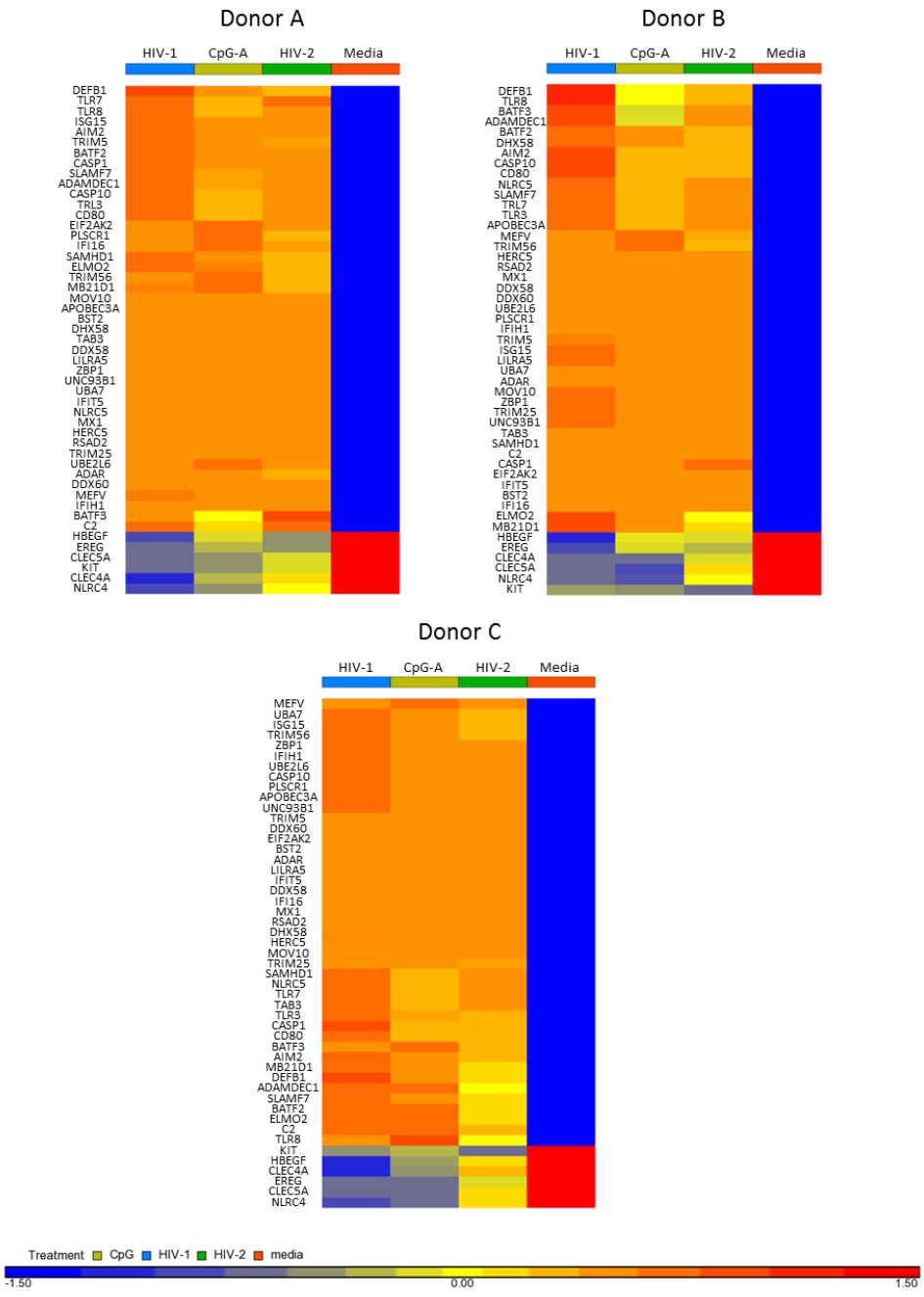

Figure 4.15. Heat map of enriched genes associated with innate immunity after 12 hours of stimulation. Each heat map represents responses from an individual donor. Each column represents a different treatment: HIV-1 is headed in blue, HIV-2 in green, CpG-A in yellow and PBMCs incubated with cell culture media alone are shown in orange. Gene expression levels are indicated by colour transitions from blue (lowest expression) to red (highest expression) according to the legend displayed below the heat maps.

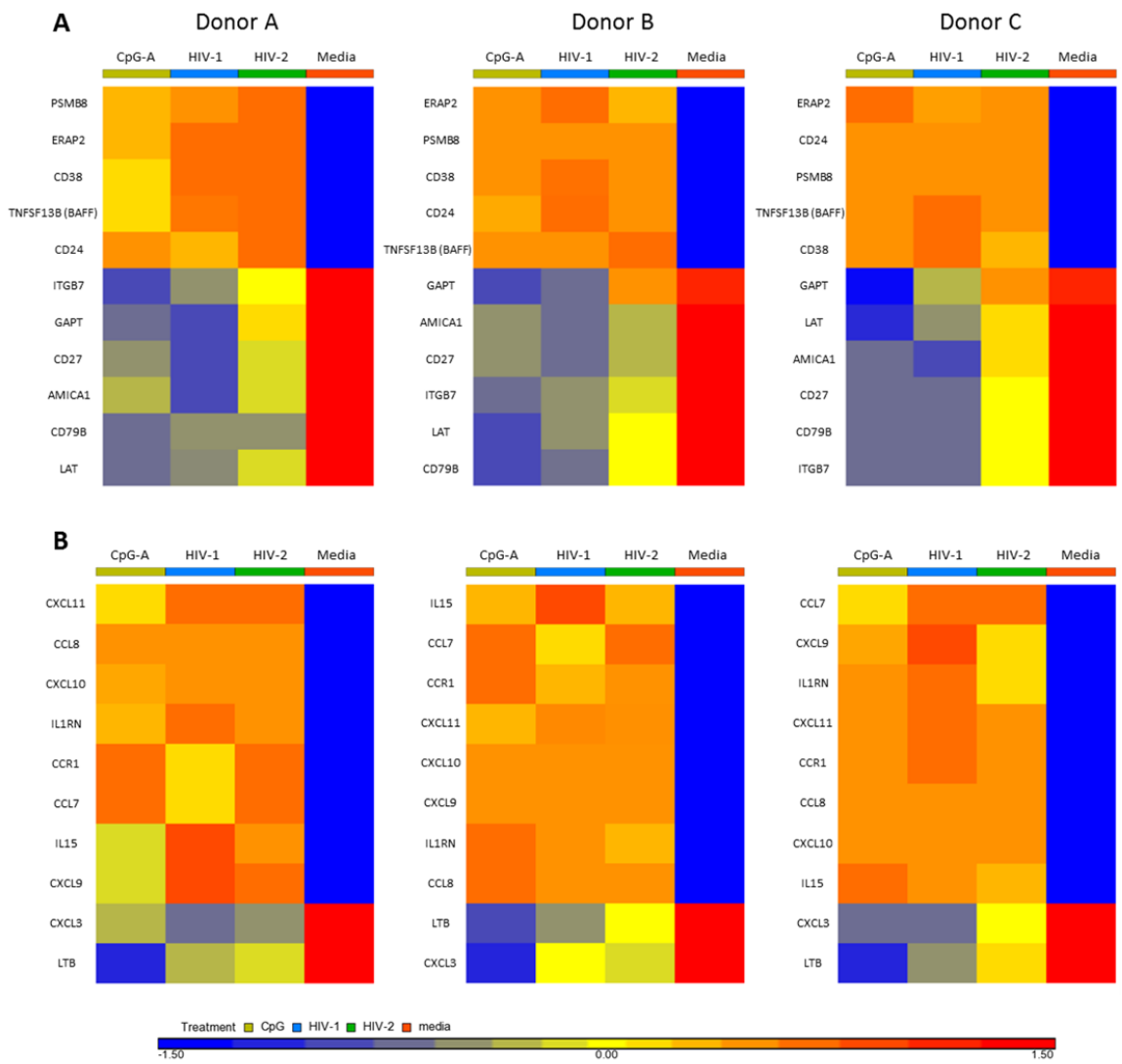

Figure 4.16. Heat map of enriched genes associated with adaptive immunity and secreted proteins after 6 hours of stimulation. Expression of (A) genes associated with the adaptive immune response and (B) cytokine and chemokine genes. Each heat map represents responses from an individual donor. Each column represents a different treatment: HIV-1 is headed in blue, HIV-2 in green, CpG-A in yellow and PBMCs incubated with cell culture media alone (unstimulated cells) are shown in orange. Gene expression levels are indicated by colour transitions from blue (lowest expression) to red (highest expression) according to the legend displayed below the heat maps.

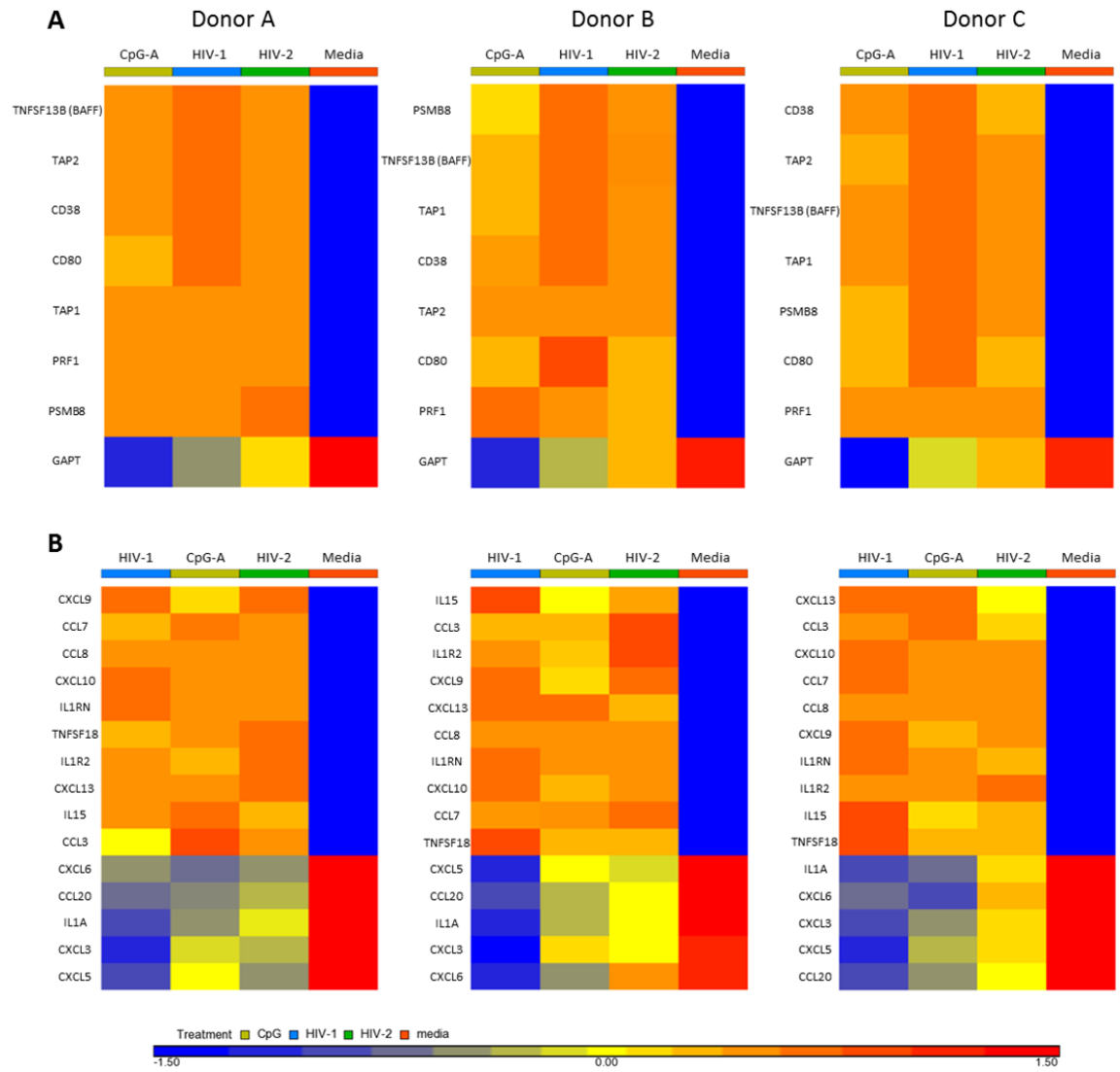

Figure 4.17. Heat map of enriched genes associated with adaptive immunity and secreted proteins after 12 hours of stimulation. Expression of (A) genes associated with the adaptive immune response and (B) cytokine and chemokine genes. Each heat map represents responses from an individual donor. Each column represents a different treatment: HIV-1 is headed in blue, HIV-2 in green, CpG-A in yellow and PBMCs incubated with cell culture media alone (unstimulated cells) are shown in orange. Gene expression levels are indicated by colour transitions from blue (lowest expression) to red (highest expression) according to the legend displayed below the heat maps.

4.4 Discussion

The aim of this chapter was to investigate the possibility that the reduced levels of type I IFN induced by HIV-2 compared to HIV-1 is caused by an immunoregulatory effect of other inflammatory mediators induced by HIV-2. This hypothesis was formulated based on the observations that PBMCs stimulated with CpG-A in the presence of HIV-2 produce less IFN-α than those stimulated with CpG-A alone. CpG-A is a synthetic TLR-9 ligand which potently activates pDC-mediated IFN-α secretion. As CpG-A exerts its effect via TLR-9 it will therefore not compete with HIV for TLR-7 ligation or, importantly, for CD4 binding to gain entry into pDCs. While HIV-1 did not alter the production of IFN-α in response to CpG-A stimulation, the addition of HIV-2 to CpG-A caused a marked reduction in the measureable level of IFN-α in cell culture supernatants compared to CpG-A alone (Figure 4.4). A similar result has previously been described whereby high concentrations of another type of CpG ODN, CpG-B (ODN 1668) was able to inhibit IFN-α secretion induced by pDC stimulation with CpG-A (Waibler *et al.*, 2008). The authors reported that this inhibition of IFN-α secretion was due to a significant increase in the secretion of the immunoregulatory cytokine IL-10, as depletion of IL-10 from the supernatants or addition of IL-10 neutralising antibodies restored CpG-A-induced IFN-α secretion in the presence of CpG-B (Waibler *et al.*, 2008).

Specific inflammatory and immunoregulatory cytokines and chemokines were subsequently chosen for analysis. A multiplex cytometric bead array (CBA) was initially used to measure nine different cytokines in PBMC culture supernatants (Figure 4.5). The assay was repeated on three separate occasions, however on each occasion upon acquisition of the sample by flow cytometry, an apparent duplicate population of beads was observed, furthermore, the required number of beads for each cytokine was unable to be obtained. The reasons for this technical problem remain unknown. One possibility is that the assay is incompatible with sample fixation with paraformaldehyde before flow cytometry analysis, which was required due to the presence of infectious HIV-1 and HIV-2 in the supernatants. I therefore decided to use the CBA results as a screen to identify potentially

measureable cytokines, which were then further quantified by ELISA. Although the ELISA is more laborious and less sensitive, it was more reliable and does not suffer the technical fault observed with the CBA, as described by others (Richens *et al.*, 2010, Timmons *et al.*, 2009). The only consistently measureable soluble proteins were IL-6 and IL-8, suggesting that other cytokines such as IL-4, IFN-γ, IL-12p70 or IL-10 are not responsible for the suppression of IFN-α responses observed with HIV-2.

From the ELISA results, only IL-6 secretion increased following viral stimulation (Figure 4.6). I therefore investigated the interaction between type I IFN and IL-6. Specifically, I tested the hypothesis that IL-6 secretion was a secondary effect of type I IFN production, and could therefore be blocked by inhibiting IFN-α/β signalling. Surprisingly, the addition of antibodies blocking either soluble IFN-α/β or the IFN-α receptor resulted in an increase in IL-6 secretion, which was independent of viral stimulation (Figure 4.7A). Depletion of pDCs from whole PBMCs, performed on one donor, and subsequent stimulation of TLR-4 with LPS, which induces IL-6 production in immune cells such as monocytes (Guha and Mackman, 2001), caused a mild raise in IL-6 secretion compared to LPS-stimulated untouched PBMCs (Figure 4.7B). This increase in IL-6 production was counteracted by the addition of exogenous type I IFN. These data suggest that constitutive type I IFN production by pDCs is required to control IL-6-mediated inflammation. This is consistent with a study conducted by Chang *et al* (2007), showing that defective type I IFN signalling in mice causes a substantial increase in LPS induced cytokines such as IL-1β and TNF-α. The same study showed that type I IFN signalling is required for LPS induced IL-10 production by monocytes, which negatively feeds back to reduce the type I IFN response (Chang *et al.*, 2007). Therefore, in this experimental set up, IL-10 production may have been reduced by blocking IFN-α/β, thereby allowing for increased IL-6 secretion. Plasmacytoid DCs perhaps secrete very low basal levels of IFN-α (undetectable by ELISA), which may explain why there was an increase in IL-6 production when blocking antibodies were added even in the absence of stimulation.

In addition to secreting type I IFN, pDCs are also known to secrete other inflammatory cytokines, such as IL-6 and TNF-α, after activation by HIV-1. However, different from IFN-α, pDCs do not secrete these cytokines in such large quantities (O'Brien *et al.*, 2011). Plasmacytoid DCs represent a minor population within PBMCs, and while they can secrete 1000 fold more IFN-α than other circulating cell types, upon *in vitro* PBMC stimulation the majority of inflammatory cytokines will most likely originate from other cells of the innate immune system, such as monocytes and mDCs.

Overall, investigation of cytokine secretion did not show a clear difference between HIV-1 and HIV-2. Therefore to further explore the possibility that HIV-2 is inducing a mechanism whereby type I IFN is reduced, a whole genome array was performed on PBMCs stimulated with either HIV-1 or HIV-2, in order to explore a wider range of pathways. CpG-A was used as a positive control for pDC activation and type I IFN induction. HIV-2 induced the differential expression of a smaller number of genes compared to HIV-1 and CpG-A at both 6 and 12 hours (Figure 4.8B and Figure 4.9B). In order to identify functional groups of genes that were differentially expressed, enrichment based on gene ontology classification was then performed on genes induced by both HIV-1 and HIV-2, as well as those induced by the two viruses separately. Gene enrichment clusters genes according to their associated functional pathways. The expression pattern of IFN genes is consistent with previous findings presented in this study (shown in Chapter 3), and shows that HIV-1 induces a greater up-regulation of type I IFN genes than HIV-2 (Figure 4.10A and Figure 4.11A). It is noteworthy that certain type I IFN genes, such as *IFNA14* and *IFNW1*, remained unchanged in response to HIV-2 compared with unstimulated cells after 12 hours. Interestingly, despite the lower levels of IFN gene expression and production induced by HIV-2, the expression pattern of IFN signalling genes (*IRF* and *STAT*) and ISGs in PBMCs was similar between HIV-1, HIV-2 and CpG-A (Figure 4.10B and Figure 4.11B). There are two signalling pathways employed to induce type I IFN secretion; pDCs are activated to produce type I IFN after ligation of TLR-7 or TLR-9 and subsequent phosphorylation of IRF-7 (Honda *et al.*, 2005c). Secreted type I IFN then induces a positive feedback loop in which ligation of the IFN receptor complex

(IFNAR1/IFNAR2) expressed on pDCs, as well as other cell types, causes the dimerisation and subsequent phosphorylation of STAT1 and STAT2 which in turn translocate to the nucleus resulting in transcription of IRF-7 and IRF-8 (Honda *et al.*, 2005c, Tailor *et al.*, 2006). Proteins from the IRF family induce transcription of IFN-α/β as well as ISGs, which play an important role in the inhibition of HIV replication (Samuel, 2001). Thus, while it is the phosphorylation of these signalling molecules which results in IFN secretion, the similar level of up-regulation of these genes signifies that they are most likely being consumed and thus replaced at a similar rate. This therefore suggests that the reduced IFN expression induced by HIV-2 is still sufficient to induce ISG expression.

Consistent with the stimulation of IFN signalling genes and ISGs, HIV-2 induces a robust innate immune response, similar to that observed with HIV-1. Of particular interest was the similar degree of up-regulation of viral restriction factors observed in response to the two viruses (Figure 4.12C and Figure 4.13C), indicating that the molecular mechanisms of viral inhibition may be equally initiated during the early stages of infection by both HIV-1 and HIV-2. The family of APOBEC proteins are polynucleotide deaminases capable of catalysing a mutation from cytosine to uracil in the viral DNA, causing hypermutation or degradation of uracil-containing DNA strands (Harris *et al.*, 2002). APOBEC proteins are packaged into new HIV virions inhibiting their replicative potential (Harris *et al.*, 2012). TRIM family members, in particular TRIM5α, inhibit HIV replication by interfering with the capsid uncoating process required for productive infection (Malim and Bieniasz, 2012, Stremlau *et al.*, 2004). Tetherin, also known as BST-2, inhibits new virion release from infected cells by 'tethering' budding virions to the host cell membrane (Neil *et al.*, 2008). SAMHD1 is a myeloid-specific protein which depletes the pool of nucleotides available, therefore halting viral replication (Laguette *et al.*, 2011, Lahouassa *et al.*, 2012). Many of these innate factors are in fact IFN inducible, as evidenced by the presence of IFN responsive promoters (Tyagi and Kashanchi, 2012), which further confirms that the level of type I IFN production by HIV-2 is sufficient to drive the innate immune response.

Although viral infection induces the expression of multiple host restriction factors, HIV has developed ways to evade these innate immune mechanisms. In particular, the HIV-1 proteins Vif and Vpu are able to counteract APOBEC3G and BST-2 respectively. HIV-2 is also able to evade restriction from BST-2 via a portion of the Env protein (Malim and Bieniasz, 2012). To date, only HIV-2 has been found to counteract the activity of SAMHD1, via its degradation by the viral protein Vpx (Harris *et al.*, 2012, Laguette *et al.*, 2011). It has been suggested that the ability of HIV-2-encoded Vpx to mediate degradation of SAMHD1 enables HIV-2 to efficiently infect dendritic cells and macrophages, thus boosting the anti-viral state and leading to enhanced immune control of the virus (Manel *et al.*, 2010). However, a recent study comparing viraemic and aviraemic HIV-2^+ patients suggested that Vpx antagonism of SAMHD1 does not correlate with viral control during HIV-2 infection, with a similar infection rate of myeloid-specific cells reported across all individuals (Yu *et al.*, 2013).

Stimulation with HIV-1 and HIV-2 caused a similar up-regulation in the expression of several genes associated with apoptosis and immunosuppression (Figure 4.12B and Figure 4.13B). In particular, infection with HIV-1 has been associated with an increase in the expression of TNF superfamily ligands and their receptors; namely TRAIL/DR5 and FasL/Fas (Herbeuval *et al.*, 2005a, Herbeuval *et al.*, 2005b, Herbeuval *et al.*, 2006). These apoptotic pathways have been proposed to play a role in the apoptosis and subsequent depletion of uninfected $CD4^+$ T cells during HIV-1 infection (Fraietta *et al.*, 2013, Herbeuval *et al.*, 2005b). TRAIL expression is known to be regulated by IFN-α on T cells, monocytes and pDCs (Griffith *et al.*, 1999, Hardy *et al.*, 2007). $CD4^+$ T cells exposed to HIV-1 *in vitro* undergo apoptosis via a TRAIL-dependent mechanism, which is inhibited by anti-type I IFN antibodies (Herbeuval *et al.*, 2005b). Similarly, apoptosis mediated by FasL/Fas can be regulated by type I IFN production (Fraietta *et al.*, 2013). The PD-L1/PD-1 pathway is another immunosuppressive pathway proposed to play a role in HIV infection and has been implicated in immune exhaustion (Boasso *et al.*, 2008b, Maier *et al.*, 2007, Yao and Chen, 2006). The binding of PD-L1 to PD-1 transduces a negative co-stimulatory signal to T cells (Freeman *et al.*, 2000). Increased levels of PD-1 are observed in T cells

from HIV-1 infected patients (Day *et al.*, 2006, Trautmann *et al.*, 2006). HIV-1 exposure *in vitro* increases PD-L1 expression on neutrophils, monocytes and $CCR5^+$ T cells (Boasso *et al.*, 2008b, Bowers *et al.*, 2014), and PBMC stimulation with either IFN-α or TLR-7/9 agonists resulted in similar PD-L1 up-regulation (Chen *et al.*, 2007, Meier *et al.*, 2008, Bowers *et al.*, 2014). It would be of interest to determine if the reduced levels of type I IFN produced after HIV-2 stimulation are sufficient to drive the up-regulation of these immune suppressive proteins.

A similar up-regulation of PRRs and associated genes was also observed following stimulation with HIV-1 and HIV-2 (Figure 4.12A and Figure 4.13A). The majority of enriched genes were found to be involved in cytoplasmic DNA and RNA sensing, including the RLRs (*DDX58*, *DDX60*, *DHX58* and *IFIH1*, also known as *MDA5*), as well as NOD-like receptors (*NOD-1* and *NLRC5*). An up-regulation in the expression of *TLR-3*, *TLR-7* and *TLR-8*, which recognise nucleic acid, was also observed, as well as an increase in the expression of *UNC93B1* which is required for the transport of TLRs from the endoplasmic reticulum to endolysosomes (Kim *et al.*, 2008). While type I IFN signalling in pDCs is the result of TLR-7 or TLR-9 ligation and subsequent IRF-7 activation, other cells which participate in inflammatory responses rely on TLR-3 and RIG-I family proteins to induce type I IFN production (Kawai and Akira, 2007).

After 6 hours a number of genes associated with the regulation of the adaptive immune response which were down-regulated following viral exposure, remained higher in PBMCs stimulated with HIV-2 compared to HIV-1 (Figure 4.16A and Figure 4.17A). These genes are associated with B cell signalling (*CD79B* and *GAPT*), T cell activation (*CD27* and *LAT*) and T cell migration (*ITGB7* and *AMICA1*). After 12 hours, there was an enrichment of genes associated with antigen processing and presentation which were up-regulated at a similar level by both HIV-1 and HIV-2, raising the possibility that peptides from both HIV-1 and HIV-2 are efficiently presented by APCs for T cell activation.

A similar pattern was observed with chemokines (*CXCL6*, *CCL20*, *CXCL3* and *CXCL5*) after 12 hours, that is, HIV-1 and CpG-A caused a greater down-regulation of these chemokines than HIV-2 (Figure 4.17B). Interestingly, CXCL3, CXCL5 and CXCL6 are all involved in the chemoattraction of neutrophils. Neutropaenia is commonly reported during HIV infection and can result in increased susceptibility to bacterial and fungal infections. Furthermore, these reduced numbers of neutrophils display a decrease in their chemotactic ability (Kuritzkes, 2000, Roilides *et al.*, 1990).

The results presented in this chapter confirmed that HIV-2 stimulation of PBMCs results in a reduced type I IFN profile compared to HIV-1, supporting the findings of decreased IFN-α protein secretion. Nonetheless, HIV-2-induced type I IFN levels are sufficient to induce similar levels of ISG expression and anti-viral restriction factors, indicative of a robust innate immune response. It is noteworthy that amidst this reduced type I IFN environment there is a preservation of adaptive immune response associated genes following PBMC stimulation with HIV-2. This unbiased gene array data highlights the fact that differential induction of type I IFN is a major difference in the innate immune response against HIV-1 and HIV-2. However, no evidence was found that HIV-2 induces the production of an inhibitory factor which reduced IFN-α secretion, suggesting that other cellular and molecular mechanisms are responsible for the differences observed between HIV-1 and HIV-2.

Chapter 5 Induction of an Antigen Presenting Phenotype

5.1 Introduction

Dendritic cells are mediators of the innate immune response (Merad *et al.*, 2013, Murphy *et al.*, 2008). They serve an important role as professional antigen presenting cells (APC), acting as sentinels to detect invading pathogens (Merad *et al.*, 2013, Murphy *et al.*, 2008). Upon engulfment of foreign agents, APCs migrate to secondary lymphoid organs and efficiently process antigens and display the peptide fragments bound to MHC molecules on the cell surface for recognition by effector cells of the adaptive immune system (Lanzavecchia and Sallusto, 2001). Importantly, professional APCs also provide the co-stimulatory signal required to promote the activation of naïve T cells. The co-stimulatory ligands, CD80 and CD86, bind to CD28 on T cells in the context of MHC-peptide recognition by the T cell receptor, thus allowing for T cell activation (Felix *et al.*, 2010).

Although the secretion of high levels of type I IFN is thought to be the main role for pDCs, they are in fact able to act as APCs. Expression of co-stimulatory molecules on dendritic cells is increased after TLR engagement and subsequent activation of the NF-κB pathway (Gilliet *et al.*, 2008). Mature pDCs, expressing high levels of MHC and co-stimulatory molecules, co-cultured with naïve allogeneic T cells exhibited a high capacity to stimulate T cell proliferation (Cella *et al.*, 2000). In a study conducted using influenza virus, Fonteneau *et al* (2003) demonstrated that pDCs were as efficient as mDCs at acquiring and presenting antigen to both $CD4^+$ and $CD8^+$ influenza-specific T cell clones. Furthermore, influenza-activated pDCs were able to re-activate anti-influenza CTL memory responses (Fonteneau *et al.*, 2003). Plasmacytoid DCs have also been reported to capture and cross present soluble viral antigens to $CD8^+$ T cells on MHC class I molecules, including HIV antigens (Hoeffel *et al.*, 2007, Lui *et al.*, 2009). Thus, the potential for pDCs to act as APCs should not be dismissed. In the context of HIV there have been several reports showing that HIV-1 induces pDC maturation *in vitro*, increasing the expression of co-

stimulatory molecules as well as the activation marker CD83 (Beignon *et al.*, 2005, Boasso *et al.*, 2011, Fonteneau *et al.*, 2004).

While the role of CD80 and CD86 in T cell co-stimulation is well described, the function of CD83 during immune responses is not fully understood. High expression of CD83 has been widely utilised as a marker of DC maturation (Lechmann *et al.*, 2002, Prazma and Tedder, 2008). Some reports have hypothesised a role for CD83 in T cell activation. In a study in which CD83 was over expressed on DCs by delivery of mRNA via electroporation, the authors reported enhanced stimulation of allogeneic T cells (Aerts-Toegaert *et al.*, 2007). Furthermore, binding of CD83 with its putative ligand on T cells favours the maturation and survival of virus-specific CTLs (Hirano *et al.*, 2006).

Several studies have shown that pDCs can be functionally dichotomous, and when activated with different CpG-rich ODN sequences follow two distinct maturation pathways. When activated with CpG-A pDCs become type I IFN producing cells, which secrete large quantities of IFN-α and show limited up-regulation of co-stimulatory molecules. Conversely, pDCs stimulated with CpG-B (ODN 2006) secrete little or no IFN-α and rather mature into efficient APCs (Jaehn *et al.*, 2008). This effect appears to be largely due to the compartmental localisation of the TLR agonist within the pDC. In particular, TLR-9 signalling within early endosomes results in an IFN-α producing phenotype, while signalling in late endosomes or lysosomes causes an increase in CD86 expression (Guiducci *et al.*, 2006, Honda *et al.*, 2005a). A study by O'Brien *et al* (2011) showed that, similar to CpG-A, HIV-1 traffics to the early endosome where it stimulates persistent IFN-α secretion via IRF-7 signalling, whereby CpG-B traffics to the lysosome, where it activates the NF-κB signalling pathway.

Myeloid DCs are efficient professional APCs and are able to capture and present viral antigen to both $CD4^+$ and $CD8^+$ T cells (Lanzavecchia and Sallusto, 2001). In particular, the ability of mDCs to cross present antigen to $CD8^+$ T cells was thought to be important during HIV-1 infection (Buseyne *et al.*,

2001). However, in contrast to pDCs, blood mDCs are not directly activated by HIV. Rather, secreted products from pDCs such as type I IFN or TNF-α induce bystander maturation of mDCs (Fonteneau *et al.*, 2004).

Monocytes represent another important population of APCs, as they are precursors for macrophages as well as DCs in some inflammatory settings, sometimes referred to as inflammatory DCs (Cheong *et al.*, 2010, Coleman and Wu, 2009, Shortman and Naik, 2007, Ziegler-Heitbrock *et al.*, 2010). Monocytes are key producers of inflammatory cytokines and chemokines and become highly activated during both HIV-1 and HIV-2 infection (Cavaleiro *et al.*, 2013).

Antigen presenting cells are essential in priming effective T cell responses. Stimulation of T lymphocytes via TCR/MHC engagement in the absence of sufficient co-stimulatory signals can lead to T cell tolerance (Williams and Bevan, 2007). Thus, the activity of APCs during HIV infection can have profound effects on T cell activation (Chougnet *et al.*, 2002). T cell dysregulation during HIV-1 infection has been well documented. Proliferation of T cells in response to antigen-specific and mitogen stimulation is progressively impaired as a result of HIV-1 infection (Clerici *et al.*, 1989). Furthermore, HIV-1^+ patients who spontaneously control the virus and maintain stable $CD4^+$ T cell counts (LTNPs) retain enhanced proliferative virus-specific T cell responses compared to HIV-1^+ progressors (Imami *et al.*, 2013, Rinaldo *et al.*, 1995, Wilson *et al.*, 2000). In contrast to HIV-1, individuals infected with HIV-2 maintain better $CD4^+$ T cell proliferative capacity and preserve a greater frequency of IL-2 and IFN-γ secreting $CD4^+$ T cells (Duvall *et al.*, 2006, Sousa *et al.*, 2001). Moreover, compared to HIV-1-specific T cell responses, which exhibit a high frequency of monofunctional $CD8^+$ T cells, HIV-2-specific $CD8^+$ T cell responses show greater polyfunctionality (Duvall *et al.*, 2008). Thus, an increased capacity in T cell functionality during HIV-2 infection potentially reflects enhanced APC function.

5.2 Hypothesis & Aims

The hypothesis for this chapter of work is that despite the reduced ability of HIV-2 to induce IFN-α secretion, PBMC stimulation with HIV-2 will result in the maturation of pDCs, mDCs and monocytes into APCs, which may account for the preservation of T cell responses observed in HIV-2 infected patients.

In order to investigate this hypothesis the following will be assessed by flow cytometry:

- Expression of the activation marker CD83, and co-stimulatory molecules on pDCs, mDCs and monocytes, following PBMC stimulation with HIV-1, HIV-2 or media alone.
- The maturation status of activated pDCs, in particular identifying pDCs actively secreting IFN-α and examining co-expression of CD86 and CD83 on IFN-α^+ cells.

5.3 Results

Plasmacytoid DC and monocyte activation was measured by examining the expression of co-stimulatory molecules CD80 and CD86, and the activation marker CD83. Myeloid DC activation was measured based on the expression of CD80, CD86 and MHC-I (HLA-ABC). All results are shown as both the frequency of expressing cells, and mean fluorescence intensity (MFI), which measures expression at the single cell level.

5.3.1 Cell Viability

Cell viability was assessed using two methods. Trypan blue exclusion (N=6) was examined after 24 hours culture under all conditions. Cell viability remained higher than 90% in all conditions analysed after 24 hours culture (Table 5.1). A statistically significant decrease in viability was found after incubation with intermediate concentrations of HIV-2 compared to media alone. PBMCs were also labelled with FVD eFluor 506 after 24 hours culture with either media alone or 13 x10^9 RNA copies/ml of HIV-1 or HIV-2 (Table 5.2). Only dead or dying cells stain positive for FVD. Due to low cell numbers

staining positive for FVD, the MFI of FVD eFluor 506 was then examined on pDCs, mDCs and monocytes rather than cell frequencies. Stimulation with both viruses resulted in a slightly higher FVD MFI on pDCs and mDCs compared to media alone, which was however only significant for HIV-2. Conversely, HIV-1 induced a significantly higher FVD MFI on monocytes compared to unstimulated cells. HIV-2 also induced a slight increase in FVD MFI on monocytes, although this was not significant when compared to media.

Overall, while viral stimulation did have minor effects on cell viability, no significant differences were found between HIV-1 and HIV-2 stimulation.

Table 5.1. Percentage cell viability after 24 hours culture measured by trypan blue exclusion. Results expressed as median (IQR) (N = 6)

Culture Condition	HIV-1	HIV-2
13 x10^9 RNA copies/ml	96.6 (94.7-97.5)	96.7 (94.1-99.4)
3.9 x10^9 RNA copies/ml	95.7 (95.3-98.1)	94.5 (92.8-95.2)*
1.3 x10^9 RNA copies/ml	93.9 (93.1-95.0)	97.3 (95.9-99.6)
0 RNA copies/ml (media alone)	97.5 (96.9-97.7)	

Percentage viability after stimulation with HIV-1, HIV-2 and media alone within individual virus concentrations was compared using a Friedman test with a Dunn's post test for multiple analyses. *HIV-2 vs media $p<0.05$

Table 5.2. FVD eFluor 506 MFI on pDC, mDC and monocytes. Results expressed as median (IQR) (N = 4)

	HIV-1	HIV-2	Media
pDCs	1230.2 (1194.4-1378-9)	1231.5 (1197.2-1442.3)*	1080.4 (1038.8-1179.3)
mDCs	1908.1 (1726.9-2108-8)	1986.4 (1748.9-2206.9)*	1726.3 (1640.4-1859.1)
Monocytes	3072.6 (2991.9-3211.0)*	2869.7 (2835.8-2966.3)	2658.2 (2649.7-2723.0)

FVD MFI after stimulation with HIV-1, HIV-2 and media alone was compared using a Friedman test with a Dunn's post test for multiple analyses.*HIV vs media $p<0.05$

5.3.2 Plasmacytoid DC Activation

Negligible CD80 expression was measured after 9 hours under all culture conditions and after 24 hours a slight increase in expression was observed (Figure 5.1). Using the highest concentration of HIV-1 (13 $x10^9$ RNA copies/ml) there was a significant increase in both the frequency of $CD80^+$ pDCs and CD80 MFI compared to unstimulated cells (Figure 5.1A & D). HIV-2 significantly increased the percentage of CD80-expressing pDCs compared to media alone when PBMCs were stimulated with an intermediate concentration of virus (3.9 $x10^9$ RNA copies/ml) (Figure 5.1B).

Stimulation of PBMCs with either virus caused an increase in CD86 expression, as expected upon pDC maturation (Figure 5.2). After 9 hours culture, HIV-2 induced an increase in the percentage of CD86 expressing pDCs compared to unstimulated cells, which reached significance using 13 $x10^9$ RNA copies/ml (Figure 5.2A). This difference however was not mirrored when examining the MFI. Both viruses induced the expression of CD86 on a significantly higher frequency of pDCs after 24 hours stimulation compared to media alone, which tested significantly positive at both high and intermediate virus concentrations for HIV-1 and at an intermediate concentration for HIV-2 (Figure 5.2A & B). CD86 expression on pDCs remained low at both 9 and 24 hours in the absence of virus.

The frequency of CD83-expressing pDCs was significantly increased after 9 and 24 hours incubation with the highest concentration of HIV-1 (13 $x10^9$ RNA copies/ml) compared to media (Figure 5.3A). High HIV-2 concentrations induced a similar up-regulation, which was significant only after 24 hours (Figure 5.3A). When intermediate virus concentrations were used (3.9 $x10^9$ RNA copies/ml), HIV-2 induced a significant increase in CD83-expressing pDCs compared to unstimulated cells after 9 hours, whereas HIV-1-induced CD83 up-regulation tested significant only after 24 hours (Figure 5.3B). Finally, when using 1.3 $x10^9$ RNA copies/ml, both HIV-1 and HIV-2 induced significant CD83 up-regulation at both 9 and 24 hours (Figure 5.3C). CD83 MFI on pDCs showed similar results (Figure 5.3D, E & F),

demonstrating that both viruses are capable of causing an up-regulation in CD83 expression on pDCs. CD83 expression on pDCs was minimal in PBMCs cultured in media alone after 9 and 24 hours.

The MFI of both BDCA2 and CD123 on pDCs was also measured after PBMC stimulation with either HIV-1 or HIV-2 (Figure 5.4). In all culture conditions, both markers were down-regulated after 24 hours of cells being in culture. No differences were observed in the MFI of the scavenger receptor BDCA2 when cells were stimulated with HIV-1, HIV-2 or media alone (Figure 5.4A, B & C). After 24 hours of exposure to HIV-2 pDCs retained a higher CD123 MFI compared to cells treated with media alone, which was significant using 3.9 $x10^9$ RNA copies/ml and 1.3 $x10^9$ RNA copies/ml (Figure 5.4E & F).

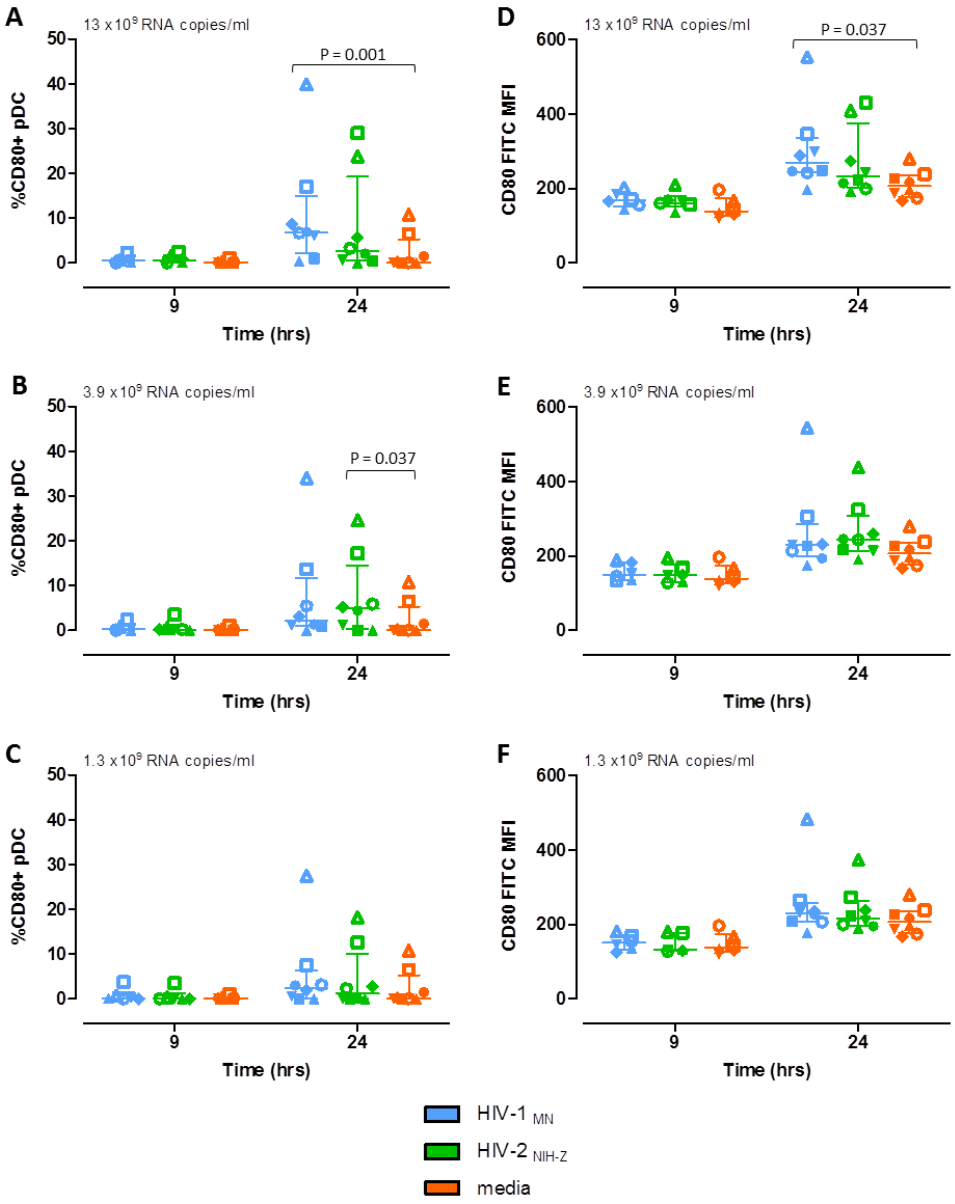

Figure 5.1. Expression of CD80 on pDCs after PBMC exposure to HIV-1 or HIV-2. CD80 expression measured as frequency of expressing pDCs (left panels, A – C) and CD80 MFI on pDCs (right panels, D – F) after 9 and 24 hours in different culture conditions. PBMCs cultured with HIV-1 are indicated in blue, HIV-2 in green and media alone (unstimulated cells) in orange. Individual donors are represented by different symbols. The concentration of virus used to stimulate PBMCs is shown in the top left of each graph. Horizontal bars represent median values and vertical lines show the interquartile range. Responses to HIV-1, HIV-2 and media alone within individual time points and virus concentrations were compared using a Friedman test with Dunn's post test.

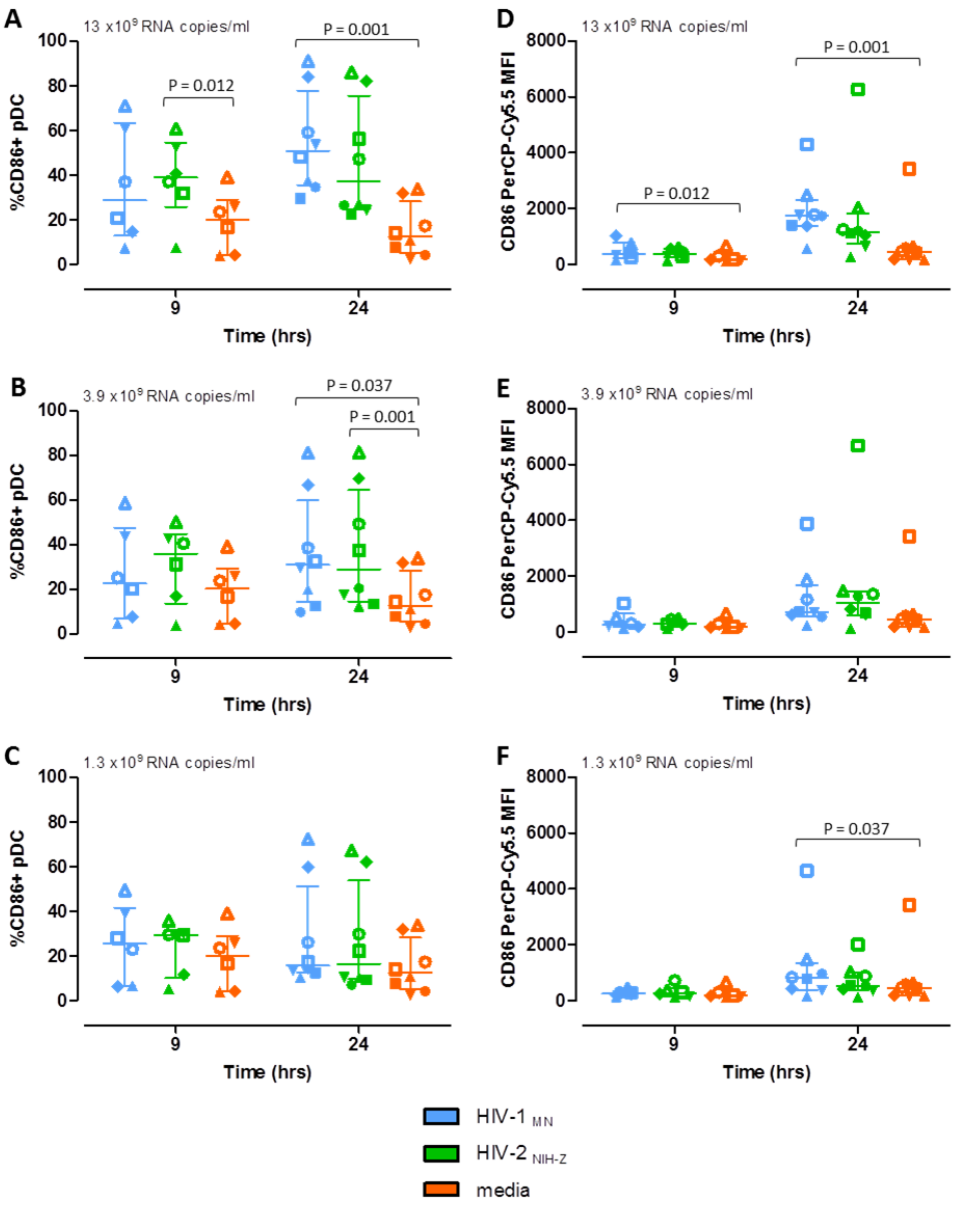

Figure 5.2. Expression of the co-stimulatory molecule CD86 on pDCs after PBMC exposure to HIV-1 or HIV-2. CD86 expression measured as frequency of expressing pDCs (left panels, A – C) and CD86 MFI on pDCs (right panels, D – F) after 9 and 24 hours in different culture conditions. PBMCs cultured with HIV-1 are indicated in blue, HIV-2 in green and media alone (unstimulated cells) in orange. Individual donors are represented by different symbols. The concentration of virus used to stimulate PBMCs is shown in the top left of each graph. Horizontal bars represent median values and vertical lines show the IQR. Responses to HIV-1, HIV-2 and media alone within individual time points and virus concentrations were compared using a Friedman test with Dunn's post test.

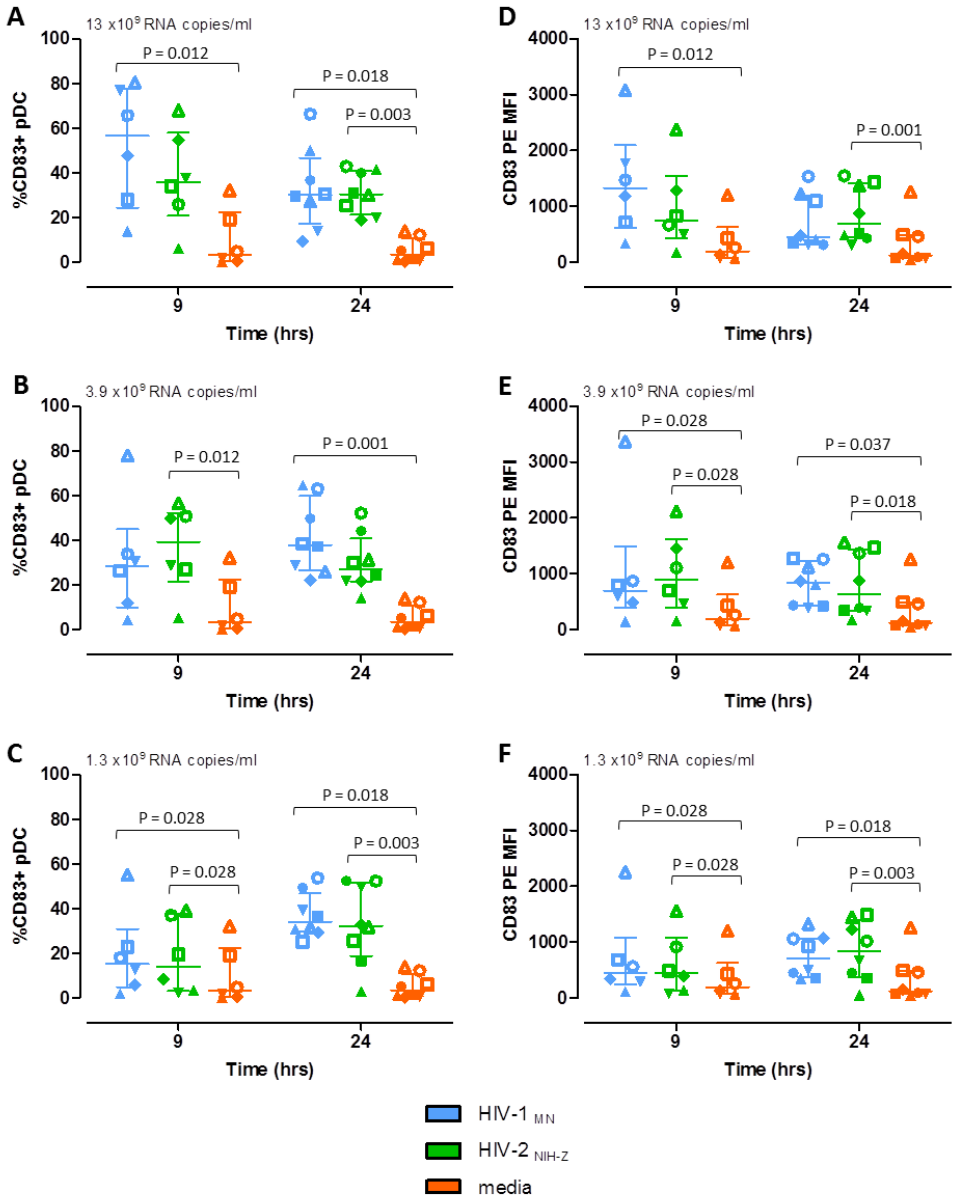

Figure 5.3. Up-regulation of the activation marker CD83 on pDCs after 9 and 24 hour incubation of PBMCs with HIV-1 or HIV-2. Left panels (A – C) show the frequency of CD83-expressing pDCs and right panels represent CD83 MFI on pDCs (D – F). Responses to HIV-1 are indicated in blue, HIV-2 in green and media alone (unstimulated cells) in orange. The concentration of virus used to stimulate PBMCs is shown in the top left of each graph. Individual donors are represented by different symbols. Horizontal bars represent median values and vertical lines show the IQR. Responses to HIV-1, HIV-2 and media alone within individual time points and virus concentrations were compared using a Friedman test with Dunn's post test.

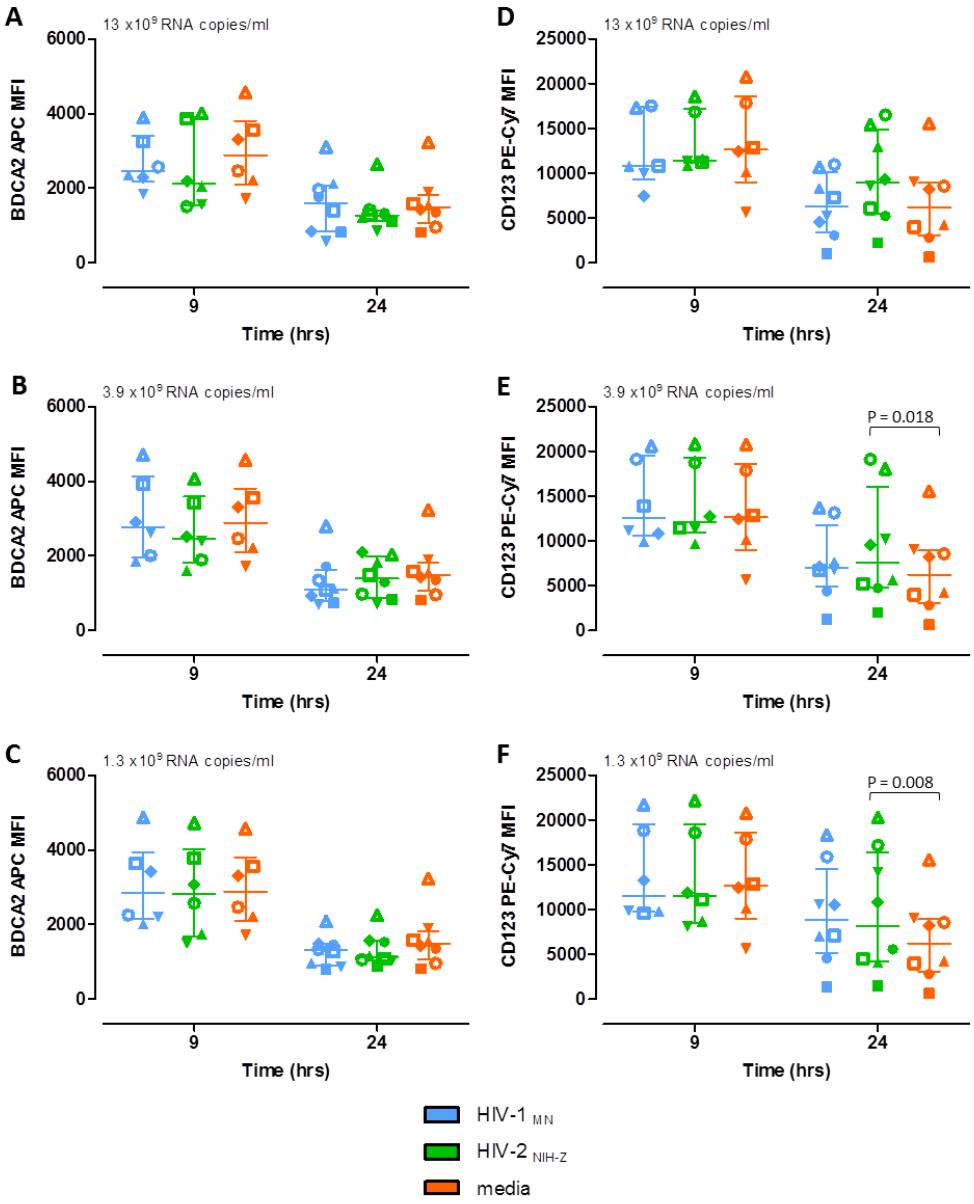

Figure 5.4. Expression of BDCA2 and CD123 on pDCs after stimulation with either HIV-1 or HIV-2. BDCA2 MFI (left panels, A – C) and CD123 MFI (right panels, D – F) of the BDCA2^{+} population after 9 and 24 hours under different culture conditions. The concentration of virus used to stimulate PBMCs is shown in the top left of each graph. PBMCs cultured with HIV-1 are indicated in blue, HIV-2 in green and media alone (unstimulated cells) in orange. Individual donors are represented by different symbols. Horizontal bars represent median values and vertical lines show the IQR. Responses to HIV-1, HIV-2 and media alone within individual time points and virus concentrations were compared using a Friedman test with Dunn's post test.

5.3.3 Monocyte Activation

Very low frequencies of CD80-expressing monocytes were measured in all culture conditions and at all time points (Figure 5.5). A non-parametric Friedman test indicated that HIV-1 caused a significant increase in the percentage of $CD80^+$ monocytes compared to unstimulated cells after 24 hours at all virus concentrations tested (Figure 5.5A, B & C), although these increases appear to be only marginal. Analysis of the MFI of CD80 on monocytes showed that after 24 hours both viruses induced a significant up-regulation of CD80 expression on a per cell basis compared to media alone (Figure 5.5D, E & F).

After 9 hours stimulation, at the highest virus concentration (13 $x10^9$ RNA copies/ml) both HIV-1 and HIV-2 induced a significantly greater proportion of monocytes to express CD86 compared to media alone (Figure 5.6A). The same was true for both intermediate and low concentrations of HIV-2, but not for HIV-1 (Figure 5.6B & C). Both HIV-1 and HIV-2 induced a significant up-regulation in CD86 expression on monocytes after 24 hours stimulation at all concentrations used. Similar results were found examining the MFI of CD86 on monocytes (Figure 5.6D, E & F).

CD83 expression on monocytes showed large variability among donors after 9 hours, independent of the culture condition (Figure 5.7). However, using 13 $x10^9$ RNA copies/ml of HIV-1, a slight increase in the frequency of $CD83^+$ monocytes was observed compared to media after 9 hours (Figure 5.7A), with a similar trend observed when examining the MFI (Figure 5.7D). At 24 hours, all concentrations of HIV-1 caused a significant up-regulation in the percentage of CD83-expressing monocytes compared to media alone (Figure 5.7A, B & C). HIV-2 also induced a significant increase in CD83 expression on monocytes compared to unstimulated cells when used at an intermediate concentration (3.9 $x10^9$ RNA copies/ml) (Figure 5.7B). Examining the MFI of CD83 on monocytes after 24 hours exposure to stimulus, high concentrations of both HIV-1 and HIV-2 induced an increase in the expression of CD83

on an individual cell basis compared to media alone (Figure 5.7D). This significance was maintained for HIV-1 using both intermediate and low concentrations (Figure 5.7E & F).

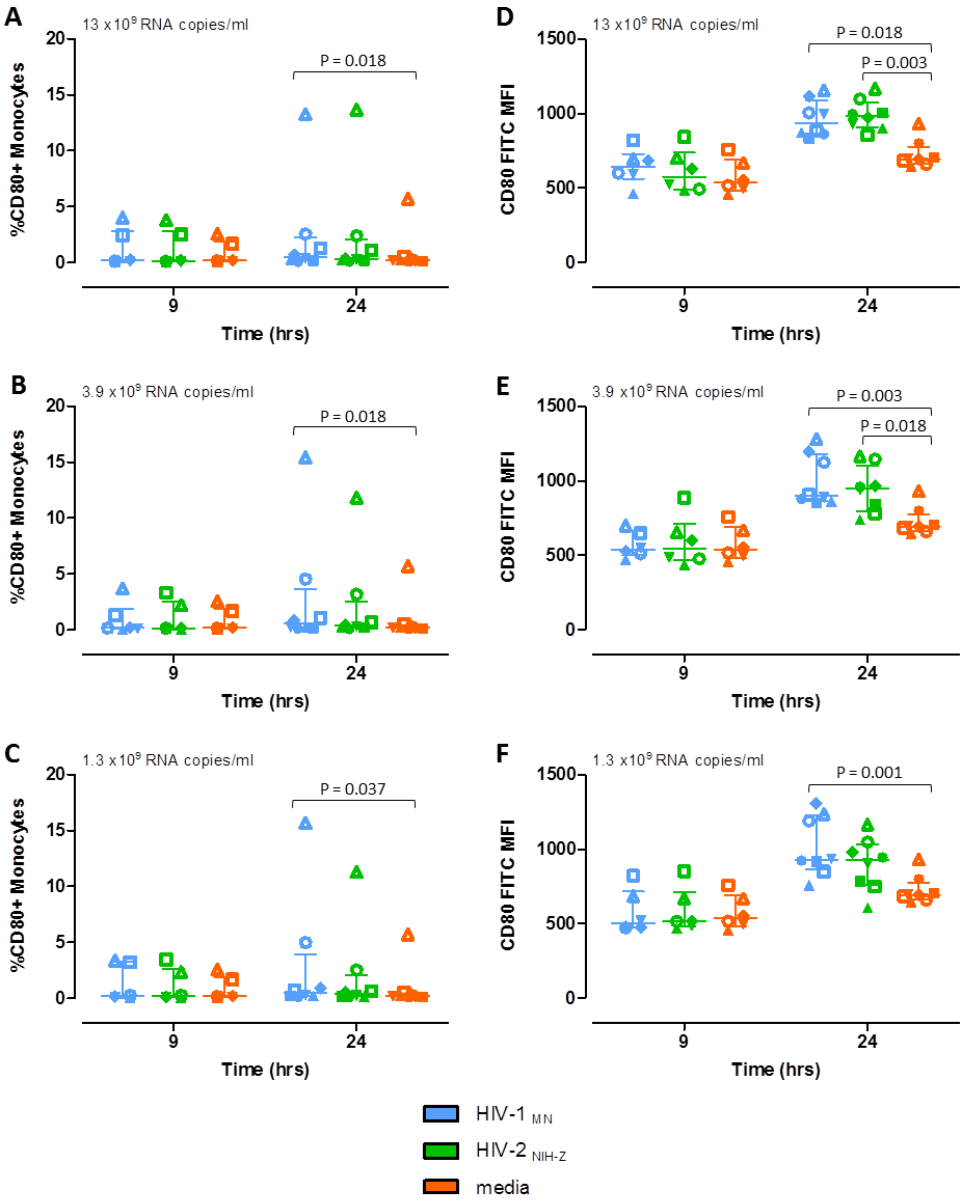

Figure 5.5. Expression of CD80 on monocytes following PBMC exposure to different concentrations of HIV-1 or HIV-2. CD80 expression measured as the frequency of expressing monocytes (left panels, A – C) and CD80 MFI on monocytes (right panels, D – F) after 9 and 24 hours. The concentration of virus used to stimulate PBMCs is shown in the top left of each graph. Responses to HIV-1 are indicated in blue, HIV-2 in green and unstimulated cells (media alone) in orange. Individual donors are represented by different symbols. Horizontal bars represent median values and vertical lines show the IQR. Responses to HIV-1, HIV-2 and media alone within individual time points and virus concentrations were compared using a Friedman test with Dunn's post test.

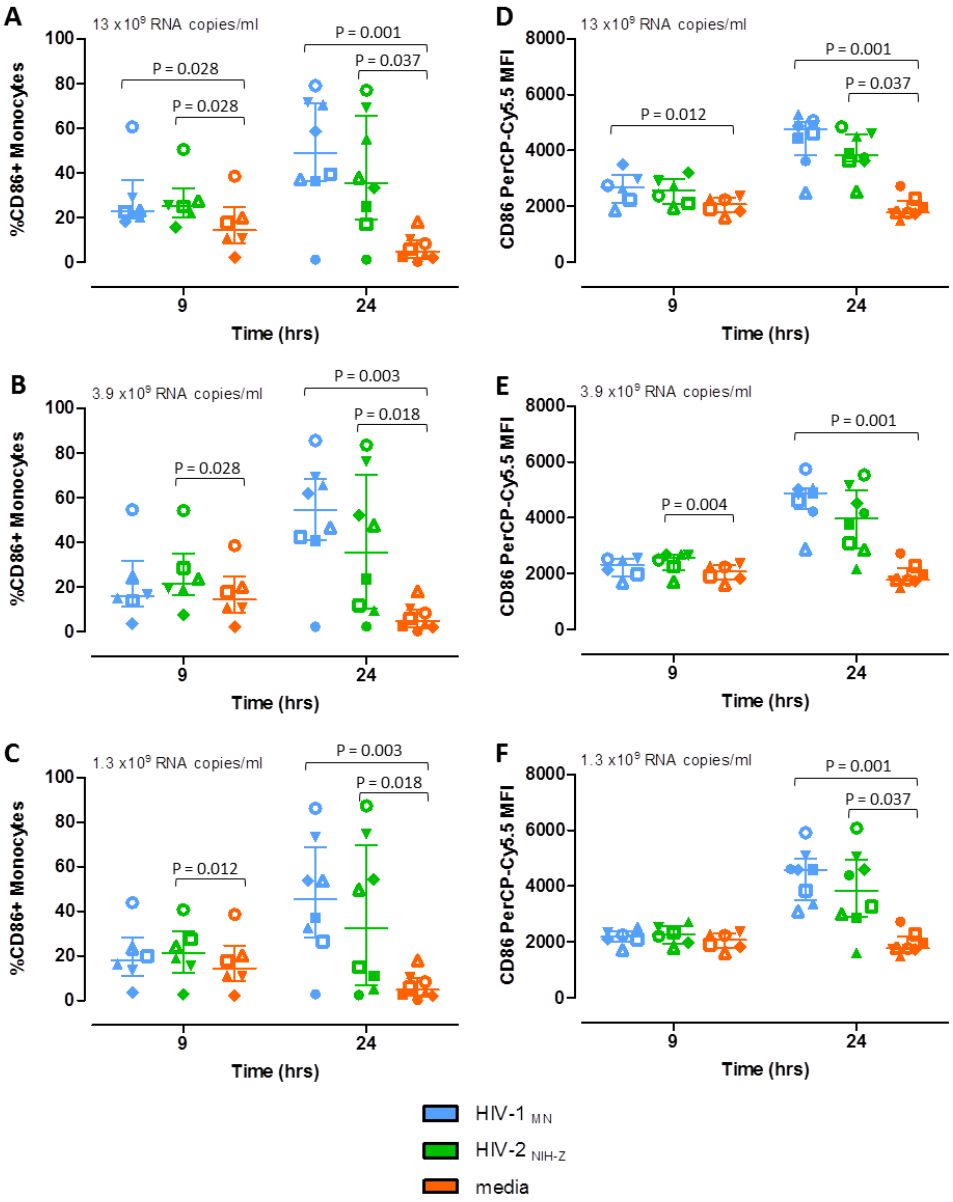

Figure 5.6. CD86 expression on monocytes after stimulation for 9 and 24 hours with HIV-1 or HIV-2. CD86 expression measured as the percentage of positive monocytes (left panels, A – C) and CD86 MFI of monocytes (right panels, D – F) after culture with different concentrations of HIV-1 or HIV-2. The concentration of virus used to stimulate PBMCs is shown in the top left of each graph. Responses to HIV-1 are indicated in blue, HIV-2 in green and media alone (unstimulated cells) in orange. Individual donors are represented by different symbols. Horizontal bars represent median values and vertical lines extend to the IQR. Responses to HIV-1, HIV-2 and media alone within individual time points and virus concentrations were compared using a Friedman test with Dunn's post test.

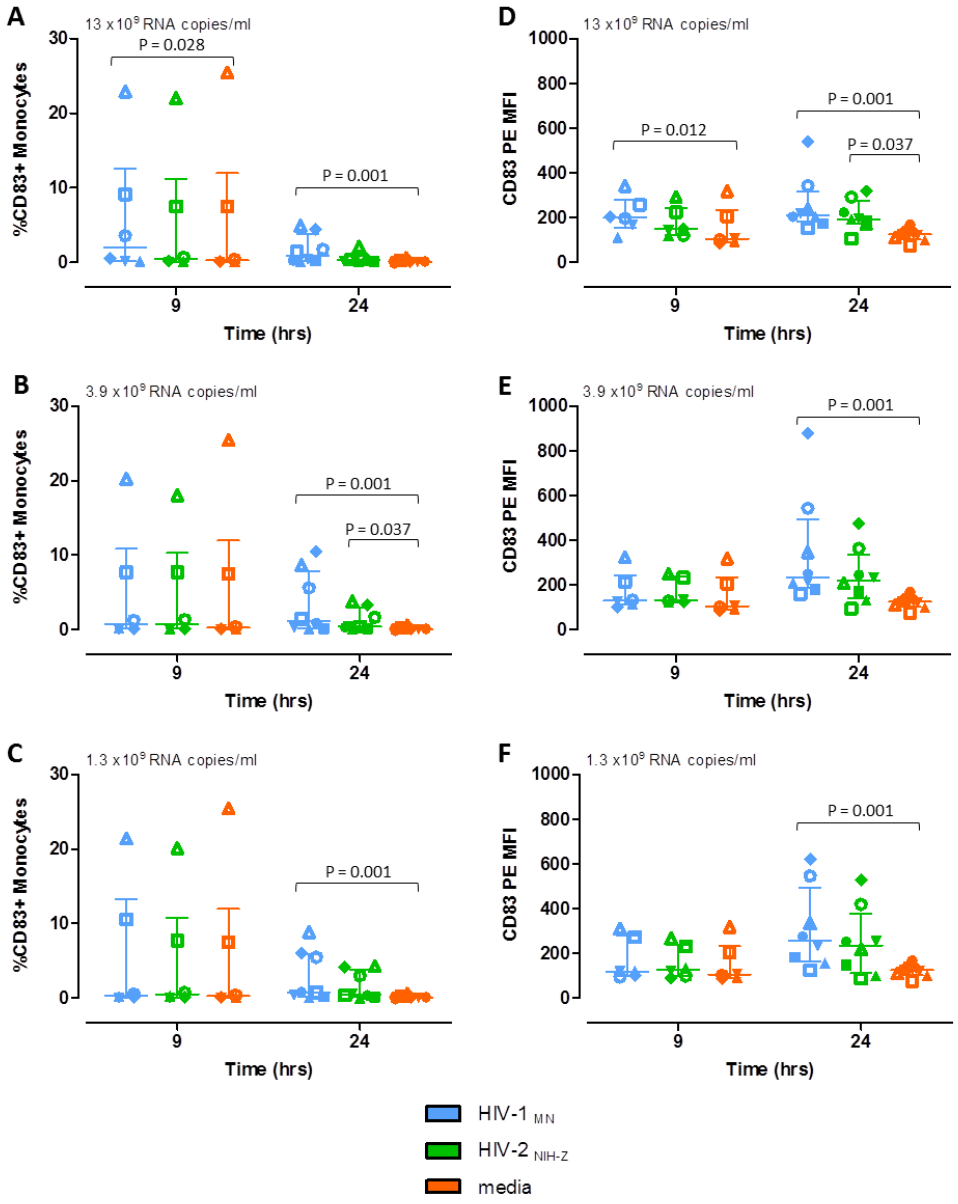

Figure 5.7. Frequency and MFI of CD83-expressing monocytes. Left panels (A – C) show the percentage of CD83^{+} monocytes and right panels (D – F) represent the MFI of CD83 on the monocyte population after stimulation with either HIV-1 or HIV-2. The concentration of virus used to stimulate PBMCs is shown in the top left of each graph. Responses to HIV-1 are indicated in blue, HIV-2 in green and media alone (unstimulated cells) in orange. Individual donors are represented by different symbols. Horizontal bars represent median values and vertical lines extend to the IQR. Responses to HIV-1, HIV-2 and media alone within individual time points and virus concentrations were compared using a Friedman test with Dunn's post test.

5.3.4 Myeloid DC Activation

Similar to monocytes, CD80 expression on mDCs was generally low and no difference was observed in CD80-expressing mDCs after PBMC incubation with HIV-1, HIV-2 or media after 9 hours (Figure 5.8). After 24 hours small increases in CD80 expression on mDCs were observed after viral stimulation, which was significant using 3.9 x10^9 RNA copies/ml of HIV-1 compared to media alone (Figure 5.8B). Analysis of CD80 expression on an individual cell basis using the MFI showed a statistically significant increase after stimulation with a high concentration of HIV-1 (13 x10^9 RNA copies/ml) after 9 hours (Figure 5.8D).

Different from CD80, both $CD86^+$ (Figure 5.9) and $HLA\text{-}ABC^+$ (Figure 5.10) mDC frequencies approached 100% under all culture conditions. CD86 MFI remained similar between HIV-1, HIV-2 and media alone at 9 hours (Figure 5.9D, E & F). Conversely, after 24 hours of culture both HIV-1 and HIV-2 were able to induce a greater level of CD86 expression per cell, which was significant using a high and intermediate concentration respectively (Figure 5.9D & E). High concentrations of HIV-1 (13 x10^9 RNA copies/ml) further increased the frequency of $HLA\text{-}ABC^+$ mDCs at 9 hours compared to unstimulated cells, whereas no effect was observed with HIV-2 (Figure 5.10A). Using the MFI to determine expression on a per cell basis, a small increase in HLA-ABC expression was observed after 9 hours incubation using an intermediate concentration of HIV-1 (3.9 x10^9 RNA copies/ml) (Figure 5.10E). No differences in HLA-ABC MFI were observed at 24 hours between any culture conditions (Figure 5.10D, E & F).

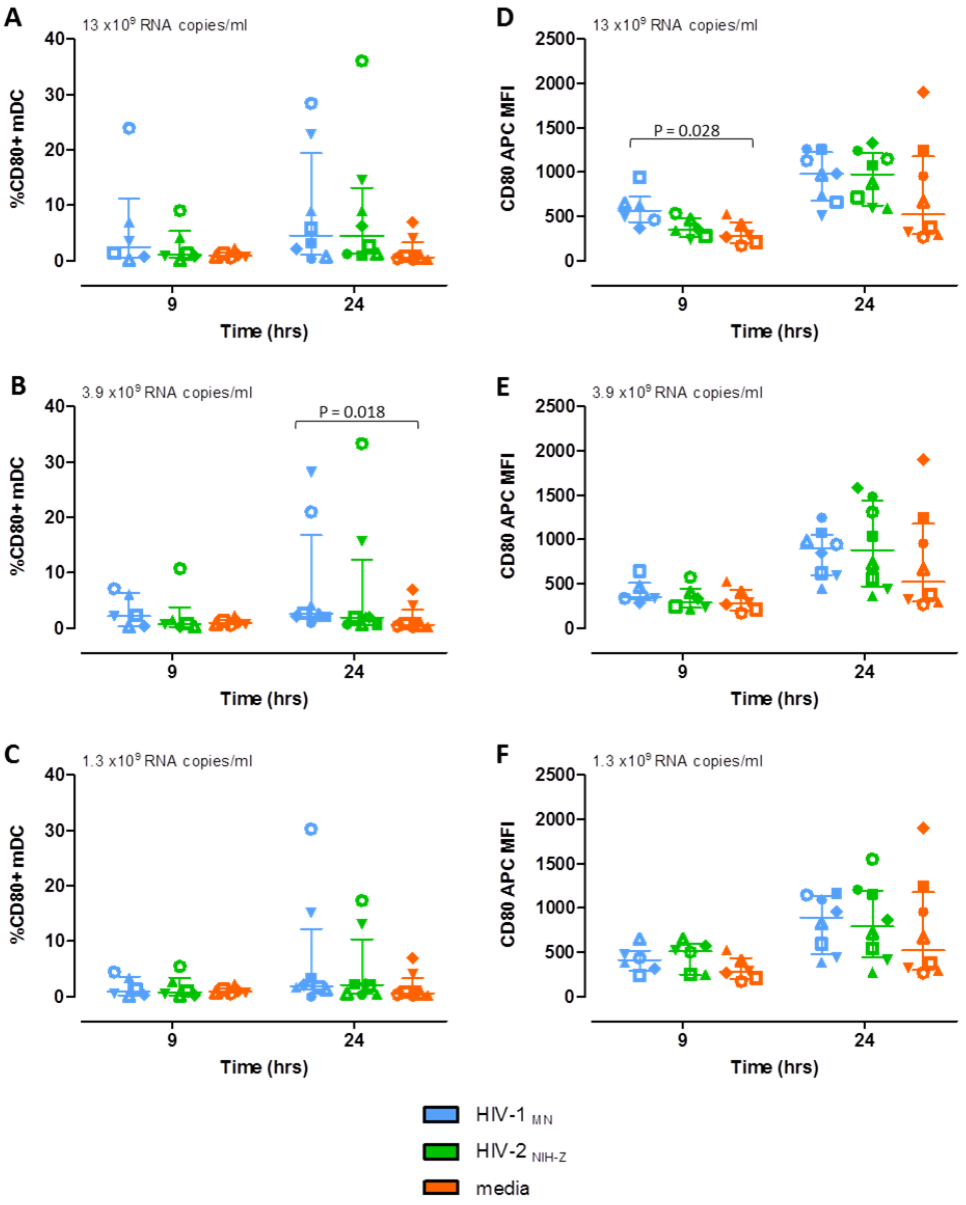

Figure 5.8. Expression of the co-stimulatory molecule CD80 on mDCs after PBMC exposure to HIV-1 and HIV-2. Left panels (A – C) show the percentage of $CD80^{+}$ mDCs and right panels (D – F) represent the MFI of CD80 on mDCs after stimulation with either HIV-1 or HIV-2 for 9 and 24 hours. The concentration of virus used to stimulate PBMCs is shown in the top left of each graph. Responses to HIV-1 are denoted in blue, HIV-2 in green and media alone (unstimulated cells) in orange. Individual donors are represented by different symbols. Horizontal bars represent median values and vertical lines show the IQR. Responses to HIV-1, HIV-2 and media alone within individual time points and virus concentrations were compared using a Friedman test with Dunn's post test.

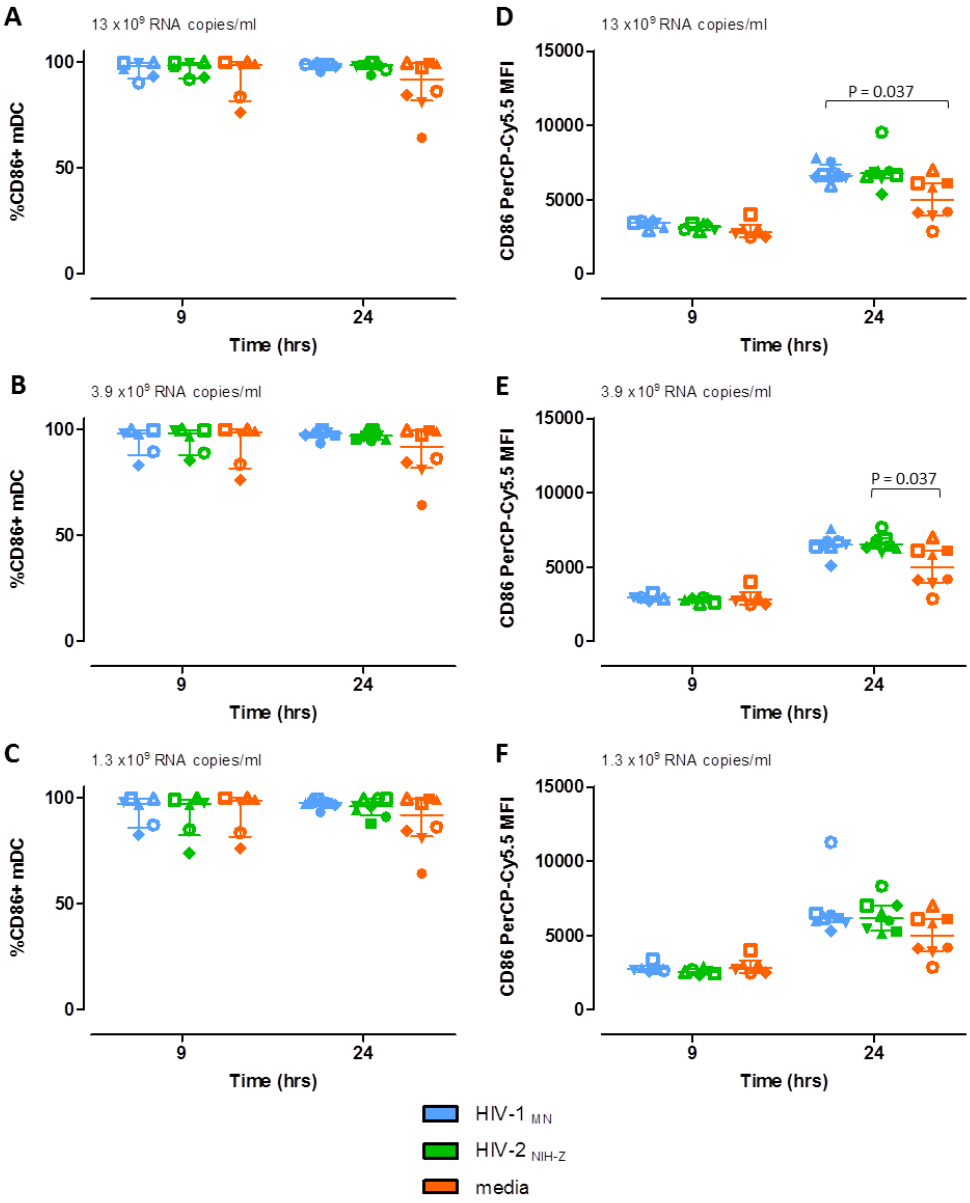

Figure 5.9. CD86 expression on mDCs following HIV-1 or HIV-2 exposure. Frequency of $CD86^{+}$ mDCs (left panels, A – C) and CD86 MFI of mDCs (right panels, D – F). The concentration of HIV-1 or HIV-2 used to stimulate PBMCs is shown in the top left of each graph. Responses to HIV-1 are indicated in blue, HIV-2 in green and media alone (unstimulated cells) in orange. Individual donors are represented by different symbols. Horizontal bars represent median values and vertical lines show the IQR. Responses to HIV-1, HIV-2 and media alone within individual time points and virus concentrations were compared using a Friedman test with Dunn's post test.

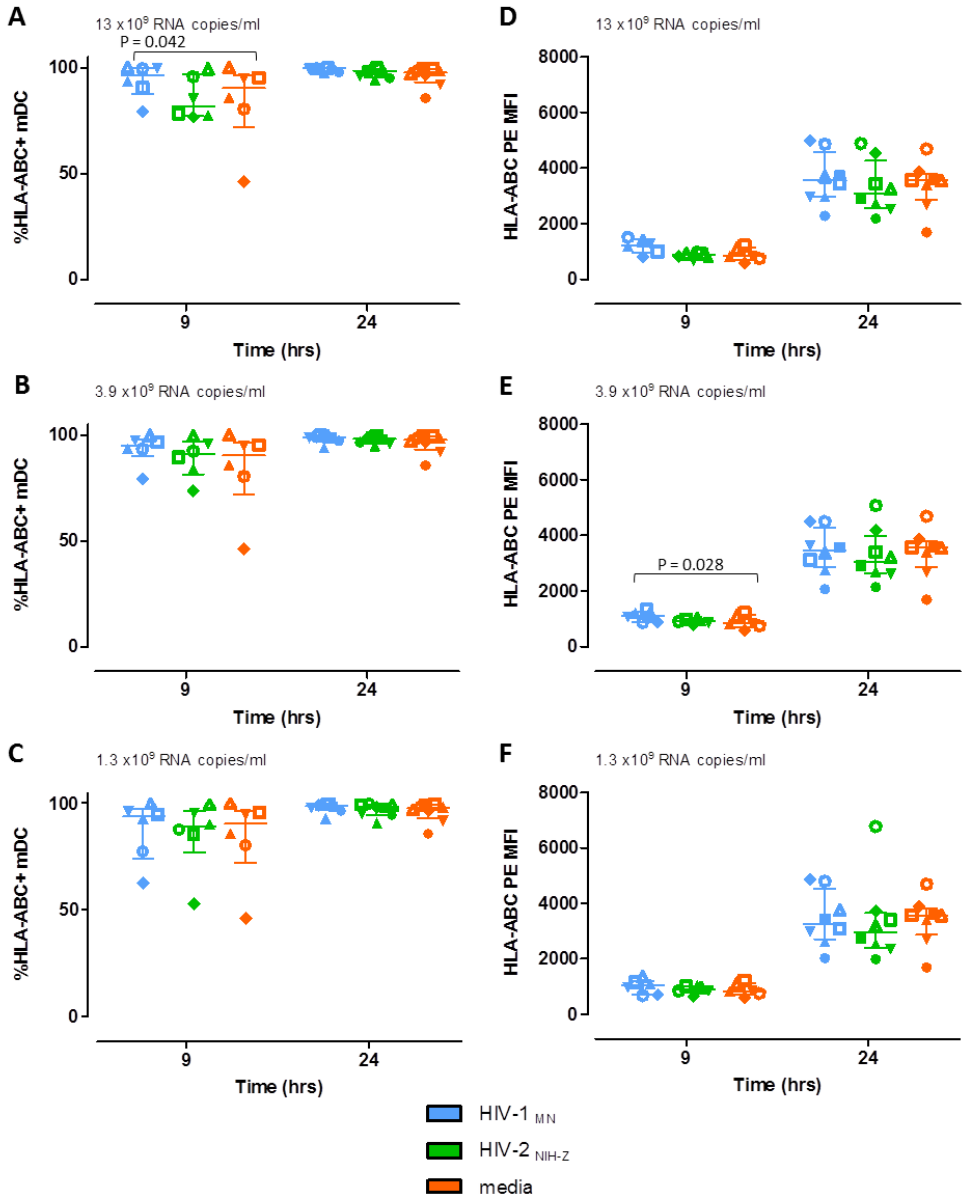

Figure 5.10. HLA-ABC expression on mDCs after PBMC stimulation. Percentage of HLA-ABC-expressing mDCs (left panels, A – C) and HLA-ABC MFI of mDCs (right panels, D – F) after stimulation with different concentrations of HIV-1 and HIV-2. Viral concentration used to stimulate PBMCs is shown in the top left of each graph. Responses to HIV-1 are shown in blue, HIV-2 is denoted in green and media alone (unstimulated cells) in orange. Individual donors are represented by different symbols. Horizontal bars represent median values and vertical lines show the IQR. Responses to HIV-1, HIV-2 and media alone within individual time points and virus concentrations were compared using a Friedman test with Dunn's post test.

5.3.5 Interferon-Secreting versus Antigen Presenting Phenotype

Using flow cytometry, pDCs were divided into cells actively secreting IFN-α (IFN-α^+), and those expressing the co-stimulatory molecule CD86 (Figure 5.11) or the activation marker CD83 (Figure 5.12) after viral stimulation. High concentrations of HIV-1 (13 x10^9 RNA copies/ml) induced a significantly greater percentage of CD86-negative IFN-α^+ pDCs after both 9 and 24 hours of stimulation. Conversely, similar concentrations of HIV-2 induced a significantly higher frequency of $CD86^+$ IFN-α-negative pDCs compared to unstimulated PBMCs at both time points tested (Figure 5.11). There was also a small, albeit statistically significant, increase in $CD86^+$ IFN-α^+ pDCs when PBMCs were stimulated with high concentrations of HIV-1 at both 9 and 24 hours. Interestingly, when low concentrations of virus were used (1.3 x10^9 RNA copies/ml), HIV-2 induced a higher percentage of IFN-α secreting pDCs, both $CD86^+$ and CD86-negative populations, but also a significantly greater proportion of $CD86^+$ IFN-α-negative pDCs at 24 hours compared to media alone. The changes in CD86-expressing and IFN-α-secreting cells were reflected in the frequency of double negative pDCs, which was significantly reduced at both 9 and 24 hours using high concentrations of HIV-2 compared to unstimulated cells, as well as with high concentrations of HIV-1 and low concentrations of HIV-2 after 24 hours of cell culture.

Under all conditions IFN-α-secreting cells were also positive for the activation marker CD83 (Figure 5.12). High concentrations of HIV-1 (13 x10^9 RNA copies/ml) induced a greater frequency of $CD83^+$ IFN-α^+ pDCs compared to media alone at both 9 and 24 hours. PBMCs exposed to low concentrations of HIV-2 (1.3 x10^9 RNA copies/ml) expressed a higher proportion of $CD83^+$ IFN-α^+ pDCs at both time points compared to media alone. Both HIV-1 and HIV-2 were able to induce a higher percentage of $CD83^+$ IFN-α-negative pDCs at 9 and 24 hours, compared to unstimulated cells. High and low concentrations of HIV-2 resulted in a significantly lower frequency of double negative cells after 9 hours of culture. Whereas after 24 hours stimulation, high concentrations of HIV-1 and low

concentrations of HIV-2 resulted in a significantly reduced frequency of double negative pDCs when compared to unstimulated cells.

The co-expression of IFN-α secretion, CD86 and CD83 was also analysed using SPICE software. Similar results were found at both 9 (Figure 5.13) and 24 hours (Figure 5.14). A small fraction of cells were identified as expressing all three markers. IFN-α-secreting pDCs made up a small fraction of pDCs, furthermore IFN-α^+ pDCs were found to always express CD83. The majority of pDCs were in fact IFN-α-negative $CD86^+$ $CD83^+$ or only positive for CD83. PBMC stimulation with HIV-2 induced a greater frequency of IFN-α-negative $CD86^+$ $CD83^+$ pDCs compared to unstimulated cells, while no significant change from media was observed after HIV-1 stimulation. Both HIV-1 and HIV-2 stimulation of PBMCs induced a significant increase in the frequency of IFN-α-negative CD86-negative $CD83^+$ pDCs compared to media alone.

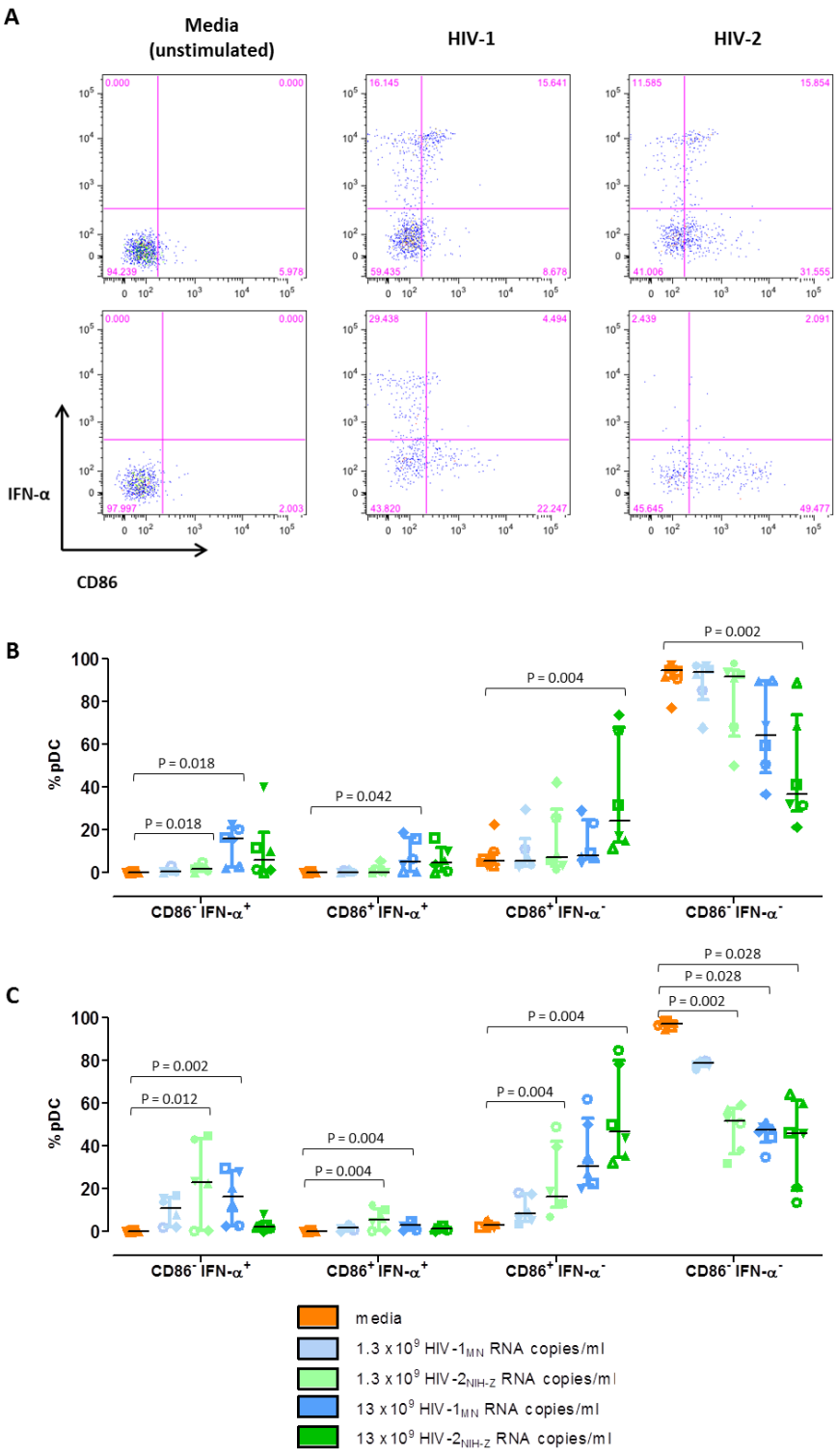

Figure 5.11. Simultaneous analysis of CD86 expression and IFN-α secretion on pDCs. (A) Flow cytometry plots of one representative donor showing IFN-α-PE on the y-axis and CD86-PerCP-Cy5.5 on the x-axis. Top and bottom row panels show results after 9 and 24 hours stimulation respectively. Percentage distribution in each quadrant is displayed. Graphs (B) and (C) show the percentage of pDCs expressing CD86, secreting IFN-α (IFN-α$^+$) or both following PBMC exposure to either HIV-1 or HIV-2 for 9 (B) and 24 hours (C). Responses to media alone (unstimulated) are represented in orange, HIV-1 in blue (light blue: low viral concentration, dark blue: high viral concentration) HIV-2 in green (light green: low viral concentration, dark green: high viral concentration). Responses to HIV-1, HIV-2 and media alone within individual time points and virus concentrations were compared using a Friedman test with Dunn's post test for multiple analyses.

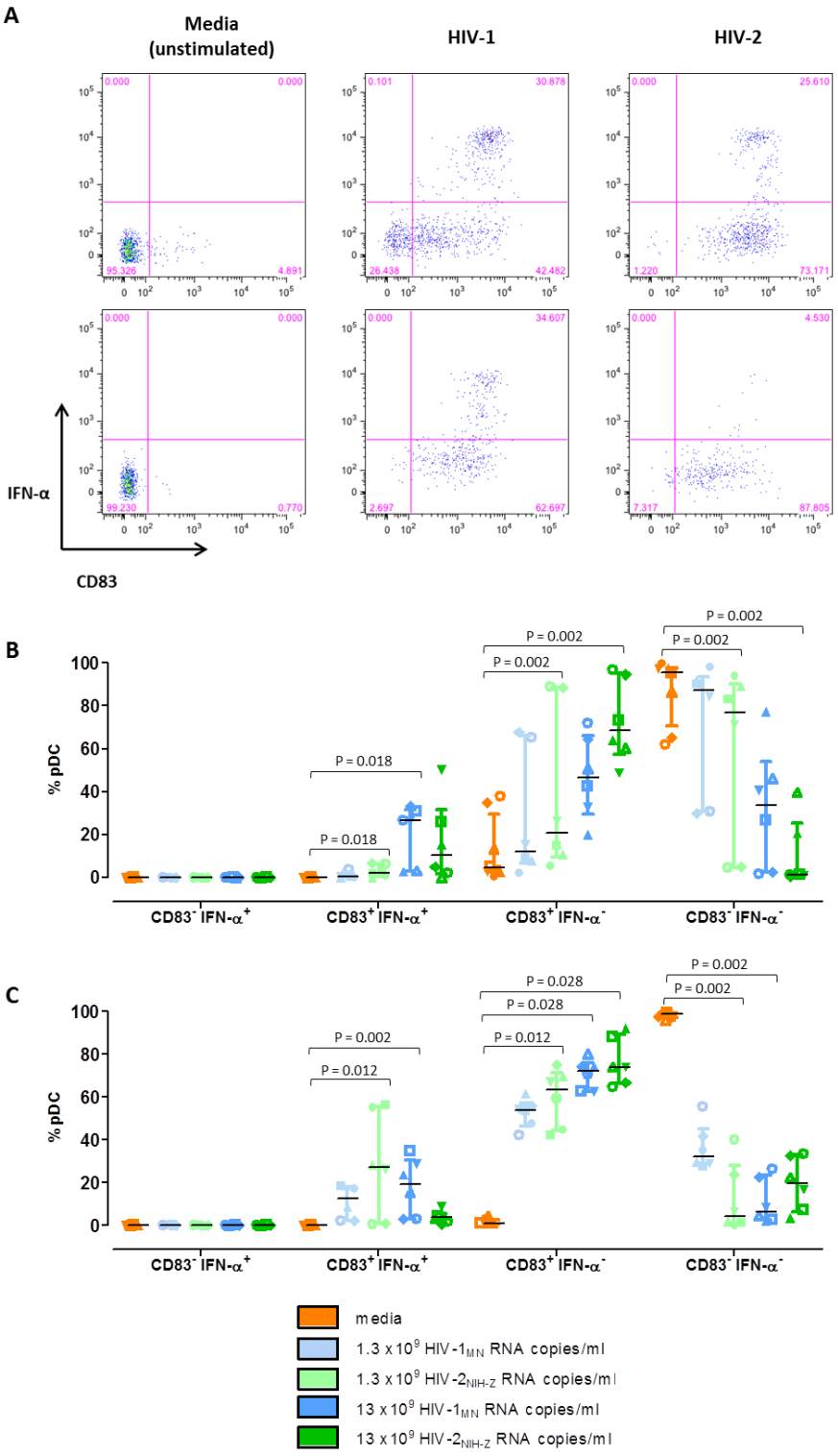

Figure 5.12. Simultaneous analysis of CD83 expression and IFN-α secretion on pDCs. (A) Flow cytometry plots of one representative donor, showing IFN-α-PE on the y-axis and CD83-BV421 on the x-axis. Top and bottom row panels show results after 9 and 24 hours stimulation respectively. Percentage distribution in each quadrant is displayed. Graphs (B) and (C) show the percentage of pDCs expressing CD83, secreting IFN-α (IFN-α^+) or both following PBMC exposure to either HIV-1 or HIV-2 for 9 (B) and 24 hours (C). Responses to media alone (unstimulated) are represented in orange, HIV-1 in blue (light blue: low viral concentration, dark blue: high viral concentration) HIV-2 in green (light green: low viral concentration, dark green: high viral concentration). Responses to HIV-1, HIV-2 and media alone within individual time points and virus concentrations were compared using a Friedman test with Dunn's post test.

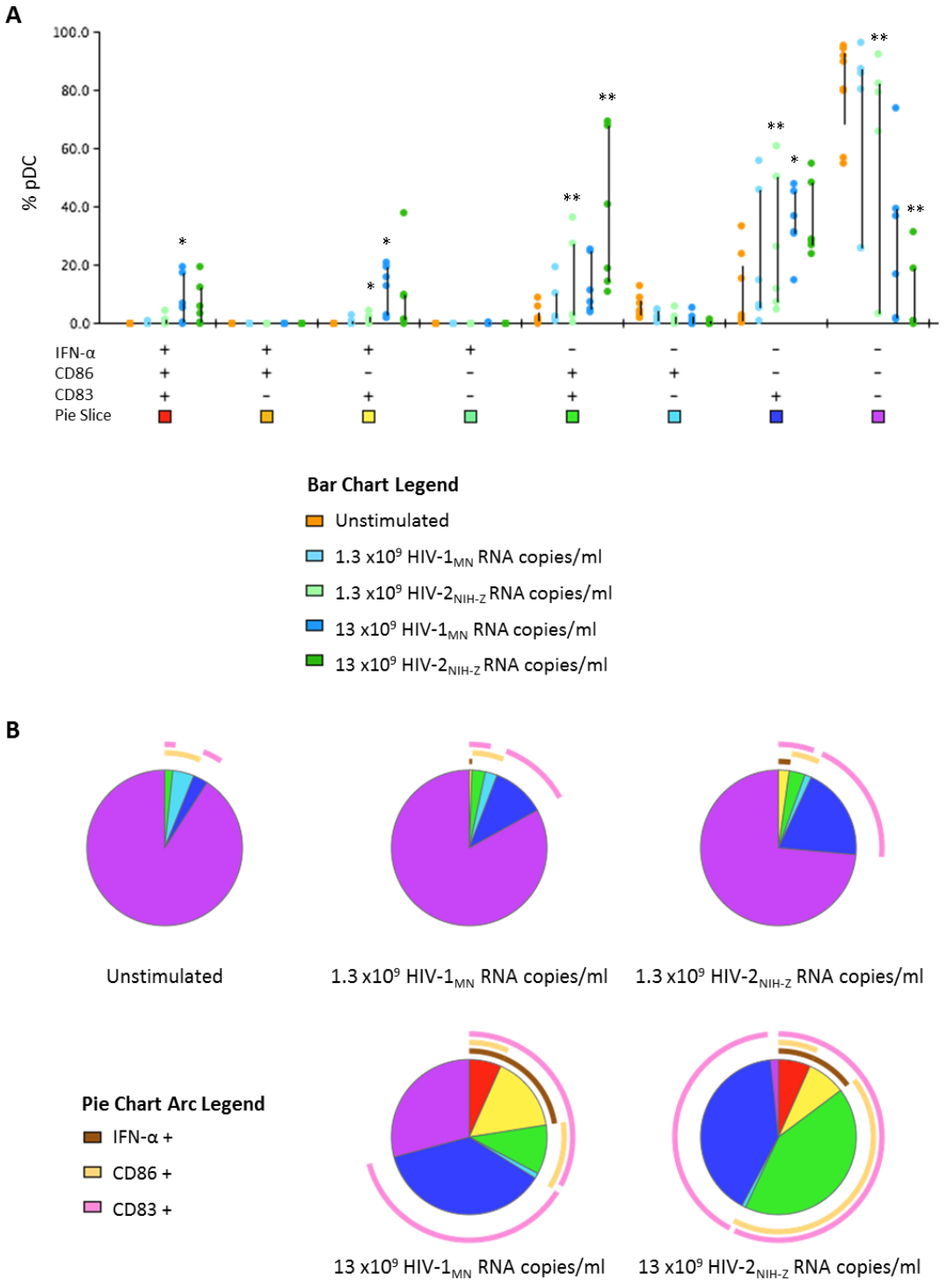

Figure 5.13. SPICE Analysis of IFN-α secretion and CD86 and CD83 expression after 9 hours. (A) Bar chart showing simultaneous expression of IFN-α, CD86 and CD83 in different combinations on pDCs. Responses to media alone (unstimulated) are represented in orange, HIV-1 in blue (light blue: low viral concentration, dark blue: high viral concentration) HIV-2 in green (light green: low viral concentration, dark green: high viral concentration). The frequency of phenotypically different pDCs within individual time points in response to media alone, HIV-1 and HIV-2 was analysed using a Friedman test with a Dunn's post test for multiple analyses. *p<0.05 **p<0.01. (B) Pie charts representing median distribution of phenotypically different pDCs. Colours of pie slices correspond to the colours shown on the x-axis of the bar chart in (A). Pie chart arcs illustrate which slices of pie express IFN-α (brown), CD86 (mustard) and CD83 (pink).

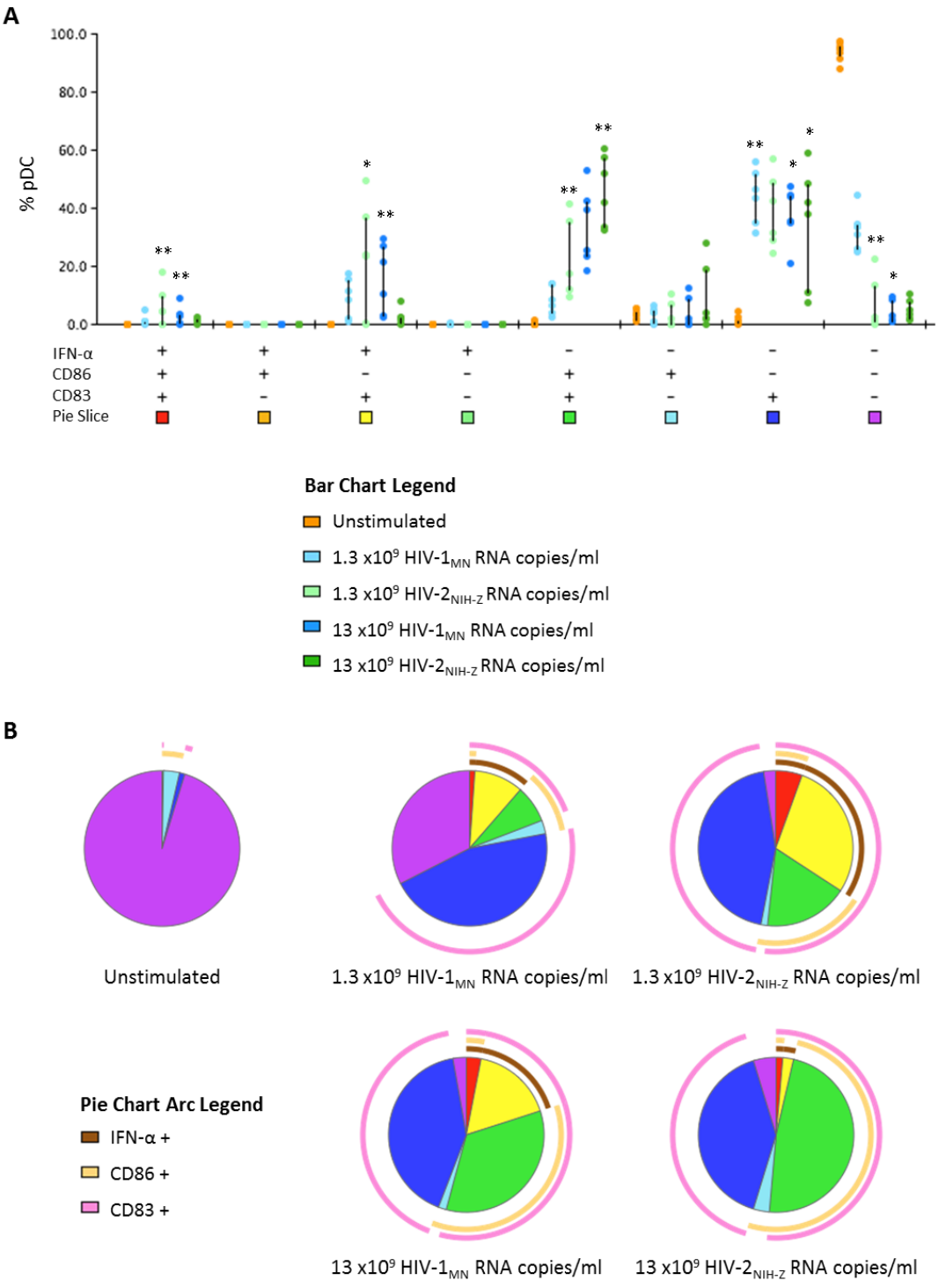

Figure 5.14. SPICE Analysis of IFN-α secretion and CD86 and CD83 expression after 24 hours. (A) Bar chart showing simultaneous expression of IFN-α, CD86 and CD83 in different combinations on pDCs. Responses to media alone (unstimulated) are represented in orange, HIV-1 in blue (light blue: low viral concentration, dark blue: high viral concentration) HIV-2 in green (light green: low viral concentration, dark green: high viral concentration). The frequency of phenotypically different pDCs within individual time points in response to media alone, HIV-1 and HIV-2 was analysed using a Friedman test with a Dunn's post test for multiple analyses. *p<0.05 **p<0.01. (B) Pie charts representing median distribution of phenotypically different pDCs. Colours of pie slices correspond to the colours shown on the x-axis of the bar chart in (A). Pie chart arcs illustrate which slices of pie express IFN-α (brown), CD86 (mustard) and CD83 (pink).

5.4 Discussion

HIV-1 is known to mature pDCs as well as mDCs and monocytes into APCs, inducing high expression of co-stimulatory molecules (Beignon *et al.*, 2005, Boasso *et al.*, 2011, Fonteneau *et al.*, 2004, Sabado *et al.*, 2010). The aim of this part of the project was to compare the effects of HIV-1 and HIV-2 stimulation of PBMCs on the maturation of pDCs, mDCs and monocytes. No expression of CD80 on pDCs was observed after 9 hours incubation under any culture condition. While CD80 expression remained low after 24 hours stimulation, the level of CD80 expression induced by both HIV-1 and HIV-2 was significantly greater compared to media alone, depending on the virus concentration used (Figure 5.1). HIV-2 induced CD86 expression on pDCs with a faster kinetic than HIV-1. In particular, using a high concentration of virus, HIV-2 induced a significantly greater frequency of CD86-expressing pDCs compared to media at 9 hours, whereas HIV-1 induced significant CD86 expression compared to media after 24 hours incubation (Figure 5.2A). A similar trend was observed using an intermediate concentration of virus, although statistical comparisons did not survive correction for multiple analyses at 9 hours. After 24 hours both HIV-1 and HIV-2 induced similar levels of CD86 expression. Expression of the activation marker CD83 on pDCs was significantly increased after stimulation with HIV-1 and HIV-2 compared to media alone after 24 hours (Figure 5.3). This was independent of the virus concentration used, although the observed change did not reach statistical significance when 3.9 $x10^9$ RNA copies/ml of HIV-2 was used. The kinetic with which CD83 was up-regulated changed according to the virus concentration used. High concentrations of HIV-1 induced a significantly greater frequency of CD83-expressing pDCs compared to media after 9 hours, while intermediate concentrations of HIV-2 induced higher CD83 expression on pDCs at 9 hours. Low concentrations of HIV-1 and HIV-2 induced a similar proportion of $CD83^+$ pDCs after 9 hours.

Overall both HIV-1 and HIV-2 induced high levels of co-stimulatory molecule and CD83 expression on pDCs, despite remarkable differences in their ability to induce IFN-α secretion, as shown in Chapter 3. This is in contrast to previous work, in which *in vitro* exposure to HIV-2 did not induce co-stimulatory

molecule expression on pDCs (Duvall *et al.*, 2007). However, the authors used purified pDCs which require additional cytokines, namely IL-3, for survival. This could potentially account for the differences in result as it has previously been shown that IL-3-induced DCs stimulate T_H2 $CD4^+$ T cell responses over T_H1 responses (Kadowaki *et al.*, 2000).

We have previously demonstrated that the induction of expression of CD80, CD86 and CD83 on pDCs is not completely reliant on the concentration of IFN-α produced. HIV-1 treated with βCD causes an alteration in the composition of the plasma membrane lipid raft by removing cholesterol, thus rendering it less efficient at inducing IFN-α secretion. Cholesterol-deprived HIV-1 preserved the ability to induce co-stimulatory molecule up-regulation on pDCs despite the inability to induce IFN-α production (Boasso *et al.*, 2011).

Based on these results and previous studies showing that phenotypic maturation of pDCs can be dissociated from IFN-α production depending on different intracellular trafficking (Guiducci *et al.*, 2006, Honda *et al.*, 2005a, O'Brien *et al.*, 2011), the simultaneous expression of CD86 and secretion of IFN-α by pDCs was examined. The aim was to determine if stimulation with HIV-1 and HIV-2 would result in functionally different mature pDCs. This was achieved using a flow cytometry based IFN-α secretion assay. One advantage of the assay used in this project is that it allows the detection of pDCs actively secreting IFN-α, rather than cells with intracellular stores of IFN-α.

Using a high concentration of virus, HIV-1 induced a greater frequency of CD86-negative IFN-α^+ pDCs and $CD86^+$ IFN-α^+ pDCs compared to media alone at both 9 and 24 hours. Conversely, HIV-2 induced a greater proportion of $CD86^+$ IFN-α-negative pDCs at both 9 and 24 hours (Figure 5.11). It is worth noting that the percentage of $CD86^+$ IFN-α^+ pDCs remained low, particularly at 24 hours, consistent with the notion that expression of co-stimulatory molecules and IFN-α secretion are distinct pDC functions (Bruel *et al.*, 2014). These results suggest that in this experimental set up, HIV-2 behaves in a

similar manner to CpG-B, inducing co-stimulatory molecule expression in preference to type I IFN. It remains to be determined whether, similar to CpG-B, HIV-2 is trafficked to the lysosomes, thus preferentially stimulating the NF-κB signalling pathway over IRF-7. Another future line of investigation would be to determine if the APC phenotype induced by HIV-2 correlates with enhanced T cell stimulation. In support of this hypothesis, CpG-B stimulated pDCs proved to be more potent at eliciting allogeneic T cell proliferation compared to both HIV-1 and CpG-A stimulated pDCs (O'Brien *et al.*, 2011). Furthermore, Fonteneau *et al* (2004) showed that the ability of pDCs to stimulate T cell proliferation correlates with the levels of co-stimulatory molecule expression on the cell surface. A study by Matsui *et al* (2009) also identified two functionally distinct subsets of pDCs based on the expression of CD2. The authors report that activated $CD2^{high}$ pDCs expressed higher levels of co-stimulatory molecules and were more efficient at inducing naïve T cell proliferation than $CD2^{low}$ pDCs (Matsui *et al.*, 2009).

Using low concentrations of virus, after 24 hours of stimulation both HIV-1 and HIV-2 induced a higher percentage of CD86-negative IFN-α^{+} pDCs compared to media alone, although for HIV-1 the statistical significance of this effect did not survive correction for multiple analyses. HIV-2 also induced a higher frequency of $CD86^{+}$ IFN-α-negative pDCs compared to unstimulated cells, while this difference was not seen using low concentrations of HIV-1. The differences in pDC activation by high and low concentrations of HIV-2 were surprising, considering that previous measurement of IFN-α by ELISA showed that HIV-1 was consistently more potent at inducing IFN-α compared to HIV-2, regardless of the concentration of virus used (shown in Chapter 3). One possible explanation for this difference in result is in the source of PBMCs used. Detection of IFN-α-secreting pDCs was conducted using whole blood obtained from healthy volunteers within the department. While assays measuring IFN-α in cell culture supernatants as well as flow cytometry looking solely at CD80, CD86 and CD83 expression were performed on blood obtained from leucocyte cones. PBMCs from both sources responded with different kinetics and potency to stimuli, which may therefore explain why low concentrations of HIV-

2 were able to induce greater IFN-α secretion than similar concentrations of HIV-1, a phenomenon that was not observed when using leucocyte cones. While whole blood is obtained from healthy volunteers the same day the PBMCs are isolated, leucocyte cones are obtained from the NHS Blood and Transplant Service, and are thus often already 24 hours old before the PBMCs are isolated from the blood. Plasmacytoid DCs are extremely fragile and often do not survive beyond 48 hours without the addition of survival factors such as IL-3. Furthermore, large variations in IFN-α-secreting cells were seen amongst samples stimulated with low concentrations of HIV-2. Increased study numbers would help elucidate whether this difference is real or an artefact of variability.

Cells expressing CD83 as well as secreting IFN-α were also examined. The results show that IFN-α secretion and expression of CD83 are not mutually exclusive. All pDCs found to be positive for IFN-α also expressed CD83 (Figure 5.12). High concentrations of HIV-1 induced a significantly greater frequency of $CD83^+$ IFN-α^+ pDCs compared to media alone. This difference was not observed for HIV-2. Conversely, independent of the concentration used, HIV-2 resulted in a significantly greater proportion of $CD83^+$ IFN-α-negative pDCs at both 9 and 24 hours compared to unstimulated cells, indicating that these cells have undergone maturation. HIV-1 also induced $CD83^+$ IFN-α-negative pDCs, although this was not statistically significant until 24 hours of stimulation.

Although the main function of pDCs is thought to be the secretion of IFN-α, these results show a much higher frequency of $CD83^+$ IFN-α-negative pDCs compared to $CD83^+$ IFN-α^+ pDCs independent of the stimulus. This demonstrates a population of mature pDCs which do not secrete IFN-α. Analysis using SPICE software revealed that a large proportion of these $CD83^+$ IFN-α-negative pDCs co-expressed CD86, indicating that they are most likely involved in APC activity. However, there was a subset of pDCs which were only positive for CD83. Perhaps this population of pDCs have been activated, and therefore express CD83, but it is yet to be determined whether they will become APCs or IFN-secreting cells. Another possibility is that this population of $CD83^+$ IFN-α-negative pDCs represent cells which

have lost the ability to secrete IFN-α due to potent viral stimulus. Indeed, pDCs activated by influenza, a strong TLR stimulus for NF-κB signalling, mature into APCs, however they then become refractory to further cytokine production (O'Brien *et al.*, 2011), or perhaps these cells are involved in the secretion of other inflammatory cytokines, such as TNF-α or IL-6. In addition, it remains to be determined whether these activated pDCs secrete species of type I IFN, other than IFN-α, which are not detected by this assay.

During maturation, pDCs down-regulate BDCA2 expression, while expression of CD123 on the other hand has been shown to increase after pDC activation (Van Brussel *et al.*, 2010). BDCA2 MFI appears to decrease between 9 and 24 hours independent of the culture condition. However, in this experimental set up there were no significant differences in the MFI of BDCA2 between unstimulated, HIV-1 and HIV-2 stimulated PBMC cultures (Figure 5.4A, B & C). Overall, while CD123 expression on pDCs was reduced from 9 to 24 hours incubation, the expression of CD123 was maintained at a higher level after 24 hours of stimulation with HIV-2 compared to unstimulated cells. This was significant compared to unstimulated cells using both intermediate and low concentrations of HIV-2 (Figure 5.4D, E & F). These results are consistent with the hypothesis that HIV-2 is not just a weaker stimulus for pDCs, but rather that differences exist between the ways in which HIV-1 and HIV-2 induce pDC maturation.

The frequencies of CD80-expressing monocytes were negligible after PBMC exposure to either HIV-1 or HIV-2. However, using the MFI as a measure of the expression of CD80 per cell, both HIV-1 and HIV-2 induced a greater level of CD80 expression compared to media alone after 24 hours (Figure 5.5D, E & F). HIV-1 and HIV-2 also induced a significantly higher proportion of monocytes to express CD86 at both 9 and 24 hours after stimulation (Figure 5.6). A mild response to virus stimulation was observed for CD83 expression on monocytes. All concentrations of HIV-1 tested induced greater CD83 expression compared to media alone, whether CD83 expression was measured as the frequency of

expressing cells or the MFI. HIV-2 was also able to induce CD83 expression to some extent on monocytes (Figure 5.7). It is likely that the increases in co-stimulatory molecules as well as CD83 on monocytes are a secondary response to IFN-α production, although expression of CD86 on monocytes is not strictly dependent on IFN-α (Boasso *et al.*, 2008b). It is possible that cell-cell interactions as well as secretion of other inflammatory cytokines from pDCs, such as TNF-α and IL-6, induce co-stimulatory molecule expression on monocytes.

It is now recognised that mDCs are not directly activated by exposure to HIV *in vitro*. While mDCs express PRRs capable of detecting viral RNA, secreted products from activated pDCs cause maturation of mDCs, increasing the expression of co-stimulatory molecules, rather than HIV itself (Fonteneau *et al.*, 2004). Results from this thesis showed that HIV-1 induced only marginal increases in CD80 expression on mDCs. No statistically significant changes in CD80 expression on mDCs were observed after incubation with HIV-2 (Figure 5.8). Conversely, almost 100% of mDCs were positive for CD86 after 24 hours independent of the culture condition (Figure 5.9A, B & C). High expression of CD86 on mDCs in the absence of stimulus has previously been reported (Sabado *et al.*, 2010) which most likely reflects their role as professional APCs. Examining the MFI of CD86 showed that both HIV-1 and HIV-2 induced CD86 expression above that of unstimulated cells (Figure 5.9D, E & F). After 24 hours it was not surprising that 100% of mDCs stained positive for HLA-ABC, as almost all human cells are known to express MHC-I. However, PBMC stimulation with the highest concentration of HIV-1 caused a more rapid up-regulation of MHC-I expression on mDCs, compared to media alone. A similar difference was not observed with HIV-2 (Figure 5.10A). This was not particularly surprising as IFN-α is known to increase MHC-I (Keir *et al.*, 2002). A previous study we conducted using an IFN-α incompetent virus showed no HLA-ABC up-regulation on mDCs in the absence of IFN-α (Boasso *et al.*, 2011). The kinetics of IFN-α secretion by HIV-1 and HIV-2 (shown in Chapter 3) revealed that HIV-1 induces IFN-α secretion at a more rapid rate than does HIV-2, which may therefore explain the HIV-1-induced increase in MHC-I expression after only 9 hours.

The slight increases in FVD staining after HIV-2 stimulation (Table 5.2), indicating a higher frequency of dead or dying cells, may reflect enhanced apoptosis due to increased cell activation. It may be helpful to differentiate apoptotic cells from dead cells, in which case Annexin V staining may be useful. Nonetheless, the small alterations in cell viability did not affect the results as dead cells were in fact excluded from analysis of the IFN-α secretion assay (gating strategy shown in Chapter 2, Figure 2.5), which showed increased CD86 and CD83 expression on pDCs after HIV-2 stimulation.

The data presented in this chapter indicate that HIV-2 is able to induce an antigen presenting phenotype in pDCs to a similar, if not greater, degree to HIV-1 after PBMC stimulation. These results may in part explain why efficient T cell proliferative and anti-viral responses are preserved during HIV-2 infection.

Chapter 6 Discussion and Conclusions

HIV-2 represents a naturally attenuated form of HIV. Patients infected with HIV-2 display a slow rate of disease progression, which is characterised by lower plasma viral loads and higher $CD4^+$ T cell counts compared to HIV-1^+ individuals (Andersson *et al.*, 2000, Marlink *et al.*, 1994, Nyamweya *et al.*, 2013). Thus, the majority of HIV-2^+ patients display a phenotype similar to HIV-1 infected long-term non-progressors (LTNPs). HIV-2 represents a unique tool to investigate the mechanisms underlying control of HIV infection, which could form the basis for designing and developing new therapeutic and prophylactic strategies.

The overall aim of this thesis was to compare the two related, yet distinct viruses, HIV-1 and HIV-2, for their abilities to activate pDCs. Chronic activation of pDCs has been hypothesised to contribute to HIV-1 immunopathogenesis (Boasso and Shearer, 2008, Miedema *et al.*, 2013). However, a recent paper by Kader *et al* (2013) demonstrated that while pDCs are the predominant producers of IFN-α during the acute stages of SIV infection in rhesus macaques, it is mainly mDCs that are responsible for IFN-α secretion during chronic disease. Thus, while pDCs may play a secondary role in type I IFN-mediated pathogenesis during chronic HIV-1 infection, they may influence the early innate response and the development of adaptive immunity during HIV exposure. Plasmacytoid DCs may contribute to HIV-1 immunopathogenesis by recruiting target cells to the site of infection (Li *et al.*, 2009), increasing apoptotic and immunosuppressive pathways in addition to increasing T cell activation (Boasso *et al.*, 2008a, Boasso *et al.*, 2008b, Fraietta *et al.*, 2013, Herbeuval *et al.*, 2005b, Rodriguez *et al.*, 2006, Lehmann *et al.*, 2014), and altering the T_H17/Treg balance at the mucosal interface (Favre *et al.*, 2009, Favre *et al.*, 2010).

Studies examining HIV-1 and HIV-2 infected patients have identified critical differences in the immune responses against HIV-1 and HIV-2 during chronic infection. However, the early events occurring

during acute infection which dramatically contribute to disease outcome cannot be investigated in chronically infected HIV-1^+ and HIV-2^+ individuals. Thus, in this study the effects of acute viral stimulation were tested by exposing PBMCs from healthy individuals to HIV-1 or HIV-2 *in vitro*. This experimental approach allowed the observation of early events differentiating HIV-1 and HIV-2 exposure in PBMCs which have not previously been exposed to HIV, thus removing any bias from existing immunity or plasma virus concentrations. Importantly, viral concentrations used in this study were normalised for RNA content. The innate immune system recognises viral nucleic acids, due to the expression of conserved PAMPs, by host expressed PRRs (Kawai and Akira, 2007). Therefore by normalising virus concentrations on RNA, cells are stimulated with equal amounts of PAMP, ensuring that any differences observed in cell activation are due to virus-host interactions and not a result of differences in viral concentrations.

Overall the major difference identified between HIV-1 and HIV-2 was the type I IFN signature. HIV-2 induced a markedly reduced type I IFN response in comparison to HIV-1. This difference was confirmed both by gene array results and at a translational level, measuring IFN-α secretion into cell culture supernatants. The strong correlation between high levels of type I IFN production, measured by ELISA, and the frequency of IFN-α-secreting pDC, identified by flow cytometry, indicated that pDCs were the main producers of type I IFN in this experimental system. These results support the hypothesis that excessive IFN-α contributes to HIV-1 immunopathogenesis.

It is worth noting that the aim of the RT-qPCR assay developed in this study was to normalise the RNA content of HIV-1 and HIV-2 against each other. Therefore a protocol was designed in which the measurement of RNA in HIV-1 and HIV-2 could be run under the same experimental conditions in order to limit variation. Measurement of the RNA concentration using the NanoDrop revealed a mean difference of 7.4 between HIV-1_{MN} and HIV-2_{NIH-Z}. A similar fold difference in RNA concentration of 8.8 was calculated using the RT-qPCR, consistent with the qPCR efficiencies. Inter-assay variability was not

assessed, as samples were run within one plate, nor was the protocol validated against clinical assays used to quantify plasma viral load. The sensitivity of the assay was limited by the RNA extraction method, whereby the lowest volume of virus which yielded RNA of both good quality and within the linear range of extraction was 12 µl. However, despite the potential limitations of the quantification and normalisation of RNA, the differences observed between HIV-1 and HIV-2 appear to be independent of virus concentration. This was particularly demonstrated in Chapter 3 (Figure 3.5), which illustrates that the differences in IFN-α secretion observed cannot be overcome by increasing the concentration of HIV-2.

Upon examination of the phenotypic maturation of pDCs, a similar up-regulation in co-stimulatory molecules, CD80 and CD86, as well as the activation marker CD83, was observed when cells were stimulated with either HIV-1 or HIV-2 compared to unstimulated PBMCs. A growing body of evidence shows that pDCs can mature into functionally dichotomous populations, either to secrete high levels of type I IFN, or act as professional APCs, expressing high levels of co-stimulatory molecules (Guiducci *et al.*, 2006, Honda *et al.*, 2005a, Jaehn *et al.*, 2008, O'Brien *et al.*, 2011). Based on this information, expression of CD86 in conjunction with the ability to secrete IFN-α was examined by flow cytometry. These results showed that HIV-2 preferentially matured pDCs into phenotypic APCs, while in contrast, HIV-1 induced a greater proportion of IFN-α-secreting pDCs.

In comparison to HIV-1^+ patients, HIV-2 infected individuals maintain greater T cell functionality throughout infection (Duvall *et al.*, 2006, Duvall *et al.*, 2008, Nyamweya *et al.*, 2013, Sousa *et al.*, 2001). Antigen presenting cells play a crucial role in priming effective T cell responses and can induce apoptosis and tolerance (Chougnet *et al.*, 2002, Williams and Bevan, 2007). Therefore, the increase in APCs in the absence of increased levels of both type I IFN and IDO may translate into the improved T cell responses documented in HIV-2^+ patients (Figure 6.1).

One limitation of the study was the sole use of lab-adapted viruses, as opposed to founder or transmitted viruses which would be more relevant for studying the early stages of infection. Founder viruses tend to use CCR5, rather than CXCR4, as a co-receptor for cellular entry. In addition, differences have been reported in terms of the replicative efficiency of founder viruses compared to lab-adapted CCR5-tropic HIV-1 isolates (Ochsenbauer *et al.*, 2012). Interestingly, founder viruses are reported to be relatively resistant to the anti-viral effects of type I IFN (Fenton-May *et al.*, 2013). High plasma concentrations of IFN-α have been reported during the acute stage of infection in HIV-1^+ patients (Stacey *et al.*, 2009), suggesting that HIV-1 founder viruses may in fact continue to replicate and establish infection in spite of increased type I IFN. Thus, the fact that founder/transmitted HIV-1 is insensitive to the anti-viral effects of type I IFN during acute infection, further supports the hypothesis that increased APC capability may be more beneficial than an excessive IFN-secreting phenotype, similar to that observed with HIV-2 in this thesis.

Spatiotemporal trafficking of TLR ligands within pDCs determines their mature phenotype. HIV-1, similar to CpG-A, has been shown to traffic to the early endosome where it stimulates persistent IFN-α secretion via IRF-7 induction. CpG-B on the other hand, traffics to the lysosome resulting in preferential activation of the NF-κB pathway and up-regulation of co-stimulatory molecules, yet weakly stimulating IFN-α/β secretion (O'Brien *et al.*, 2011). As expected, CpG-B activated pDCs proved to be more efficient APCs, compared to HIV-1 activated pDCs (O'Brien *et al.*, 2011). The results presented in this thesis suggest that HIV-2 behaves in a similar fashion to the synthetic ligand CpG-B in terms of pDC activation, thus further corroborating the hypothesis that pDC maturation during HIV-2 infection contributes to enhanced T cell responses.

The lower levels of IFN-α induced by HIV-2 as well as the reduced activity of the immunosuppressive enzyme IDO, may both contribute to the lower levels of immune activation and apoptosis observed in HIV-2 infected individuals. Type I IFN can induce the expression of apoptotic and immunosuppressive

ligands, namely TRAIL and PD-L1, which have been associated with HIV-1 disease progression (Boasso *et al.*, 2008b, Griffith *et al.*, 1999, Hardy *et al.*, 2007, Herbeuval *et al.*, 2005a, Herbeuval *et al.*, 2005b, Maier *et al.*, 2007, Yao and Chen, 2006). Furthermore, IDO has been implicated in HIV-1 immunopathogenesis, both inhibiting anti-viral T cell responses and altering the T_H17/Treg ratio (Favre *et al.*, 2009, Favre *et al.*, 2010, Potula *et al.*, 2005). The lower induction by HIV-2 of mechanisms which dampen the immune response may in part explain the more efficient T cell responses and better disease outcome compared to HIV-1 infection.

Studies performed in non-human primate models have also demonstrated striking differences in the type I IFN response between the non-pathogenic natural hosts of SIV, the sooty mangabey and African green monkey, and disease susceptible SIV infection of rhesus macaques (Bosinger *et al.*, 2009, Harris *et al.*, 2010, Jacquelin *et al.*, 2009). Similar to the results described in this thesis, stimulation of PBMCs from sooty mangabeys with SIV_{SM}, from which HIV-2 originates, fails to elicit potent IFN-α secretion, in contrast to PBMCs from the rhesus macaque (Bosinger *et al.*, 2013, Mandl *et al.*, 2008). However, NF-κB signalling pathways in both sooty mangabey and rhesus macaque pDCs remains intact, secreting similar levels of pro-inflammatory cytokines such as TNF-α (Mandl *et al.*, 2008). This suggests that differential maturation of pDCs may occur in the natural host of SIV compared to pathogenic SIV infection, suggesting that pDC activation is a major contributing factor to immune dysregulation and therefore disease progression.

Importantly, the reduced levels of IFN-α secreted in response to HIV-2 were still sufficient to induce a robust innate immune response, epitomised by similar up-regulation of ISG expression following HIV-1 and HIV-2 stimulation of PBMCs. Furthermore, a similar increase in both mDC and monocyte activation, as measured by co-stimulatory molecule expression, was observed after PBMC culture with HIV-1 and HIV-2. Gene array data also showed that the expression of genes involved in antigen processing and presentation were similarly up-regulated in response to HIV-1 and HIV-2, suggesting

that the molecular pathways required for efficient antigen presentation are maintained in response to HIV-2 stimulation.

HIV-1-infected patients with pre-existing HIV-2 infection display a slower disease progressing phenotype, characterised by higher $CD4^+$ T cell counts compared to HIV-1 mono-infected patients (Esbjornsson *et al.*, 2012). Thus, HIV-2 infection is not only less pathogenic than HIV-1, but might also be beneficial in the context of co-infection. A previous study reported that the simultaneous exposure of pDCs to the synthetic TLR-9 ligands, CpG-A and CpG-B, resulted in activated pDCs with a phenotype more similar to that induced by CpG-B alone, namely an increase in co-stimulatory molecule expression over type I IFN secretion (Jaehn *et al.*, 2008). Consistent with this report, IFN-α secretion in response to CpG-A was significantly reduced when PBMCs were simultaneously treated with HIV-2, highlighting the dominant effect of HIV-2 on reducing pDC-mediated IFN-α secretion, most likely by driving pDCs down the maturation pathway to become APCs over IFN-producing cells. It is therefore possible that in patients with pre-existing HIV-2 infection, HIV-1 fails to induce an inflammatory response dominated by IFN-α. The lack of type I IFN-induced immunosuppressive mechanisms may translate into the development of more efficient adaptive responses and a slower disease progressing phenotype in co-infected patients.

A recent study examined the effect of TLR-7/9 inhibition *in vivo* during acute SIV infection, and showed no reduction in immune activation or viral load (Kader *et al.*, 2013). The results documented in this thesis suggest that rather than blocking pDC activation entirely by inhibiting TLR-7/9 activation, an improvement in disease outcome may be established by pushing pDCs into APCs rather than IFN-producing cells. HIV-1 infected patients who efficiently control viral replication below detection level in the absence of ART (elite controllers) show enhanced antigen-presenting cell capabilities compared to both HIV^+ patients with progressive disease and HIV-negative individuals (Huang *et al.*, 2010). This

was documented as an increased ability to induce both $CD4^+$ and $CD8^+$ allogeneic T cell proliferation *in vitro*, suggesting that APCs play a critical role in regulating viral control.

Collectively these data demonstrate that HIV types which cause different disease phenotypes *in vivo* can be characterized by their effect on pDC maturation *in vitro*. The conditioning of pDCs during the acute stages of infection may contribute to disease outcome, depending on whether the response is dominated by IFN-α or an APC phenotype. The dominant effect of HIV-2 on pDC differentiation over the synthetic TLR-9 ligand, CpG-A, suggests that manipulation of pDC activity may be considered to enhance the efficiency of prophylactic strategies by limiting IFN-α responses and enhancing APC maturation at the time of immunisation or viral exposure.

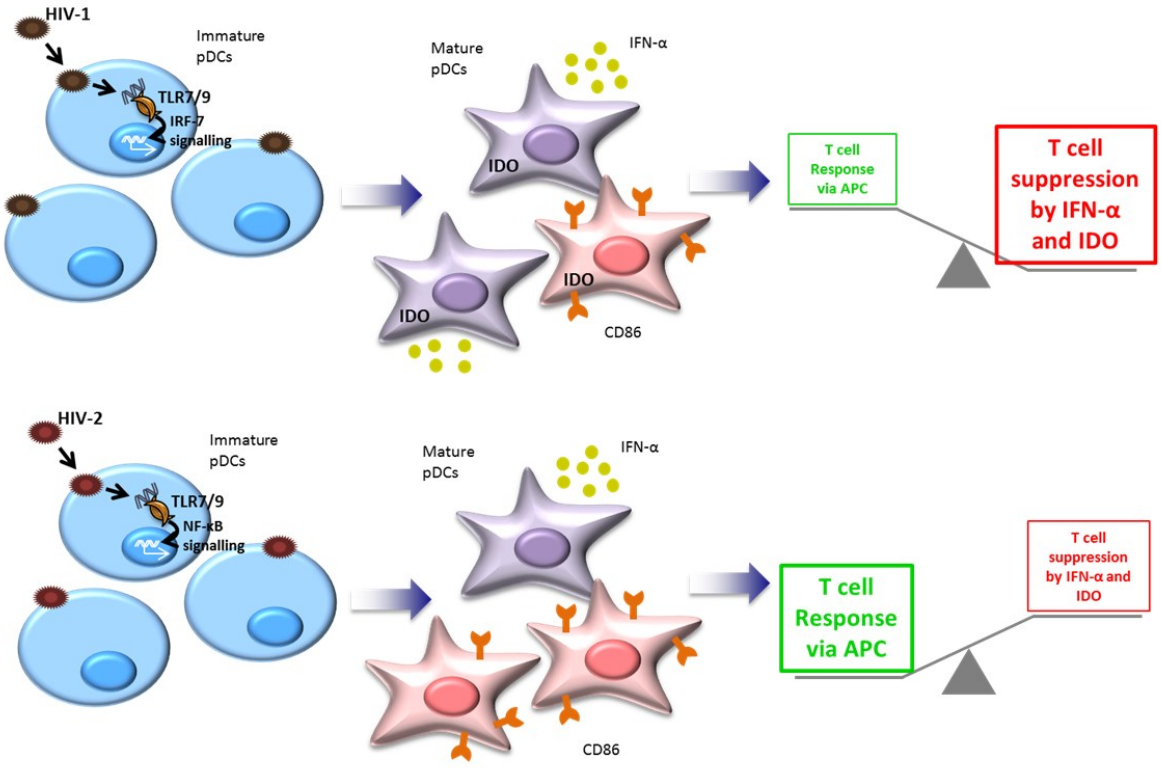

Figure 6.1. HIV-1 versus HIV-2 activation of pDCs. The preferential activation of IFN-producing regulatory pDCs by HIV-1 (top panel) may contribute to poorer disease outcome, characterised by early suppression of T cell responses. Conversely, pDC activation by HIV-2 (shown in the bottom panel) induces a greater number of CD86 expressing cells, which may lead to more efficient T cell responses and slower disease progression. The secretion of IFN-α also leads to maturation of other APCs, such as mDCs and monocytes, which occurs in the setting of both HIV-1 and HIV-2 stimulation, despite the lower levels of type I IFN induced by HIV-2.

6.1 Future Work

There are many possible avenues to take in terms of future work on the contribution pDCs make to HIV-1 immunopathogenesis. Some of the important questions to ask include the following:

Does the different pDC maturation state translate into differences in T cell activation *in vitro*?

Perhaps the first step would be to investigate if pDC activation by HIV-2, leading to the expression of CD86 in the absence of high concentrations of IFN-α and IDO, would in fact lead to a more efficient T cell response compared to that induced by HIV-1. This could be achieved by co-culturing HIV-1 or HIV-2 activated pDCs with allogeneic T cells and measuring subsequent T cell proliferation. Furthermore, it would be of interest to determine if these *in vitro* observations also hold true *in vivo*. To this end, the phenotype of mature pDCs from acutely infected HIV-1 and HIV-2 individuals could be compared.

Is the difference in pDC maturation between HIV-1 and HIV-2 due to trafficking and intracellular signalling?

If spatiotemporal trafficking of TLR ligands is important for determining the phenotype of mature pDCs, it may be interesting to explore if HIV-2 does indeed preferentially traffic to lysosomes. An important question is then: what causes preferential trafficking to either the lysosome or the endosome? The differences in the trafficking of CpG subtypes and thus their abilities to either induce high levels of IFN-α or co-stimulatory molecule expression have been attributed to their secondary and tertiary structure rather than sequence (Guiducci *et al.*, 2006). The authors found that multimeric CpG localised primarily within endosomes and induced greater IFN-α secretion compared to single-stranded CpG structures which were mainly found within lysosomes (Guiducci *et al.*, 2006). We have previously published work utilising fluorescently labelled HIV-1 (Boasso *et al.*, 2011), which could be used in conjunction with confocal microscopy or technologies such as ImageStream (flow cytometry integrated with microscopy), in order to examine viral intracellular trafficking. If this question were addressed, it might be possible to investigate whether HIV-1 can be modified in order to behave more

like HIV-2. The use of HIV-1 and HIV-2 chimeras could provide useful information, whereby the HIV-2 genome is encased within the HIV-1 envelope and similarly the other way around; HIV-1 genome within the HIV-2 envelope. This may help to identify whether the viral envelope proteins or the RNA sequence contribute to the differences in pDC maturation induced by HIV-1 and HIV-2. As discussed, we have previously shown that by modifying the structure of the lipid raft within the plasma membrane of the virus, HIV-1 fails to induce an excessive type I IFN response, but retains the ability to up-regulate co-stimulatory markers on DCs and monocytes (Boasso *et al.*, 2011), suggesting that the viral envelope proteins are an important determining factor of pDC differentiation.

Does the altered pDC maturation during primary HIV-2 infection protect against subsequent HIV-1 infection?

The hypothesis that HIV-2-induced pDC maturation is dominant over HIV-1 responses should also be explored. This study has shown that HIV-2 responses are dominant over CpG-A-induced IFN-α secretion, which signals through TLR-9. A potential *in vitro* study would be to test whether HIV-2 pre-incubation with PBMCs also inhibits subsequent HIV-1-induced responses. However, I decided to exclude this experiment from this investigation due to the potential confounding effect of viral competition for pDC entry via CD4 or TLR-7 ligation.

A previous study has demonstrated that CpG-B treatment of pDCs inhibited the IFN-α response to subsequent stimulation with the RNA encoded vesicular stomatitis virus (VSV) (Waibler *et al.*, 2008). Therefore, an alternative *in vivo* approach could be to treat macaques with CpG-B ODN, subsequently challenge the animals with SIV and investigate any alterations in DC maturation. This approach may also help elucidate whether pDC manipulation, potentially by CpG-B, would be useful at the time of vaccination.

Furthering our understanding of the mechanisms that govern the capabilities of pDCs to act as either APCs or immune-dampening regulatory cells is important not only for viral infections, but will also aid in the research of autoimmune diseases, cancer and other immunologic conditions, such as transplant rejection, in which pDCs have been shown to play a crucial role.

References

Abbas, A. K., Murphy, K. M. & Sher, A. (1996). Functional diversity of helper T lymphocytes. *Nature,* 383**,** 787-93.

Abbey, J. L. & O'Neill, H. C. (2008). Expression of T-cell receptor genes during early T-cell development. *Immunol Cell Biol,* 86**,** 166-74.

Aerts-Toegaert, C., Heirman, C., Tuyaerts, S., Corthals, J., Aerts, J. L., Bonehill, A., Thielemans, K. & Breckpot, K. (2007). CD83 expression on dendritic cells and T cells: correlation with effective immune responses. *Eur J Immunol,* 37**,** 686-95.

Agy, M. B., Acker, R. L., Sherbert, C. H. & Katze, M. G. (1995). Interferon treatment inhibits virus replication in HIV-1- and SIV-infected CD4+ T-cell lines by distinct mechanisms: evidence for decreased stability and aberrant processing of HIV-1 proteins. *Virology,* 214**,** 379-86.

Akira, S., Hirano, T., Taga, T. & Kishimoto, T. (1990). Biology of multifunctional cytokines: IL 6 and related molecules (IL 1 and TNF). *FASEB J,* 4**,** 2860-7.

Alatrakchi, N., Damond, F., Matheron, S., Beretta-Tempelhoff, S., Campa, P., Carcelain, G., Brun-Vezinet, F. & Autran, B. (2006). Proliferative, IFNgamma and IL-2-producing T-cell responses to HIV-2 in untreated HIV-2 infection. *Aids,* 20**,** 29-34.

Andersson, J., Boasso, A., Nilsson, J., Zhang, R., Shire, N. J., Lindback, S., Shearer, G. M. & Chougnet, C. A. (2005). The prevalence of regulatory T cells in lymphoid tissue is correlated with viral load in HIV-infected patients. *J Immunol,* 174**,** 3143-7.

Andersson, S., Norrgren, H., da Silva, Z., Biague, A., Bamba, S., Kwok, S., Christopherson, C., Biberfeld, G. & Albert, J. (2000). Plasma viral load in HIV-1 and HIV-2 singly and dually infected individuals in Guinea-Bissau, West Africa: significantly lower plasma virus set point in HIV-2 infection than in HIV-1 infection. *Arch Intern Med,* 160**,** 3286-93.

Appay, V. & Sauce, D. (2008). Immune activation and inflammation in HIV-1 infection: causes and consequences. *J Pathol,* 214**,** 231-41.

Arthur, L. O., Bess, J. W., Jr., Chertova, E. N., Rossio, J. L., Esser, M. T., Benveniste, R. E., Henderson, L. E. & Lifson, J. D. (1998). Chemical inactivation of retroviral infectivity by targeting nucleocapsid protein zinc fingers: a candidate SIV vaccine. *AIDS Res Hum Retroviruses,* 14 Suppl 3**,** S311-9.

Arts, E. J. & Wainberg, M. A. (1996). Mechanisms of nucleoside analog antiviral activity and resistance during human immunodeficiency virus reverse transcription. *Antimicrob Agents Chemother,* 40**,** 527-40.

Asselin-Paturel, C. & Trinchieri, G. (2005). Production of type I interferons: plasmacytoid dendritic cells and beyond. *J Exp Med,* 202**,** 461-5.

Baenziger, S., Heikenwalder, M., Johansen, P., Schlaepfer, E., Hofer, U., Miller, R. C., Diemand, S., Honda, K., Kundig, T. M., Aguzzi, A. & Speck, R. F. (2009). Triggering TLR7 in mice induces immune activation and lymphoid system disruption, resembling HIV-mediated pathology. *Blood,* 113**,** 377-88.

Banchereau, J. & Steinman, R. M. (1998). Dendritic cells and the control of immunity. *Nature,* 392**,** 245-52.

Barletta, J. M., Edelman, D. C. & Constantine, N. T. (2004). Lowering the detection limits of HIV-1 viral load using real-time immuno-PCR for HIV-1 p24 antigen. *Am J Clin Pathol,* 122**,** 20-7.

Barre-Sinoussi, F., Chermann, J. C., Rey, F., Nugeyre, M. T., Chamaret, S., Gruest, J., Dauguet, C., Axler-Blin, C., Vezinet-Brun, F., Rouzioux, C., Rozenbaum, W. & Montagnier, L. (1983). Isolation of a T-lymphotropic retrovirus from a patient at risk for acquired immune deficiency syndrome (AIDS). *Science,* 220**,** 868-71.

Barron, M. A., Blyveis, N., Palmer, B. E., MaWhinney, S. & Wilson, C. C. (2003). Influence of plasma viremia on defects in number and immunophenotype of blood dendritic cell subsets in human immunodeficiency virus 1-infected individuals. *J Infect Dis,* 187**,** 26-37.

Beignon, A. S., McKenna, K., Skoberne, M., Manches, O., DaSilva, I., Kavanagh, D. G., Larsson, M., Gorelick, R. J., Lifson, J. D. & Bhardwaj, N. (2005). Endocytosis of HIV-1 activates plasmacytoid dendritic cells via Toll-like receptor-viral RNA interactions. *J Clin Invest,* 115**,** 3265-75.

Berger, E. A., Murphy, P. M. & Farber, J. M. (1999). Chemokine receptors as HIV-1 coreceptors: roles in viral entry, tropism, and disease. *Annu Rev Immunol,* 17**,** 657-700.

Berrey, M. M., Schacker, T., Collier, A. C., Shea, T., Brodie, S. J., Mayers, D., Coombs, R., Krieger, J., Chun, T. W., Fauci, A., Self, S. G. & Corey, L. (2001). Treatment of primary human immunodeficiency virus type 1 infection with potent antiretroviral therapy reduces frequency of rapid progression to AIDS. *J Infect Dis,* 183**,** 1466-75.

Birx, D. L., Redfield, R. R., Tencer, K., Fowler, A., Burke, D. S. & Tosato, G. (1990). Induction of interleukin-6 during human immunodeficiency virus infection. *Blood,* 76**,** 2303-10.

Boasso, A., Hardy, A. W., Anderson, S. A., Dolan, M. J. & Shearer, G. M. (2008a). HIV-induced type I interferon and tryptophan catabolism drive T cell dysfunction despite phenotypic activation. *PLoS One,* 3**,** e2961.

Boasso, A., Hardy, A. W., Landay, A. L., Martinson, J. L., Anderson, S. A., Dolan, M. J., Clerici, M. & Shearer, G. M. (2008b). PDL-1 upregulation on monocytes and T cells by HIV via type I interferon: restricted expression of type I interferon receptor by CCR5-expressing leukocytes. *Clin Immunol,* 129**,** 132-44.

Boasso, A., Herbeuval, J. P., Hardy, A. W., Anderson, S. A., Dolan, M. J., Fuchs, D. & Shearer, G. M. (2007). HIV inhibits CD4+ T-cell proliferation by inducing indoleamine 2,3-dioxygenase in plasmacytoid dendritic cells. *Blood,* 109**,** 3351-9.

Boasso, A., Herbeuval, J. P., Hardy, A. W., Winkler, C. & Shearer, G. M. (2005). Regulation of indoleamine 2,3-dioxygenase and tryptophanyl-tRNA-synthetase by CTLA-4-Fc in human CD4+ T cells. *Blood,* 105**,** 1574-81.

Boasso, A., Royle, C. M., Doumazos, S., Aquino, V. N., Biasin, M., Piacentini, L., Tavano, B., Fuchs, D., Mazzotta, F., Lo Caputo, S., Shearer, G. M., Clerici, M. & Graham, D. R. (2011). Overactivation of plasmacytoid dendritic cells inhibits antiviral T-cell responses: a model for HIV immunopathogenesis. *Blood,* 118**,** 5152-62.

Boasso, A. & Shearer, G. M. (2008). Chronic innate immune activation as a cause of HIV-1 immunopathogenesis. *Clin Immunol,* 126**,** 235-42.

Borden, E. C., Sen, G. C., Uze, G., Silverman, R. H., Ransohoff, R. M., Foster, G. R. & Stark, G. R. (2007). Interferons at age 50: past, current and future impact on biomedicine. *Nat Rev Drug Discov,* 6**,** 975-90.

Bosinger, S. E., Johnson, Z. P., Folkner, K. A., Patel, N., Hashempour, T., Jochems, S. P., Del Rio Estrada, P. M., Paiardini, M., Lin, R., Vanderford, T. H., Hiscott, J. & Silvestri, G. (2013). Intact type I Interferon production and IRF7 function in sooty mangabeys. *PLoS Pathog,* 9**,** e1003597.

Bosinger, S. E., Li, Q., Gordon, S. N., Klatt, N. R., Duan, L., Xu, L., Francella, N., Sidahmed, A., Smith, A. J., Cramer, E. M., Zeng, M., Masopust, D., Carlis, J. V., Ran, L., Vanderford, T. H., Paiardini, M., Isett, R. B., Baldwin, D. A., Else, J. G., Staprans, S. I., Silvestri, G., Haase, A. T. & Kelvin, D. J. (2009). Global genomic analysis reveals rapid control of a robust innate response in SIV-infected sooty mangabeys. *J Clin Invest,* 119**,** 3556-72.

Bowers, N. L., Helton, E. S., Huijbregts, R. P., Goepfert, P. A., Heath, S. L. & Hel, Z. (2014). Immune Suppression by Neutrophils in HIV-1 Infection: Role of PD-L1/PD-1 Pathway. *PLoS Pathog,* 10**,** e1003993.

Bratke, K., Klein, C., Kuepper, M., Lommatzsch, M. & Virchow, J. C. (2011). Differential development of plasmacytoid dendritic cells in Th1- and Th2-like cytokine milieus. *Allergy,* 66**,** 386-95.

Brenchley, J. M., Paiardini, M., Knox, K. S., Asher, A. I., Cervasi, B., Asher, T. E., Scheinberg, P., Price, D. A., Hage, C. A., Kholi, L. M., Khoruts, A., Frank, I., Else, J., Schacker, T., Silvestri, G. & Douek, D. C. (2008). Differential Th17 CD4 T-cell depletion in pathogenic and nonpathogenic lentiviral infections. *Blood,* 112**,** 2826-35.

Brenchley, J. M., Price, D. A. & Douek, D. C. (2006a). HIV disease: fallout from a mucosal catastrophe? *Nat Immunol,* 7**,** 235-9.

Brenchley, J. M., Price, D. A., Schacker, T. W., Asher, T. E., Silvestri, G., Rao, S., Kazzaz, Z., Bornstein, E., Lambotte, O., Altmann, D., Blazar, B. R., Rodriguez, B., Teixeira-Johnson, L., Landay, A., Martin, J. N., Hecht, F. M., Picker, L. J., Lederman, M. M., Deeks, S. G. & Douek, D. C. (2006b). Microbial translocation is a cause of systemic immune activation in chronic HIV infection. *Nat Med,* 12**,** 1365-71.

Brenchley, J. M., Schacker, T. W., Ruff, L. E., Price, D. A., Taylor, J. H., Beilman, G. J., Nguyen, P. L., Khoruts, A., Larson, M., Haase, A. T. & Douek, D. C. (2004). CD4+ T cell depletion during all stages of HIV disease occurs predominantly in the gastrointestinal tract. *J Exp Med,* 200**,** 749-59.

Brown, K. N., Wijewardana, V., Liu, X. & Barratt-Boyes, S. M. (2009). Rapid influx and death of plasmacytoid dendritic cells in lymph nodes mediate depletion in acute simian immunodeficiency virus infection. *PLoS Pathog,* 5**,** e1000413.

Bruel, T., Dupuy, S., Demoulins, T., Rogez-Kreuz, C., Dutrieux, J., Corneau, A., Cosma, A., Cheynier, R., Dereuddre-Bosquet, N., Le Grand, R. & Vaslin, B. (2014). Plasmacytoid dendritic cell dynamics tune interferon-alfa production in SIV-infected cynomolgus macaques. *PLoS Pathog,* 10**,** e1003915.

Buseyne, F., Le Gall, S., Boccaccio, C., Abastado, J. P., Lifson, J. D., Arthur, L. O., Riviere, Y., Heard, J. M. & Schwartz, O. (2001). MHC-I-restricted presentation of HIV-1 virion antigens without viral replication. *Nat Med,* 7**,** 344-9.

Cadogan, M. & Dalgleish, A. G. (2008). HIV immunopathogenesis and strategies for intervention. *Lancet Infect Dis,* 8**,** 675-84.

Campbell-Yesufu, O. T. & Gandhi, R. T. (2011). Update on human immunodeficiency virus (HIV)-2 infection. *Clin Infect Dis,* 52**,** 780-7.

Cannavo, G., Paiardini, M., Galati, D., Cervasi, B., Montroni, M., De Vico, G., Guetard, D., Bocchino, M. L., Picerno, I., Magnani, M., Silvestri, G. & Piedimonte, G. (2001). Abnormal intracellular kinetics of cell-cycle-dependent proteins in lymphocytes from patients infected with human immunodeficiency virus: a novel biologic link between immune activation, accelerated T-cell turnover, and high levels of apoptosis. *Blood,* 97**,** 1756-64.

Canque, B., Rosenzwajg, M., Gey, A., Tartour, E., Fridman, W. H. & Gluckman, J. C. (1996). Macrophage inflammatory protein-1alpha is induced by human immunodeficiency virus infection of monocyte-derived macrophages. *Blood,* 87**,** 2011-9.

Cavaleiro, R., Baptista, A. P., Foxall, R. B., Victorino, R. M. & Sousa, A. E. (2009a). Dendritic cell differentiation and maturation in the presence of HIV type 2 envelope. *AIDS Res Hum Retroviruses,* 25**,** 425-31.

Cavaleiro, R., Baptista, A. P., Soares, R. S., Tendeiro, R., Foxall, R. B., Gomes, P., Victorino, R. M. & Sousa, A. E. (2009b). Major depletion of plasmacytoid dendritic cells in HIV-2 infection, an attenuated form of HIV disease. *PLoS Pathog,* 5**,** e1000667.

Cavaleiro, R., Tendeiro, R., Foxall, R. B., Soares, R. S., Baptista, A. P., Gomes, P., Valadas, E., Victorino, R. M. & Sousa, A. E. (2013). Monocyte and myeloid dendritic cell activation occurs throughout HIV type 2 infection, an attenuated form of HIV disease. *J Infect Dis,* 207**,** 1730-42.

Cecchinato, V., Trindade, C. J., Laurence, A., Heraud, J. M., Brenchley, J. M., Ferrari, M. G., Zaffiri, L., Tryniszewska, E., Tsai, W. P., Vaccari, M., Parks, R. W., Venzon, D., Douek, D. C., O'Shea, J. J. & Franchini, G. (2008). Altered balance between Th17 and Th1 cells at mucosal sites predicts AIDS progression in simian immunodeficiency virus-infected macaques. *Mucosal Immunol,* 1**,** 279-88.

Cella, M., Facchetti, F., Lanzavecchia, A. & Colonna, M. (2000). Plasmacytoid dendritic cells activated by influenza virus and CD40L drive a potent TH1 polarization. *Nat Immunol,* 1**,** 305-10.

Cella, M., Jarrossay, D., Facchetti, F., Alebardi, O., Nakajima, H., Lanzavecchia, A. & Colonna, M. (1999). Plasmacytoid monocytes migrate to inflamed lymph nodes and produce large amounts of type I interferon. *Nat Med,* 5**,** 919-23.

Chang, E. Y., Guo, B., Doyle, S. E. & Cheng, G. (2007). Cutting edge: involvement of the type I IFN production and signaling pathway in lipopolysaccharide-induced IL-10 production. *J Immunol,* 178**,** 6705-9.

Chase, A. J., Yang, H. C., Zhang, H., Blankson, J. N. & Siliciano, R. F. (2008). Preservation of FoxP3+ regulatory T cells in the peripheral blood of human immunodeficiency virus type 1-infected elite suppressors correlates with low CD4+ T-cell activation. *J Virol,* 82**,** 8307-15.

Chen, L., Zhang, Z., Chen, W., Li, Y., Shi, M., Zhang, J., Wang, S. & Wang, F. S. (2007). B7-H1 up-regulation on myeloid dendritic cells significantly suppresses T cell immune function in patients with chronic hepatitis B. *J Immunol,* 178**,** 6634-41.

Cheong, C., Matos, I., Choi, J. H., Dandamudi, D. B., Shrestha, E., Longhi, M. P., Jeffrey, K. L., Anthony, R. M., Kluger, C., Nchinda, G., Koh, H., Rodriguez, A., Idoyaga, J., Pack, M., Velinzon, K., Park, C. G. & Steinman, R. M. (2010). Microbial stimulation fully differentiates monocytes to DC-SIGN/CD209(+) dendritic cells for immune T cell areas. *Cell,* 143**,** 416-29.

Chougnet, C., Shearer, G. M. & Landay, A. L. (2002). The Role of Antigen-presenting Cells in HIV Pathogenesis. *Curr Infect Dis Rep,* 4**,** 266-271.

Clavel, F., Guetard, D., Brun-Vezinet, F., Chamaret, S., Rey, M. A., Santos-Ferreira, M. O., Laurent, A. G., Dauguet, C., Katlama, C., Rouzioux, C. & et al. (1986). Isolation of a new human retrovirus from West African patients with AIDS. *Science,* 233**,** 343-6.

Clerici, M., Stocks, N. I., Zajac, R. A., Boswell, R. N., Lucey, D. R., Via, C. S. & Shearer, G. M. (1989). Detection of three distinct patterns of T helper cell dysfunction in asymptomatic, human immunodeficiency virus-seropositive patients. Independence of CD4+ cell numbers and clinical staging. *J Clin Invest,* 84**,** 1892-9.

Cocchi, F., DeVico, A. L., Garzino-Demo, A., Arya, S. K., Gallo, R. C. & Lusso, P. (1995). Identification of RANTES, MIP-1 alpha, and MIP-1 beta as the major HIV-suppressive factors produced by CD8+ T cells. *Science,* 270**,** 1811-5.

Coleman, C. M. & Wu, L. (2009). HIV interactions with monocytes and dendritic cells: viral latency and reservoirs. *Retrovirology,* 6**,** 51.

Colonna, M., Trinchieri, G. & Liu, Y. J. (2004). Plasmacytoid dendritic cells in immunity. *Nat Immunol,* 5**,** 1219-26.

Cotter, R. L., Zheng, J., Che, M., Niemann, D., Liu, Y., He, J., Thomas, E. & Gendelman, H. E. (2001). Regulation of human immunodeficiency virus type 1 infection, beta-chemokine production, and CCR5 expression in CD40L-stimulated macrophages: immune control of viral entry. *J Virol,* 75**,** 4308-20.

Dalgleish, A. G., Beverley, P. C., Clapham, P. R., Crawford, D. H., Greaves, M. F. & Weiss, R. A. (1984). The CD4 (T4) antigen is an essential component of the receptor for the AIDS retrovirus. *Nature,* 312**,** 763-7.

Day, C. L., Kaufmann, D. E., Kiepiela, P., Brown, J. A., Moodley, E. S., Reddy, S., Mackey, E. W., Miller, J. D., Leslie, A. J., DePierres, C., Mncube, Z., Duraiswamy, J., Zhu, B., Eichbaum, Q., Altfeld, M., Wherry, E. J., Coovadia, H. M., Goulder, P. J., Klenerman, P., Ahmed, R., Freeman, G. J. & Walker, B. D. (2006). PD-1 expression on HIV-specific T cells is associated with T-cell exhaustion and disease progression. *Nature,* 443**,** 350-4.

de Silva, T. I., Cotten, M. & Rowland-Jones, S. L. (2008). HIV-2: the forgotten AIDS virus. *Trends Microbiol,* 16**,** 588-95.

de Silva, T. I., Peng, Y., Leligdowicz, A., Zaidi, I., Li, L., Griffin, H., Blais, M. E., Vincent, T., Saraiva, M., Yindom, L. M., van Tienen, C., Easterbrook, P., Jaye, A., Whittle, H., Dong, T. & Rowland-Jones, S. L. (2013). Correlates of T-cell-mediated viral control and phenotype of CD8(+) T cells in HIV-2, a naturally contained human retroviral infection. *Blood,* 121**,** 4330-9.

Derby, N., Martinelli, E. & Robbiani, M. (2011). Myeloid dendritic cells in HIV-1 infection. *Curr Opin HIV AIDS,* 6**,** 379-84.

Donaghy, H., Gazzard, B., Gotch, F. & Patterson, S. (2003). Dysfunction and infection of freshly isolated blood myeloid and plasmacytoid dendritic cells in patients infected with HIV-1. *Blood,* 101**,** 4505-11.

Duvall, M. G., Jaye, A., Dong, T., Brenchley, J. M., Alabi, A. S., Jeffries, D. J., van der Sande, M., Togun, T. O., McConkey, S. J., Douek, D. C., McMichael, A. J., Whittle, H. C., Koup, R. A. & Rowland-Jones, S. L. (2006). Maintenance of HIV-specific CD4+ T cell help distinguishes HIV-2 from HIV-1 infection. *J Immunol,* 176**,** 6973-81.

Duvall, M. G., Lore, K., Blaak, H., Ambrozak, D. A., Adams, W. C., Santos, K., Geldmacher, C., Mascola, J. R., McMichael, A. J., Jaye, A., Whittle, H. C., Rowland-Jones, S. L. & Koup, R. A. (2007). Dendritic cells are less susceptible to human immunodeficiency virus type 2 (HIV-2) infection than to HIV-1 infection. *J Virol,* 81**,** 13486-98.

Duvall, M. G., Precopio, M. L., Ambrozak, D. A., Jaye, A., McMichael, A. J., Whittle, H. C., Roederer, M., Rowland-Jones, S. L. & Koup, R. A. (2008). Polyfunctional T cell responses are a hallmark of HIV-2 infection. *Eur J Immunol,* 38**,** 350-63.

Effros, R. B. & Pawelec, G. (1997). Replicative senescence of T cells: does the Hayflick Limit lead to immune exhaustion? *Immunol Today,* 18**,** 450-4.

Eggena, M. P., Barugahare, B., Jones, N., Okello, M., Mutalya, S., Kityo, C., Mugyenyi, P. & Cao, H. (2005). Depletion of regulatory T cells in HIV infection is associated with immune activation. *J Immunol,* 174**,** 4407-14.

Engelman, A. & Cherepanov, P. (2012). The structural biology of HIV-1: mechanistic and therapeutic insights. *Nat Rev Microbiol,* 10**,** 279-90.

Epple, H. J., Loddenkemper, C., Kunkel, D., Troger, H., Maul, J., Moos, V., Berg, E., Ullrich, R., Schulzke, J. D., Stein, H., Duchmann, R., Zeitz, M. & Schneider, T. (2006). Mucosal but not peripheral FOXP3+ regulatory T cells are highly increased in untreated HIV infection and normalize after suppressive HAART. *Blood,* 108**,** 3072-8.

Esbjornsson, J., Mansson, F., Kvist, A., Isberg, P. E., Nowroozalizadeh, S., Biague, A. J., da Silva, Z. J., Jansson, M., Fenyo, E. M., Norrgren, H. & Medstrand, P. (2012). Inhibition of HIV-1 disease progression by contemporaneous HIV-2 infection. *N Engl J Med,* 367**,** 224-32.

Estes, J. D., Li, Q., Reynolds, M. R., Wietgrefe, S., Duan, L., Schacker, T., Picker, L. J., Watkins, D. I., Lifson, J. D., Reilly, C., Carlis, J. & Haase, A. T. (2006). Premature induction of an immunosuppressive regulatory T cell response during acute simian immunodeficiency virus infection. *J Infect Dis,* 193**,** 703-12.

Fallarino, F., Grohmann, U., You, S., McGrath, B. C., Cavener, D. R., Vacca, C., Orabona, C., Bianchi, R., Belladonna, M. L., Volpi, C., Santamaria, P., Fioretti, M. C. & Puccetti, P. (2006). The combined effects of tryptophan starvation and tryptophan catabolites down-regulate T cell receptor zeta-chain and induce a regulatory phenotype in naive T cells. *J Immunol,* 176**,** 6752-61.

Favre, D., Lederer, S., Kanwar, B., Ma, Z. M., Proll, S., Kasakow, Z., Mold, J., Swainson, L., Barbour, J. D., Baskin, C. R., Palermo, R., Pandrea, I., Miller, C. J., Katze, M. G. & McCune, J. M. (2009). Critical loss of the balance between Th17 and T regulatory cell populations in pathogenic SIV infection. *PLoS Pathog,* 5**,** e1000295.

Favre, D., Mold, J., Hunt, P. W., Kanwar, B., Loke, P., Seu, L., Barbour, J. D., Lowe, M. M., Jayawardene, A., Aweeka, F., Huang, Y., Douek, D. C., Brenchley, J. M., Martin, J. N., Hecht, F. M., Deeks, S. G. &

McCune, J. M. (2010). Tryptophan catabolism by indoleamine 2,3-dioxygenase 1 alters the balance of TH17 to regulatory T cells in HIV disease. *Sci Transl Med,* 2**,** 32ra36.

Felix, N. J., Suri, A., Salter-Cid, L., Nadler, S. G., Gujrathi, S., Corbo, M. & Aranda, R. (2010). Targeting lymphocyte co-stimulation: from bench to bedside. *Autoimmunity,* 43**,** 514-25.

Fenton-May, A. E., Dibben, O., Emmerich, T., Ding, H., Pfafferott, K., Aasa-Chapman, M. M., Pellegrino, P., Williams, I., Cohen, M. S., Gao, F., Shaw, G. M., Hahn, B. H., Ochsenbauer, C., Kappes, J. C. & Borrow, P. (2013). Relative resistance of HIV-1 founder viruses to control by interferon-alpha. *Retrovirology,* 10**,** 146.

Fidler, S., Porter, K., Ewings, F., Frater, J., Ramjee, G., Cooper, D., Rees, H., Fisher, M., Schechter, M., Kaleebu, P., Tambussi, G., Kinloch, S., Miro, J. M., Kelleher, A., McClure, M., Kaye, S., Gabriel, M., Phillips, R., Weber, J. & Babiker, A. (2013). Short-course antiretroviral therapy in primary HIV infection. *N Engl J Med,* 368**,** 207-17.

Finkel, T. H., Tudor-Williams, G., Banda, N. K., Cotton, M. F., Curiel, T., Monks, C., Baba, T. W., Ruprecht, R. M. & Kupfer, A. (1995). Apoptosis occurs predominantly in bystander cells and not in productively infected cells of HIV- and SIV-infected lymph nodes. *Nat Med,* 1**,** 129-34.

Fitzgerald-Bocarsly, P. (1993). Human natural interferon-alpha producing cells. *Pharmacol Ther,* 60**,** 39-62.

Fonteneau, J. F., Gilliet, M., Larsson, M., Dasilva, I., Munz, C., Liu, Y. J. & Bhardwaj, N. (2003). Activation of influenza virus-specific CD4+ and CD8+ T cells: a new role for plasmacytoid dendritic cells in adaptive immunity. *Blood,* 101**,** 3520-6.

Fonteneau, J. F., Larsson, M., Beignon, A. S., McKenna, K., Dasilva, I., Amara, A., Liu, Y. J., Lifson, J. D., Littman, D. R. & Bhardwaj, N. (2004). Human immunodeficiency virus type 1 activates plasmacytoid dendritic cells and concomitantly induces the bystander maturation of myeloid dendritic cells. *J Virol,* 78**,** 5223-32.

Foxall, R. B., Cortesao, C. S., Albuquerque, A. S., Soares, R. S., Victorino, R. M. & Sousa, A. E. (2008). Gag-specific CD4+ T-cell frequency is inversely correlated with proviral load and directly correlated with immune activation in infection with human immunodeficiency virus type 2 (HIV-2) but not HIV-1. *J Virol,* 82**,** 9795-9.

Fraietta, J. A., Mueller, Y. M., Yang, G., Boesteanu, A. C., Gracias, D. T., Do, D. H., Hope, J. L., Kathuria, N., McGettigan, S. E., Lewis, M. G., Giavedoni, L. D., Jacobson, J. M. & Katsikis, P. D. (2013). Type I interferon upregulates Bak and contributes to T cell loss during human immunodeficiency virus (HIV) infection. *PLoS Pathog,* 9**,** e1003658.

Freeman, G. J., Long, A. J., Iwai, Y., Bourque, K., Chernova, T., Nishimura, H., Fitz, L. J., Malenkovich, N., Okazaki, T., Byrne, M. C., Horton, H. F., Fouser, L., Carter, L., Ling, V., Bowman, M. R., Carreno, B. M., Collins, M., Wood, C. R. & Honjo, T. (2000). Engagement of the PD-1 immunoinhibitory receptor by a novel B7 family member leads to negative regulation of lymphocyte activation. *J Exp Med,* 192**,** 1027-34.

Friberg, M., Jennings, R., Alsarraj, M., Dessureault, S., Cantor, A., Extermann, M., Mellor, A. L., Munn, D. H. & Antonia, S. J. (2002). Indoleamine 2,3-dioxygenase contributes to tumor cell evasion of T cell-mediated rejection. *Int J Cancer,* 101**,** 151-5.

Fuchs, D., Moller, A. A., Reibnegger, G., Werner, E. R., Werner-Felmayer, G., Dierich, M. P. & Wachter, H. (1991). Increased endogenous interferon-gamma and neopterin correlate with increased degradation of tryptophan in human immunodeficiency virus type 1 infection. *Immunol Lett,* 28**,** 207-11.

Gallo, S. A., Reeves, J. D., Garg, H., Foley, B., Doms, R. W. & Blumenthal, R. (2006). Kinetic studies of HIV-1 and HIV-2 envelope glycoprotein-mediated fusion. *Retrovirology,* 3**,** 90.

Gary-Gouy, H., Lebon, P. & Dalloul, A. H. (2002). Type I interferon production by plasmacytoid dendritic cells and monocytes is triggered by viruses, but the level of production is controlled by distinct cytokines. *J Interferon Cytokine Res,* 22**,** 653-9.

Geissmann, F., Manz, M. G., Jung, S., Sieweke, M. H., Merad, M. & Ley, K. (2010). Development of monocytes, macrophages, and dendritic cells. *Science,* 327**,** 656-61.

Gerstoft, J., Malchow-Moller, A., Bygbjerg, I., Dickmeiss, E., Enk, C., Halberg, P., Haahr, S., Jacobsen, M., Jensen, K., Mejer, J., Nielsen, J. O., Thomsen, H. K., Sondergaard, J. & Lorenzen, I. (1982). Severe acquired immunodeficiency in European homosexual men. *Br Med J (Clin Res Ed),* 285**,** 17-9.

Gilliet, M., Cao, W. & Liu, Y. J. (2008). Plasmacytoid dendritic cells: sensing nucleic acids in viral infection and autoimmune diseases. *Nat Rev Immunol,* 8**,** 594-606.

Gilliet, M. & Liu, Y. J. (2002). Generation of human CD8 T regulatory cells by CD40 ligand-activated plasmacytoid dendritic cells. *J Exp Med,* 195**,** 695-704.

Giorgi, J. V., Hultin, L. E., McKeating, J. A., Johnson, T. D., Owens, B., Jacobson, L. P., Shih, R., Lewis, J., Wiley, D. J., Phair, J. P., Wolinsky, S. M. & Detels, R. (1999). Shorter survival in advanced human immunodeficiency virus type 1 infection is more closely associated with T lymphocyte activation than with plasma virus burden or virus chemokine coreceptor usage. *J Infect Dis,* 179**,** 859-70.

Giorgi, J. V., Liu, Z., Hultin, L. E., Cumberland, W. G., Hennessey, K. & Detels, R. (1993). Elevated levels of CD38+ CD8+ T cells in HIV infection add to the prognostic value of low CD4+ T cell levels: results of 6 years of follow-up. The Los Angeles Center, Multicenter AIDS Cohort Study. *J Acquir Immune Defic Syndr,* 6**,** 904-12.

Golding, A., Rosen, A., Petri, M., Akhter, E. & Andrade, F. (2010). Interferon-alpha regulates the dynamic balance between human activated regulatory and effector T cells: implications for antiviral and autoimmune responses. *Immunology,* 131**,** 107-17.

Gottlieb, M. S., Schroff, R., Schanker, H. M., Weisman, J. D., Fan, P. T., Wolf, R. A. & Saxon, A. (1981). Pneumocystis carinii pneumonia and mucosal candidiasis in previously healthy homosexual men: evidence of a new acquired cellular immunodeficiency. *N Engl J Med,* 305**,** 1425-31.

Goujon, C., Moncorge, O., Bauby, H., Doyle, T., Ward, C. C., Schaller, T., Hue, S., Barclay, W. S., Schulz, R. & Malim, M. H. (2013). Human MX2 is an interferon-induced post-entry inhibitor of HIV-1 infection. *Nature,* 502**,** 559-62.

Griffith, T. S., Wiley, S. R., Kubin, M. Z., Sedger, L. M., Maliszewski, C. R. & Fanger, N. A. (1999). Monocyte-mediated tumoricidal activity via the tumor necrosis factor-related cytokine, TRAIL. *J Exp Med,* 189**,** 1343-54.

Gringeri, A., Musicco, M., Hermans, P., Bentwich, Z., Cusini, M., Bergamasco, A., Santagostino, E., Burny, A., Bizzini, B. & Zagury, D. (1999). Active anti-interferon-alpha immunization: a European-

Israeli, randomized, double-blind, placebo-controlled clinical trial in 242 HIV-1--infected patients (the EURIS study). *J Acquir Immune Defic Syndr Hum Retrovirol,* 20**,** 358-70.

Gringeri, A., Santagostino, E., Cusini, M., Muca-Perja, M., Marinoni, A., Mannucci, P. M., Burny, A., Criscuolo, M., Lu, W., Andrieru, J. M., Mbika, J. P., Lachgar, A., Fall, L. S., Chams, V., Feldman, M., Hermans, P., Zagury, J. F., Bizzini, B., Musicco, M. & Zagury, D. (1996). Absence of clinical, virological, and immunological signs of progression in HIV-1-infected patients receiving active anti-interferon-alpha immunization: a 30-month follow-up report. *J Acquir Immune Defic Syndr Hum Retrovirol,* 13**,** 55-67.

Grohmann, U., Orabona, C., Fallarino, F., Vacca, C., Calcinaro, F., Falorni, A., Candeloro, P., Belladonna, M. L., Bianchi, R., Fioretti, M. C. & Puccetti, P. (2002). CTLA-4-Ig regulates tryptophan catabolism in vivo. *Nat Immunol,* 3**,** 1097-101.

Guha, M. & Mackman, N. (2001). LPS induction of gene expression in human monocytes. *Cell Signal,* 13**,** 85-94.

Guiducci, C., Ott, G., Chan, J. H., Damon, E., Calacsan, C., Matray, T., Lee, K. D., Coffman, R. L. & Barrat, F. J. (2006). Properties regulating the nature of the plasmacytoid dendritic cell response to Toll-like receptor 9 activation. *J Exp Med,* 203**,** 1999-2008.

Guyader, M., Emerman, M., Sonigo, P., Clavel, F., Montagnier, L. & Alizon, M. (1987). Genome organization and transactivation of the human immunodeficiency virus type 2. *Nature,* 326**,** 662-9.

Haase, A. T. (2010). Targeting early infection to prevent HIV-1 mucosal transmission. *Nature,* 464**,** 217-23.

Hahn, B. H., Shaw, G. M., De Cock, K. M. & Sharp, P. M. (2000). AIDS as a zoonosis: scientific and public health implications. *Science,* 287**,** 607-14.

Hansmann, A., Schim van der Loeff, M. F., Kaye, S., Awasana, A. A., Sarge-Njie, R., O'Donovan, D., Ariyoshi, K., Alabi, A., Milligan, P. & Whittle, H. C. (2005). Baseline plasma viral load and CD4 cell percentage predict survival in HIV-1- and HIV-2-infected women in a community-based cohort in The Gambia. *J Acquir Immune Defic Syndr,* 38**,** 335-41.

Hardy, A. W., Graham, D. R., Shearer, G. M. & Herbeuval, J. P. (2007). HIV turns plasmacytoid dendritic cells (pDC) into TRAIL-expressing killer pDC and down-regulates HIV coreceptors by Toll-like receptor 7-induced IFN-alpha. *Proc Natl Acad Sci U S A,* 104**,** 17453-8.

Harris, L. D., Tabb, B., Sodora, D. L., Paiardini, M., Klatt, N. R., Douek, D. C., Silvestri, G., Muller-Trutwin, M., Vasile-Pandrea, I., Apetrei, C., Hirsch, V., Lifson, J., Brenchley, J. M. & Estes, J. D. (2010). Downregulation of robust acute type I interferon responses distinguishes nonpathogenic simian immunodeficiency virus (SIV) infection of natural hosts from pathogenic SIV infection of rhesus macaques. *J Virol,* 84**,** 7886-91.

Harris, R. S., Hultquist, J. F. & Evans, D. T. (2012). The restriction factors of human immunodeficiency virus. *J Biol Chem,* 287**,** 40875-83.

Harris, R. S., Petersen-Mahrt, S. K. & Neuberger, M. S. (2002). RNA editing enzyme APOBEC1 and some of its homologs can act as DNA mutators. *Mol Cell,* 10**,** 1247-53.

Hecht, F. M., Wang, L., Collier, A., Little, S., Markowitz, M., Margolick, J., Kilby, J. M., Daar, E., Conway, B. & Holte, S. (2006). A multicenter observational study of the potential benefits of initiating combination antiretroviral therapy during acute HIV infection. *J Infect Dis,* 194**,** 725-33.

Heikenwalder, M., Polymenidou, M., Junt, T., Sigurdson, C., Wagner, H., Akira, S., Zinkernagel, R. & Aguzzi, A. (2004). Lymphoid follicle destruction and immunosuppression after repeated CpG oligodeoxynucleotide administration. *Nat Med,* 10**,** 187-92.

Herbeuval, J. P., Boasso, A., Grivel, J. C., Hardy, A. W., Anderson, S. A., Dolan, M. J., Chougnet, C., Lifson, J. D. & Shearer, G. M. (2005a). TNF-related apoptosis-inducing ligand (TRAIL) in HIV-1-infected patients and its in vitro production by antigen-presenting cells. *Blood,* 105**,** 2458-64.

Herbeuval, J. P., Grivel, J. C., Boasso, A., Hardy, A. W., Chougnet, C., Dolan, M. J., Yagita, H., Lifson, J. D. & Shearer, G. M. (2005b). CD4+ T-cell death induced by infectious and noninfectious HIV-1: role of type 1 interferon-dependent, TRAIL/DR5-mediated apoptosis. *Blood,* 106**,** 3524-31.

Herbeuval, J. P., Hardy, A. W., Boasso, A., Anderson, S. A., Dolan, M. J., Dy, M. & Shearer, G. M. (2005c). Regulation of TNF-related apoptosis-inducing ligand on primary CD4+ T cells by HIV-1: role of type I IFN-producing plasmacytoid dendritic cells. *Proc Natl Acad Sci U S A,* 102**,** 13974-9.

Herbeuval, J. P., Nilsson, J., Boasso, A., Hardy, A. W., Kruhlak, M. J., Anderson, S. A., Dolan, M. J., Dy, M., Andersson, J. & Shearer, G. M. (2006). Differential expression of IFN-alpha and TRAIL/DR5 in lymphoid tissue of progressor versus nonprogressor HIV-1-infected patients. *Proc Natl Acad Sci U S A,* 103**,** 7000-5.

Hirahara, K., Poholek, A., Vahedi, G., Laurence, A., Kanno, Y., Milner, J. D. & O'Shea, J. J. (2013). Mechanisms underlying helper T-cell plasticity: implications for immune-mediated disease. *J Allergy Clin Immunol,* 131**,** 1276-87.

Hirano, N., Butler, M. O., Xia, Z., Ansen, S., von Bergwelt-Baildon, M. S., Neuberg, D., Freeman, G. J. & Nadler, L. M. (2006). Engagement of CD83 ligand induces prolonged expansion of CD8+ T cells and preferential enrichment for antigen specificity. *Blood,* 107**,** 1528-36.

Hirsch, V. M. (2004). What can natural infection of African monkeys with simian immunodeficiency virus tell us about the pathogenesis of AIDS? *AIDS Rev,* 6**,** 40-53.

Hoeffel, G., Ripoche, A. C., Matheoud, D., Nascimbeni, M., Escriou, N., Lebon, P., Heshmati, F., Guillet, J. G., Gannage, M., Caillat-Zucman, S., Casartelli, N., Schwartz, O., De la Salle, H., Hanau, D., Hosmalin, A. & Maranon, C. (2007). Antigen crosspresentation by human plasmacytoid dendritic cells. *Immunity,* 27**,** 481-92.

Honda, K., Ohba, Y., Yanai, H., Negishi, H., Mizutani, T., Takaoka, A., Taya, C. & Taniguchi, T. (2005a). Spatiotemporal regulation of MyD88-IRF-7 signalling for robust type-I interferon induction. *Nature,* 434**,** 1035-40.

Honda, K. & Taniguchi, T. (2006). IRFs: master regulators of signalling by Toll-like receptors and cytosolic pattern-recognition receptors. *Nat Rev Immunol,* 6**,** 644-58.

Honda, K., Yanai, H., Mizutani, T., Negishi, H., Shimada, N., Suzuki, N., Ohba, Y., Takaoka, A., Yeh, W. C. & Taniguchi, T. (2004). Role of a transductional-transcriptional processor complex involving MyD88 and IRF-7 in Toll-like receptor signaling. *Proc Natl Acad Sci U S A,* 101**,** 15416-21.

Honda, K., Yanai, H., Negishi, H., Asagiri, M., Sato, M., Mizutani, T., Shimada, N., Ohba, Y., Takaoka, A., Yoshida, N. & Taniguchi, T. (2005b). IRF-7 is the master regulator of type-I interferon-dependent immune responses. *Nature,* 434**,** 772-7.

Honda, K., Yanai, H., Takaoka, A. & Taniguchi, T. (2005c). Regulation of the type I IFN induction: a current view. *Int Immunol,* 17**,** 1367-78.

Huang, J., Burke, P. S., Cung, T. D., Pereyra, F., Toth, I., Walker, B. D., Borges, L., Lichterfeld, M. & Yu, X. G. (2010). Leukocyte immunoglobulin-like receptors maintain unique antigen-presenting properties of circulating myeloid dendritic cells in HIV-1-infected elite controllers. *J Virol,* 84**,** 9463-71.

Huengsberg, M., Winer, J. B., Gompels, M., Round, R., Ross, J. & Shahmanesh, M. (1998). Serum kynurenine-to-tryptophan ratio increases with progressive disease in HIV-infected patients. *Clin Chem,* 44**,** 858-62.

Hufert, F. T., van Lunzen, J., Janossy, G., Bertram, S., Schmitz, J., Haller, O., Racz, P. & von Laer, D. (1997). Germinal centre CD4+ T cells are an important site of HIV replication in vivo. *Aids,* 11**,** 849-57.

Imami, N., Westrop, S. J., Grageda, N. & Herasimtschuk, A. A. (2013). Long-Term Non-Progression and Broad HIV-1-Specific Proliferative T-Cell Responses. *Front Immunol,* 4**,** 58.

Isaacs, A. & Lindenmann, J. (1957). Virus interference. I. The interferon. *Proc R Soc Lond B Biol Sci,* 147**,** 258-67.

Jacquelin, B., Mayau, V., Targat, B., Liovat, A. S., Kunkel, D., Petitjean, G., Dillies, M. A., Roques, P., Butor, C., Silvestri, G., Giavedoni, L. D., Lebon, P., Barre-Sinoussi, F., Benecke, A. & Muller-Trutwin, M. C. (2009). Nonpathogenic SIV infection of African green monkeys induces a strong but rapidly controlled type I IFN response. *J Clin Invest,* 119**,** 3544-55.

Jaehn, P. S., Zaenker, K. S., Schmitz, J. & Dzionek, A. (2008). Functional dichotomy of plasmacytoid dendritic cells: antigen-specific activation of T cells versus production of type I interferon. *Eur J Immunol,* 38**,** 1822-32.

Jain, V., Hartogensis, W., Bacchetti, P., Hunt, P. W., Hatano, H., Sinclair, E., Epling, L., Lee, T. H., Busch, M. P., McCune, J. M., Pilcher, C. D., Hecht, F. M. & Deeks, S. G. (2013). Antiretroviral therapy initiated within 6 months of HIV infection is associated with lower T-cell activation and smaller HIV reservoir size. *J Infect Dis,* 208**,** 1202-11.

Janssen, E. M., Lemmens, E. E., Wolfe, T., Christen, U., von Herrath, M. G. & Schoenberger, S. P. (2003). CD4+ T cells are required for secondary expansion and memory in CD8+ T lymphocytes. *Nature,* 421**,** 852-6.

Jassoy, C., Harrer, T., Rosenthal, T., Navia, B. A., Worth, J., Johnson, R. P. & Walker, B. D. (1993). Human immunodeficiency virus type 1-specific cytotoxic T lymphocytes release gamma interferon, tumor necrosis factor alpha (TNF-alpha), and TNF-beta when they encounter their target antigens. *J Virol,* 67**,** 2844-52.

Jaye, A., Sarge-Njie, R., Schim van der Loeff, M., Todd, J., Alabi, A., Sabally, S., Corrah, T. & Whittle, H. (2004). No differences in cellular immune responses between asymptomatic HIV type 1- and type 2-infected Gambian patients. *J Infect Dis,* 189**,** 498-505.

Jego, G., Palucka, A. K., Blanck, J. P., Chalouni, C., Pascual, V. & Banchereau, J. (2003). Plasmacytoid dendritic cells induce plasma cell differentiation through type I interferon and interleukin 6. *Immunity,* 19**,** 225-34.

Jenabian, M. A., Patel, M., Kema, I., Kanagaratham, C., Radzioch, D., Thebault, P., Lapointe, R., Tremblay, C., Gilmore, N., Ancuta, P. & Routy, J. P. (2013). Distinct tryptophan catabolism and Th17/Treg balance in HIV progressors and elite controllers. *PLoS One,* 8**,** e78146.

Jones, M., Davidson, A., Hibbert, L., Gruenwald, P., Schlaak, J., Ball, S., Foster, G. R. & Jacobs, M. (2005). Dengue virus inhibits alpha interferon signaling by reducing STAT2 expression. *J Virol,* 79**,** 5414-20.

Josefsson, L., Palmer, S., Faria, N. R., Lemey, P., Casazza, J., Ambrozak, D., Kearney, M., Shao, W., Kottilil, S., Sneller, M., Mellors, J., Coffin, J. M. & Maldarelli, F. (2013). Single cell analysis of lymph node tissue from HIV-1 infected patients reveals that the majority of CD4+ T-cells contain one HIV-1 DNA molecule. *PLoS Pathog,* 9**,** e1003432.

Kader, M., Smith, A. P., Guiducci, C., Wonderlich, E. R., Normolle, D., Watkins, S. C., Barrat, F. J. & Barratt-Boyes, S. M. (2013). Blocking TLR7- and TLR9-mediated IFN-alpha production by plasmacytoid dendritic cells does not diminish immune activation in early SIV infection. *PLoS Pathog,* 9**,** e1003530.

Kadowaki, N., Antonenko, S., Lau, J. Y. & Liu, Y. J. (2000). Natural interferon alpha/beta-producing cells link innate and adaptive immunity. *J Exp Med,* 192**,** 219-26.

Kawai, T. & Akira, S. (2007). Antiviral signaling through pattern recognition receptors. *J Biochem,* 141**,** 137-45.

Kawai, T., Sato, S., Ishii, K. J., Coban, C., Hemmi, H., Yamamoto, M., Terai, K., Matsuda, M., Inoue, J., Uematsu, S., Takeuchi, O. & Akira, S. (2004). Interferon-alpha induction through Toll-like receptors involves a direct interaction of IRF7 with MyD88 and TRAF6. *Nat Immunol,* 5**,** 1061-8.

Kaye, J., Hsu, M. L., Sauron, M. E., Jameson, S. C., Gascoigne, N. R. & Hedrick, S. M. (1989). Selective development of CD4+ T cells in transgenic mice expressing a class II MHC-restricted antigen receptor. *Nature,* 341**,** 746-9.

Keir, M. E., Stoddart, C. A., Linquist-Stepps, V., Moreno, M. E. & McCune, J. M. (2002). IFN-alpha secretion by type 2 predendritic cells up-regulates MHC class I in the HIV-1-infected thymus. *J Immunol,* 168**,** 325-31.

Khader, S. A., Gaffen, S. L. & Kolls, J. K. (2009). Th17 cells at the crossroads of innate and adaptive immunity against infectious diseases at the mucosa. *Mucosal Immunol,* 2**,** 403-11.

Kim, Y. M., Brinkmann, M. M., Paquet, M. E. & Ploegh, H. L. (2008). UNC93B1 delivers nucleotide-sensing toll-like receptors to endolysosomes. *Nature,* 452**,** 234-8.

Kobayashi, S., Hamamoto, Y., Kobayashi, N. & Yamamoto, N. (1990). Serum level of TNF alpha in HIV-infected individuals. *Aids,* 4**,** 169-70.

Komanduri, K. V., Donahoe, S. M., Moretto, W. J., Schmidt, D. K., Gillespie, G., Ogg, G. S., Roederer, M., Nixon, D. F. & McCune, J. M. (2001). Direct measurement of CD4+ and CD8+ T-cell responses to CMV in HIV-1-infected subjects. *Virology,* 279**,** 459-70.

Kuritzkes, D. R. (2000). Neutropenia, neutrophil dysfunction, and bacterial infection in patients with human immunodeficiency virus disease: the role of granulocyte colony-stimulating factor. *Clin Infect Dis,* 30**,** 256-60.

Kwa, S., Kannanganat, S., Nigam, P., Siddiqui, M., Shetty, R. D., Armstrong, W., Ansari, A., Bosinger, S. E., Silvestri, G. & Amara, R. R. (2011). Plasmacytoid dendritic cells are recruited to the colorectum and contribute to immune activation during pathogenic SIV infection in rhesus macaques. *Blood,* 118**,** 2763-73.

Laguette, N., Sobhian, B., Casartelli, N., Ringeard, M., Chable-Bessia, C., Segeral, E., Yatim, A., Emiliani, S., Schwartz, O. & Benkirane, M. (2011). SAMHD1 is the dendritic- and myeloid-cell-specific HIV-1 restriction factor counteracted by Vpx. *Nature,* 474**,** 654-7.

Lahouassa, H., Daddacha, W., Hofmann, H., Ayinde, D., Logue, E. C., Dragin, L., Bloch, N., Maudet, C., Bertrand, M., Gramberg, T., Pancino, G., Priet, S., Canard, B., Laguette, N., Benkirane, M., Transy, C., Landau, N. R., Kim, B. & Margottin-Goguet, F. (2012). SAMHD1 restricts the replication of human immunodeficiency virus type 1 by depleting the intracellular pool of deoxynucleoside triphosphates. *Nat Immunol,* 13**,** 223-8.

Lanzavecchia, A. & Sallusto, F. (2001). Regulation of T cell immunity by dendritic cells. *Cell,* 106**,** 263-6.

Layne, S. P., Merges, M. J., Dembo, M., Spouge, J. L., Conley, S. R., Moore, J. P., Raina, J. L., Renz, H., Gelderblom, H. R. & Nara, P. L. (1992). Factors underlying spontaneous inactivation and susceptibility to neutralization of human immunodeficiency virus. *Virology,* 189**,** 695-714.

Le, T., Wright, E. J., Smith, D. M., He, W., Catano, G., Okulicz, J. F., Young, J. A., Clark, R. A., Richman, D. D., Little, S. J. & Ahuja, S. K. (2013). Enhanced CD4+ T-cell recovery with earlier HIV-1 antiretroviral therapy. *N Engl J Med,* 368**,** 218-30.

Lechmann, M., Berchtold, S., Hauber, J. & Steinkasserer, A. (2002). CD83 on dendritic cells: more than just a marker for maturation. *Trends Immunol,* 23**,** 273-5.

Lehmann, C., Jung, N., Forster, K., Koch, N., Leifeld, L., Fischer, J., Mauss, S., Drebber, U., Steffen, H. M., Romerio, F., Fatkenheuer, G. & Hartmann, P. (2014). Longitudinal Analysis of Distribution and Function of Plasmacytoid Dendritic Cells in Peripheral Blood and Gut Mucosa of HIV Infected Patients. *J Infect Dis,* 209**,** 940-9.

Leligdowicz, A., Yindom, L. M., Onyango, C., Sarge-Njie, R., Alabi, A., Cotten, M., Vincent, T., da Costa, C., Aaby, P., Jaye, A., Dong, T., McMichael, A., Whittle, H. & Rowland-Jones, S. (2007). Robust Gag-specific T cell responses characterize viremia control in HIV-2 infection. *J Clin Invest,* 117**,** 3067-74.

Letvin, N. L. & Walker, B. D. (2003). Immunopathogenesis and immunotherapy in AIDS virus infections. *Nat Med,* 9**,** 861-6.

Levy, J. A. (2009). HIV pathogenesis: 25 years of progress and persistent challenges. *Aids,* 23**,** 147-60.

Li, Q., Estes, J. D., Schlievert, P. M., Duan, L., Brosnahan, A. J., Southern, P. J., Reilly, C. S., Peterson, M. L., Schultz-Darken, N., Brunner, K. G., Nephew, K. R., Pambuccian, S., Lifson, J. D., Carlis, J. V. & Haase, A. T. (2009). Glycerol monolaurate prevents mucosal SIV transmission. *Nature,* 458**,** 1034-8.

Lin, R. Y., Nygren, E. J., Valinsky, J. E. & Ralph, H. E. (1988). T cell immunophenotypes and DR antigen expression in intravenous drug users. Relationship to human immunodeficiency virus serology. *Int Arch Allergy Appl Immunol,* 87**,** 263-8.

Liu, Y. J. (2001). Dendritic cell subsets and lineages, and their functions in innate and adaptive immunity. *Cell,* 106**,** 259-62.

Liu, Z., Cumberland, W. G., Hultin, L. E., Prince, H. E., Detels, R. & Giorgi, J. V. (1997). Elevated CD38 antigen expression on CD8+ T cells is a stronger marker for the risk of chronic HIV disease progression to AIDS and death in the Multicenter AIDS Cohort Study than CD4+ cell count, soluble immune activation markers, or combinations of HLA-DR and CD38 expression. *J Acquir Immune Defic Syndr Hum Retrovirol,* 16**,** 83-92.

Lo, C. C., Schwartz, J. A., Johnson, D. J., Yu, M., Aidarus, N., Mujib, S., Benko, E., Hyrcza, M., Kovacs, C. & Ostrowski, M. A. (2012). HIV delays IFN-alpha production from human plasmacytoid dendritic cells and is associated with SYK phosphorylation. *PLoS One,* 7**,** e37052.

Lore, K., Betts, M. R., Brenchley, J. M., Kuruppu, J., Khojasteh, S., Perfetto, S., Roederer, M., Seder, R. A. & Koup, R. A. (2003). Toll-like receptor ligands modulate dendritic cells to augment cytomegalovirus- and HIV-1-specific T cell responses. *J Immunol,* 171**,** 4320-8.

Lui, G., Manches, O., Angel, J., Molens, J. P., Chaperot, L. & Plumas, J. (2009). Plasmacytoid dendritic cells capture and cross-present viral antigens from influenza-virus exposed cells. *PLoS One,* 4**,** e7111.

Lyles, R. H., Munoz, A., Yamashita, T. E., Bazmi, H., Detels, R., Rinaldo, C. R., Margolick, J. B., Phair, J. P. & Mellors, J. W. (2000). Natural history of human immunodeficiency virus type 1 viremia after seroconversion and proximal to AIDS in a large cohort of homosexual men. Multicenter AIDS Cohort Study. *J Infect Dis,* 181**,** 872-80.

Machuca, A., Ding, L., Taffs, R., Lee, S., Wood, O., Hu, J. & Hewlett, I. (2004). HIV type 2 primary isolates induce a lower degree of apoptosis "in vitro" compared with HIV type 1 primary isolates. *AIDS Res Hum Retroviruses,* 20**,** 507-12.

Maier, H., Isogawa, M., Freeman, G. J. & Chisari, F. V. (2007). PD-1:PD-L1 interactions contribute to the functional suppression of virus-specific CD8+ T lymphocytes in the liver. *J Immunol,* 178**,** 2714-20.

Malim, M. H. & Bieniasz, P. D. (2012). HIV Restriction Factors and Mechanisms of Evasion. *Cold Spring Harb Perspect Med,* 2**,** a006940.

Malleret, B., Maneglier, B., Karlsson, I., Lebon, P., Nascimbeni, M., Perie, L., Brochard, P., Delache, B., Calvo, J., Andrieu, T., Spreux-Varoquaux, O., Hosmalin, A., Le Grand, R. & Vaslin, B. (2008). Primary infection with simian immunodeficiency virus: plasmacytoid dendritic cell homing to lymph nodes, type I interferon, and immune suppression. *Blood,* 112**,** 4598-608.

Manches, O., Fernandez, M. V., Plumas, J., Chaperot, L. & Bhardwaj, N. (2012). Activation of the noncanonical NF-kappaB pathway by HIV controls a dendritic cell immunoregulatory phenotype. *Proc Natl Acad Sci U S A,* 109**,** 14122-7.

Manches, O., Frleta, D. & Bhardwaj, N. (2013). Dendritic cells in progression and pathology of HIV infection. *Trends Immunol*.

Manches, O., Munn, D., Fallahi, A., Lifson, J., Chaperot, L., Plumas, J. & Bhardwaj, N. (2008). HIV-activated human plasmacytoid DCs induce Tregs through an indoleamine 2,3-dioxygenase-dependent mechanism. *J Clin Invest,* 118**,** 3431-9.

Mandl, J. N., Barry, A. P., Vanderford, T. H., Kozyr, N., Chavan, R., Klucking, S., Barrat, F. J., Coffman, R. L., Staprans, S. I. & Feinberg, M. B. (2008). Divergent TLR7 and TLR9 signaling and type I interferon production distinguish pathogenic and nonpathogenic AIDS virus infections. *Nat Med,* 14**,** 1077-87.

Manel, N., Hogstad, B., Wang, Y., Levy, D. E., Unutmaz, D. & Littman, D. R. (2010). A cryptic sensor for HIV-1 activates antiviral innate immunity in dendritic cells. *Nature,* 467**,** 214-7.

Marchetti, G., Tincati, C. & Silvestri, G. (2013). Microbial translocation in the pathogenesis of HIV infection and AIDS. *Clin Microbiol Rev,* 26**,** 2-18.

Marlink, R., Kanki, P., Thior, I., Travers, K., Eisen, G., Siby, T., Traore, I., Hsieh, C. C., Dia, M. C., Gueye, E. H. & et al. (1994). Reduced rate of disease development after HIV-2 infection as compared to HIV-1. *Science,* 265**,** 1587-90.

Martinez-Steele, E., Awasana, A. A., Corrah, T., Sabally, S., van der Sande, M., Jaye, A., Togun, T., Sarge-Njie, R., McConkey, S. J., Whittle, H. & Schim van der Loeff, M. F. (2007). Is HIV-2- induced AIDS different from HIV-1-associated AIDS? Data from a West African clinic. *Aids,* 21**,** 317-24.

Martinson, J. A., Montoya, C. J., Usuga, X., Ronquillo, R., Landay, A. L. & Desai, S. N. (2009). Chloroquine modulates HIV-1-induced plasmacytoid dendritic cell alpha interferon: implication for T-cell activation. *Antimicrob Agents Chemother,* 54**,** 871-81.

Martinson, J. A., Roman-Gonzalez, A., Tenorio, A. R., Montoya, C. J., Gichinga, C. N., Rugeles, M. T., Tomai, M., Krieg, A. M., Ghanekar, S., Baum, L. L. & Landay, A. L. (2007). Dendritic cells from HIV-1 infected individuals are less responsive to toll-like receptor (TLR) ligands. *Cell Immunol,* 250**,** 75-84.

Mathan, T. S., Figdor, C. G. & Buschow, S. I. (2013). Human plasmacytoid dendritic cells: from molecules to intercellular communication network. *Front Immunol,* 4**,** 372.

Matsui, T., Connolly, J. E., Michnevitz, M., Chaussabel, D., Yu, C. I., Glaser, C., Tindle, S., Pypaert, M., Freitas, H., Piqueras, B., Banchereau, J. & Palucka, A. K. (2009). CD2 distinguishes two subsets of human plasmacytoid dendritic cells with distinct phenotype and functions. *J Immunol,* 182**,** 6815-23.

McKenna, K., Beignon, A. S. & Bhardwaj, N. (2005). Plasmacytoid dendritic cells: linking innate and adaptive immunity. *J Virol,* 79**,** 17-27.

McKnight, A., Dittmar, M. T., Moniz-Periera, J., Ariyoshi, K., Reeves, J. D., Hibbitts, S., Whitby, D., Aarons, E., Proudfoot, A. E., Whittle, H. & Clapham, P. R. (1998). A broad range of chemokine receptors are used by primary isolates of human immunodeficiency virus type 2 as coreceptors with CD4. *J Virol,* 72**,** 4065-71.

Mehandru, S., Poles, M. A., Tenner-Racz, K., Horowitz, A., Hurley, A., Hogan, C., Boden, D., Racz, P. & Markowitz, M. (2004). Primary HIV-1 infection is associated with preferential depletion of CD4+ T lymphocytes from effector sites in the gastrointestinal tract. *J Exp Med,* 200**,** 761-70.

Meier, A., Bagchi, A., Sidhu, H. K., Alter, G., Suscovich, T. J., Kavanagh, D. G., Streeck, H., Brockman, M. A., LeGall, S., Hellman, J. & Altfeld, M. (2008). Upregulation of PD-L1 on monocytes and dendritic cells by HIV-1 derived TLR ligands. *Aids,* 22**,** 655-8.

Mellor, A. L. & Munn, D. H. (2003). Tryptophan catabolism and regulation of adaptive immunity. *J Immunol,* 170**,** 5809-13.

Merad, M., Sathe, P., Helft, J., Miller, J. & Mortha, A. (2013). The dendritic cell lineage: ontogeny and function of dendritic cells and their subsets in the steady state and the inflamed setting. *Annu Rev Immunol,* 31**,** 563-604.

Meyaard, L., Otto, S. A., Jonker, R. R., Mijnster, M. J., Keet, R. P. & Miedema, F. (1992). Programmed death of T cells in HIV-1 infection. *Science,* 257**,** 217-9.

Michel, P., Balde, A. T., Roussilhon, C., Aribot, G., Sarthou, J. L. & Gougeon, M. L. (2000). Reduced immune activation and T cell apoptosis in human immunodeficiency virus type 2 compared with type 1: correlation of T cell apoptosis with beta2 microglobulin concentration and disease evolution. *J Infect Dis,* 181**,** 64-75.

Miedema, F., Hazenberg, M. D., Tesselaar, K., van Baarle, D., de Boer, R. J. & Borghans, J. A. (2013). Immune Activation and Collateral Damage in AIDS Pathogenesis. *Front Immunol,* 4**,** 298.

Migueles, S. A., Weeks, K. A., Nou, E., Berkley, A. M., Rood, J. E., Osborne, C. M., Hallahan, C. W., Cogliano-Shutta, N. A., Metcalf, J. A., McLaughlin, M., Kwan, R., Mican, J. M., Davey, R. T., Jr. & Connors, M. (2009). Defective human immunodeficiency virus-specific CD8+ T-cell polyfunctionality, proliferation, and cytotoxicity are not restored by antiretroviral therapy. *J Virol,* 83**,** 11876-89.

Miller, C. J., Li, Q., Abel, K., Kim, E. Y., Ma, Z. M., Wietgrefe, S., La Franco-Scheuch, L., Compton, L., Duan, L., Shore, M. D., Zupancic, M., Busch, M., Carlis, J., Wolinsky, S. & Haase, A. T. (2005). Propagation and dissemination of infection after vaginal transmission of simian immunodeficiency virus. *J Virol,* 79**,** 9217-27.

Moseman, E. A., Liang, X., Dawson, A. J., Panoskaltsis-Mortari, A., Krieg, A. M., Liu, Y. J., Blazar, B. R. & Chen, W. (2004). Human plasmacytoid dendritic cells activated by CpG oligodeoxynucleotides induce the generation of CD4+CD25+ regulatory T cells. *J Immunol,* 173**,** 4433-42.

Moutsopoulos, N. M., Vazquez, N., Greenwell-Wild, T., Ecevit, I., Horn, J., Orenstein, J. & Wahl, S. M. (2006). Regulation of the tonsil cytokine milieu favors HIV susceptibility. *J Leukoc Biol,* 80**,** 1145-55.

Munier, M. L. & Kelleher, A. D. (2007). Acutely dysregulated, chronically disabled by the enemy within: T-cell responses to HIV-1 infection. *Immunol Cell Biol,* 85**,** 6-15.

Munn, D. H., Sharma, M. D., Baban, B., Harding, H. P., Zhang, Y., Ron, D. & Mellor, A. L. (2005). GCN2 kinase in T cells mediates proliferative arrest and anergy induction in response to indoleamine 2,3-dioxygenase. *Immunity,* 22**,** 633-42.

Munn, D. H., Sharma, M. D., Hou, D., Baban, B., Lee, J. R., Antonia, S. J., Messina, J. L., Chandler, P., Koni, P. A. & Mellor, A. L. (2004a). Expression of indoleamine 2,3-dioxygenase by plasmacytoid dendritic cells in tumor-draining lymph nodes. *J Clin Invest,* 114**,** 280-90.

Munn, D. H., Sharma, M. D. & Mellor, A. L. (2004b). Ligation of B7-1/B7-2 by human CD4+ T cells triggers indoleamine 2,3-dioxygenase activity in dendritic cells. *J Immunol,* 172**,** 4100-10.

Munn, D. H., Zhou, M., Attwood, J. T., Bondarev, I., Conway, S. J., Marshall, B., Brown, C. & Mellor, A. L. (1998). Prevention of allogeneic fetal rejection by tryptophan catabolism. *Science,* 281**,** 1191-3.

Murphy, K., Travers, P. & Walport, M. (2008). *Janeway's Immunobiology,* New York, USA, Garland Science.

Murray, S. M., Down, C. M., Boulware, D. R., Stauffer, W. M., Cavert, W. P., Schacker, T. W., Brenchley, J. M. & Douek, D. C. (2010). Reduction of immune activation with chloroquine therapy during chronic HIV infection. *J Virol,* 84**,** 12082-6.

Neil, S. J., Zang, T. & Bieniasz, P. D. (2008). Tetherin inhibits retrovirus release and is antagonized by HIV-1 Vpu. *Nature,* 451**,** 425-30.

Nilsson, J., Boasso, A., Velilla, P. A., Zhang, R., Vaccari, M., Franchini, G., Shearer, G. M., Andersson, J. & Chougnet, C. (2006). HIV-1-driven regulatory T-cell accumulation in lymphoid tissues is associated with disease progression in HIV/AIDS. *Blood,* 108**,** 3808-17.

Nyamweya, S., Hegedus, A., Jaye, A., Rowland-Jones, S., Flanagan, K. L. & Macallan, D. C. (2013). Comparing HIV-1 and HIV-2 infection: Lessons for viral immunopathogenesis. *Rev Med Virol,* 23**,** 221-40.

O'Brien, M., Manches, O., Sabado, R. L., Baranda, S. J., Wang, Y., Marie, I., Rolnitzky, L., Markowitz, M., Margolis, D. M., Levy, D. & Bhardwaj, N. (2011). Spatiotemporal trafficking of HIV in human plasmacytoid dendritic cells defines a persistently IFN-alpha-producing and partially matured phenotype. *J Clin Invest,* 121**,** 1088-101.

Ochando, J. C., Homma, C., Yang, Y., Hidalgo, A., Garin, A., Tacke, F., Angeli, V., Li, Y., Boros, P., Ding, Y., Jessberger, R., Trinchieri, G., Lira, S. A., Randolph, G. J. & Bromberg, J. S. (2006). Alloantigen-presenting plasmacytoid dendritic cells mediate tolerance to vascularized grafts. *Nat Immunol,* 7**,** 652-62.

Ochsenbauer, C., Edmonds, T. G., Ding, H., Keele, B. F., Decker, J., Salazar, M. G., Salazar-Gonzalez, J. F., Shattock, R., Haynes, B. F., Shaw, G. M., Hahn, B. H. & Kappes, J. C. (2012). Generation of transmitted/founder HIV-1 infectious molecular clones and characterization of their replication capacity in CD4 T lymphocytes and monocyte-derived macrophages. *J Virol,* 86**,** 2715-28.

Ondondo, B. O., Rowland-Jones, S. L., Dorrell, L., Peterson, K., Cotten, M., Whittle, H. & Jaye, A. (2008). Comprehensive analysis of HIV Gag-specific IFN-gamma response in HIV-1- and HIV-2-infected asymptomatic patients from a clinical cohort in The Gambia. *Eur J Immunol,* 38**,** 3549-60.

Oswald-Richter, K., Grill, S. M., Shariat, N., Leelawong, M., Sundrud, M. S., Haas, D. W. & Unutmaz, D. (2004). HIV infection of naturally occurring and genetically reprogrammed human regulatory T-cells. *PLoS Biol,* 2**,** E198.

Ou, C. Y., Kwok, S., Mitchell, S. W., Mack, D. H., Sninsky, J. J., Krebs, J. W., Feorino, P., Warfield, D. & Schochetman, G. (1988). DNA amplification for direct detection of HIV-1 in DNA of peripheral blood mononuclear cells. *Science,* 239**,** 295-7.

Paiardini, M., Cervasi, B., Reyes-Aviles, E., Micci, L., Ortiz, A. M., Chahroudi, A., Vinton, C., Gordon, S. N., Bosinger, S. E., Francella, N., Hallberg, P. L., Cramer, E., Schlub, T., Chan, M. L., Riddick, N. E., Collman, R. G., Apetrei, C., Pandrea, I., Else, J., Munch, J., Kirchhoff, F., Davenport, M. P., Brenchley, J. M. & Silvestri, G. (2011). Low levels of SIV infection in sooty mangabey central memory CD T cells are associated with limited CCR5 expression. *Nat Med,* 17**,** 830-6.

Paiardini, M., Galati, D., Cervasi, B., Cannavo, G., Galluzzi, L., Montroni, M., Guetard, D., Magnani, M., Piedimonte, G. & Silvestri, G. (2001). Exogenous interleukin-2 administration corrects the cell cycle perturbation of lymphocytes from human immunodeficiency virus-infected individuals. *J Virol,* 75**,** 10843-55.

Pallotta, M. T., Orabona, C., Volpi, C., Vacca, C., Belladonna, M. L., Bianchi, R., Servillo, G., Brunacci, C., Calvitti, M., Bicciato, S., Mazza, E. M., Boon, L., Grassi, F., Fioretti, M. C., Fallarino, F., Puccetti, P. & Grohmann, U. (2011). Indoleamine 2,3-dioxygenase is a signaling protein in long-term tolerance by dendritic cells. *Nat Immunol,* 12**,** 870-8.

Pandrea, I. V., Gautam, R., Ribeiro, R. M., Brenchley, J. M., Butler, I. F., Pattison, M., Rasmussen, T., Marx, P. A., Silvestri, G., Lackner, A. A., Perelson, A. S., Douek, D. C., Veazey, R. S. & Apetrei, C. (2007). Acute loss of intestinal CD4+ T cells is not predictive of simian immunodeficiency virus virulence. *J Immunol,* 179**,** 3035-46.

Pantaleo, G. & Fauci, A. S. (1996). Immunopathogenesis of HIV infection. *Annu Rev Microbiol,* 50**,** 825-54.

Papagno, L., Appay, V., Sutton, J., Rostron, T., Gillespie, G. M., Ogg, G. S., King, A., Makadzanhge, A. T., Waters, A., Balotta, C., Vyakarnam, A., Easterbrook, P. J. & Rowland-Jones, S. L. (2002). Comparison between HIV- and CMV-specific T cell responses in long-term HIV infected donors. *Clinical and Experimental Immunology,* 130**,** 509-17.

Paton, N. I., Goodall, R. L., Dunn, D. T., Franzen, S., Collaco-Moraes, Y., Gazzard, B. G., Williams, I. G., Fisher, M. J., Winston, A., Fox, J., Orkin, C., Herieka, E. A., Ainsworth, J. G., Post, F. A., Wansbrough-Jones, M. & Kelleher, P. (2012). Effects of hydroxychloroquine on immune activation and disease progression among HIV-infected patients not receiving antiretroviral therapy: a randomized controlled trial. *JAMA,* 308**,** 353-61.

Patterson, S., Rae, A., Hockey, N., Gilmour, J. & Gotch, F. (2001). Plasmacytoid dendritic cells are highly susceptible to human immunodeficiency virus type 1 infection and release infectious virus. *J Virol,* 75**,** 6710-3.

Payvandi, F., Amrute, S. & Fitzgerald-Bocarsly, P. (1998). Exogenous and endogenous IL-10 regulate IFN-alpha production by peripheral blood mononuclear cells in response to viral stimulation. *J Immunol,* 160**,** 5861-8.

Perfetto, S. P., Ambrozak, D., Nguyen, R., Chattopadhyay, P. & Roederer, M. (2006). Quality assurance for polychromatic flow cytometry. *Nat Protoc,* 1**,** 1522-30.

Picker, L. J. & Watkins, D. I. (2005). HIV pathogenesis: the first cut is the deepest. *Nat Immunol,* 6**,** 430-2.

Piconi, S., Parisotto, S., Rizzardini, G., Passerini, S., Terzi, R., Argenteri, B., Meraviglia, P., Capetti, A., Biasin, M., Trabattoni, D. & Clerici, M. (2011). Hydroxychloroquine drastically reduces immune activation in HIV-infected, antiretroviral therapy-treated immunologic nonresponders. *Blood,* 118**,** 3263-72.

Pitcher, C. J., Quittner, C., Peterson, D. M., Connors, M., Koup, R. A., Maino, V. C. & Picker, L. J. (1999). HIV-1-specific CD4+ T cells are detectable in most individuals with active HIV-1 infection, but decline with prolonged viral suppression. *Nat Med,* 5**,** 518-25.

Popper, S. J., Sarr, A. D., Gueye-Ndiaye, A., Mboup, S., Essex, M. E. & Kanki, P. J. (2000). Low plasma human immunodeficiency virus type 2 viral load is independent of proviral load: low virus production in vivo. *J Virol,* 74**,** 1554-7.

Popper, S. J., Sarr, A. D., Travers, K. U., Gueye-Ndiaye, A., Mboup, S., Essex, M. E. & Kanki, P. J. (1999). Lower human immunodeficiency virus (HIV) type 2 viral load reflects the difference in pathogenicity of HIV-1 and HIV-2. *J Infect Dis,* 180**,** 1116-21.

Potula, R., Poluektova, L., Knipe, B., Chrastil, J., Heilman, D., Dou, H., Takikawa, O., Munn, D. H., Gendelman, H. E. & Persidsky, Y. (2005). Inhibition of indoleamine 2,3-dioxygenase (IDO) enhances elimination of virus-infected macrophages in an animal model of HIV-1 encephalitis. *Blood,* 106**,** 2382-90.

Prazma, C. M. & Tedder, T. F. (2008). Dendritic cell CD83: a therapeutic target or innocent bystander? *Immunol Lett,* 115**,** 1-8.

Rammensee, H. G., Falk, K. & Rotzschke, O. (1993). MHC molecules as peptide receptors. *Curr Opin Immunol,* 5**,** 35-44.

Reeves, J. D. & Doms, R. W. (2002). Human immunodeficiency virus type 2. *J Gen Virol,* 83**,** 1253-65.

Reizis, B. (2010). Regulation of plasmacytoid dendritic cell development. *Curr Opin Immunol,* 22**,** 206-11.

Richens, J. L., Urbanowicz, R. A., Metcalf, R., Corne, J., O'Shea, P. & Fairclough, L. (2010). Quantitative validation and comparison of multiplex cytokine kits. *J Biomol Screen,* 15**,** 562-8.

Rinaldo, C., Huang, X. L., Fan, Z. F., Ding, M., Beltz, L., Logar, A., Panicali, D., Mazzara, G., Liebmann, J., Cottrill, M. & et al. (1995). High levels of anti-human immunodeficiency virus type 1 (HIV-1) memory cytotoxic T-lymphocyte activity and low viral load are associated with lack of disease in HIV-1-infected long-term nonprogressors. *J Virol,* 69**,** 5838-42.

Rodriguez, B., Lederman, M. M., Jiang, W., Bazdar, D. A., Garate, K., Harding, C. V. & Sieg, S. F. (2006). Interferon-alpha differentially rescues CD4 and CD8 T cells from apoptosis in HIV infection. *Aids,* 20**,** 1379-89.

Roilides, E., Mertins, S., Eddy, J., Walsh, T. J., Pizzo, P. A. & Rubin, M. (1990). Impairment of neutrophil chemotactic and bactericidal function in children infected with human immunodeficiency virus type 1 and partial reversal after in vitro exposure to granulocyte-macrophage colony-stimulating factor. *J Pediatr,* 117**,** 531-40.

Royle, C. M., Tsai, M. H., Tabarrini, O., Massari, S., Graham, D. R., Aquino, V. N. & Boasso, A. (2013). Modulation of HIV-1-Induced Activation of Plasmacytoid Dendritic Cells by 6-Desfluoroquinolones. *AIDS Res Hum Retroviruses*.

Rubbert, A., Behrens, G. & Ostrowski, M. 2012. Pathogenesis of HIV-1 Infection. *In:* HOFFMANN, C. & ROCKSTROH, J. K. (eds.) *HIV 2012/2013.* www.hivbook.com: Medizin Fokus Verlag.

Russell, J. H. & Ley, T. J. (2002). Lymphocyte-mediated cytotoxicity. *Annu Rev Immunol,* 20**,** 323-70.

Rutz, M., Metzger, J., Gellert, T., Luppa, P., Lipford, G. B., Wagner, H. & Bauer, S. (2004). Toll-like receptor 9 binds single-stranded CpG-DNA in a sequence- and pH-dependent manner. *Eur J Immunol,* 34**,** 2541-50.

Sabado, R. L., O'Brien, M., Subedi, A., Qin, L., Hu, N., Taylor, E., Dibben, O., Stacey, A., Fellay, J., Shianna, K. V., Siegal, F., Shodell, M., Shah, K., Larsson, M., Lifson, J., Nadas, A., Marmor, M., Hutt, R., Margolis, D., Garmon, D., Markowitz, M., Valentine, F., Borrow, P. & Bhardwaj, N. (2010). Evidence of dysregulation of dendritic cells in primary HIV infection. *Blood,* 116**,** 3839-52.

Sabat, R., Grutz, G., Warszawska, K., Kirsch, S., Witte, E., Wolk, K. & Geginat, J. (2010). Biology of interleukin-10. *Cytokine Growth Factor Rev,* 21**,** 331-44.

Sakurai, K., Zou, J. P., Tschetter, J. R., Ward, J. M. & Shearer, G. M. (2002). Effect of indoleamine 2,3-dioxygenase on induction of experimental autoimmune encephalomyelitis. *J Neuroimmunol,* 129**,** 186-96.

Samuel, C. E. (2001). Antiviral actions of interferons. *Clin Microbiol Rev,* 14**,** 778-809, table of contents.

Santini, S. M., Lapenta, C., Logozzi, M., Parlato, S., Spada, M., Di Pucchio, T. & Belardelli, F. (2000). Type I interferon as a powerful adjuvant for monocyte-derived dendritic cell development and activity in vitro and in Hu-PBL-SCID mice. *J Exp Med,* 191**,** 1777-88.

Sato, M., Hata, N., Asagiri, M., Nakaya, T., Taniguchi, T. & Tanaka, N. (1998). Positive feedback regulation of type I IFN genes by the IFN-inducible transcription factor IRF-7. *FEBS Lett,* 441**,** 106-10.

Schmidt, B., Ashlock, B. M., Foster, H., Fujimura, S. H. & Levy, J. A. (2005). HIV-infected cells are major inducers of plasmacytoid dendritic cell interferon production, maturation, and migration. *Virology,* 343**,** 256-66.

Schramm, B., Penn, M. L., Palacios, E. H., Grant, R. M., Kirchhoff, F. & Goldsmith, M. A. (2000). Cytopathicity of human immunodeficiency virus type 2 (HIV-2) in human lymphoid tissue is coreceptor dependent and comparable to that of HIV-1. *J Virol,* 74**,** 9594-600.

Schreibelt, G., Tel, J., Sliepen, K. H., Benitez-Ribas, D., Figdor, C. G., Adema, G. J. & de Vries, I. J. (2010). Toll-like receptor expression and function in human dendritic cell subsets: implications for dendritic cell-based anti-cancer immunotherapy. *Cancer Immunol Immunother,* 59**,** 1573-82.

Sharpe, A. H. & Freeman, G. J. (2002). The B7-CD28 superfamily. *Nat Rev Immunol,* 2**,** 116-26.

Shortman, K. & Naik, S. H. (2007). Steady-state and inflammatory dendritic-cell development. *Nat Rev Immunol,* 7**,** 19-30.

Siegal, F. P., Kadowaki, N., Shodell, M., Fitzgerald-Bocarsly, P. A., Shah, K., Ho, S., Antonenko, S. & Liu, Y. J. (1999). The nature of the principal type 1 interferon-producing cells in human blood. *Science,* 284**,** 1835-7.

Silvestri, G. (2005). Naturally SIV-infected sooty mangabeys: are we closer to understanding why they do not develop AIDS? *J Med Primatol,* 34**,** 243-52.

Silvestri, G., Sodora, D. L., Koup, R. A., Paiardini, M., O'Neil, S. P., McClure, H. M., Staprans, S. I. & Feinberg, M. B. (2003). Nonpathogenic SIV infection of sooty mangabeys is characterized by limited bystander immunopathology despite chronic high-level viremia. *Immunity,* 18**,** 441-52.

Simon, V., Ho, D. D. & Abdool Karim, Q. (2006). HIV/AIDS epidemiology, pathogenesis, prevention, and treatment. *Lancet,* 368**,** 489-504.

Smith, R. A., Gottlieb, G. S., Anderson, D. J., Pyrak, C. L. & Preston, B. D. (2008). Human immunodeficiency virus types 1 and 2 exhibit comparable sensitivities to Zidovudine and other nucleoside analog inhibitors in vitro. *Antimicrob Agents Chemother,* 52**,** 329-32.

Sousa, A. E., Carneiro, J., Meier-Schellersheim, M., Grossman, Z. & Victorino, R. M. (2002). CD4 T cell depletion is linked directly to immune activation in the pathogenesis of HIV-1 and HIV-2 but only indirectly to the viral load. *J Immunol,* 169**,** 3400-6.

Sousa, A. E., Chaves, A. F., Loureiro, A. & Victorino, R. M. (2001). Comparison of the frequency of interleukin (IL)-2-, interferon-gamma-, and IL-4-producing T cells in 2 diseases, human immunodeficiency virus types 1 and 2, with distinct clinical outcomes. *J Infect Dis,* 184**,** 552-9.

Stacey, A. R., Norris, P. J., Qin, L., Haygreen, E. A., Taylor, E., Heitman, J., Lebedeva, M., DeCamp, A., Li, D., Grove, D., Self, S. G. & Borrow, P. (2009). Induction of a striking systemic cytokine cascade prior to peak viremia in acute human immunodeficiency virus type 1 infection, in contrast to more modest and delayed responses in acute hepatitis B and C virus infections. *J Virol,* 83**,** 3719-33.

Stefano, K. A., Collman, R., Kolson, D., Hoxie, J., Nathanson, N. & Gonzalez-Scarano, F. (1993). Replication of a macrophage-tropic strain of human immunodeficiency virus type 1 (HIV-1) in a hybrid cell line, CEMx174, suggests that cellular accessory molecules are required for HIV-1 entry. *J Virol,* 67**,** 6707-15.

Stremlau, M., Owens, C. M., Perron, M. J., Kiessling, M., Autissier, P. & Sodroski, J. (2004). The cytoplasmic body component TRIM5alpha restricts HIV-1 infection in Old World monkeys. *Nature,* 427**,** 848-53.

Tailor, P., Tamura, T. & Ozato, K. (2006). IRF family proteins and type I interferon induction in dendritic cells. *Cell Res,* 16**,** 134-40.

Taylor, K. E. & Mossman, K. L. (2013). Recent advances in understanding viral evasion of type I interferon. *Immunology,* 138**,** 190-7.

Teh, H. S., Kisielow, P., Scott, B., Kishi, H., Uematsu, Y., Bluthmann, H. & von Boehmer, H. (1988). Thymic major histocompatibility complex antigens and the alpha beta T-cell receptor determine the CD4/CD8 phenotype of T cells. *Nature,* 335**,** 229-33.

Teijaro, J. R., Ng, C., Lee, A. M., Sullivan, B. M., Sheehan, K. C., Welch, M., Schreiber, R. D., de la Torre, J. C. & Oldstone, M. B. (2013). Persistent LCMV infection is controlled by blockade of type I interferon signaling. *Science,* 340**,** 207-11.

Tesselaar, K., Arens, R., van Schijndel, G. M., Baars, P. A., van der Valk, M. A., Borst, J., van Oers, M. H. & van Lier, R. A. (2003). Lethal T cell immunodeficiency induced by chronic costimulation via CD27-CD70 interactions. *Nat Immunol,* 4**,** 49-54.

Timmons, B. W., Hamadeh, M. J. & Tarnopolsky, M. A. (2009). Two methods for determining plasma IL-6 in humans at rest and following exercise. *Eur J Appl Physiol,* 105**,** 13-8.

Trabattoni, D., Saresella, M., Biasin, M., Boasso, A., Piacentini, L., Ferrante, P., Dong, H., Maserati, R., Shearer, G. M., Chen, L. & Clerici, M. (2003). B7-H1 is up-regulated in HIV infection and is a novel surrogate marker of disease progression. *Blood,* 101**,** 2514-20.

Trautmann, L., Janbazian, L., Chomont, N., Said, E. A., Gimmig, S., Bessette, B., Boulassel, M. R., Delwart, E., Sepulveda, H., Balderas, R. S., Routy, J. P., Haddad, E. K. & Sekaly, R. P. (2006). Upregulation of PD-1 expression on HIV-specific CD8+ T cells leads to reversible immune dysfunction. *Nat Med,* 12**,** 1198-202.

Tyagi, M. & Kashanchi, F. (2012). New and novel intrinsic host repressive factors against HIV-1: PAF1 complex, HERC5 and others. *Retrovirology,* 9**,** 19.

Ullum, H., Cozzi Lepri, A., Bendtzen, K., Victor, J., Gotzsche, P. C., Phillips, A. N., Skinhoj, P. & Klarlund Pedersen, B. (1997). Low production of interferon gamma is related to disease progression in HIV

infection: evidence from a cohort of 347 HIV-infected individuals. *AIDS Res Hum Retroviruses,* 13**,** 1039-46.

UNAIDS 2013. Global report: UNAIDS report on the global AIDS epidemic 2013. http://www.unaids.org/en/media/unaids/contentassets/documents/epidemiology/2013/gr2013/UNAIDS_Global_Report_2013_en.pdf.

Vaccari, M., Fenizia, C., Ma, Z. M., Hryniewicz, A., Boasso, A., Doster, M. N., Miller, C. J., Lindegardh, N., Tarning, J., Landay, A. L., Shearer, G. M. & Franchini, G. (2013). Transient Increase of Interferon-Stimulated Genes and No Clinical Benefit by Chloroquine Treatment During Acute Simian Immunodeficiency Virus Infection of Macaques. *AIDS Res Hum Retroviruses*.

Van Brussel, I., Van Vre, E. A., De Meyer, G. R., Vrints, C. J., Bosmans, J. M. & Bult, H. (2010). Expression of dendritic cell markers CD11c/BDCA-1 and CD123/BDCA-2 in coronary artery disease upon activation in whole blood. *J Immunol Methods,* 362**,** 168-75.

Veazey, R. S., DeMaria, M., Chalifoux, L. V., Shvetz, D. E., Pauley, D. R., Knight, H. L., Rosenzweig, M., Johnson, R. P., Desrosiers, R. C. & Lackner, A. A. (1998). Gastrointestinal tract as a major site of CD4+ T cell depletion and viral replication in SIV infection. *Science,* 280**,** 427-31.

Veazey, R. S., Mansfield, K. G., Tham, I. C., Carville, A. C., Shvetz, D. E., Forand, A. E. & Lackner, A. A. (2000). Dynamics of CCR5 expression by CD4(+) T cells in lymphoid tissues during simian immunodeficiency virus infection. *J Virol,* 74**,** 11001-7.

Vlotides, G., Sorensen, A. S., Kopp, F., Zitzmann, K., Cengic, N., Brand, S., Zachoval, R. & Auernhammer, C. J. (2004). SOCS-1 and SOCS-3 inhibit IFN-alpha-induced expression of the antiviral proteins 2,5-OAS and MxA. *Biochem Biophys Res Commun,* 320**,** 1007-14.

von Sydow, M., Sonnerborg, A., Gaines, H. & Strannegard, O. (1991). Interferon-alpha and tumor necrosis factor-alpha in serum of patients in various stages of HIV-1 infection. *AIDS Res Hum Retroviruses,* 7**,** 375-80.

Waibler, Z., Anzaghe, M., Konur, A., Akira, S., Muller, W. & Kalinke, U. (2008). Excessive CpG 1668 stimulation triggers IL-10 production by cDC that inhibits IFN-alpha responses by pDC. *Eur J Immunol,* 38**,** 3127-37.

Weiss, L., Haeffner-Cavaillon, N., Laude, M., Gilquin, J. & Kazatchkine, M. D. (1989). HIV infection is associated with the spontaneous production of interleukin-1 (IL-1) in vivo and with an abnormal release of IL-1 alpha in vitro. *Aids,* 3**,** 695-9.

Widner, B., Werner, E. R., Schennach, H., Wachter, H. & Fuchs, D. (1997). Simultaneous measurement of serum tryptophan and kynurenine by HPLC. *Clin Chem,* 43**,** 2424-6.

Williams, M. A. & Bevan, M. J. (2007). Effector and memory CTL differentiation. *Annu Rev Immunol,* 25**,** 171-92.

Wilson, E. B., Yamada, D. H., Elsaesser, H., Herskovitz, J., Deng, J., Cheng, G., Aronow, B. J., Karp, C. L. & Brooks, D. G. (2013). Blockade of chronic type I interferon signaling to control persistent LCMV infection. *Science,* 340**,** 202-7.

Wilson, J. D., Imami, N., Watkins, A., Gill, J., Hay, P., Gazzard, B., Westby, M. & Gotch, F. M. (2000). Loss of CD4+ T cell proliferative ability but not loss of human immunodeficiency virus type 1 specificity equates with progression to disease. *J Infect Dis,* 182**,** 792-8.

Yao, S. & Chen, L. (2006). Reviving exhausted T lymphocytes during chronic virus infection by B7-H1 blockade. *Trends Mol Med,* 12**,** 244-6.

Yu, H., Usmani, S. M., Borch, A., Kramer, J., Sturzel, C. M., Khalid, M., Li, X., Krnavek, D., van der Ende, M. E., Osterhaus, A. D., Gruters, R. A. & Kirchhoff, F. (2013). The efficiency of Vpx-mediated SAMHD1 antagonism does not correlate with the potency of viral control in HIV-2-infected individuals. *Retrovirology,* 10**,** 27.

Zhang, S., Zhang, H. & Zhao, J. (2009). The role of CD4 T cell help for CD8 CTL activation. *Biochem Biophys Res Commun,* 384**,** 405-8.

Zheng, N. N., Kiviat, N. B., Sow, P. S., Hawes, S. E., Wilson, A., Diallo-Agne, H., Critchlow, C. W., Gottlieb, G. S., Musey, L. & McElrath, M. J. (2004). Comparison of human immunodeficiency virus (HIV)-specific T-cell responses in HIV-1- and HIV-2-infected individuals in Senegal. *J Virol,* 78**,** 13934-42.

Ziegler-Heitbrock, L., Ancuta, P., Crowe, S., Dalod, M., Grau, V., Hart, D. N., Leenen, P. J., Liu, Y. J., MacPherson, G., Randolph, G. J., Scherberich, J., Schmitz, J., Shortman, K., Sozzani, S., Strobl, H., Zembala, M., Austyn, J. M. & Lutz, M. B. (2010). Nomenclature of monocytes and dendritic cells in blood. *Blood,* 116**,** e74-80.

Appendix

Appendix 1 Virus Normalisation

The main objective of this study was to compare pDC responses to HIV-1 and HIV-2. It was therefore important that any effect observed reflected differences in the molecular and biological characteristics of the viruses, and not differences in the amount of TLR ligand present in the culture system. Due to the fact that pDC activation is mediated by TLR-7 sensing of viral RNA (Mathan *et al.*, 2013), concentrations of HIV-1 and HIV-2 were normalised based on the viral RNA content measured by qPCR. Other methods of virus quantification, such as measurement of total protein content, carry the disadvantage that the total protein content of HIV-1 and HIV-2 preparations can vary greatly depending on the cell line and culture conditions used to grow the viruses, and may not reflect the number of viral particles. An alternative and often utilised approach is to quantify the capsid proteins, p24 for HIV-1 and p26 for HIV-2, by ELISA. However, there is limited information on p26 and it is not known if the levels of p26 capsid protein per virion is comparable to p24. Furthermore, currently available ELISA kits for p26 quantification actually use the SIV p27 ELISA which has been shown to be cross reactive with HIV-2. In addition, the reported numbers of p24 per HIV-1 particle vary between 1200 to 3000 molecules/virion (Barletta *et al.*, 2004, Layne *et al.*, 1992), rendering the estimation of the number of virions in culture unreliable. However, as many studies do quote p24 values for HIV-1, p24 was quantified as a comparison, as described below.

A 1.1 p24 Quantification of HIV-1

Quantification of p24 antigen in purified HIV-1_{MN} was performed using a commercially available ELISA kit (PerkinElmer Life Sciences, Waltham, MA, USA). Results are shown in Appendix Table 1.1. According to the manufacturer's protocol, 20 µl of 5% Triton X-100 was added to all wells of the supplied pre-coated microplate. The supplied standard was appropriately diluted in PBS and serially diluted 1:2 to generate a range from 4000 pg/ml to 12.5 pg/ml. A control was also prepared from the

standard at a concentration of 100 pg/ml and used four times in each plate to monitor inter- and intra-assay variability. Purified virus to be measured was diluted appropriately in PBS, and PBS was also used as a negative control. Diluted standards, controls and samples were added in volumes of 200 µl in duplicate to the microplate. The plate was incubated at 37°C for two hours then washed six times with diluted wash buffer and the wells aspirated and tapped dry. 100 µl of pre-diluted detector antibody was then added to each well and the plate was incubated for one hour at 37°C. After six washes, 100 µl of diluted streptavidin-horseradish peroxidase (SA-HRP) concentrate, prepared in SA-HRP diluent as per the manufacturer's instructions, was added to each well and the plate incubated at room temperature for 30 minutes. After a further six washes, 100 µl of freshly prepared o-Phenylenediamine dihydrochloride (OPD) substrate solution (1 tablet/11 ml substrate diluent), was added to each well and the plate incubated at room temperature in the dark for approximately 10 minutes. The reaction was then terminated with 100 µl stop solution and the absorbance measured at 492 nm with a reference reading at 620 nm using a plate reader (Infinite M200 Pro, Tecan).

Appendix Table 1.1. p24 quantification of HIV-1_{MN} propagated in H9 cells

HIV-1 RNA copies/ml	HIV-1 p24 (ng/ml)
$1.3x\ 10^9$	66.9
$3.9x\ 10^9$	200.6
$13x\ 10^9$	668.7

Appendix 2 Optimisation of qPCR

Initially a one-step RT-qPCR protocol was tested in order to quantify viral RNA. However, amplification curves generated using the HIV-1 primers published in the literature, SK38 & SK39 (Ou *et al.*, 1988), did not follow the typical sigmoid profile (Appendix Figure 2.1). This unusual profile was not due to the amplification of contaminants or primer-dimers as confirmed by the single peak observed in the melting curve. In order to optimise the assay, different primer concentrations and annealing temperatures as low as 56°C were tested, however neither of these methods corrected the amplification curves. Re-examination of the HIV-1 amplified sequence revealed that the GC content was 38%, whereas the GC content for the HIV-2 amplicon was 50%. Consistent with the lower GC content, the melting temperatures of the HIV-1 and HIV-2 products were approximately 74°C and 79°C, respectively. Thus, it is possible that the thermoprofile optimal for the amplification of HIV-2 was not suitable for the HIV-1 sequence with low GC content. A new set of HIV-1 primers was designed to amplify a sequence with a similar GC content as the HIV-2 amplicon. In addition, a two-step RT-qPCR protocol was used which enables the generation and storage of cDNA for future use, thus eliminating the need for multiple RNA extractions. This method ensured optimal amplification profiles and PCR efficiencies for both HIV-1 and HIV-2. This method was subsequently used to normalise all virus isolates (as described in full in Chapter 2, Section 2.2.2).

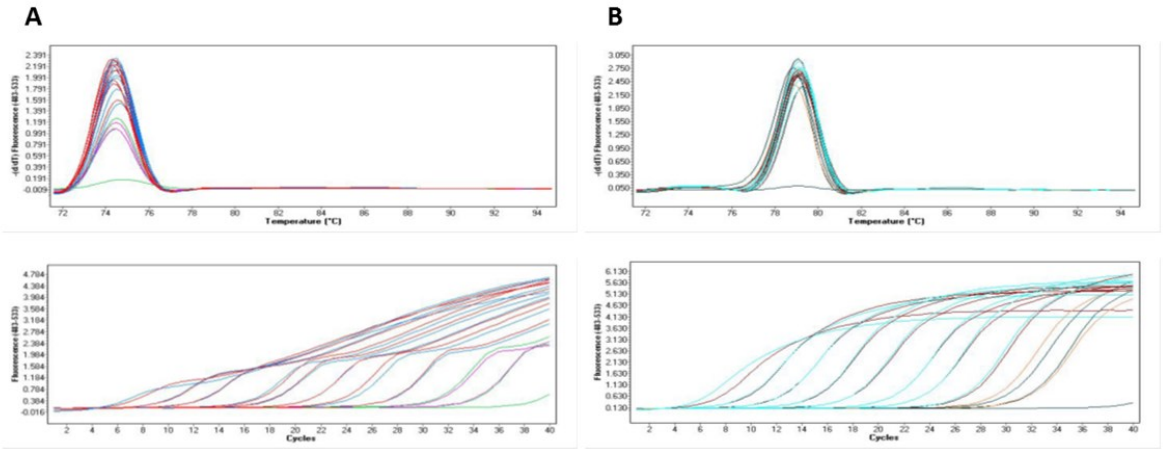

Appendix Figure 2.1. One-step RT-qPCR. Melting curves (top row) and amplification curves (bottom row) for HIV-1 (A) and HIV-2 (B).

Appendix 3 Flow Cytometry Set-up & QC

Voltage settings on the LSR-II (Becton Dickinson) were optimised and monitored throughout the course of this study. Methodology used was based on a published protocol by Perfetto *et al* (Perfetto *et al.*, 2006) and was performed using single peak rainbow and 8 peak calibration beads (Becton Dickinson).

Starting from a setting of 300 volts for the PMT (photomultiplier tube), a mixture of single peak and negative (unstained) beads were initially acquired and 5000 events recorded on the FITC detector, gradually increasing the voltage by 50 volts until the positive peak was no longer visualised on scale (Appendix Figure 3.1). This was repeated for every detector as shown in Appendix Figure 3.1. Based on the result, a range of voltages was chosen for each parameter which gave the lowest background (negative signal) and highest signal.

Plus size anti-mouse compensations beads (Becton Dickinson) were stained individually using the antibodies listed in Chapter 2 (Section 2.4.1). Beads were then acquired on the appropriate detector (FITC, PE, PerCP-Cy5.5, PE-Cy7, APC, APC-Cy7 or Pacific Blue) within the range of voltages chosen (as indicated in Appendix Figure 3.1), gradually increasing the voltage by 10 volts. The optimal voltage for each detector was subsequently chosen as the lowest voltage at which the primary detector MFI (fluorochrome to which the antibody is conjugated) was higher than the secondary detectors MFI.

Single peak rainbow beads were then acquired on the flow cytometer using the optimal voltages chosen for each detector. The MFI of the peak for each fluorochrome was measured. These values then represented the 'target MFI'.

Each day on which samples were acquired on the LSR-II, the single peak rainbow beads were first acquired and the voltages for each detector adjusted until the 'target MFI' was achieved. In addition, 8 peak beads were acquired using these daily voltages and the CV recorded of the 7th brightest bead, giving a measurement of the precision of the flow cytometer over time. Appendix Figure 3.2 illustrates the monitoring of both the PMT voltages and CV over time.

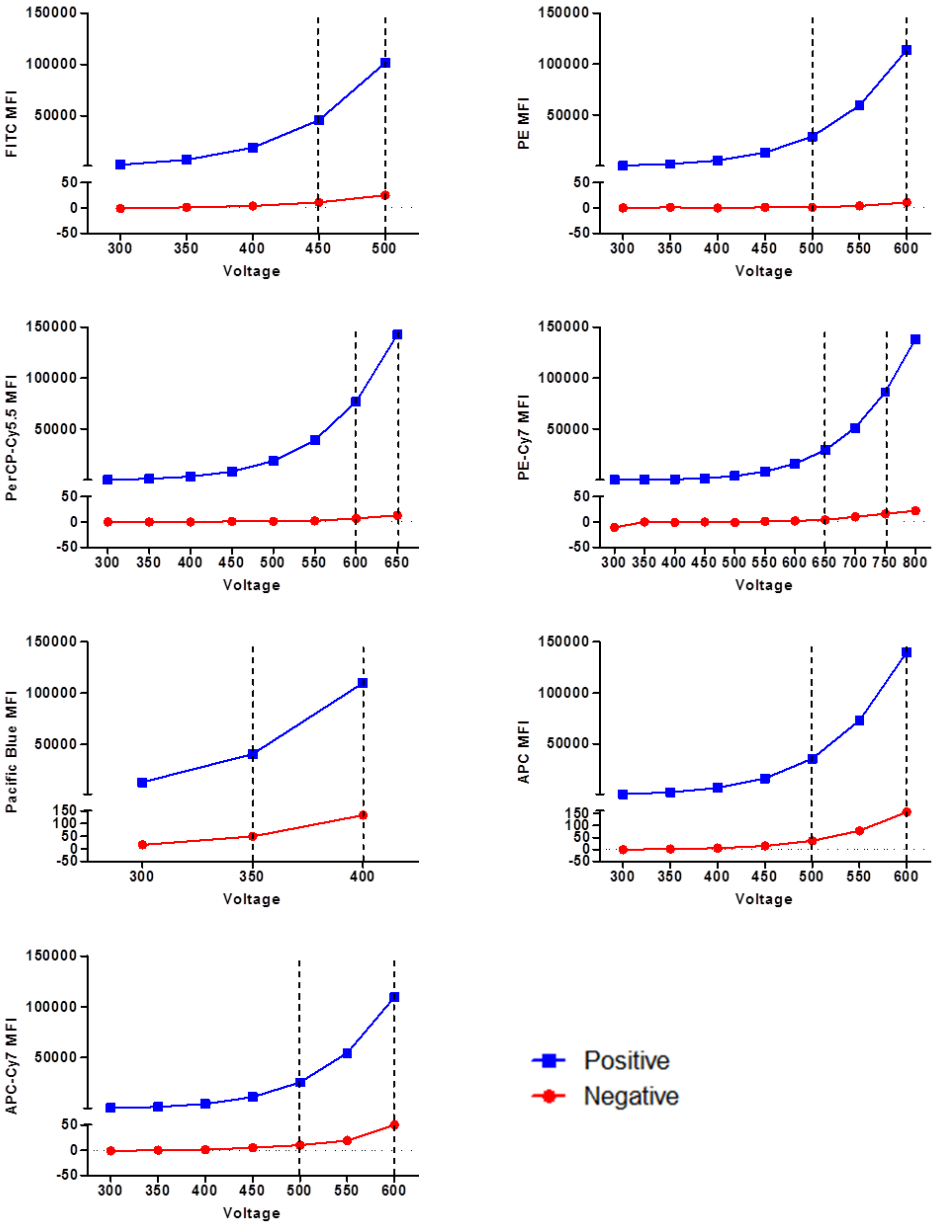

Appendix Figure 3.1. Signal to noise for each detector. The MFI of positive single peak beads is shown in blue and the MFI of negative beads is represented in red. The range of voltages chosen for optimisation are denoted by the vertical dashed lines.

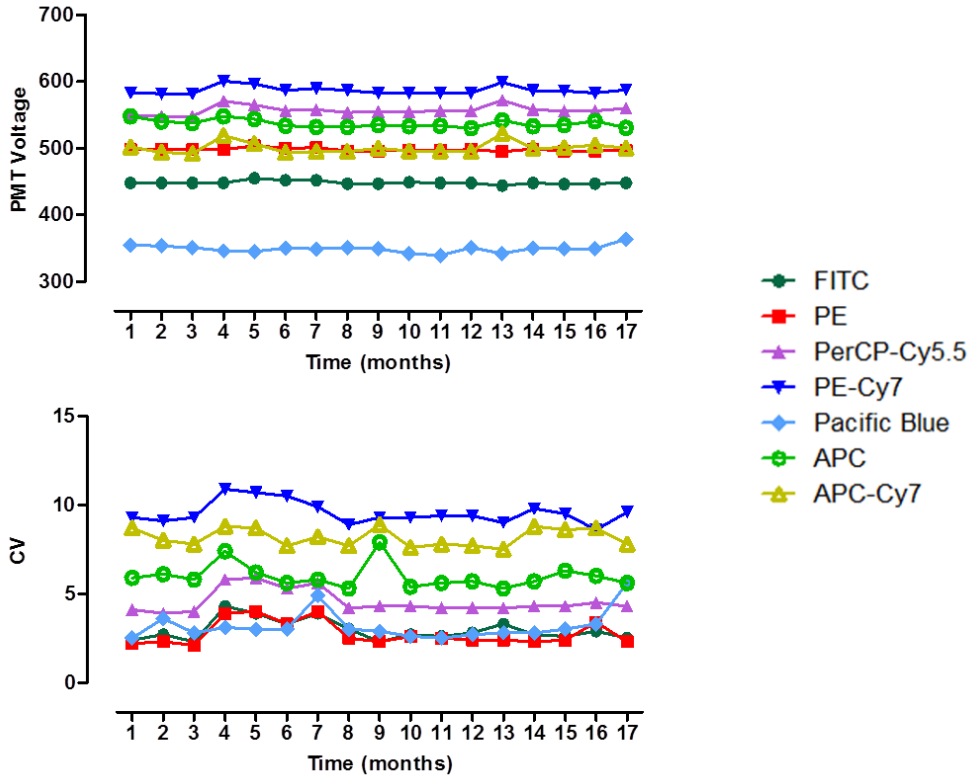

Appendix Figure 3.2. Monitoring PMT voltages and CV. Voltages (top graph) and CV (bottom graph) for each PMT were monitored over time. Each value shows one representative day for each month.

Appendix 4 Confirmation of mDC Gating Strategy

In order to confirm the identity of the Lineage-negative HLA-DR$^+$ CD11c$^+$ cells identified as mDCs (Chapter 2, Section 2.4.1, Figure 2.2), an alternative gating strategy was also employed. This identifies mDCs based on the expression of CD11c as well as the unique marker BDCA1 (BioLegend), thus negating the need for HLA-DR (Appendix Figure 4.1A - D). Back-gating shows that Lineage-negative CD11c$^+$ BDCA1$^+$ identifies the same population of cells as Lineage-negative HLA-DR$^+$ (Appendix Figure 4.1E)

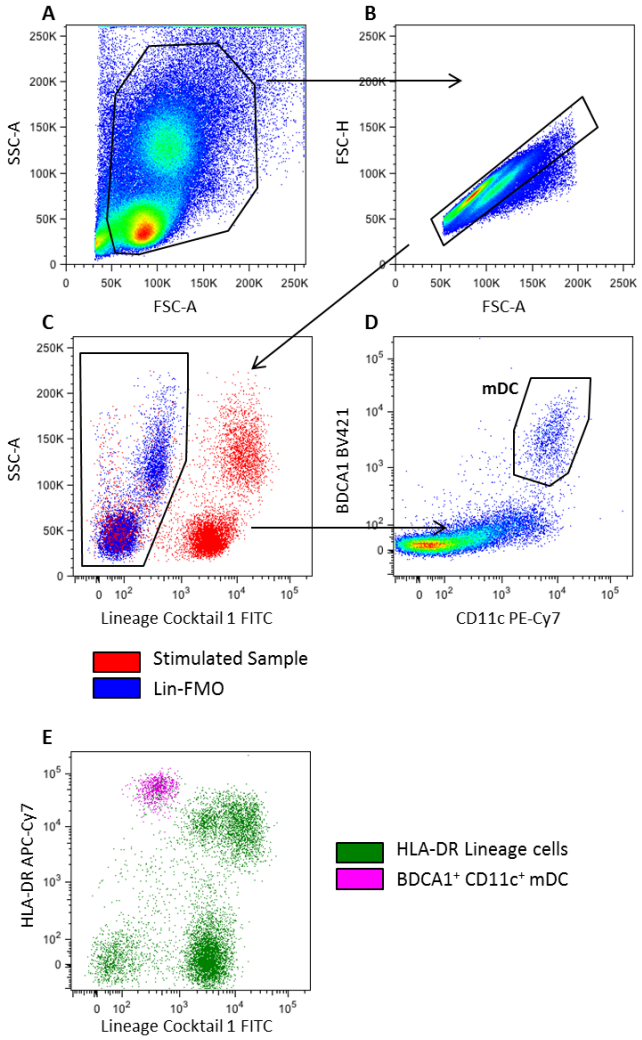

Appendix Figure 4.1. Alternative mDC gating strategy. (A) PBMCs were gated based on side scatter (SSC-A) and forward scatter (FSC-A). (B) Doublets were excluded using FSC height (FSC-H) versus FSC-A. (C) Myeloid DCs were identified as Lineage$^-$ (C) and CD11c$^+$ BDCA1$^+$ (D). In (C) Fluorescence-minus-one (FMO) for Lineage-FITC is displayed in blue to show the separation between the negative and positive population. (E) Back-gating shows the cells identified as mDC in (D), displayed in pink, against a scatter plot of HLA-DR vs Lineage.

Appendix 5 Microarray Gene Lists

Appendix Tables 5.1 and 5.2 show lists of genes differentially regulated by HIV-2 only compared to unstimulated cells (media only), as determined by ANOVA. After 6 (Appendix Table 5.1) and 12 hours (Appendix Table 5.2), HIV-2 induced the differential expression of 21 and 22 genes respectively. Tables only include information of characterised probe sets.

Gene enrichment was performed on three separate lists of genes: those up-regulated or down-regulated by HIV-1 and not HIV-2 compared to media (Appendix Tables 5.3 and 5.6), those regulated by HIV-2 and not HIV-1 (Appendix Tables 5.4 and 5.7) and those regulated by both viruses (Appendix Tables 5.5 and 5.8), as determined by ANOVA. The gene enrichment method clusters genes according to their functional pathways, restricting analysis to functional groups with more than 2 genes, which therefore helps to narrow down the number of differentially altered genes. Enriched genes were then further classified into subgroups based on gene ontology according to the online database AmiGO (http://amigo1.geneontology.org/cgi-bin/amigo/go.cgi, Version 1.8, GO database release 2013-11-09) and available literature and displayed as heat maps (shown in Chapter 4, Section 4.3.4).

Functional information on genes was retrieved from the GeneCards Human Gene Database (Weizmann Institute of Science, Rehovot, Israel, available online http://www.genecards.org/, last updated on 23rd October 2013). Regulation of all genes in virus-stimulated cells is statistically significant compared to media (p-value <0.05 after Benjamini & Hochberg correction).

Appendix Table 5.1. Genes differentially regulated by HIV-2 compared to unstimulated cells after 6 hours stimulation.

Gene Symbol	RefSeq	Fold-Change (HIV-2 vs media)	Function
RGS1	NM_002922	2.01	Attenuates the signalling activity of G-proteins
KIAA1217	NM_019590	2.02	Required for normal development of intervertebral disks (By similarity)
RAB39A	ENST00000320578	2.03	Plays a role in the maturation and acidification of phagosomes that engulf pathogens
USP30-AS1	NR_038996	2.04	RNA gene
TMEM229B	ENST00000555638	2.10	Transmembrane protein
LGALS9C	NM_001040078	2.08	Binds galactosides
LGALS9B	ENST00000423676	2.19	Binds galactosides
LGALS3BP	NM_005567	2.13	It appears to be implicated in immune response associated with NK cell cytotoxicity. LGALS3BP has been found elevated in the serum of patients with cancer and in those infected by HIV.
LOC100507459	ENST00000414676	2.06	RNA gene
OLIG2	ENST00000333337	2.02	Required for oligodendrocyte and motor neuron specification in the spinal cord
P2RY13	NM_176894	2.19	Receptor for ADP
FLJ32255	AK056817	2.03	Uncategorised gene
NFE2L3	NM_004289	2.07	Activates erythroid-specific, globin gene expression

Appendix Table 5.2. Genes differentially regulated by HIV-2 compared to unstimulated cells after 12 hours stimulation.

Gene Symbol	RefSeq	Fold-Change (HIV-2 vs media)	Function
GBP6	NM_198460	2.05111	Guanylate-binding proteins, such as GBP6, are induced by interferon and hydrolyze GTP to both GDP and GMP
CHI3L2	ENST00000445067	2.04439	Lectin that binds chitooligosaccharides and other glycans with high affinity, but not heparin.
LOC400236	NR_036500	2.16306	RNA gene
CLUAP1	NM_015041	2.01855	Required for cilia biogenesis.
SPP1	NM_001251830	2.2934	Probably important to cell-matrix interaction
TMEM178B	NM_001195278	2.22449	Transmembrane protein
INHBA	ENST00000242208	2.04872	The inhibin beta A subunit joins the alpha subunit to form a pituitary FSH secretion inhibitor.

Appendix Table 5.3. Enriched genes regulated by HIV-1 after 6 hours stimulation.

Gene symbol	RefSeq	Fold Change (HIV-1 vs media)	Function
LY9	NM_001033667	-2.34	T-lymphocyte surface antigen
MAP3K8	AB209539	2.42	Member of the serine/threonine protein kinase family
MAP4K2	NM_004579	-2.26	Member of the serine/threonine protein kinase family
BATF2	NM_138456	2.09	AP-1 family transcription factor that controls the differentiation of lineage-specific cells in the immune system
ITGB7	ENST00000267082	-2.02	Codes for integrin beta-7. Integrin alpha-4/beta-7 is an adhesion molecule that mediates lymphocyte migration to gut-associated lymphoid tissue. Binds to HIV-1 gp120
RGCC	NM_014059	-2.15	Regulator of cell cycle
IGHG1	BC019046	-2.03	Immunoglobulin
LAT	NM_014387	-2.24	Required for TCR signalling both in mature T-cells and during their development.
CD79B	NM_000626	-2.01	Interacts with CD79A and involved in initiation of the signal transduction cascade activated by the B-cell antigen receptor complex (BCR) which leads to internalization of the complex, trafficking to late endosomes and antigen presentation.
IL1RN	NM_173842	2.16	IL-1 receptor antagonist
KIT	NM_000222	-2.02	Tyrosine-protein kinase that acts as cell-surface receptor for the cytokine KITLG/SCF.
CXCL3	NM_002090	-2.10	Has chemotactic activity for neutrophils
GAPT	ENST00000396776	-2.49	Negatively regulates B-cell proliferation following stimulation through the B-cell receptor
ERAP2	NM_022350	2.04	Aminopeptidase that plays a central role in peptide trimming, a step required for the generation of most HLA class I-binding peptides
EGR1	NM_001964	-2.47	Transcriptional regulator
HBEGF	ENST00000230990	-2.89	Growth factor. May be involved in macrophage-mediated cellular proliferation.
LTB	ENST00000482429	-2.16	Cytokine that binds to LTBR/TNFRSF3. May play a specific role in immune response regulation
IFNA4	NM_021068	20.81	Type I IFN
IFNA7	NM_021057	27.67	Type I IFN
IFNA10	NM_002171	12.75	Type I IFN
IFNA17	NM_021268	21.42	Type I IFN
IFNA14	NM_002172	5.14	Type I IFN

Appendix Table 5.4. Enriched genes regulated by HIV-2 after 6 hours stimulation.

Gene symbol	RefSeq	Fold Change (HIV-2 vs media)	Function
TIPIN	ENST00000261881	2.07	Required for normal progression of S-phase. Important for cell survival after DNA damage or replication stress
CCR1	ENST00000296140	2.06	Receptor for a C-C type chemokine. Binds to MIP-1-α and RANTES and less efficiently to MIP-1-β
CISH	NM_013324	2.38	Belongs to the SOCS family proteins form part of a classical negative feedback system that regulates cytokine signal transduction
GPR171	NM_013308	2.16	Orphan receptor
SIT1	NM_014450	-2.01	Negatively regulates TCR-mediated signalling in T-cells. Involved in positive selection of T-cells

Appendix Table 5.5. Enriched genes regulated by both HIV-1 and HIV-2 after 6 hours stimulation.

Gene symbol	RefSeq	Fold Change (HIV-1 vs media)	Fold Change (HIV-2 vs media)	Function
ISG15	ENST00000379389	5.40	5.09	Ubiquitin-like protein that is conjugated to intracellular target proteins upon activation by IFN-α and IFN-β.
MOV10	NM_020963	2.32	2.18	Probable RNA helicase. Required for RNA-mediated gene silencing
MNDA	NM_002432	4.77	4.60	May act as a transcriptional activator/repressor in the myeloid lineage
FASLG	ENST00000367721	2.78	2.79	Ligand for Fas. Interaction of Fas with this ligand is critical in triggering apoptosis of some types of cells such as lymphocytes
CFH	NM_000186	2.31	2.36	Regulation of complement activation
GBP3	NM_018284	2.23	2.14	Member of the guanylate-binding protein (GBP) family. GBPs specifically bind guanine nucleotides (GMP, GDP, and GTP). Exhibits anti-viral activity
GBP1	NM_002053	4.95	4.26	Member of the guanylate-binding protein (GBP) family. Exhibits anti-viral activity. Induced by interferon.
AIM2	NM_004833	2.08	2.18	Involved in innate immune response by recognizing cytosolic double-stranded DNA and inducing caspase-1-activating inflammasome formation in macrophages. Interferon inducible
BATF3	NM_018664	2.14	2.17	This gene encodes a member of the basic leucine zipper protein family. Functions as a transcriptional repressor. Involved in DC differentiation
FAS	NM_000043	2.53	2.44	Interaction of Fas with its ligand is critical in triggering apoptosis of some types of cells such as lymphocytes
IFIT2	NM_001547	8.37	8.06	IFN-induced antiviral protein which inhibits expression of viral mRNA
IFIT3	NM_001031683	5.23	5.26	IFN-induced antiviral protein which acts as an inhibitor of cellular as well as viral processes, cell migration, proliferation, signalling, and viral replication
IFIT1	NM_001548	4.86	4.99	Interferon-induced antiviral protein that inhibits expression of viral mRNA

Appendix Table 5.5 continued

IFIT5	NM_012420	2.41	2.46	Interferon-induced protein that acts as a sensor of viral single-stranded RNA
SERPING 1	NM_000062	6.59	5.29	Involved in the regulation of the complement cascade
IFITM3	ENST00000399808	2.06	2.03	IFN-induced antiviral protein which inhibits the entry of viruses to the host cell cytoplasm, permitting endocytosis, but preventing subsequent viral fusion and release of viral contents into the cytosol. Active against HIV-1
IRF7	NM_004031	2.50	2.51	Key transcriptional regulator of type I IFN-dependent immune responses
TRIM5	NM_033092	2.11	2.08	Member of the TRIM family of proteins. Capsid-specific restriction factor that prevents infection from non-host-adapted retroviruses. Blocks viral replication early in the life cycle, after viral entry but before reverse transcription. Also acts as a pattern recognition receptor that activates innate immune signalling in response to the retroviral capsid lattice.
UBE2L6	NM_198183	2.42	2.62	Ubiquitin-conjugating enzyme, involved in ubiquitination
UNC93B 1	NM_030930	2.29	2.49	Required for the transport of a subset of TLRs (including TLR3, TLR7 and TLR9) from the endoplasmic reticulum to endolysosomes where they can engage pathogen nucleotides and activate signalling cascades.
AMICA1	NM_001098526	-3.07	-2.16	May function in transmigration of leukocytes through epithelial and endothelial tissues
CD27	ENST00000266557	-2.99	-2.17	The protein encoded by this gene is a member of the TNF-receptor superfamily. It binds to ligand CD70. Contributes to T and B cell activation
OAS1	ENST00000202917	3.14	3.24	Interferon-induced, dsRNA-activated antiviral enzyme.
OAS3	NM_006187	2.33	2.24	Interferon-induced, dsRNA-activated antiviral enzyme.
OAS2	ENST00000392583	2.12	2.15	Interferon-induced, dsRNA-activated antiviral enzyme.
STAT2	NM_005419	2.49	2.41	Mediates signalling by type I IFN
IFNG	ENST00000229135	9.44	8.28	Type II IFN. Produced by lymphocytes activated by specific antigens or mitogens
OASL	NM_003733	3.06	3.11	Does not have 2'-5'-OAS activity, but can bind double-stranded RNA. Displays antiviral activity.
TNFSF13 B	NM_006573	3.08	3.16	Also known as BAFF. This cytokine is expressed in B cell lineage cells, and acts as a potent B cell activator
RPS6KA5	NM_004755	2.32	2.11	Serine/threonine-protein kinase. Involved in the regulation inflammatory genes
PML	NM_033240	3.21	3.07	Member of the TRIM family of proteins. Exhibits antiviral activity.
ISG20	ENST00000306072	2.82	2.74	Exonuclease with specificity for single-stranded RNA and, to a lesser extent for DNA. Involved in the antiviral function of IFN against RNA viruses
IRF8	ENST00000268638	2.24	2.13	Transcription factor. Specifically binds to the upstream regulatory region of type I IFN and IFN-inducible MHC class I genes.
MEFV	ENST00000219596	2.47	2.37	Modulator of innate immunity
CCL7	NM_006273	2.70	3.23	Secreted chemokine which attracts macrophages during inflammation
CCL8	NM_005623	43.19	37.47	Secreted chemokine. By recruiting leukocytes to sites of inflammation this cytokine may contribute to the antiviral state against HIV infection
IFI35	NM_005533	2.54	2.53	IFN induced protein

Appendix Table 5.5 continued

DHX58	NM_024119	2.47	2.53	Acts as a regulator of DDX58/RIG-I and IFIH1/MDA5 mediated antiviral signalling
TRIM25	NM_005082	2.16	2.16	Member of the TRIM family of proteins. Involved in innate immune defense against viruses by mediating ubiquitination of DDX58
SECTM1	NM_003004	3.73	3.33	Transmembrane and secreted protein
PMAIP1	ENST00000316660	2.60	2.70	Promotes activation of caspases and apoptosis
BST2	ENST00000252593	2.42	2.53	IFN-induced antiviral host restriction factor which efficiently blocks the release of diverse mammalian enveloped viruses by directly tethering budding virions to the membranes of infected cells
RSAD2	NM_080657	5.29	4.86	Interferon-inducible antiviral protein. Active against HIV-1
CASP10	NM_032974	3.68	3.50	Involved in the activation cascade of caspases responsible for apoptosis execution.
EIF2AK2	ENST00000233057	2.09	2.02	IFN-induced dsRNA-dependent serine/threonine-protein kinase. Exhibits antiviral activity.
IFIH1	ENST00000263642	4.11	4.01	Cytoplasmic sensor of viral nucleic acids Plays a in the activation of a cascade of antiviral responses including the induction of type I IFN and pro-inflammatory cytokines. Also known as MDA5.
IRS1	NM_005544	2.08	2.13	May mediate the control of various cellular processes by insulin
SAMHD1	ENST00000262878	2.52	2.53	Host restriction nuclease that blocks early-stage virus replication in dendritic and other myeloid cells
ZBP1	NM_030776	2.99	2.97	Cytoplasmic DNA sensor which induces type I IFN production
MX1	NM_001144925	2.47	2.36	IFN-induced GTPase with antiviral activity against a wide range of RNA viruses and some DNA viruses
APOL1	NM_003661	4.96	4.53	May play a role in lipid exchange and transport throughout the body
APOBEC 3A	NM_145699	2.38	2.37	Member of the cytidine deaminase protein family with restriction activity against viruses and foreign DNA
PLSCR1	NM_021105	2.83	2.60	May play a role in the antiviral response of IFN by amplifying and enhancing the IFN response through increased expression of select subset of potent antiviral genes
TNFSF10	NM_003810	4.25	4.24	Also known as TRAIL, a cytokine that induces apoptosis
CD38	NM_001775	2.51	2.31	A multifunctional ectoenzyme widely expressed in cells and tissues especially in leukocytes
HERC5	NM_016323	3.96	3.76	Ubiquitin ligase. Acts as a positive regulator of innate antiviral response in cells induced by IFN
EXOSC9	NM_001034194	2.18	2.11	A component of the human exosome, which processes and degrades RNA in the nucleus and cytoplasm
IL15	NM_172175	2.66	2.16	Cytokine that stimulates the proliferation of T-lymphocytes
TLR3	NM_003265	2.64	3.19	Nucleotide-sensing TLR which is activated by double-stranded RNA
CXCL9	NM_002416	27.74	18.72	Secreted chemokine which attracts activated T-cells
CXCL10	NM_001565	16.40	15.69	Secreted chemokine which attracts monocytes and T-lymphocytes
CXCL11	NM_005409	32.66	28.99	Secreted chemokine which attracts activated T-cells
DDX60	NM_017631	2.49	2.27	Positively regulates DDX58/RIG-I- and IFIH1/MDA5-

Appendix Table 5.5 continued

				dependent type I IFN and IFN inducible gene expression in response to viral infection. Binds ssRNA, dsRNA and dsDNA
PSMB8	NM_004159	2.12	2.14	Proteasome subunit. Involved in antigen processing to generate class I binding peptides
BAK1	NM_001188	2.08	2.00	In the presence of an appropriate stimulus, accelerates programmed cell death by binding to, and antagonizing the anti-apoptotic action of BCL2
MB21D1	NM_138441	2.59	2.39	Cytosolic DNA sensor
NOD1	NM_006092	2.37	2.14	Intracellular pattern-recognition receptor (PRR)
DEFB1	ENST00000297439	3.39	2.80	Defensins form a family of microbicidal and cytotoxic peptides made by neutrophils
IFNA8	NM_002170	40.12	11.44	Type I IFN
IFNA1	NM_024013	146.58	44.67	Type I IFN
IFNB1	NM_002176	7.44	2.96	Type I IFN
IFNW1	NM_002177	8.61	3.44	Type I IFN
IFNA21	NM_002175	65.80	17.56	Type I IFN
IFNA16	NM_002173	63.56	18.61	Type I IFN
IFNA5	NM_002169	19.56	7.23	Type I IFN
IFNA13	NM_006900	44.92	13.95	Type I IFN
IFNA2	NM_000605	14.91	5.73	Type I IFN
DDX58	NM_014314	3.66	3.59	Also known as RIG-I. Acts as a cytoplasmic sensor of viral nucleic acids and induces expression of type I IFN and pro-inflammatory cytokines
TLR7	NM_016562	2.84	3.02	Nucleotide-sensing TLR which is activated by single-stranded RNA
TAB3	ENST00000467136	2.19	2.59	TGF-β activated kinase. Functions in the NF-κB signal transduction pathway
CD24	NM_013230	2.37	2.50	Modulates B-cell activation responses

Appendix Table 5.6. Enriched genes regulated by HIV-1 after 12 hours stimulation.

Gene symbol	RefSeq	Fold-Change (HIV-1 vs media)	Function
ADAR	ENST00000292205	2.01	IFN-inducible RNA editing enzyme. Proposed to stimulate both the release and infectivity of HIV-1 viral particles
CLEC4A	NM_016184	-2.69	Member of the C-type lectin family of proteins. Also known as DCIR. May play a role in modulating DC differentiation and/or maturation.
NLRC4	ENST00000404025	-2.28	Member of the NOD-like receptor family of PRRs.
ELMO2	NM_133171	2.18	Involved in cytoskeletal rearrangements required for phagocytosis of apoptotic cells and cell motility
CXCL6	NM_002993	-2.60	Secreted chemokine which attracts neutrophil granulocytes
CXCL3	NM_002090	-3.87	Has chemotactic activity for neutrophils
GAPT	ENST00000396776	-2.22	Negatively regulates B-cell proliferation following stimulation through the B-cell receptor
VEGFA	NM_001025366	-2.04	Growth factor active in angiogenesis, vasculogenesis and endothelial cell growth
IRF5	NM_032643	2.27	Transcription factor involved in the induction of type I IFN and inflammatory cytokines upon virus infection. Activated by TLR7 or TLR8 signalling
ENPP2	ENST00000518109	2.04	Hydrolyzes lysophospholipids to produce lysophosphatidic acid (LPA) in extracellular fluids
IFNB1	NM_002176	4.51	Type I IFN
IFNW1	NM_002177	5.36	Type I IFN
IFNA10	NM_002171	9.37	Type I IFN
IFNA14	NM_002172	3.52	Type I IFN
IFNA2	NM_000605	10.20	Type I IFN

Appendix Table 5.7. Enriched genes regulated by HIV-2 after 12 hours stimulation.

Gene symbol	RefSeq	Fold-Change (HIV-2 vs media)	Function
CCL3	NM_002983	2.01	Chemokine also known as MIP-1-α. Binds to CCR1, CCR4 and CCR5. One of the major HIV-suppressive factors produced by $CD8^+$ T cells. Recombinant MIP-1-α induces a dose-dependent inhibition of HIV-1, HIV-2, and SIV

Appendix Table 5.8. Enriched genes regulated by both HIV-1 and HIV-2 after 12 hours stimulation

Gene symbol	RefSeq	Fold Change (HIV-1 vs media)	Fold Change (HIV-2 vs media)	Function
ISG15	ENST00000379389	15.11	11.64	Ubiquitin-like protein that is conjugated to intracellular target proteins upon activation by IFN-α and IFN-β
IFI44L	NM_006820	3.49	3.41	Antiviral IFN inducible protein.
MOV10	NM_020963	3.78	3.58	Probable RNA helicase. Required for RNA-mediated gene silencing
MNDA	NM_002432	13.11	10.33	May act as a transcriptional activator/repressor in the myeloid lineage
IFI16	NM_005531	2.12	2.08	IFN induced. Binds viral DNA in the cytoplasm
SLAMF7	ENST00000368043	4.08	3.31	Mediates NK cell activation
FASLG	ENST00000367721	2.68	2.28	Ligand for Fas. Interaction of Fas with this ligand is critical in triggering apoptosis of some types of cells such as lymphocytes
GBP3	NM_018284	3.64	2.96	Member of the guanylate-binding protein (GBP) family. GBPs specifically bind guanine nucleotides (GMP, GDP, and GTP). Exhibits anti-viral activity
GBP1	NM_002053	8.77	7.42	Member of the guanylate-binding protein (GBP) family. Exhibits anti-viral activity. Induced by interferon.
GBP2	ENST00000464839	3.26	2.90	Member of the guanylate-binding protein (GBP) family. Exhibits anti-viral activity. Induced by interferon.
AIM2	NM_004833	4.53	3.43	Involved in innate immune response by recognizing cytosolic double-stranded DNA and inducing caspase-1-activating inflammasome formation in macrophages. Interferon inducible
TNFSF18	ENST00000404377	2.30	2.07	Cytokine member of the TNF ligand family. Regulates T-cell responses.
BATF3	NM_018664	2.84	2.59	This gene encodes a member of the basic leucine zipper protein family. Functions as a transcriptional repressor. Involved in DC differentiation
FAS	NM_000043	3.22	2.83	Interaction of Fas with its ligand is critical in triggering apoptosis of some types of cells such as lymphocytes
IFIT2	NM_001547	21.01	16.97	IFN-induced antiviral protein which inhibits expression of viral mRNA
IFIT3	NM_001031683	16.99	15.30	IFN-induced antiviral protein which acts as an inhibitor of cellular as well as viral processes, cell migration, proliferation, signalling, and viral replication
IFIT1	NM_001548	14.37	13.05	Interferon-induced antiviral protein that inhibits expression of viral mRNA
IFIT5	NM_012420	3.38	3.32	Interferon-induced protein that acts as a sensor of viral single-stranded RNA
PRF1	NM_005041	2.53	2.46	Perforin 1. One of the key cytotoxic proteins involved in secretory granule-dependent cell death.
TRIM22	NM_006074	2.83	2.75	Member of the TRIM family of proteins. Interferon-induced antiviral protein involved in cell innate immunity. The antiviral activity could in part be mediated by the ubiquitination of viral proteins. Plays a role in restricting the replication of HIV-1

Appendix Table 5.8 continued

SERPING1	NM_000062	19.31	18.00	Involved in the regulation of the complement cascade
IRF7	NM_004031	4.63	4.48	Key transcriptional regulator of type I IFN-dependent immune responses
TRIM5	NM_033092	3.37	3.17	Member of the TRIM family of proteins. Capsid-specific restriction factor that prevents infection from non-host-adapted retroviruses. Blocks viral replication early in the life cycle, after viral entry but before reverse transcription. Also acts as a pattern recognition receptor that activates innate immune signalling in response to the retroviral capsid lattice
UBE2L6	NM_198183	3.25	3.05	Ubiquitin-conjugating enzyme, involved in ubiquitination
BATF2	NM_138456	3.06	2.53	Member of the basic leucine zipper protein family. Functions as a transcriptional repressor. Involved in DC differentiation
UNC93B1	NM_030930	3.11	2.98	Required for the transport of a subset of TLRs (including TLR3, TLR7 and TLR9) from the endoplasmic reticulum to endolysosomes where they can engage pathogen nucleotides and activate signalling cascades.
CASP1	NM_001257118	2.30	2.16	Member of the caspase family of proteins. Plays a central role in the execution of apoptosis
OAS1	ENST00000202917	8.08	7.48	Interferon-induced, dsRNA-activated antiviral enzyme.
OAS3	NM_006187	8.79	8.45	Interferon-induced, dsRNA-activated antiviral enzyme.
OAS2	ENST00000392583	3.81	3.67	Interferon-induced, dsRNA-activated antiviral enzyme.
P2RX7	NR_033948	4.54	3.48	Receptor for ATP that acts as a ligand-gated ion channel. Responsible for ATP-dependent lysis of macrophages through the formation of membrane pores.
STAT2	NM_005419	4.37	4.13	Mediates signalling by type I IFN
OASL	NM_003733	5.31	4.98	Does not have 2'-5'-OAS activity, but can bind double-stranded RNA. Displays antiviral activity.
TNFSF13B	NM_006573	4.50	4.13	Also known as BAFF. This cytokine is expressed in B cell lineage cells, and acts as a potent B cell activator
PML	NM_033240	5.65	4.84	Member of the TRIM family of proteins. Exhibits antiviral activity.
ISG20	ENST00000306072	4.62	4.48	Exonuclease with specificity for single-stranded RNA and, to a lesser extent for DNA. Involved in the antiviral function of IFN against RNA viruses
NLRC5	ENST00000262510	2.16	2.03	Member of the NOD-like receptor family of proteins. Probable regulator of the NF-κB and type I interferon signalling pathways.
IRF8	ENST00000268638	2.33	2.17	Transcription factor. Specifically binds to the upstream regulatory region of type I IFN and IFN-inducible MHC class I genes
MEFV	ENST00000219596	5.00	4.53	Modulator of innate immunity
CCL7	NM_006273	8.52	9.11	Secreted chemokine which attracts macrophages during inflammation
CCL8	NM_005623	109.02	102.64	Secreted chemokine. By recruiting leukocytes to sites of inflammation this cytokine may contribute to the antiviral state against HIV infection
IFI35	NM_005533	5.68	5.48	IFN induced protein

Appendix Table 5.8 continued

DHX58	NM_024119	4.57	3.95	Acts as a regulator of DDX58/RIG-I and IFIH1/MDA5 mediated antiviral signalling
TRIM25	NM_005082	3.04	2.80	Member of the TRIM family of proteins. Involved in innate immune defense against viruses by mediating ubiquitination of DDX58
SECTM1	NM_003004	6.73	5.89	Transmembrane and secreted protein
PMAIP1	ENST00000316660	2.67	2.37	Promotes activation of caspases and apoptosis
AXL	NM_021913	8.83	6.35	Receptor tyrosine kinase that transduces signals from the extracellular matrix into the cytoplasm. Plays a role in regulating many physiological processes including cell survival, cell proliferation, migration and differentiation. Also involved in the inhibition of TLR-mediated innate immune response.
BST2	ENST00000252593	4.20	4.35	IFN-induced antiviral host restriction factor which efficiently blocks the release of diverse mammalian enveloped viruses by directly tethering budding virions to the membranes of infected cells
PRKD2	NM_016457	2.53	2.46	Serine/threonine-protein kinase. Involved in the regulation of cell proliferation via MAPK1/3 (ERK1/2) signalling, oxidative stress-induced NF-κB activation, inhibition of HDAC7 transcriptional repression, signalling downstream of TCR and cytokine production, and plays a role in Golgi membrane trafficking, angiogenesis, secretory granule release and cell adhesion.
LILRA5	NM_021250	3.11	2.98	Member of the leukocyte immunoglobulin-like receptor (LIR) family. May play a role in triggering innate immune responses.
RSAD2	NM_080657	16.11	14.56	Interferon-inducible antiviral protein. Active against HIV-1
IL1R2	NR_048564	2.97	3.55	Non-signalling receptor for IL1A, IL1B and IL1RN. Reduces IL1B activities. Serves as a decoy receptor by competitive binding to IL1B and preventing its binding to IL1R1
IL1RN	NM_173842	4.12	3.45	IL-1 receptor antagonist
CASP10	NM_032974	4.03	3.24	Involved in the activation cascade of caspases responsible for apoptosis execution.
CCL20	NM_004591	-6.95	-3.67	Chemotactic factor that attracts lymphocytes, DCs and neutrophils, but not monocytes.
EIF2AK2	ENST00000233057	3.70	3.64	IFN-induced dsRNA-dependent serine/threonine-protein kinase. Exhibits antiviral activity.
IL1A	NM_000575	-5.61	-2.81	Produced by activated macrophages. IL-1 proteins are involved in the inflammatory response.
IFIH1	ENST00000263642	7.04	6.15	Cytoplasmic sensor of viral nucleic acids Plays a in the activation of a cascade of antiviral responses including the induction of type I IFN and pro-inflammatory cytokines. Also known as MDA5.
STAT1	NM_007315	3.25	3.07	Mediates signalling by type I IFN
RBCK1	NM_031229	2.75	2.63	E3 ubiquitin-protein ligase (promotes ubiquitination)
THBD	ENST00000377103	-7.78	-3.66	Thrombomodulin. Involved in the anticoagulation pathway. Also known as BDCA-3 expressed on a subset of DCs.
SAMHD1	ENST00000262878	2.20	2.11	Host restriction nuclease that blocks early-stage virus replication in dendritic and other myeloid cells

Appendix Table 5.8 continued

ZBP1	NM_030776	6.27	5.63	Cytoplasmic DNA sensor which induces type I IFN production
MX1	NM_001144925	4.97	4.65	IFN-induced GTPase with antiviral activity against a wide range of RNA viruses and some DNA viruses
APOL1	NM_003661	6.64	5.14	May play a role in lipid exchange and transport throughout the body
APOBEC3A	NM_145699	4.84	4.60	Member of the cytidine deaminase protein family with restriction activity against viruses and foreign DNA
OSM	NM_020530	-2.77	-2.10	Growth regulator. It regulates cytokine production, including IL-6, G-CSF and GM-CSF from endothelial cells
UBA7	NM_003335	2.77	2.60	Ubiquitin activating enzyme.
CD80	NM_005191	5.83	4.31	Involved in the co-stimulatory signal essential for T-lymphocyte activation
PLSCR1	NM_021105	3.41	3.16	May play a role in the antiviral response of IFN by amplifying and enhancing the IFN response through increased expression of select subset of potent antiviral genes
TNFSF10	NM_003810	6.91	6.32	Also known as TRAIL, a cytokine that induces apoptosis
CD38	NM_001775	8.04	6.36	A multifunctional ectoenzyme widely expressed in cells and tissues especially in leukocytes
KIT	NM_000222	-2.39	-2.37	Tyrosine-protein kinase that acts as cell-surface receptor for the cytokine KITLG/SCF.
EREG	NM_001432	-2.49	-2.08	Ligand of the EGF receptor/EGFR and ERBB4. May be a mediator of localized cell proliferation.
CXCL13	NM_006419	5.04	4.18	Chemotactic for B-lymphocytes but not for T-lymphocytes, monocytes and neutrophils.
HERC5	NM_016323	10.16	8.99	Ubiquitin ligase. Acts as a positive regulator of innate antiviral response in cells induced by IFN
IL15	NM_172175	3.54	2.66	Cytokine that stimulates the proliferation of T-lymphocytes
TLR3	NM_003265	4.37	3.79	Nucleotide-sensing TLR which is activated by double-stranded RNA
CXCL5	NM_002994	-5.76	-2.79	This chemokine involved in neutrophil activation
CXCL9	NM_002416	21.38	20.60	Secreted chemokine which attracts activated T-cells
CXCL10	NM_001565	35.30	27.93	Secreted chemokine which attracts monocytes and T-lymphocytes
DDX60	NM_017631	4.26	4.10	Positively regulates DDX58/RIG-I- and IFIH1/MDA5-dependent type I IFN and IFN inducible gene expression in response to viral infection. Binds ssRNA, dsRNA and dsDNA
PRLR	NM_000949	10.41	5.79	This is a receptor for the anterior pituitary hormone prolactin.
HBEGF	ENST00000230990	-4.75	-2.70	Growth factor. May be involved in macrophage-mediated cellular proliferation.
EDN1	NM_001955	3.18	2.53	Endothelins are endothelium-derived vasoconstrictor peptides
C2	NM_000063	2.71	2.51	Component C2 which is part of the classical pathway of the complement system
CFB	ENST00000425368	6.95	4.93	Complement factor B, a component of the alternative pathway of complement activation
TAP2	NM_018833	3.19	3.00	Involved in the transport of antigens from the cytoplasm to the endoplasmic reticulum for association with MHC class I molecules

Appendix Table 5.8 continued

PSMB8	NM_004159	2.34	2.24	Proteasome subunit. Involved in antigen processing to generate class I binding peptides
TAP1	NM_000593	2.93	2.80	Involved in the transport of antigens from the cytoplasm to the endoplasmic reticulum for association with MHC class I molecules
MB21D1	NM_138441	2.72	2.14	Cytosolic DNA sensor
TRIM56	ENST00000306085	2.42	2.19	Member of the TRIM family of proteins. E3 ubiquitin-protein ligase involved in innate immune defense against viruses. Activates production of IFN-β.
NOD1	NM_006092	2.87	2.47	Intracellular pattern-recognition receptor (PRR)
CLEC5A	NM_013252	-7.08	-3.51	Member of the C-type lectin family of proteins. Regulates inflammatory responses
ADAMDEC1	NM_001145271	2.74	2.15	This encoded protein is thought to be a secreted protein belonging to the disintegrin metalloproteinase family. Its expression is up-regulated during dendritic cells maturation. This protein may play an important role in dendritic cell function and their interactions with germinal center T cells
DEFB1	ENST00000297439	6.90	4.11	Defensins form a family of microbicidal and cytotoxic peptides made by neutrophils
ENPP2	NM_006209	2.38	2.28	Hydrolyzes lysophospholipids to produce lysophosphatidic acid (LPA) in extracellular fluids
CD274	NM_014143	4.68	3.78	Also known as PDL-1. Involved in the co-stimulatory signal. Interaction with its receptor PD-1 inhibits T-cell proliferation and cytokine production
PDCD1LG2	NM_025239	2.91	2.59	Also known as PDL-1 2. Involved in the co-stimulatory signal. Interaction with its receptor PD-1 inhibits T-cell proliferation and cytokine production
IFNA8	NM_002170	42.79	5.25	Type I IFN
IFNA1	NM_024013	151.13	16.37	Type I IFN
IFNA21	NM_002175	106.44	9.40	Type I IFN
IFNA4	NM_021068	29.48	2.48	Type I IFN
IFNA7	NM_021057	31.84	2.62	Type I IFN
IFNA16	NM_002173	69.25	8.04	Type I IFN
IFNA17	NM_021268	33.93	3.35	Type I IFN
IFNA5	NM_002169	14.39	2.84	Type I IFN
IFNA13	NM_006900	55.21	5.76	Type I IFN
DDX58	NM_014314	5.59	5.39	Also known as RIG-I. Acts as a cytoplasmic sensor of viral nucleic acids and induces expression of type I IFN and pro-inflammatory cytokines
TLR7	NM_016562	4.90	4.48	Nucleotide-sensing TLR which is activated by single-stranded RNA
TLR8	NM_138636	2.37	2.02	Nucleotide-sensing TLR
TAB3	ENST00000467136	4.60	4.30	TGF-β activated kinase. Functions in the NF-κB signal transduction pathway